Function and failure mechanisms of dual mobility bearings for total hip replacement

Mackenzie Taylor Smeeton

Submitted in accordance with the requirements for the degree of
Doctor of Philosophy

The University of Leeds
School of Mechanical Engineering

December 2022

The candidate confirms that the work submitted is her own, except where work which has formed part of jointly authored publications has been included. The contribution of the candidate and the other authors to this work has been explicitly indicated below. The candidate confirms that appropriate credit has been given within the thesis where reference has been made to the work of others.

Chapters 4 and 5 include elements from one jointly authored publication:

> Matthew Peter Shuttleworth, Oliver Vickers, Mackenzie Smeeton, Tim Board, Graham Isaac, Peter Culmer, Sophie Williams, Robert William Kay. 2023. Inertial Tracking System for Monitoring Dual Mobility Implants In Vitro. *Sensors*. 23(2), 904.

With regards to the research presented in Chapters 4 and 5, the author's work constitutes all aspects of the methodological design, development, formal investigation, data analysis and data visualisation presented in this Thesis.

M.P. Shuttleworth was responsible for the development, validation and calibration of the tracker and provided technical assistance for the use of this device within a hip simulator. His assistance is directly acknowledged within this Thesis, where appropriate.

Acknowledgements

First and foremost, I would like to acknowledge and thank DePuy Synthes for financially supporting this project through an industrial CASE studentship and for providing the components used in this Thesis for testing.

In addition, I would like to thank my primary supervisor Professor Sophie Williams for your endless support, guidance, and expertise. This PhD was not without its challenges – whether it be the Covid-19 pandemic, simulator breakdowns, or personal setbacks – but you have supported me through each difficulty with compassion, resolve and a sense of humility and humour that is truly admirable. I am sincerely grateful to have been one of your researchers.

I would also like to thank to remainder of my supervision team: Professor Graham Isaac, Professor Ruth Wilcox, Dr James Anderson, and Professor Tim Board. It was a real pleasure working with you all. I am also grateful to Professor Douglas van Citters from Dartmouth College for his collaborative efforts in providing dual mobility retrievals on loan for this work, and to Dr Matthew Shuttleworth for sharing his expertise in in-vitro sensing of dual mobility implants.

I'd also like to say a sincere thanks to all the technical staff who have supported this project. It was your know-how that got me through some of my most challenging days. I'd like to say a special thanks to Andrew Stockdale and Camille Hammersley for your assistance and companionship throughout this process.

To my wonderful colleagues in iMBE, I truly could not have done this without you. You have been there to share in each of my experiences – the good and the bad – and to find humour in every situation. Without you all, I'm sure I would have lost my sanity long ago. :-) I'll deeply miss working with each of you.

Finally, I'd like to thank my family and friends. A special thanks to my parents Marc and Christina who have always supported my passion for education, to 'M2 and D2' Jo and Andy for taking me in during my many years at University as your American daughter, and to 'mum and dad' Mark and Maxine for making a point to celebrate each and every of my little victories along the way. Most importantly, I'd like to thank my dearest friend Cassie for your unwavering (and transatlantic!) support throughout

this process, and to my loving husband Sam for believing in me through all my moments of self-doubt.

Abstract

Dual Mobility (DM) Total Hip Replacements (THRs) were introduced to combat the complex challenge of hip dislocation for at-risk patients. These are characterised by an unconstrained polyethylene liner therefore introducing a secondary articulating surface between the liner and acetabular component. Despite their emerging use, the in-vivo function of these implants is not well understood. Early evidence suggests that DM THRs may perform poorer than conventional designs, and failure mechanisms unique to these implants remain a concern. Therefore, the aim of this study was to improve the current understanding of DM function and failure mechanisms.

It was clear that current characterisation and in-vitro testing methodologies reported in the literature are not suitable for the novel geometry and function of DM THRs. Therefore, two novel methods were developed in this Thesis: a geometric characterisation method to assess surface damage across the articulating surfaces of DM polyethylene liners, and an in-vitro motion tracking method to investigate the mechanisms of DM liner motion. These methods may be used to improve next-generation implant designs and identify best- and worst-case operating conditions thus providing clinicians with more informed surgical guidelines (e.g., optimal component positions) and patient demographics for which these implants should be used.

In addition, the function and failure mechanisms of DM THRs were investigated through a multi-method retrieval analysis (n=20 implants) and in-vitro motion tracking, which was the first study to directly observe the behaviour of DM liners under physiologically relevant loading, displacement, and lubrication conditions. These studies identified a primary articulation site (i.e., between the femoral head and liner) and rotational capabilities of the liner within the acetabular shell. Additionally, highly variable damage patterns were observed across the collection of retrieved components and poor intra- and inter-component repeatability of the liner motion was identified in-vitro. This provides evidence that DM motion is not driven purely by implant design but instead may be sensitive to a variety of other factors (e.g., component position, soft tissue interactions). Therefore, it is possible that small changes to the in-vivo environment may have a significant impact on the behaviour and thus long-term performance of DM THRs.

Table of Contents

List of tables

List of figures

Abbreviations

AHS	Anatomical Hip Simulator
ARPD	Adverse reaction to particulate debris
CMM	Coordinate measuring machine
CoC	Ceramic-on-ceramic
CoP	Ceramic-on-polyethylene
CoPoM	Ceramic-on-polyethylene-on-metal
DM	Dual mobility
EAD	Extra-articular dislocation
EDX	Energy-dispersive x-ray analysis
EM17	Electromechanical Hip Simulator
IPD	Intraprosthetic dislocation
MoM	Metal-on-metal
MoP	Metal-on-polyethylene
MoPoM	Metal-on-polyethylene-on-metal
NOF	Neck of femur
PE	Polyethylene
PSCE	Probe-shaft contact error
PTFE	Polytetrafluoroethylene
ROM	Range of motion
SEM	Scanning electron microscope
THR	Total hip replacement
UHMWPE	Ultra-high molecular weight polyethylene
XLPE	Cross-linked polyethylene

Chapter 1 – Introduction

1.1 – The natural hip

The acetabulofemoral joint, commonly known as the hip joint, is the ball-and-socket joint between the femur and pelvis as shown in Figure 1.1. The hip joint is comprised of two bony structures: the proximal femur (the 'ball') and the acetabulum of the pelvis (the 'socket'). The surfaces of these bony structures are covered with articular cartilage, a smooth tissue which facilitates the frictionless movement of and a uniform load distribution throughout the joint (Buckwalter et al., 2005; Byrne et al., 2010). A ring of fibrous cartilage surrounds the rim of the acetabulum, known as the labrum, in order to deepen the joint. The hip is inherently stable due to its deep socket and high conformity of its bony structures. Four ligaments act to reinforce the joint and further enhance its stability (Bowman et al., 2010). Three ligaments – the iliofemoral, pubofemoral and ischiofemoral ligaments – encapsulate the joint while the fourth, the ligamentum teres, lies within the joint to connect the femoral head and acetabulum.

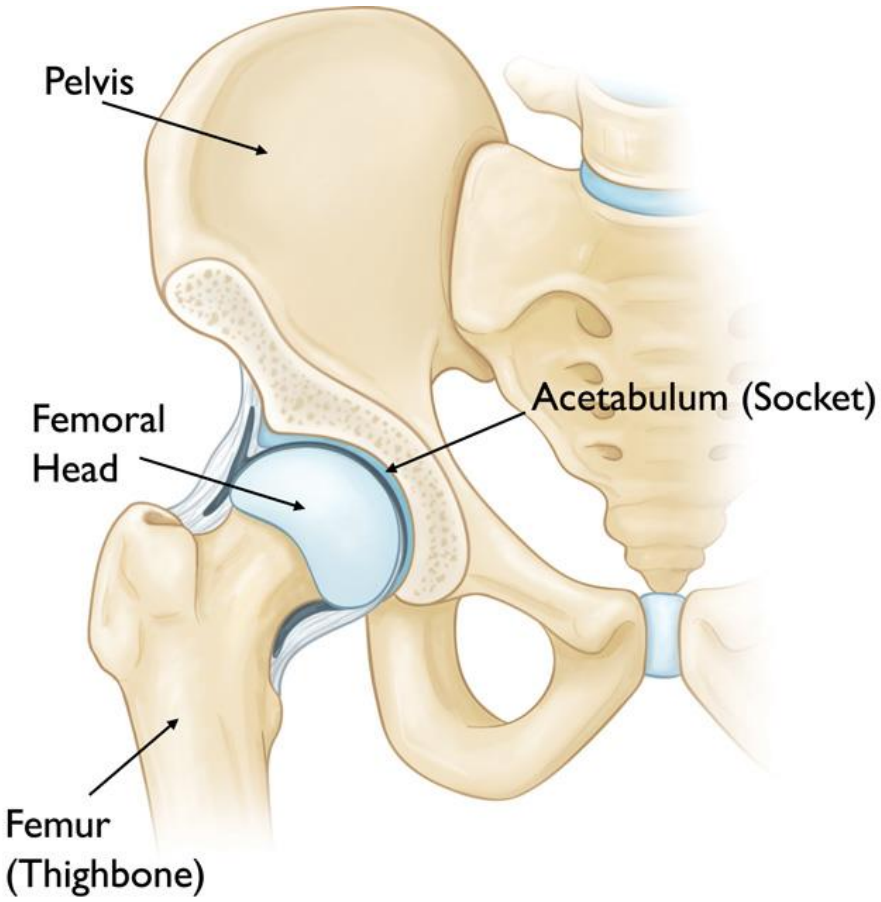

Figure 1.1 – The hip, also known as the acetabulofemoral joint, is comprised of two bony structures: the femoral head (i.e., at the proximal femur) and the acetabulum. Articular cartilage can be found on the surfaces of these bony structures and acts to facilitate the frictionless movement of the joint. Image is reproduced with permission from OrthoInfo © American Academy of Orthopaedic Surgeons. http://orthoinfo.aaos.org.

The hip joint is weight-bearing and can move with three degrees of freedom: flexion/extension, abduction/adduction and internal/external rotation. Translational displacement in the anterior-posterior and medial-lateral axes are also possible. Throughout a typical gait cycle (Figure 1.2), the load experienced at the hip takes on a double-peak profile as depicted in Figure 1.3. It has been reported that, on average, a load of roughly 2.5 times body weight is transferred through the joint during level walking (Bergmann et al., 2001). However, a high degree of variation has been shown to exist between patients in these studies.

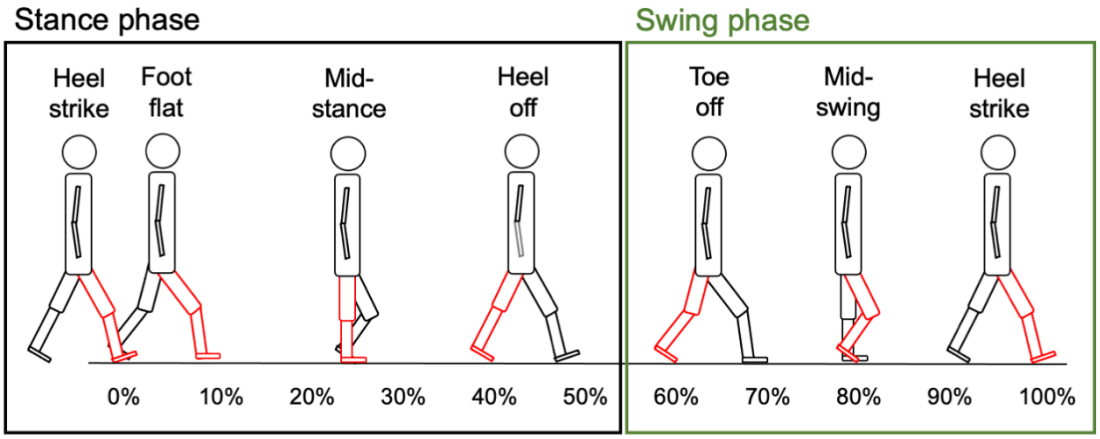

Figure 1.2 – Schematic illustrating the gait (i.e., walking) cycle, which includes a stance and swing phase. Figure produced by Author.

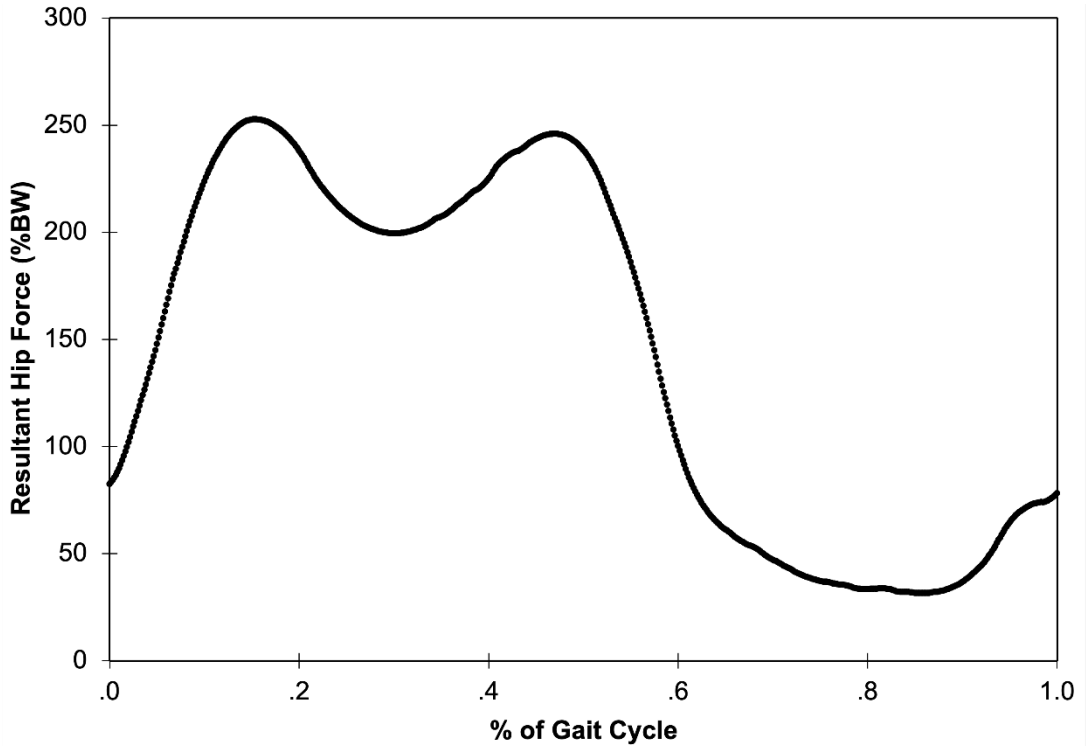

Figure 1.3 – An example of the double-peak profile which represents the resultant forces experienced at the hip during the gait cycle. Figure produced using data taken from a single patient as part of a study by Bergmann et al (2016).

1.2 – Total hip replacement

1.2.1 – Clinical need

A number of pathologies of the hip can arise, mainly due to the avascular nature of articular cartilage which does not possess inherent regenerative properties. The

cartilage is therefore susceptible to degeneration due to conditions such as osteoarthritis. Osteoarthritis is a progressive musculoskeletal disease which is predicted to affect nearly 15% of the world's population (Udgata, 2014). It is characterised by the roughening and loss of articular cartilage, ultimately leading to joint pain and stiffness. There is no cure for osteoarthritis and therefore, for patients with severe symptoms not managed by the available, yet limited, alternative therapies and lifestyle changes, it is usually recommended to replace the joint to reduce pain and improve function. Several other complications exist for which joint replacement is recommended, such as a fracture of the Neck of the Femur (NOF) or rheumatoid arthritis.

A Total Hip Replacement (THR), also known as total hip arthroplasty, is a procedure in which the natural hip is replaced with an artificial prosthesis to restore the joint's structural and functional properties following disease or trauma. During the surgery, the damaged natural hip is removed and replaced while the patient is either given general or spinal anaesthesia. It is one of the most commonly performed elective surgeries within the UK, with a large majority (nearly 90%) being performed solely for the treatment of osteoarthritis (Kärrholm et al., 2017; Australian Orthopaedic Association, 2018; National Joint Registry, 2022). The number of THRs performed annually in the UK has been steadily rising, as illustrated in Figure 1.4, due to an increasing life expectancy and incidence of obesity. However, fewer primary THRs were performed in 2020 and 2021 due to the COVID-19 pandemic.

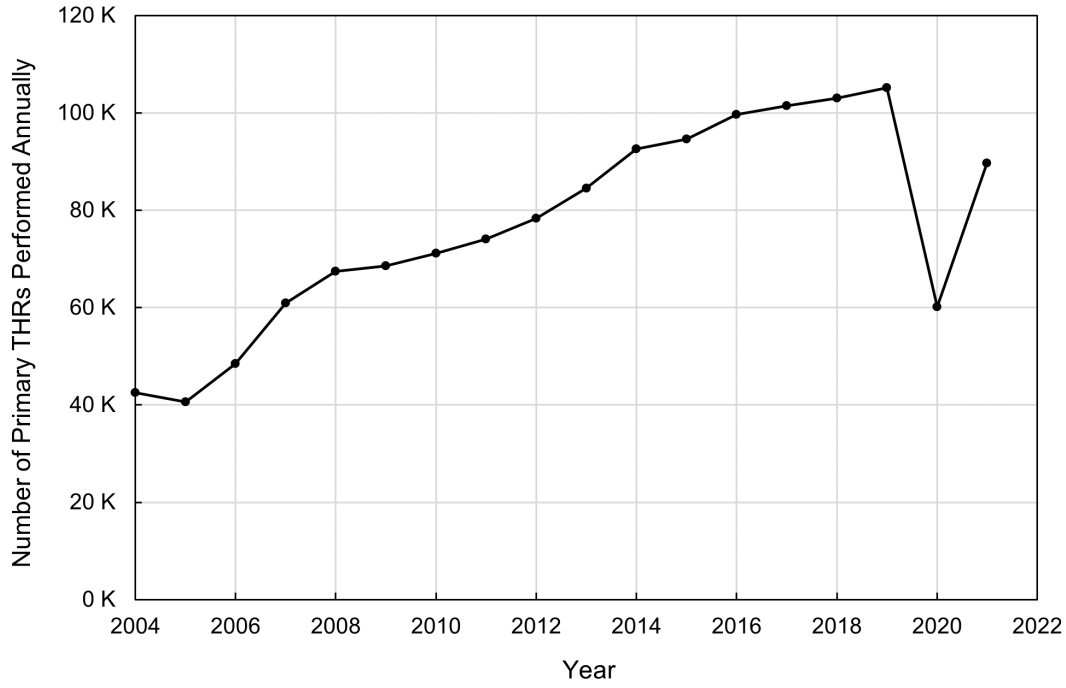

Figure 1.4 – The number of primary THRs performed annually in the UK, as reported by the National Joint Registry (2021). A drop in the number of primary THRs performed in 2020 and 2021 were observed due to the COVID-19 pandemic.

1.2.2 – Implant design

A conventional THR is comprised of femoral and acetabular components, as shown in Figure 1.5. Femoral components include the femoral stem and femoral head, which may be monobloc (i.e., manufactured as a single component) or modular (i.e., manufactured as separate components which are assembled in theatre). The majority of primary THRs performed in the UK utilise modular femoral designs which provide surgeons with a wider selection of implants to suit individual patients' anatomy and needs (National Joint Registry, 2022). The femoral stem is positioned within the shaft of the femur and fixed using cement (i.e., artificial fixation using PMMA bone cement) or cementless methods (i.e., biological fixation arising from the porous surface coating which the host's bone grows into). A femoral head lies atop of the stem and acts as one of the articulating surfaces of the joint. It can range in diameter from 22.2-mm upwards. Femoral stems are usually manufactured from a metallic alloy, whilst femoral heads can be either metallic or ceramic in composition.

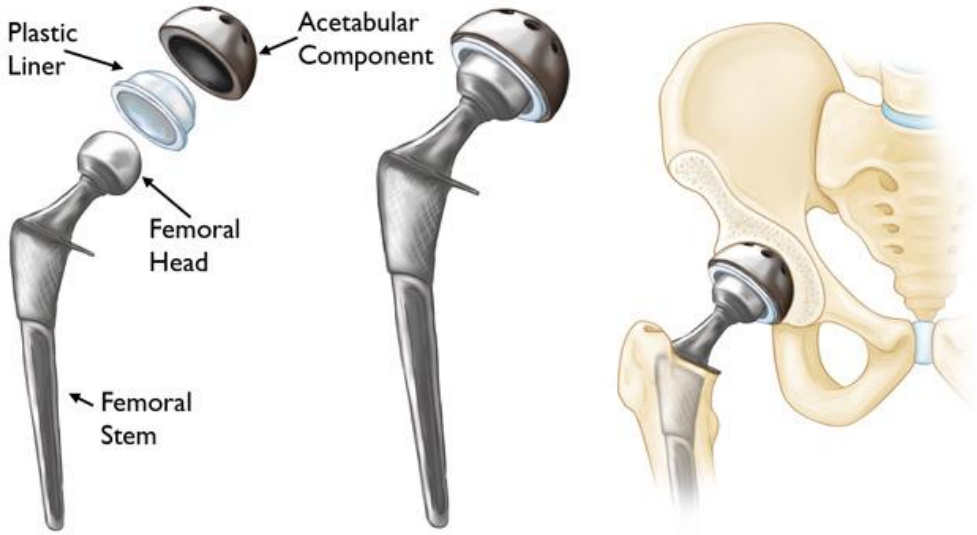

Figure 1.5 – A conventional total hip replacement. This image is reproduced with permission from OrthoInfo © American Academy of Orthopaedic Surgeons. http://orthoinfo.aaos.org.

The natural acetabulum may be replaced with either a cemented cup or a modular acetabular shell with a liner insert. Cemented cups are polyethylene components which are cemented directly into the pelvis. Alternatively, acetabular shells are metallic and are fixed with bone cement, screws, cementless methods (i.e., biological fixation due to its porous coating) or a combination of these. A liner insert is then placed within the acetabular shell, which can be manufactured from polymeric, metallic, or ceramic materials. It is either the cemented cup or the liner insert which forms the complimentary articulating surface to the femoral head.

As discussed, THR components may be manufactured from metallic (i.e., cobalt-chrome, titanium, and stainless-steel alloys), polymeric (i.e., polyethylene) or ceramic (i.e., alumina, zirconia, and alumina-zirconia composites) biomaterials. The most commonly implanted THR features a metallic femoral head which articulates against a polyethylene liner or cup, which is denoted as a Metal-on-Polyethylene (MoP) bearing. A number of other bearing surface combinations exist, including Ceramic-on-Polyethylene (CoP), Ceramic-on-Ceramic (CoC), Ceramic-on-Metal (CoM) and Metal-on-Metal (MoM).

1.2.3 – Polyethylene

In 1962, Sir John Charnley pioneered the use of Ultra-High Molecular Weight Polyethylene (UHMWPE) as an orthopaedic biomaterial which has since continued to be widely used due to its mechanical properties, resistance to wear and chemical

inertness (Kurtz, 2015a). UHMWPE will also be referred to as ‘conventional’ polyethylene in this chapter, in contrast to Crosslinked Polyethylene (XLPE) which will be further discussed in Section 1.2.3.2.

1.2.3.1 – Manufacturing and sterilisation process

The production process of polyethylene is described in Figure 1.6. All medical grade UHMWPE is produced from resin powder manufactured by Ticona under the tradenames GUR 1020 (3.5×10^6 g/amol) and GUR 1050 ($5.5\text{-}6 \times 10^6$ g/mol) (Kurtz, 2015b). The first step of the manufacturing process is consolidating the resin powder into a solid form, which is done through processes such as compression moulding or ram extrusion to create a bulk material, or direct compression moulding to create a crude, semi-finished shape (Kurtz, 2015b). Following this, a machining step is used to shape the bulk material into the final component.

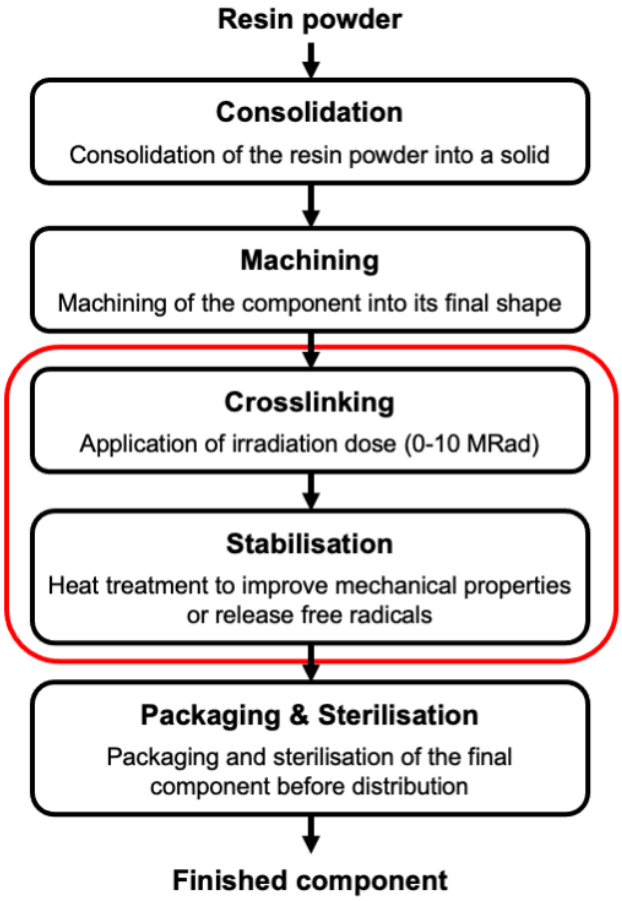

Figure 1.6 – The manufacturing process of polyethylene components for THRs begins with UHMWPE resin powder. All medical grade UHMWPE resin is produced by Ticona under the tradenames GUR 1020 and GUR 1050. The powder is first consolidated to create a solid component which may later be machined into its final shape. As an optional step (denoted in the red box), the component may be cross-linked in order to improve the polymer's wear resistance, which is followed by a stabilisation treatment (to minimise the effects of oxidation). All components are packaged and sterilised before distribution.

Various sterilisation and packaging options are available for polyethylene components. Historically, polyethylene components were sterilised with gamma irradiation (25-40 kGy dose) in gas-permeable packaging (Kurtz, 2015c). However, the irradiation process triggers a complex chemical reaction which generates macroradicals within the polymers thus subjecting the material to oxidative degradation, embrittlement and weakened mechanical properties (Muratoglu, 2009; Kurtz, 2015c). Therefore, the use of barrier packaging (i.e., non-permeable packaging filled with an inert gas) has since been adopted to minimise the effects of oxidation during shelf storage (Kurtz, 2015c).

Alternative sterilisation processes are available which do not expose the polyethylene to irradiation, including ethylene oxide and gas plasma sterilisation. Ethylene oxide sterilisation involves the diffusion of ethylene oxide, a highly toxic gas, through the polyethylene component (Kurtz, 2015c). Similarly, gas plasma sterilisation relies on the diffusion of ionised gas, such as hydrogen peroxide or peracetic acid, at low temperatures (Kurtz, 2015c). These processes do not alter the mechanical properties of the material or require the component to be stored in barrier packaging and therefore have since been widely adopted by large orthopaedic companies.

1.2.3.2 – Crosslinked polyethylene

Crosslinking is an additional manufacturing step which may improve the wear resistance of UHMWPE by exposing the polymer to ionising radiation. The degree of crosslinking is dependent on the dose of radiation applied, which is typically between 50 and 100 kGy (Muratoglu, 2009). As previously described, the irradiation process results in the formation of macroradicals which may then recombine to generate crosslinks throughout the polymer. This process increases the polymer's resistance to wear by reducing plastic deformation which occurs at the surface (Muratoglu, 2009). However, the crosslinks formed during the irradiation process adversely affect the material's mechanical properties, including the ductility, yield strength and elongation to failure (McKellop et al., 1999; Gomoll et al., 2002; Muratoglu, 2009). Additionally, the residual and uncombined macroradicals also dispose the polymer to oxidative degeneration.

A stabilisation treatment is required to remove a portion of the residual macroradicals and minimise the effects of radiation. This may be in the form of a heat treatment (i.e., annealing or remelting) or by doping the polymer with an antioxidant (e.g., vitamin E). Remelting and annealing are forms of the stabilisation process which involve heating the polyethylene to just above or just below the melting point, respectively. Remelting the polyethylene allows the macroradicals to crosslink but may adversely affect the mechanical properties due to a decrease in crystallinity (Muratoglu, 2009; Atwood et al., 2011). Annealing, on the other hand, produces XLPE which retains its mechanical properties but with a potential for residual macroradicals to be left behind thus leaving the implant prone to oxidative degeneration (Atwood et al., 2011; Manley, 2015).

1.2.4 – Mechanisms of THR component damage

Polyethylene components (i.e., acetabular liners, cemented cups) become worn and damaged through the course of an implant's lifespan. This is due to the repetitive loading and displacement conditions experienced at the hip, along with other factors such as the introduction of particulate debris into the joint space. This can ultimately lead to the penetration of the femoral head into the liner and/or the generation of surface damage. Seven modes of UHMWPE damage have previously been described in a study by Hood, Wright, and Burstein (1983), which includes scratching, pitting, embedded debris, deformation, burnishing, abrasion, and delamination as shown in Figure 1.7.

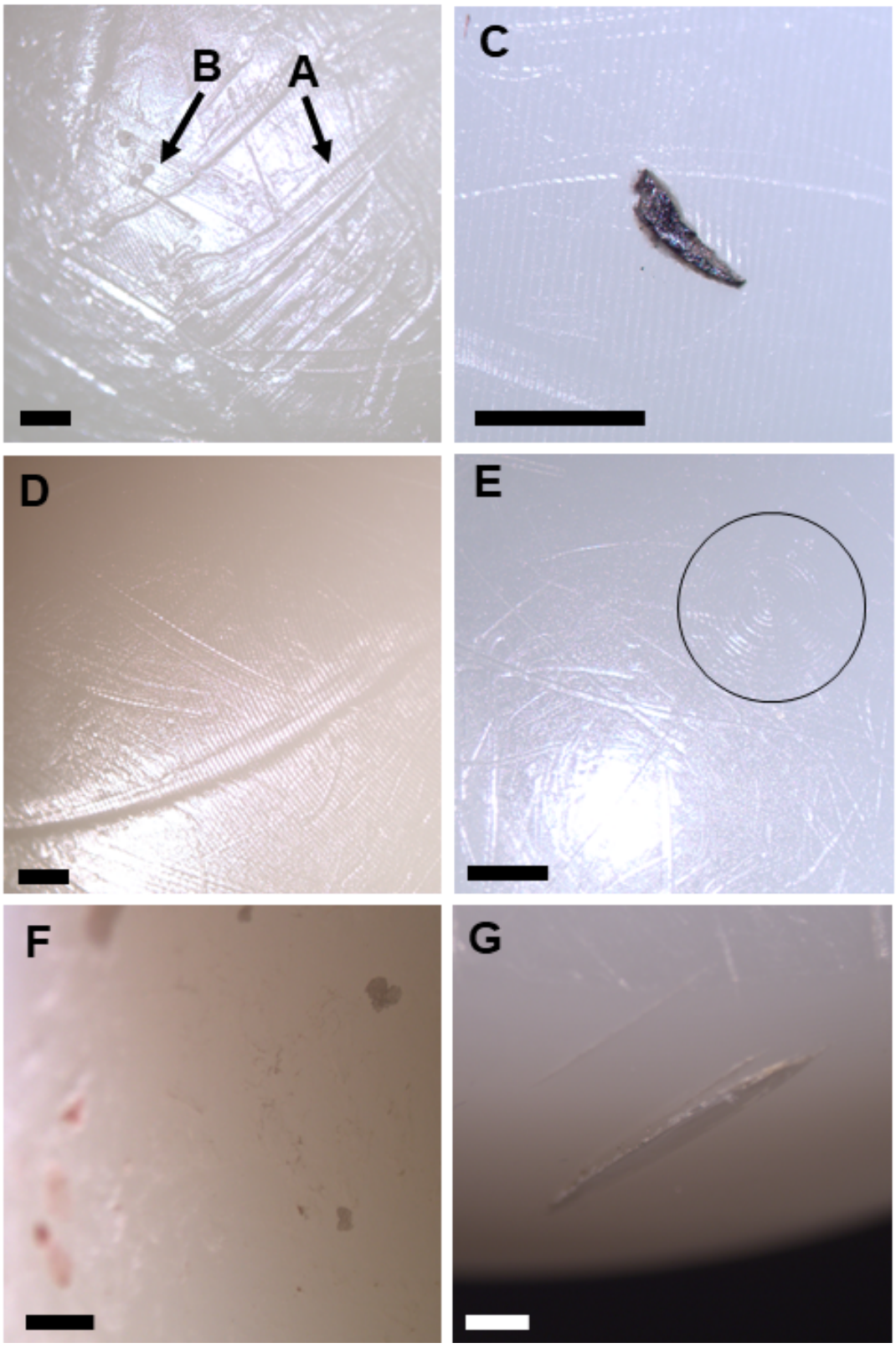

Figure 1.7 – Damage mechanisms identified on the surfaces of polyethylene orthopaedic components, which includes scratching (A), pitting (B), embedded debris (C), deformation (D), burnishing (E), abrasion (F) and delamination (G). All scale bars represent a unit length of 1 mm.

The penetration of the femoral head into the liner can occur over time due to several mechanisms, which include creep (i.e., early plastic flow) or wear (i.e., material loss). Creep is responsible for the initial deformation of the polyethylene which occurs predominantly within the first six months post-implantation, known as the 'bedding-in' period (Glyn-Jones et al., 2008). A study by Glyn-Jones et al reported the mean penetration due to creep to be 0.27- and 0.26-mm for conventional and highly crosslinked polyethylene liners, respectively (Glyn-Jones et al., 2008). Polyethylene wear, on the other hand, is caused by a loss of material which therefore generates wear debris. Polyethylene wear debris is created due to an interaction of surface asperities at the articulating interface. As the polyethylene articulates against a hard surface (i.e., the femoral head), macroscopic asperities on the polymer surface (e.g., one to 10 μm in height) deform and create localised stress concentrations. This leads to fatigue failure of the material following cyclic loading and ultimately generates polyethylene wear debris (Fisher, 1994). Any microscopic asperities on the hard surface may also generate smaller-scale polyethylene wear debris through an abrasive mechanism (Fisher, 1994). This wear debris within the joint triggers a response from local macrophages which causes a net bone resorption during a process known as osteolysis. This can cause aseptic loosening of the implant, which continues to be the most common reason for long-term THR failure (National Joint Registry, 2022), although improved materials (e.g., XLPE, see Section 1.2.3.2) which provide increased resistance to wear have minimised this risk in new-generation devices.

For example, the use of XLPE has been shown to significantly decrease the linear penetration rate of the femoral head into the liner and therefore polyethylene wear is no longer a contemporary failure mechanism of modern THR devices (Rames et al., 2019; Moon et al., 2021). A systematic review by Kurtz et al reported the mean penetration rate for conventional and crosslinked polyethylene to be 0.137 and 0.042 mm/year, respectively (Kurtz et al., 2011). Other factors known to affect the wear rate of polyethylene include a patient's activity levels (i.e. implant sliding distance), weight (i.e. applied load) and surface roughnesses at the articulating interfaces (Fisher and Dowson, 1991; Schmalzried et al., 2000). According to a review by Dumbleton et al, a linear wear rate which is greater than 0.1 mm/year is indicative of osteolysis (Dumbleton et al., 2002). This is supported by a study which analysed 48 primary THRs at a minimum of 10 years follow-up, which reported no findings of osteolysis for any components with a wear rate less than 0.1 mm/year (Dowd et al., 2000).

THR components constructed from hard materials, such as metallics or ceramics, are also at risk of becoming damaged. Metallic surfaces are particularly disposed to damage when third body debris, such as bone cement or delaminated porous coating, enters the joint space. This elicits an abrasive mechanism which creates fine surface scratches with heaped-up edges (Jasty et al., 1994). This has been observed on both stainless steel (Isaac et al., 1986) and CoCr (Jasty et al., 1994) femoral heads. Ceramics are stronger than metals and generally considered to be scratch resistant. However, the presence of metal transfer patches can affect the tribology of the joint thus increasing surface roughness and encouraging wear of the polyethylene counterface (Eberhardt et al., 2009; Merola et al., 2016). Ceramics also carry a small risk of catastrophic fracture although the risk of this has been significantly reduced with improved manufacturing methods and materials (e.g., composite ceramics).

1.3 – Revision total hip replacement

Despite the successes of conventional THRs, approximately 3% of all primary THRs recorded in the National Joint Registry had an associated revision surgery (National Joint Registry, 2022). The purpose of a revision surgery is to replace a failed implant, whether it be a single component or the entire prosthesis. Revisions are complex surgical procedures which involve increased operation time, blood loss and length of hospital stay when compared to primary THRs (Barrack et al., 1999). The most common reasons for a primary (i.e., first time) revision in the UK include aseptic loosening, joint instability, Adverse Reaction to Particulate Debris (ARPD), periprosthetic fracture, infection and pain as shown in Table 1.1.

Table 1.1 – The most common reasons for revision of a primary THR in the UK, as reported by the 19th Annual National Joint Registry (2021). It should be noted that multiple causes may be reported for a single revision. Additionally, ARPD is likely underestimated due to changes in the data collection protocol.

Cause	n	% of all revisions
All revisions	**40,387**	**100%**
Aseptic loosening	9,962	25%
Instability	7,028	17%
Periprosthetic fracture	6,355	16%
Infection	6,159	15%
ARPD	5,991	15%
Pain	5,019	12%

1.3.1 – Dislocation

Dislocation is defined as a mechanical failure in which the femoral head disassociates from the socket and moves in an anterior or, more commonly, a posterior direction (Zahar et al., 2013). Dislocation has been reported as the most common indication for THR revision within the first two years (Kärrholm et al., 2017; National Joint Registry, 2022). In addition, the prevalence of hip dislocation is likely to be underestimated as joint registries only report dislocations which result in a THR revision surgery but exclude those treated with closed reductions (Devane et al., 2012).

The management of joint instability remains one of the most complex and challenging complications associated with THRs, particularly for at-risk patients. Instability-related revision procedures often yield poor outcomes, with re-revision rates reported as great as 13.7% (Kärrholm et al., 2017). These types of revisions are also known to come at a great economic cost, with one study showing a 48% increase in expenses when compared to a primary THR (Sanchez-Sotelo et al., 2006).

The cause of implant instability and dislocation is multifactorial. Certain patient populations are at an increased risk of dislocation, including those with a neuromuscular condition, spinal fusion, or abductor deficiency. Neuromuscular conditions (e.g., cerebral palsy), for example, cause muscular imbalances which may result in subluxation or dislocation of the hip if it is abnormally loaded. Spinal fusions cause a reduction in pelvic mobility, leaving patients vulnerable to dislocation

particularly when moving from a standing to seated position (Buckland et al., 2017). The hip is also susceptible to dislocation in the presence of an abductor deficiency, as this causes inadequate soft tissue tension which is critical in stabilising the joint. Abductor deficiencies may be a result of patient anatomy (i.e., natural laxity of tissues), THR implant positioning or APRD-associated soft tissue necrosis. Additionally, hip dislocation may be caused by implant- or surgical-related mechanisms such as impingement, component malpositioning or wear (Wera et al., 2012).

Impingement is a recognised mechanism which may result in implant dislocation, alongside other complications such as pain and increased polyethylene wear (Malik et al., 2007). Prosthetic impingement occurs when the femoral neck abuts against the acetabular liner at extreme Ranges of Motion (ROM). This causes the bearing's centre of rotation to shift from the centre of the femoral head to the impingement site (i.e., at the liner rim) thus allowing the femoral head to 'lever out' and subluxate and/or dislocate (Kluess et al., 2007). Anterior impingement (i.e., during a sitting or squat position) results in posterior dislocation of the head, which is the most common mode of hip dislocation. The incidence of impingement is influenced by various factors, such as the implant's head-to-neck ratio (i.e., the difference in the radius of the head and neck) as shown in Figure 1.8. As the head-to-neck ratio is increased (i.e., by increasing the head size and/or reducing the neck thickness), the ROM is increased thus decreasing the risk of impingement. Other factors, such as the liner geometry and component positioning, may also influence the incidence of impingement (Malik et al., 2007). A study by Waddell et al reported evidence of impingement among 77% of analysed retrieved liners from conventional THRs (Waddell et al., 2019).

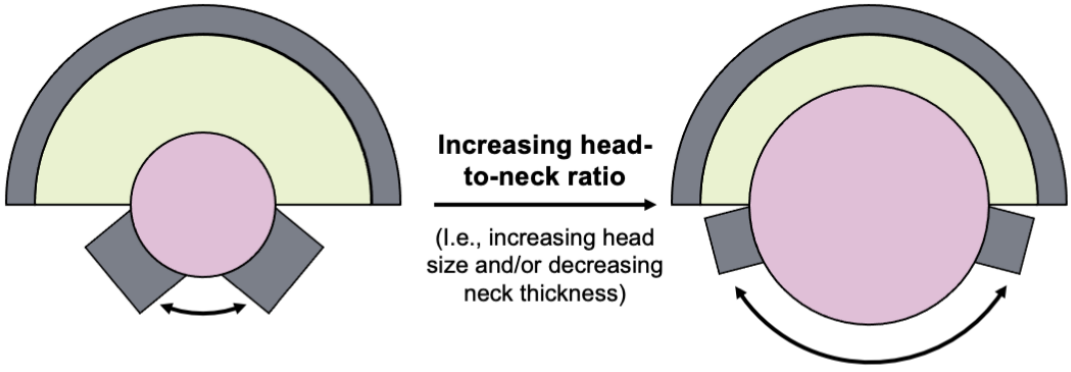

Figure 1.8 – The influence of head-to-neck ratio on ROM before impingement. Image adapted from a concept by Malik et al (Malik et al., 2007).

1.4 – Dual mobility total hip replacement

1.4.1 – Overview and nomenclature

Dual Mobility (DM) THRs, also known as unconstrained tripolar bearings, were introduced in the 1970s to overcome the challenges associated with joint instability and recurrent dislocation. These bearings consist of a femoral head which articulates within an unconstrained and mobile polyethylene liner (Figure 1.9) thus creating two articulating surfaces: an inner articulation between the femoral head and liner, and an outer articulation between the liner and acetabular component. At extreme ranges of motion, the femoral neck abuts the liner thus activating the outer articulation (Figure 1.10) and allowing for an additional 10° to 15° of motion (Darrith et al., 2018). In theory, the two articulating surfaces should not move simultaneously (Darrith et al., 2018) however the in-vivo kinematic function of DM polyethylene liners are not well understood.

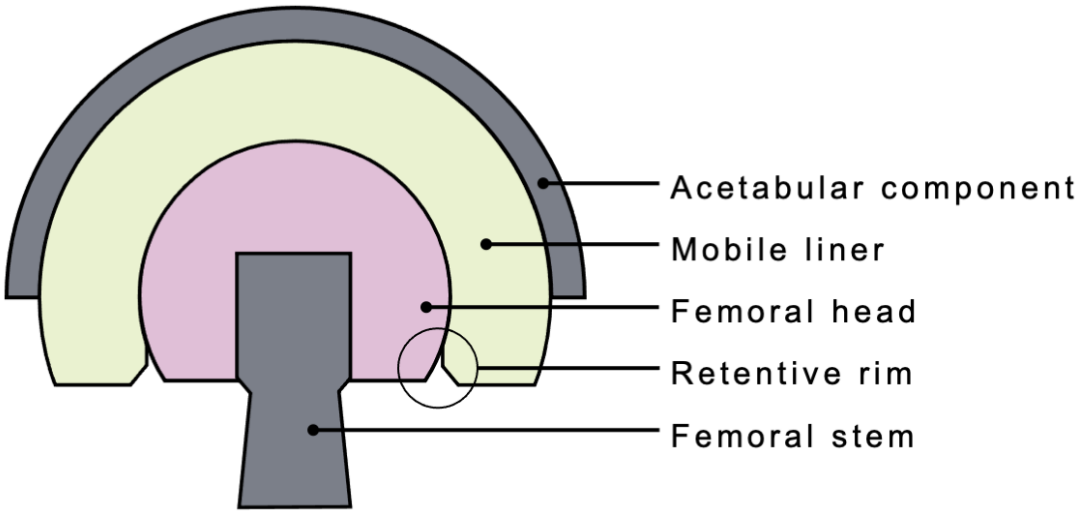

Figure 1.9 – Schematic illustrating a dual mobility bearing, which consists of four key components: a femoral stem, femoral head, mobile polyethylene liner and acetabular component. The femoral head is encapsulated within the mobile liner due to a characteristic feature of the mobile liner known as the retentive rim, which has a diameter smaller than that of the femoral head.

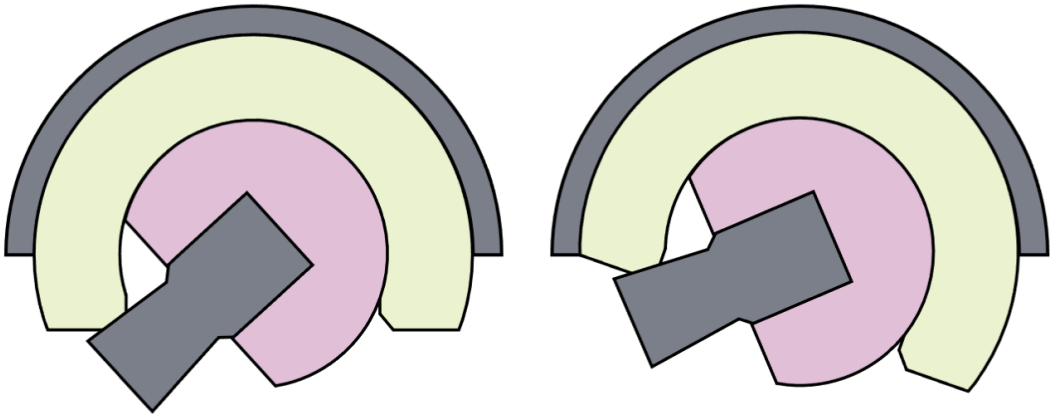

Figure 1.10 – For a dual mobility bearing at extreme ranges of motion, the femoral neck abuts against the inner rim of the mobile liner (left) and thus activates the outer articulation (right). This allows for an additional 10° to 15° degrees of motion (Darrith et al., 2018).

Naming conventions for DM bearings vary in the literature and therefore it is important to clarify the nomenclature in which DM components will be referred to in this thesis. These terms are defined in Figure 1.9. In summary, the ‘femoral head’ is defined as the component affixed to the femoral stem and is identical to those found in conventional or unipolar THRs. These can be made of both metallic and ceramic materials. The ‘liner’ refers to the unconstrained polyethylene component which assembles onto the femoral head. Both the internal (concave) and external (convex) surfaces of a DM liner act as articulating sites for DM bearings, making them differ from conventional liners in both their design and function. In addition, the opening of the mobile liner is referred to as the ‘retentive bore,’ which is a feature unique to DM THRs. The diameter of the retentive bore is less than that of the femoral head, thus causing the femoral head to become encapsulated within the liner through a snap-fit assembly mechanism. This means the head must be inserted into the liner intraoperatively through the use of a vice clamp. One study reports cracking at the retentive rim of 35% of DM liners, following axial insertion and extraction of the femoral head (Malatray et al., 2017) however these effects are not well understood. Finally, the acetabular component refers to the metallic component(s) affixed into the acetabulum. In the context of DM bearings, this can refer to either a monobloc acetabular shell or a modular acetabular shell with a metal insert.

DM constructs consist of three articulating interfaces. The first, which will be referred to as the internal articulating site, is the interface between the femoral head and liner.

The outer articulation refers to the interface between the liner and acetabular component. Finally, the interface between the femoral neck and retentive bore is often referred to as the ‘third’ bearing surface. This interface is particularly important, as impingement at this site is thought to cause activation of the outer articulation.

Two predominant material combinations exist for DM bearings. DM implants with a metal head are referred to as a Metal-on-Polyethylene-on-Metal (MoPoM) bearing, whilst implants with a ceramic head are referred to as a Ceramic-on-Polyethylene-on-Metal (CoPoM) bearing. Various implant sizes are available for DM constructs. These are often described by the outer diameter of the acetabular component in relation to the diameter of the femoral head (e.g., 47/22-mm or 69/28-mm). For example, a 69/28-mm DM bearing consists of a 28-mm diameter femoral head and an acetabular component which has a 69-mm outer diameter.

1.4.2 – Implant design

The DM concept was developed in the late 1970s by Professor Gilles Bousquet. The first DM THR to make it to market (Novae® Tripod, Serf) consisted of a monobloc, hemispherical, stainless-steel shell coated with porous plasma sprayed alumina, which was fixed using two taper pegs and one screw (Philippot et al., 2009; Cuthbert et al., 2019). The liner was five eighths of a sphere and constructed from UHMWPE (Philippot et al., 2009; Cuthbert et al., 2019). The femoral head was metallic and 22.2-mm in diameter, and all components were concentric (Philippot et al., 2009; Cuthbert et al., 2019).

Since the late 1990s, a number of developments have led to a new generation of DM bearings (Laura, H. Hothi, et al., 2017). For example, femoral head sizes have increased to 28-mm and thinner femoral necks are being employed to increase the head-to-neck ratio thus increasing stability. New-generation acetabular shells are available as both monobloc and modular components, and feature hemispherical, sub-hemispherical or anatomical designs. For reference, hemispherical shells span 180° whilst sub-hemispherical shells typically span between 152° and 166° (Morlock et al., 2011). Sub-hemispherical shells allow for a greater range of motion but increase the likelihood of joint dislocation or edge loading (Morlock et al., 2011; Sandiford and Skinner, 2014). Alternatively, anatomical designs incorporate a cut-out at the rim of the shell in order to avoid irritation of the psoas tendon (Laura, H. Hothi, et al., 2017). In order to improve the bio-integration of the shell, hydroxyapatite and

titanium plasma spray coatings have replaced the previously used alumina coating (Philippot et al., 2013).

With regards to the liner, the molecular density of the polyethylene has been increased and the geometry of the liner's internal rim has been modified (e.g., inclusion of a chamfer) (Philippot et al., 2013). This modification has allowed for an increased retention of the femoral head and a greater range of motion before impingement occurs, thus reducing wear at the rim (Philippot et al., 2013; Laura, H. Hothi, et al., 2017). In addition, some new-generation DM liners utilised cross-linked polyethylene for increased wear performance. However, mechanical properties such as fatigue resistance and elasticity are affected by the crosslinking process and thus it is speculated that this may make the mobile liner more prone to fracture (Gaudin et al., 2017). One study reported no significant difference in the incidence of cracking at the retentive bore between DM liners made from UHMWPE and XLPE (Malatray et al., 2017) although further studies are required to better understand this relationship.

Some new-generation DM bearings also feature eccentric designs. This means the femoral head and liner do not share the same centre of rotation, as illustrated in Figure 1.11 (Fabry, Woernle, et al., 2014). These constructs benefit from a self-centering mechanism under force application which further reduces the risk of joint dislocation (Fabry, Woernle, et al., 2014).

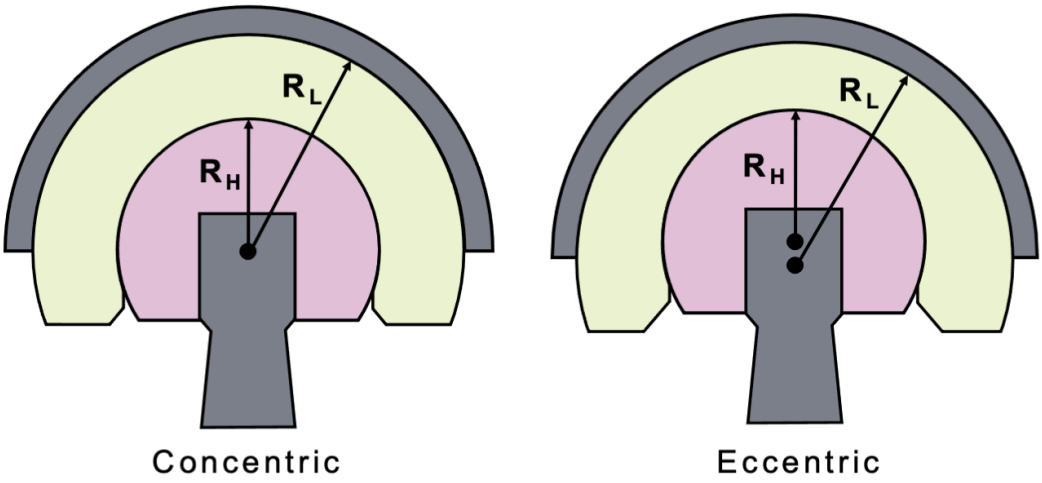

Figure 1.11 – Concentric dual mobility bearings (left) have a shared centre of rotation for the femoral head (R_H) and mobile liner (R_L). On the other hand, eccentric dual mobility systems (right) do not have a shared centre of rotation which creates an inherent self-centering mechanism under force application.

1.4.3 – Clinical evidence to date

A number of DM bearings have been introduced to the market by large orthopaedic companies such as DePuy Synthes, Corin Group, Smith & Nephew and Stryker (Laura, H. Hothi, et al., 2017). In the UK, the use of DM bearings within primary THR has been steadily rising in both elective and trauma settings and has since become more common than hip resurfacing (National Joint Registry, 2022). In addition, DM constructs were used in approximately 10% of elective primary and 20% of revision THRs in the United States in 2020 (American Joint Replacement Registry, 2022). Furthermore, nearly 30% of revisions secondary to dislocation or hip instability were treated with a DM prosthesis (American Joint Replacement Registry, 2022).

Due to their enhanced stability, these bearings have also been successfully used to treat high-risk patients such as those with neuromuscular conditions (Sanders et al., 2013), abductor deficiencies (Ozden et al., 2018; Klemt et al., 2020), spinal fusions (Mudrick et al., 2015; Nessler et al., 2020) and skeletal cancers (Philippeau et al., 2010; Zoccali et al., 2017). Additionally, DM THRs have been successfully used to treat fractures of the neck of the femur (NOF) (Adam et al., 2012; Canton et al., 2019). In fact, the use of DM bearings in primary THR secondary to a fractured NOF is steadily increasing in the UK (Figure 1.12). By 2021, DMs were used in roughly 9% of all fractured NOF-related primary THRs (National Joint Registry, 2022).

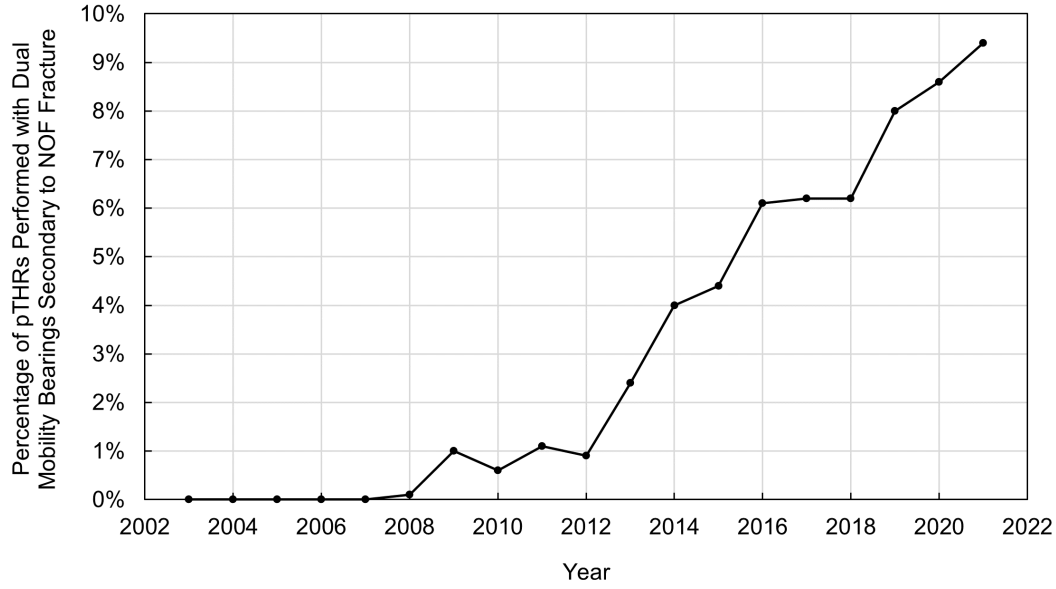

Figure 1.12 – Use of DM bearings in the UK for primary THR secondary to NOF fracture. Graph produced from data reported in the 19th Annual National Joint Registry.

So far, DM bearings have yielded promising results. A large majority of the published DM literature reports survivorship data which has been summarised in a systematic review by Darrith, Courtney and Della Valle (2018). The survivorship of DM bearings has been reported as 98.0% for primary THR at a mean of 8.5 years and 96.6% for revision THR at a mean of 5.4 years (Darrith et al., 2018). However, early joint registry data suggests that DM bearings have a higher rate of revision within the first five years when compared against conventional unipolar designs (American Academy of Orthopaedic Surgeons, 2019; National Joint Registry, 2022). However, small sample sizes make it challenging to draw any conclusions at present although this trend should continue to be closely monitored.

DM bearings have shown to significantly decrease the incidence of impingement when compared with conventional bearings (Scott et al., 2018). In addition, it has been suggested that DM bearings provide a similar ROM to large diameter (e.g. 36-mm) conventional THRs (Klingenstein et al., 2013). For these reasons, it is no surprise that DM bearings have shown enhanced joint stability and decreased dislocation rates in both primary and revision THR (Combes et al., 2013; Prudhon et al., 2013; Darrith et al., 2018; Reina et al., 2019). A systematic review by Reina et al (2019) reported a markedly lower dislocation rate for DM bearings in comparison to conventional THRs. For example, the study reported a 6.8% and 0.9% risk of dislocation for conventional and DM bearings, respectively, following primary THR ($p<0.001$, mean 7.6 years follow-up). For revision THR, the associated risks were reported to be 7.1% and 2.2%, respectively ($p<0.01$, mean 4.1 years follow-up).

1.4.4 – Joint mechanics

The stability of DM THRs arises from a combination of the fundamental principles of both the Charnley and McKee-Farrar prostheses. Charnley's low friction arthroplasty relied on maximising the difference in outer diameters between the liner and femoral head to decrease the joint's frictional torque and thus the wear of the polyethylene. DM bearings incorporate this principle at the inner articulation whereby a small femoral head (e.g., 22- or 28-mm diameter) articulates against a large polyethylene liner. However, by mobilising the liner, the effective head size of the bearing increases by at least 80% when compared to conventional bearings (Scott et al., 2018). Therefore, DM constructs also incorporate the principles described by McKee-Farrar at the outer articulation. The McKee-Farrar principle relies on the use of a large head size and head-to-neck ratio (i.e., the ratio of the femoral head radius to the femoral

neck radius). This improves stability through two mechanisms: increasing the jump distance (i.e., the distance in which the head must move to dislocate from the joint) and decreasing the incidence of impingement.

Indeed, a number of studies in the literature have confirmed the theoretical benefits of DM THRs. It has been reported that these bearings have a significantly lower incidence of impingement (Scott et al., 2018) and increased posterior jump distance (Heffernan et al., 2014) in comparison to conventional bearings, suggesting that they provide improved stability. Additionally, a computational study by Klingstein et al (2013) reported the ROM of DM bearings to be superior to conventional THRs with a 28-mm femoral head. The ROM of these DM THRs has been reported to be '120° in flexion, 10° in extension, 30° in adduction, 45° in abduction, 25° in internal rotation and 25° in external rotation' (Agarwala et al., 2020).

It is clear that the mechanisms which underpin the improved stability of DM implants are well understood. However, limited studies have assessed the joint mechanics of these constructs particularly in relation to the motion of the unconstrained polyethylene liner. One study assessed the in-vivo motion of DM liners through static and dynamic radiostereometry (Jørgensen et al., 2022). The study reported that 75% of the liners were able to move one year post-operatively and provided some evidence to suggest that DM liner motion may occur without contact between the femoral neck and liner (i.e., the 'third' bearing site). However, the study was limited to a total of 16 patients and was only able to assess dynamic liner motion through one, non-weight bearing motion.

Cadaveric models have also been used to assess the function of DM THRs, particularly in relation to the role of the surrounding soft tissues. For example, one study used cadaveric models to assess how various THR designs, including conventional, DM and hip resurfacings, influenced the function of the hip capsule (Logishetty et al., 2019). The hip capsule is made up of several ligaments which provides a stabilising mechanism to the natural hip as it wraps around the joint and becomes taut. This mechanism was shown to be lost following the implantation of a conventional THR, which has a femoral head smaller than that of the native hip thus allowing the capsule to become slack. This is especially detrimental to those prone to dislocation. Conversely, hip resurfacing kept this mechanism intact although these are not always a suitable option for those requiring a THR. The study showed that DM bearings, instead, lie somewhere in the middle. The stability mechanism from the

hip capsule was shown to be partially restored with these bearings, dependent on the position of the mobile liner. A separate study attempted to visualise the relative motions of the DM liner by using cadaveric models, which showed anterior soft tissue impingement at low flexion angles as the femur moved from a flexed to extended position (Nebergall et al., 2016). The study also analysed retrieved DM liners (see Section 1.5.1) and reported circumferential deformation at the rim and chamfer, suggesting that the liner may rotate within the acetabular component. This hypothesis was supported by an alternative retrieval analysis which observed similar circumferential wear stripes on all retrieved liners which presented with no additional pathology (Geringer et al., 2011).

Although these studies provide useful information about the possible in-vivo mechanics and soft tissue interactions of DM bearings, they are limited in their numbers and often rely on small samples sizes or cadaveric tissue which may present with varying levels of tissue laxity and thus alter the results of the analysis. Further studies are required to better understand the in-vivo mechanics of these implants, particularly in relation to the motions of the unconstrained liner. In-vitro methods to assess these functions under a variety of conditions (e.g., in a hip joint simulator) would be advantageous but have not been identified in the literature at present.

1.4.5 – Failure mechanisms

Despite their success, complications unique to DM bearings such as accelerated polyethylene wear (due to the multiple wear surfaces) and a failure mechanism known as Intraprosthetic Dislocation (IPD) remain a concern. IPD is the dislocation of the femoral head from the mobile liner which occurs due to a progressive degeneration of the liner's retentive bore (Figure 1.13). This complication is serious and can result in metal-on-metal articulation between the femoral head and acetabular shell, thus producing metallic wear debris and requiring revision surgery. IPD should not be confused with Extra-Articular Dislocation (EAD), whereby the adjoined femoral head and liner dislocates from the acetabular shell (Figure 1.14). The mechanisms which cause IPD may be categorised into three types (Philippot et al., 2013). Type I is known as 'pure IPD' whereby accelerated polyethylene wear leads to a degradation of the retentive bore and thus a dislocation of the femoral head (Philippot et al., 2013). Type II IPD occurs in conjunction with a seizing of the mobile liner due to arthrofibrosis however the order in which these events occur remains unclear (Philippot et al., 2013). Type III IPD occurs secondary to cup loosening (Philippot et al., 2013).

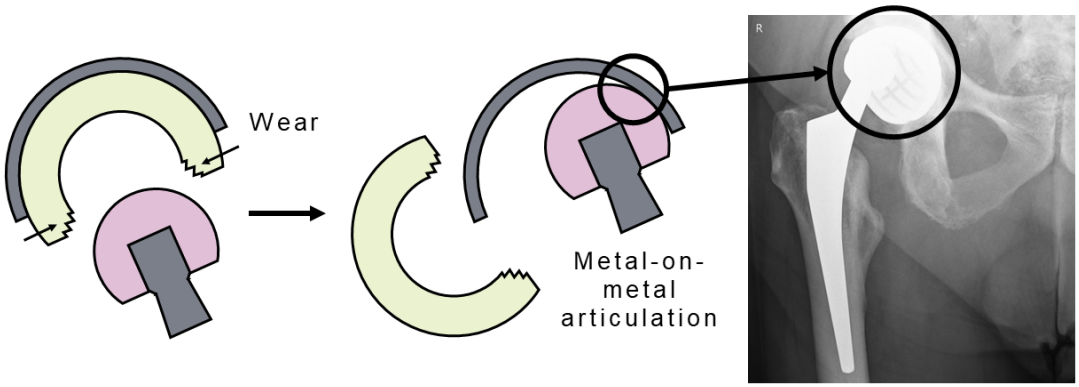

Figure 1.13 – Schematic illustrating intraprosthetic dislocation (IPD), whereby the femoral head dislocates from the mobile liner following degradation of the liner's retentive rim. If the femoral head is metallic, this can result in metal-on-metal articulation of the femoral head and liner. Image adapted from Langlois et al (2014).

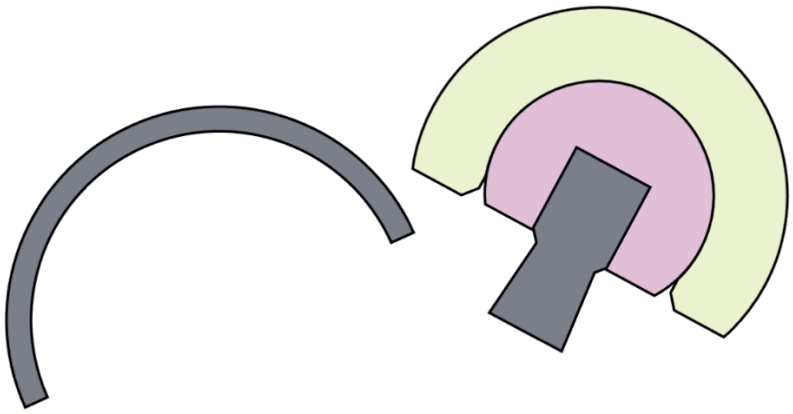

Figure 1.14 – Schematic illustrating extra-articular dislocation of a DM bearing, whereby the conjoined head and liner dislocate from the acetabular shell.

The incidence of IPD among first generation bearings has been reported as high as 4% (Philippot et al., 2013; Darrith et al., 2018). Second generation DM designs have aimed to reduce the risk of IPD by altering the liner geometry (i.e. adding chamfers to decrease contact stresses at the retentive rim), using larger femoral heads, increasing the density of or cross-linking the polyethylene and adding surface coatings onto the outer surface of the acetabular shell (i.e. to improve biointegration and reduce the risk of cup loosening) (Philippot et al., 2013). The literature suggests that these design alterations have eliminated the occurrence of IPD however this could be due to a lack of long-term follow-up (Vielpeau et al., 2011; Darrith et al., 2018; Neri et al., 2019). IPD is a complication which presents itself in the long term

following progressive polyethylene wear and thus it is unclear whether the new-generation bearings have indeed decreased the incidence of IPD or instead lengthened the timeframe in which it occurs (Neri et al., 2019). Studies with longer follow-ups are required to investigate this.

Despite concerns relating to IPD and accelerated polyethylene wear, a limited number of studies have assessed the performance of DM liners. The wear rates of conventional and DM bearings have been directly compared through in-vitro simulator testing, and no significant differences were noted under standard gait conditions (Saikko and Shen, 2010; Loving et al., 2015; Gaudin et al., 2017). Additionally, in-vitro studies have suggested that the wear performance of DM bearings may not be significantly impacted by adverse conditions such as high cup inclination angle (Saikko and Shen, 2010; Loving et al., 2015) or dynamic separation (Netter et al., 2014). Although these studies have yielded promising results, small sample sizes were used, and further investigation is required to comprehensively understand the performance of DM bearings under a variety of physiological conditions.

Overall, there is a notable lack of prospective, high quality and long-term studies relating to DM bearings. A large majority of DM-based research is retrospective, with few studies analysing retrievals (see Section 1.5.1) or experimentally testing components in-vitro. This could be due to a shortfall in available and suitable methodologies. The geometric and functional differences of DM bearings mean these types of implants cannot be easily or sufficiently evaluated with current methodologies which have been developed for conventional THRs. Therefore, there is an unmet need for appropriate experimental testing and characterisation methodologies to be developed to adequately assess the function and failure mechanisms of DM bearings.

1.5 – Methods to assess the performance and failure of THRs

It is important to understand the mechanical function and failure modes of THR components so that the implant design and thus long-term performance may be improved. This section will discuss three common approaches for assessing the performance of hip implants, including the analysis of retrieved (i.e., ex-vivo) components, in-vitro hip simulation and computational analyses.

1.5.1 – Analysis of retrieved implants

Retrievals, also known as explants, are orthopaedic implants which have been removed from a patient after a period of service time in-vivo. Implants may be removed for several reasons, such as post-operative infection, mechanical failure of the implant or patient death. Retrieval analyses allow for clinically relevant implant damage, which was generated as a result of the complex displacement and loading conditions at the hip, to be characterised. In the presence of available patient information (e.g., gender, age, BMI) and/or medical imaging (e.g., x-rays, CT), this data may be further stratified according to pertinent patient and/or surgical factors.

Explanted components may be used to support theories about the mechanisms responsible for the healthy and effective functioning of THRs in-vivo. This was the case in a study by Engh et al which analysed histological samples taken from retrieved porous-coated femoral stems (Engh et al., 1987). The study assessed the mechanism of fixation for each stem and was able to show that biological fixation by bone ingrowth is encouraged with a tight press fit of the stem into the femoral shaft. In a similar manner, retrievals can provide a wealth of information about the incidence, severity and motivating mechanisms behind different modes of component failure such as impingement (Yamaguchi et al., 2000; Shon et al., 2005) or surface damage and wear (Isaac et al., 1986; Jasty et al., 1994; Tipper et al., 2000). A limited number of studies have inspected retrieved DM components, which may be due to their limited availability. Most commonly, these studies assess DM liners for evidence of damage (D'Apuzzo et al., 2016) or impingement (Adam et al., 2014; Nebergall et al., 2016; Laura, H.S. Hothi, et al., 2017; Scott et al., 2018). Surface measurements have also been taken of retrieved DM liners using a coordinate measuring machine (Adam et al., 2014; D'Apuzzo et al., 2016), microCT scanner (Laura, H.S. Hothi, et al., 2017) or Talyrond 365 (Laura, H.S. Hothi, et al., 2017). The findings from these analyses will be further explored in Section 1.6.

Despite the benefits of retrieval analyses, a number of limitations should be acknowledged in relation to these studies. No pre-service information (e.g., as-manufactured geometry or weight) is available for these types of components and thus only the end point conditions may be assessed. In addition, patient factors such as pre-existing comorbidities, activity levels, reason for revision and BMI may differ amongst a collection of samples. These factors can influence the performance and longevity of the implant, although this data is not always available during retrieval analyses. The availability of supplemental information can vary, as does the quality

of associated medical images. Finally, explants may become damaged as a result of the retrievals process (e.g., contact with surgical instruments or in transit) thus biasing the degree of damage observed.

1.5.2 – In-vitro hip simulation

Hip simulators are tuneable machines which approximate physiological displacement and loading conditions to facilitate the pre-clinical testing and quality control of THRs or support clinical findings. These machines can provide accelerated wear data by simulating extreme conditions (Affatato et al., 2012). This allows researchers to gain an understanding of the wear and tribological processes taking place within the bearing. Hip simulators were first introduced in the 1960s in order to facilitate Charnley's laboratory studies (Smith and Joyce, 2017). Since then, a variety of hip simulators have been developed which differ according to factors such as the number of available stations (e.g., single station or multi-station), degrees of freedom (e.g., biaxial or triaxial) and component orientation (e.g., inverted or anatomical).

To generate clinically relevant data, simulators should run with conditions which are as close to physiological as possible. Idealised standard gait conditions of the hip are specified in ISO 14242-1 for hip simulation studies. It is recommended that implants are subjected to a double-peak axial loading profile and idealised rotational displacements in flexion/extension, abduction/adduction and internal/external rotation at a frequency of 1 Hz, as shown in Figure 1.15. Additionally, the temperature should be similar to that inside the body ($37° \pm 2°$ C) and the implants should be submerged in a suitable lubricant. Commonly, new-born or foetal calf serum diluted in deionised water is used as the lubricant. This should have a protein concentration of 30 g/L $\pm$ 2 g/L, which is similar to that found in the native synovial fluid. Controlling the protein concentration is essential, as it has been shown previously that this can have a significant effect on the wear rate of polyethylene (Wang et al., 1998). It is also common practice to include small concentrations of sodium azide within the lubricant to prevent microbial growth throughout testing.

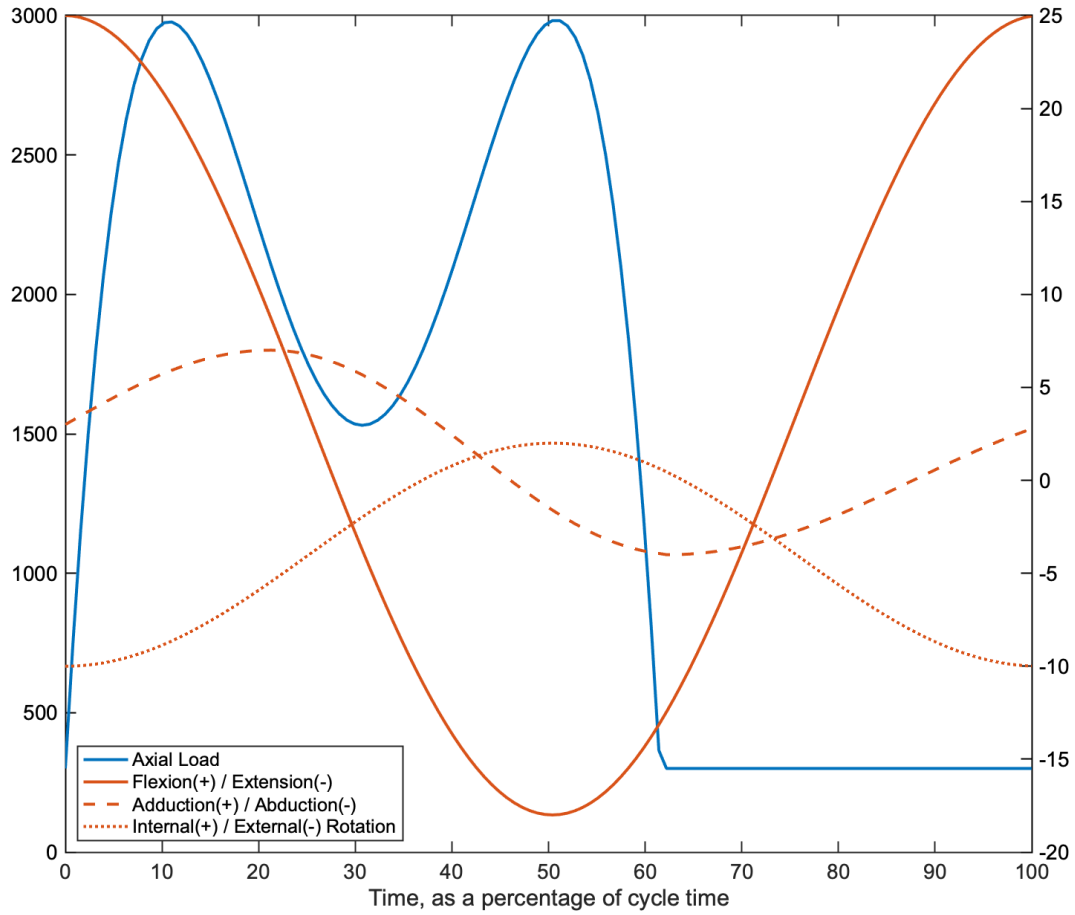

Figure 1.15 – The recommended double-peak load profile for a hip simulator during one cycle, as recommended by ISO 14242-1.

Simulators offer the advantage of allowing researchers to precisely understand the service conditions, which may be modified to suit a variety of different studies. However, simulators are run with approximated operating conditions and therefore cannot entirely represent the physiological conditions experienced in-vivo. These types of studies are also costly and labour intensive, and only allow limited information to be collected mid-test (i.e., to preserve the component's integrity).

Simulators can be used to analyse how implant function (e.g., wear, friction) is affected by different materials and bearing combinations (Wroblewski et al., 1996; McKellop et al., 1999; Firkins et al., 2001; Brockett et al., 2007). Simulators can also be used to replicate adverse test conditions, such as the introduction of third body particles (Bragdon et al., 2005) or edge loading whereby the loaded region shifts towards the rim of the acetabular shell therefore increases local stresses and implant damage (Leslie et al., 2009; Al-Hajjar et al., 2013).

Unlike conventional bearings, there are a limited number of studies (n=4) which have experimentally tested DM bearings within a hip joint simulator. These studies have investigated their performance under standard conditions (Gaudin et al., 2017), increased cup inclination angles (Saikko and Shen, 2010; Loving et al., 2015) and impingement, immobilisation and abrasion conditions (Loving et al., 2013). These studies are in agreement that there is no significant difference between the wear rates of conventional and DM liners (Saikko and Shen, 2010; Loving et al., 2015; Gaudin et al., 2017). Additionally, studies by Saikko et al (2010) and Loving et al (2015) have also reported no significant increase in the wear of DM liners at a high cup inclination angle (65° in-vivo), suggesting that the liner's mobility may lessen the effects of edge loading by orientating itself in a position which minimises stress concentrations (Saikko and Shen, 2010; Loving et al., 2015). A separate study investigated the effects of bearing immobilisation in an attempt to replicate soft tissue fibrosis, an issue specific to DM (Loving et al., 2013). This included two conditions: immobilisation of the inner bearing and immobilisation of the outer bearing. The study reported wear rates of a similar magnitude to conventional bearings whilst the outer bearing was immobilised. However, a significantly higher wear rate was reported once the inner bearing was immobilised, due to the increase in effective head size. This study has proven to be a strong first step towards the development of suitable experimental methods for DM bearings. A limitation of this study, however, is that each of the clinical conditions were investigated independently. No study has been identified which explores the combined effects of these clinical conditions to replicate worst-case operating scenarios.

1.5.3 – Computational studies

Validated computational models may be used to predict THR implant function under a variety of conditions. These models may be mathematical approximations or rely on Finite Element Analysis (FEA) or Computer-Aided Design (CAD). Computational models have been used to assess conventional THRs in a variety of studies. For example, FEA has been used to investigate the stability and micromotion of cementless femoral stems directly after implantation (Bah et al., 2011) or to predict the likelihood of cracking in the cement mantle of cemented femoral stems (Jeffers et al., 2007). Additionally, CAD models of THR components and cadaveric pelvises have been used to identify how various factors such as component design and position may influence their Range of Motion (ROM), incidence of impingement and

likelihood of dislocation (Scifert et al., 1999; McCarthy et al., 2016). Computational models have also been used to study the effects of adverse conditions, such as edge loading or dynamic separation (Liu et al., 2018; Etchels et al., 2019).

Several studies have investigated the performance of DM THRs using computational models. For example, FEA and CAD models have been used to investigate the ROM of DM implants in comparison to alternative designs such as conventional THRs or hip resurfacings (Klingenstein et al., 2013; Heffernan et al., 2014; Terrier et al., 2017). These studies suggest a comparable ROM between DM implants and large diameter (i.e., 36-mm) conventional THRs. Additionally, a study by Heffernan et al (2014) suggests that sub-hemispheric DM shells provide a superior ROM in comparison to anatomic or modular designs. Computational studies have also been utilised to investigate the posterior horizontal dislocation distance of DM implants (Heffernan et al., 2014; Klemt et al., 2020), or to predict their performance under adverse test conditions such as increased cup inclination angle (Uddin, 2015) or microseparation (Netter et al., 2014). These studies suggest DM implants have an increased dislocation distance in comparison to conventional THRs thus providing further evidence of their increased stability. Additionally, data suggests DM implants perform favourably under adverse test conditions. Finally, the kinematics of eccentric DM liners have been investigated in a computational motion analysis study (Fabry, Woernle, et al., 2014). This provided some evidence that DM implants primarily articulate at their inner bearing surface (i.e., between the femoral head and liner) although changes in the radial clearance may influence this motion and result in increased use of the outer bearing.

In summary, computational modelling may be used to predict the performance, failure, and kinematic function of THR implants under a variety of conditions. These models may also be used to inform and optimise the development of experimental studies. However, specialist knowledge is required to build and validate the complex models which can be a time consuming and computationally expensive process. Additionally, experimental studies are often required to validate the models or to provide important input factors such as frictional coefficients.

1.5.4 – Summary

Typically, the performance and mechanical failure modes of THRs are assessed through a combination of experimental studies (e.g., hip simulation), explant analyses

and clinical findings (e.g., survivorship data). In addition, computational research can be used to strengthen our understanding of THR function although these studies are often underpinned or validated through experimental data (e.g., friction data of articulation sites). Experimental studies allow implants to be tested under controlled and repeatable conditions which may be easily modified to represent a variety of pertinent patient, surgical and/or implant factors. However, these studies cannot recreate the complex in-vivo environment and, in the case of long-term wear simulation, may be expensive and time consuming. Alternatively, explant analysis provides an opportunity to gather information about the in-vivo damage mechanisms of THR components. Results from these studies may be dependent on the specific patient factors which are challenging to stratify without appropriate and sufficient supplementary data. Additionally, adequate sample sizes can be difficult to obtain when less common THR designs are being assessed, such as DMs. Therefore, the most effective way to assess implant function is through a combination of the described methods.

1.6 – Methods to characterise THR component damage

1.6.1 – Polyethylene liners

Polyethylene is a predominant orthopaedic biomaterial which is used in the majority of all primary THRs performed within the UK (National Joint Registry, 2022). Polyethylene wear debris is often a limiting factor for the long-term survivorship of THRs and therefore it is critical to understand the mechanical failure mechanisms of these components. A range of methods are available to characterise the physiochemical changes which occur to polyethylene liners after being serviced in-vivo or in-vitro. However, these methods are often designed for conventional liners and thus may not be suitable for implants which deviate from their typical geometry or function, such as in the case of DMs. Therefore, this section will review current characterisation methodologies and how, if at all, these have been applied to DM polyethylene liners. This section will focus particularly on non-destructive methods which preserve the component's structure throughout the analysis.

The wear of a polyethylene liner is typically quantified by linear wear rates (i.e., penetration depth) or volumetric wear rates (i.e., volume of material loss). In order to determine these metrics, the pre-service and worn surfaces must be compared. For in-vitro tested liners, this pre-service reference geometry may be captured directly from the specimens prior to testing. Conversely, no pre-service information is

available for retrieved liners and thus the unworn reference geometry must be approximated. This may be achieved by measuring as-manufactured samples or by referencing component drawings provided by the manufacturer, although these approaches do not account for the variability between components due to manufacturing tolerances. Alternatively, the reference geometry may be approximated through various curve or sphere fitting algorithms (Pryce, 2019; Hua and Li, 2020).

Current methods which have been developed to characterise conventional liners are not adequate for the DM system. The mobilisation of DM liners means that they are prone to wear on both their inner and outer surfaces and therefore, unlike conventional liners, both surfaces must be investigated. It is true that conventional liners may experience wear at their outer surfaces due to 'backside wear' (i.e., micromotion between the liner and shell) however these effects are likely to be minimal and therefore are rarely considered during wear analyses (Akbari et al., 2011; Reyna et al., 2016). Additionally, due to the presence of a retentive bore, the internal surface adjacent to the rim on a DM liner is not easily visible or accessible. This makes visual assessments, imaging, and probe-based measurements more complex.

1.6.1.1 – Visual assessment

The surfaces of polyethylene liners may be visually assessed for evidence of potential damage mechanisms or impingement. A visual scoring system was developed by Hood and colleagues for the assessment of UHMWPE damage found on total knee replacement components as discussed previously in Section 1.2.4. This identified seven modes of UHMWPE damage including: scratching, pitting, embedded debris, deformation, abrasion, burnishing and delamination. The scoring system involves first dividing the explant surface into zones. Each zone should receive a score ranging from zero (no damage) to three (severe damage) for each of the seven damage modes, depending on its extent and severity. A score of zero should be assigned when the damage mode is not present, whilst a score of one, two or three represents the damage mode being present on up to 10%, between 10-50%, or over 50% of the zone's surface area, respectively. The summation of scores from each zone yields the components total damage score.

The Hood system has already been expanded for the analysis of both conventional (Bradford et al., 2004; Schroder et al., 2011; Pang et al., 2015) and DM liners

(D'Apuzzo et al., 2016; Spece et al., 2018). For conventional liners, it is common practice to divide the internal surface into quadrants, as depicted in Figure 1.16A. This would yield a maximum damage score of 84 (4 quadrants x 7 damage modes x maximum score of 3) if the component is scored against all seven damage modes. However, not all studies include delamination as a mode of damage (Bradford et al., 2004). Thus far, two studies have applied the Hood scoring system to DM liners (D'Apuzzo et al., 2016; Spece et al., 2018). In both studies, the inner surface was divided into quadrants and scored in the same way as conventional liners (Figure 1.16A). For the outer surface, a study by Spece et al divided this area into three circumferential regions: the pole, equator and rim (Figure 1.16B) while another study by D'Apuzzo et al further divided these three regions into quadrants (Figure 1.16C). The total damage score is therefore equal to the summation of the scores from both the inner and outer surfaces.

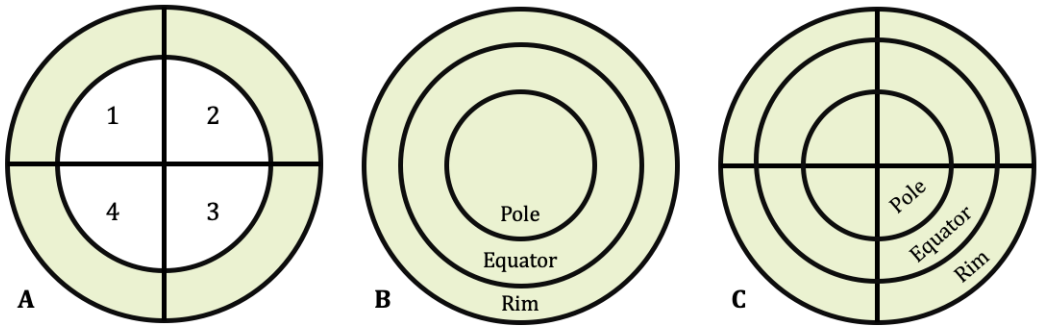

Figure 1.16 – A view of the inner (A) and outer (B, C) surfaces of a polyethylene liner, divided into regions to facilitate visual inspection methods as developed by Hood et al. When using the Hood scoring system to assess damage on polyethylene liners, the liner surface is often divided into zones. Conventional liners must only be investigated at their inner surface, which is often divided into quadrants (A). Both the inner and outer surfaces of dual mobility liners, on the other hand, must be investigated due to the mobilisation of the liner. The inner surface is similar to that of a conventional bearing, and thus is divided into quadrants in the same manner (A). The outer surface, however, has been divided into either three regions (B) or 12 regions (C), according to the literature.

Using this system, the predominant damage mechanisms of DM liners have previously been reported to be scratching, pitting and embedded debris (D'Apuzzo et al., 2016; Spece et al., 2018). D'Apuzzo and colleagues (2016) observed a greater damage score at the inner surface in comparison to the outer, suggesting that the inner articulation may be the predominant bearing surface in-vivo. At the outer surface, greater damage scores were noted at the equator and rim than at the pole

(D'Apuzzo et al., 2016; Spece et al., 2018). Although the Hood scoring system has shown to be a useful method in identifying the predominant damage mechanisms, the method is limited by the subjectivity which is introduced during the scoring process. As Hood and colleagues describe, the scores are related to not only the extent of a damage mode (i.e., the surface area in which the damage covers) but also the severity. For example, this means that a large number of small scratches (covering over 50% of the bearing surface) may be given a score of three similarly to a small number of severe scratches (covering less than 50% of the surface area). Therefore, multiple independent examiners should grade the surfaces to reduce bias and subjectivity where possible, and the agreement between them should be high.

An alternative to damage scoring systems which provides similar semi-quantitative outputs is by photogrammetry, or the process of obtaining measurements directly from photographs. This process is already widely employed when determining the in-vivo displacement and micromotion of THR components via a method known as Radiostereometric Analysis or RSA. Photogrammetry is used less commonly to evaluate the surface damage of polyethylene components although it has the potential to be a powerful tool. For example, Grochowsky et al have developed a photogrammetric method to analyse polyethylene tibial inserts used in knee replacements (Grochowsky et al., 2006). The method involves first outlining the damage areas of the component surface with a black permanent marker, and then digitally photographing and analysing the surface using a publicly available software package such as ImageJ. This is a cheap, simple and effective method to determine the area of damage relative to the total surface area. This method has since been applied to one study analysing the backside wear of conventional polyethylene THR liners (Akbari et al., 2011). However, this method relies on the user correctly outlining the damaged regions and does not account for the curvature of the surface. This would be particularly challenging in the context of DM liners due to their supra-hemispheric geometry which makes it impossible to photograph the full articulating surface in one image.

Another visual inspection method which has been applied to DM liners is a simple binary scoring system designed to assess the liner for evidence of impingement. This involves assigning a score of one if there is noticeable deformation or the creation of a raised lip at the rim, suggesting the occurrence of femoral neck impingement. Alternatively, a score of zero is assigned when there is no evidence of impingement. This method has been used in a number of studies (Nebergall et al., 2016; Laura,

H.S. Hothi, et al., 2017; Scott et al., 2018), and has shown to be an effective way to identify the incidence of impingement among THR liners including DM. For example, a study by Scott et al used this method and reported a significant decrease in the incidence of impingement among DM (21.5%) and conventional liners (77%, $p<0.001$) (Scott et al., 2018). This suggests that DM liners are less susceptible to impingement damage and thus subluxation or dislocation of the joint than conventional THRs.

1.6.1.2 – Geometric assessment

Due to their high precision, Coordinate Measuring Machines (CMMs) have been used for the geometric assessment of orthopaedic devices. A CMM is an instrument which utilises a probe attachment to trace along the specimen and record discrete coordinate points in the X-, Y- and Z-planes to generate a point cloud of the surface. The accuracy of these measurements is typically a function of the total scanning length although, for the assessment of conventional polyethylene liners, is typically below a threshold of 1 μm. This data may later be manipulated to determine wear parameters such as penetration depth or volumetric change, or to generate surface deviation heatmaps to visualise areas of damage. Geometric assessment has been widely adopted in the literature to assess both retrieved (Goldvasser et al., 2014; Holdcroft and Van Citters, 2018) and simulator-tested (Estok et al., 2005; Trommer et al., 2015) conventional liners. Studies have shown geometric assessment methods to estimate the degree of volumetric wear within 0.76 to 4.1 mm^3 of known gravimetric data (Uddin et al., 2016; Wang et al., 2016; Hua and Li, 2020).

CMM-based wear analysis has shown to be a more reliable and convenient method to determine linear and volumetric wear of THR liners in comparison to previously used techniques (Hall et al., 1995; Uddin, 2014; Uddin et al., 2016). Previous methods relied on radiographic or shadowgraph techniques to calculate the depth, d, and angle, β, at which the centre of the femoral head had penetrated into the liner. By doing this, the wear volume could be approximated indirectly by use of a mathematical formula (Kabo et al., 1991). A study by Hall et al compared indirect radiographic and shadowgraph methods to assess volumetric wear against a direct measurement method (i.e. using a CMM) (Hall et al., 1995). The study suggests that mathematical formulae may overestimate the true wear value by up to 25%, especially in the case of a non-hemispherical liner, and thus CMM-based methods are superior for the determination of volumetric wear. Alternatively, roundness

measuring machines have also been utilised to geometrically assess polyethylene liners for linear wear (Haraguchi et al., 2001; Ito et al., 2001; Bergiers et al., 2019). However, these machines can only provide measurements along one axis (e.g., longitudinal) and therefore cannot provide information relating to the entire bearing surface such as wear maps. For this reason, CMMs have often been employed in more recent studies which require geometric assessment of THR components.

A limited number of studies have used geometric measurements to analyse the surfaces of DM liners although the methods vary from study to study (Geringer et al., 2011; Adam et al., 2014; D'Apuzzo et al., 2016). D'Apuzzo and colleagues used helical traces to measure both surfaces of DM liners which had previously been sectioned at the retentive rim (D'Apuzzo et al., 2016). On the other hand, Geringer et al opted for circumferential traces to measure these surfaces (Geringer et al., 2011). In both cases, surface traces were focused at the equatorial regions and did not include the poles, either because the probe was unable to reach (D'Apuzzo et al., 2016) or because it was deemed unnecessary (Geringer et al., 2011). Likewise, data was not inclusive of the rim however the reasoning for this was not explicitly specified in either study. D'Apuzzo et al separately measured the retentive rim of liners used in a lever out study to assess for rim damage following a simulated dislocation; however, these scans were exclusive to this region and did not extend into the articulating surfaces. In addition, both studies approximated the reference geometry using scans from pristine liners in order to calculate the penetration depth or volumetric change and did not consider the component-to-component manufacturing variations. An alternative approach was described by Adam et al, in which 85 points were acquired at the surface of the inner bearing to determine a mean surface diameter, ∅ (Adam et al., 2014). The Penetration Depth (PD), in this case, was then calculated by comparing the mean surface diameter against the theoretical diameter ($\emptyset_{Th}$) and surface shape defects (SD) as described by Equation 1.

$$PD = \frac{[(\emptyset + SD) - \emptyset_{Th}]}{2} \quad (1)$$

Examples of geometric assessment of DM liners is limited in the literature although these studies have provided some information about the function and performance of these implants. For example, it has been shown that the penetration depth is significantly higher at the internal surface of retrieved DM liners (0.04 ± 0.01 mm) than at the outer surface (0.02 ± 0.03 mm; $p<0.001$) which suggests that the internal

bearing acts as the primary articulation site (D'Apuzzo et al., 2016). Additionally, circumferential wear stripes were observed in the equatorial regions of retrieved DM liners which presented with no additional pathology (e.g., arthrofibrosis) thus implying the liners have an ability to ratchet within the acetabular shell (Geringer et al., 2011).

However, there has been no published methodology which allows for a comprehensive scan of the entire bearing surface, from pole to rim, on either side of a DM liner. Improvements to these methodologies would allow for more comprehensive assessments to be facilitated so that the in-vivo function of these implants may be better understood.

1.6.1.3 – Micro-computed tomography

Micro-Computed Tomography, also known as microCT, is an imaging technique which uses x-rays to generate cross-sectional images and a three-dimensional reconstruction of a specimen. The process relies on the emission of x-rays which pass through the specimen and onto a detector. This generates a two-dimensional cross-sectional image known as a slice. The specimen is then rotated by a fraction of a degree, and the imaging process is repeated until the specimen has rotated either 180 or 360 degrees. A process known as post-processing then converts the 2-dimensional slices into a 3-dimensional reconstruction.

Validated methods are available in the literature which utilise microCT to assess the penetration depth (Bowden et al., 2005) and volumetric wear (Teeter, Naudie, et al., 2010) of conventional polyethylene liners, and to generate surface deviation heatmaps. These methods have been used to evaluate the failure mechanisms of XLPE liners (Pang et al., 2015; Choudhury et al., 2018). Additionally, microCT provides the unique ability to non-destructively evaluate sub-surface cracking in polyethylene components which has often been applied to tibial inserts from total knee replacements (Teeter, Yuan, et al., 2010). However, the use of a microCT scanner is a lengthy process that is limited by the scanning time, which can be upwards of 4 hours per liner of a conventional geometry (Bowden et al., 2005). Large datafiles (approximately a gigabyte in size) are generated which can be difficult and time-consuming to work with. Expert knowledge is required in order to manipulate the files at early stages of the process and large infrastructural investments must be in place in order to support the high costs of the equipment and software.

Thus far, two studies have been identified which use microCT for the evaluation of DM liners (Laura, H.S. Hothi, et al., 2017; Malatray et al., 2017). One study used microCT to investigate the effects of femoral neck geometry on the deformation at the retentive rim (Laura, H.S. Hothi, et al., 2017). In this case, microCT was used only to validate findings from separate analyses and thus was used for a small data set (n=2). A separate study relied on microCT to examine the incidence of sub-surface cracking following the snap-fit assembly of the femoral head and liner (Malatray et al., 2017). The study was conducted in response to concerns that introducing XLPE into DM liners would cause fractures at the retentive rim. Interestingly, the study reported no significant difference in sub-surface crack formation between conventional and cross-linked polyethylene. While microCT has been used, in a limited capacity, to examine surface damage and sub-surface cracking of DM liners, no studies have been identified which use microCT to calculate the volumetric wear of DM components.

1.6.2 – Femoral heads and acetabular components

It is well documented that the counterface which articulates against polyethylene has a significant effect on the wear and long-term survivorship of a THR (Fisher and Dowson, 1991; Cooper et al., 1993; Blunt and Jiang, 2000). This surface is constructed from a hard material, such as a metal or ceramic. In the case of DM constructs, three counterface surfaces exist: the femoral head (i.e., the inner counterface), the acetabular component (i.e., the outer counterface) and the femoral neck (i.e., the ‘third’ bearing). However, only a limited number of studies have assessed the surface damage on the counterfaces of DM bearings.

Methodologies to characterise damage on the convex surfaces of femoral heads have previously been developed and published in the literature. However, the need for such methods to analyse a large concave counterface, such as the articulating surface of a DM acetabular component, is limited to a lesser number of applications and therefore fewer published methodologies are available. This section will present two common and well-established methodologies to characterise hard, spherical surfaces and discuss how they may be applied to the analysis of DM bearings.

1.6.2.1 – Optical microscopy and photogrammetry

Optical microscopy is a qualitative analysis method which allows for hard counterface surfaces to be inspected for signs of damage, with a working resolution as low as 200 nm. A wide range of microscopes may be used, but it is important that the equipment

uses reflected light, rather than transmitted light, due to the opacity of metals and ceramics. The microscopy process is quick, simple, and accessible to most researchers. Therefore, it is no surprise that optical microscopes have been widely employed for the surface analysis of femoral heads (Jasty et al., 1994; Hall et al., 1997; Fisher et al., 2002; Wimmer et al., 2003). In a study by Jasty et al, surface scratches on retrieved cobalt-chrome femoral heads were noted to present with 'sharp edges with heaped-up boundaries' (Jasty et al., 1994). This suggests that they were caused by third body debris entering the joint space. The study also reported a greater incidence of surface damage for uncemented components when compared to their cemented counterparts. This can be explained by the porous surface coatings of uncemented bearings which are likely to generate additional third body debris thus accelerating surface damage.

Images obtained from optical microscopes or digital cameras may be post-processed using photogrammetry to obtain semi-quantitative data such as scratch length, scratch width, or pit diameter. Photogrammetry has successfully been used for the analysis of metallic joint replacement components in the ankle (Stratton-Powell, 2018), knee (Arnholt et al., 2016) and hip (Fredette et al., 2015; Dall'Ava et al., 2020). Often, these studies use photogrammetry to determine the percentage of the total surface area in which a particular damage mode extends. For example, a study by Fredette et al used digital photogrammetry in order to calculate the surface area of metal transfer patches found on retrieved femoral heads (Fredette et al., 2015). In the case of Dall'Ava et al, however, photogrammetry was used in order to quantify the level of bony attachment on the backside of uncemented acetabular shells (Dall'Ava et al., 2020).

It should be noted that photographing the surfaces of highly reflective metallic components is challenging, particularly when the aim is to visualise areas of surface damage. An imaging technique has been developed by Heiner et al which has shown to be a simple and effective solution to enhance image quality (Heiner et al., 2013). Additionally, the use of focus-bracketing can be used when imaging surfaces with a large degree of curvature (e.g. femoral heads) in order to ensure the entire image is in focus (Fredette et al., 2015).

In summary, optical microscopy is a simple and useful tool to qualitatively or semi-quantitatively characterise the surfaces of hard components of varying shapes, sizes and materials. The use of optical microscopy has been identified in one study which

examined the surfaces of DM counterfaces following in-vitro simulation testing (Saikko and Shen, 2010). Photogrammetry is a useful method in order to generate semi-quantitative data from images but has not yet been applied to DM bearings, to the author's knowledge.

1.6.2.2 – Surface roughness analysis

In a pioneering study by Dowson et al, it was revealed that the surface roughness of the counterface in a THR had significant effects on the wear rate of polyethylene (Dowson et al., 1985). The study reported that a tenfold increase in the surface roughness (Ra) of femoral heads (from 0.01 μm to 0.1 μm) resulted in 13-times increase in polyethylene wear. For this reason, it has since been of great interest to examine the surface roughness of orthopaedic counterfaces to better understand the underlying wear mechanisms.

Surface roughness measurements are quantified by use of a profilometer. A profilometer is an instrument which relies on either contacting or optical methods to detect vertical displacements (in the z-plane) at the surface of a material. Contacting profilometers operate by running a diamond stylus along a surface profile (i.e., a line) while recording vertical displacements of the stylus. By repeating this process to scan multiple, closely spaced parallel profiles, contacting methods may also be used to determine roughness values over an area. This profilometry method is advantageous in environments where surface contaminants or strong surface reflections are present as they do not interfere with the measurements. However, due to the force exerted by the stylus, contacting methods can damage some surfaces and thus are not recommended for materials which are easily scratched or damaged. Optical profilometers, on the other hand, offer a non-contacting method for measuring surface roughness using interference principles or a laser stylus.

As previously described, the roughness of a surface may be determined over a profile or an area. Values derived from a profile are often denoted as R-values (e.g. Ra, Rq, etc.) while values derived over an area are denoted as S-values (e.g. Sa, Sq, etc.). There exists a large range of surface roughness parameters which may be determined, as described in ISO 4287-1997. Some of the most commonly employed parameters are detailed in Table 1.2 and illustrated in Figure 1.17.

Table 1.2 – A list of common surface roughness parameters which may be calculated from a surface profile (i.e. a line). These values may also be derived over an area, denoted by an S-value (e.g. Sa, Sq, St, Sp, Sv).

Parameter	Abbreviation	Definition
Sampling length	l	The wavelength of the filter, which is used to distinguish between waviness and roughness. It is also known as the cut-off length.
Evaluation length	L	The length of the profile which is used to evaluate the surface parameters. This is suggested to be at least 5x the sampling length.
Mean line	M	A reference line which divides the profile. It is the line from which all deviation measurements are measured.
Mean roughness	Ra	The mean of the absolute values of all profile deviations measured within one evaluation length.
Root mean square roughness	Rq	The mean of the root mean squares of all profile deviations measured over one evaluation length.
Peak to valley height	Rt	The distance (or amplitude) between the highest peak and lowest valley over one evaluation length.
Maximum peak height	Rp	The distance between the highest peak and mean line over one evaluation length.
Maximum valley depth	Rv	The distance between the lowest valley and mean line over one evaluation length.
Skewness	Rsk	A measurement of symmetry about the mean line. Positive skewness values indicate that there are likely to be more peaks and surface asperities while negative values indicate that valleys and troughs are more predominant.

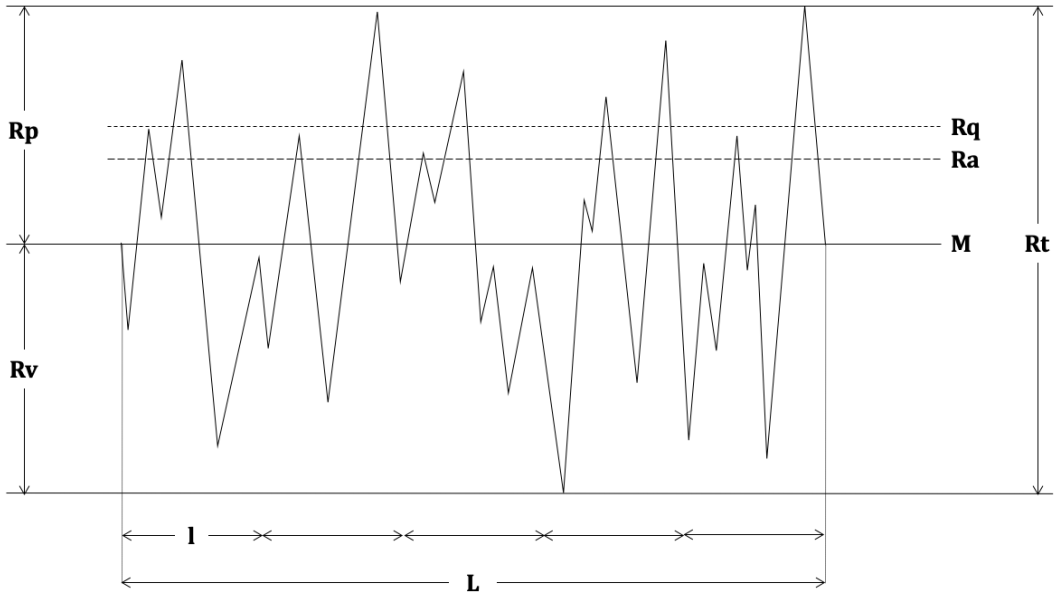

Figure 1.17 – Schematic illustrating a sample surface profile of evaluation length L. The mean line, M, divides the profile and acts as a reference from which all deviations are measured. Ra and Rq represent the mean roughness and root mean square roughness values of the profile, respectively. Rt represents the peak to valley height. Rp and Rv represent the maximum peak and maximum valley heights, respectively.

The measurement of surface roughness values has been a widely employed technique used in the literature to characterise orthopaedic components. Most commonly, this has been in order to evaluate the surfaces of metallic or ceramic femoral heads (Hall et al., 1997; Barbour et al., 2000; Goldsmith et al., 2000; Smith et al., 2001; Eberhardt et al., 2009; Merola et al., 2016). For example, a study by Eberhardt et al used contacting profilometry to compare the surface roughness of nonimplanted femoral heads to those with noticeable metal transfer patches (Eberhardt et al., 2009). The study showed there was a significant increase in the surface roughness in the presence of metal transfer patches, suggesting that they can have an effect on the performance and longevity of a THR. For example, the mean surface roughness (Ra) of nonimplanted CoCr femoral heads was reported to be 0.012 ± 0.002 μm while metal transfer patches had an increased mean roughness of 0.380 ± 0.308 μm. Another study by Smith and colleagues used an optical profilometer to determine the surface roughness of metal-on-metal bearing components (i.e. the femoral head and acetabular shell) (Smith et al., 2001). The study highlighted a key limitation of optical profilometers, which involves the space constraints introduced by the size of the instrument's lens. For this reason, it may not

be possible to measure small-diameter shells (less than 28-mm in the case of Smith et al) with optical profilometry.

To the author's knowledge, profilometry has only been used to determine the surface roughness of the femoral neck (Laura, H.S. Hothi, et al., 2017) and mobile liner (Geringer et al., 2011; Loving et al., 2013) of DM bearings. No studies have been identified which analyse the femoral head or acetabular shell of this type of bearing. However, these surfaces could be analysed using methods already developed for the analysis of standard femoral heads and MoM acetabular shells.

1.6.3 – Summary

A variety of methods are available to characterise the surface damage of in-vitro tested and retrieved THR components. These are summarised in Table 1.3.

Table 1.3 – Summary of common characterisation methodologies to assess the articulating surfaces of THR components.

Method	Purpose	Advantages	Limitations
Polyethylene components			
Visual inspection	To identify predominant modes of surface damage	- Simple methodology - No equipment requirements - Easy to adapt to any orthopaedic articulating surface	- Manual process - Intra- and inter-rater subjectivity in assigning damage scores
Geometric assessment	To visualise the shape, location, and extent of the surface damage, and to approximate linear and volumetric wear	- Quick, automated process	- Requires pre-service surface geometry to be approximated if this information is not available (i.e., retrievals) - Cannot distinguish between wear and deformation of the material
MicroCT	To identify sub-surface material changes	- High resolution	- Time consuming - Challenging to work with large datafiles
Hard components (i.e., metallic or ceramic)			
Optical microscopy	To identify predominant modes of surface damage	- Simple - Equipment is readily available in more laboratory settings	- Only provides qualitative outputs - Challenging to photograph reflective surfaces
Photogrammetry	To semi-quantitatively assess surface damage	- Automated - Can be completed with publicly available software (e.g., ImageJ)	- Relies on high quality surfaces images with adequate visualisation of surface damage - Reliability of data decreases with surface curvature
Contacting or optical profilometry	To characterise the surface roughness of a component	- Simple	- Optical methods may not be suitable for concave surfaces - Contacting methods may not be suitable for easily damaged surfaces

1.7 – Project aims and objectives

1.7.1 – Rationale

DM bearings were developed to combat the complex challenge of hip dislocation for at-risk patients and are characterised by an unconstrained polyethylene liner. New-generation DM designs have shown good survivorship and decreased rates of impingement and prosthetic dislocation in comparison to conventional, unipolar designs (Darrith et al., 2018; Scott et al., 2018). Despite their emerging use in both elective and acute orthopaedic settings, the in-vivo function of these implants is not well understood. Early joint registry data suggests DM implants may be susceptible to higher rates of early failure (<5 years) than conventional THRs, and failure mechanisms unique to these constructs, such as accelerated polyethylene wear and IPD, remain a concern.

It is important to understand the in-vivo functional mechanisms of these constructs as they are implanted more frequently and within more diverse patient populations especially in light of early National Joint Registry data which suggests possible unfavourable performance of these implants in comparison to conventional THRs (National Joint Registry, 2022). However, few studies have investigated the kinematics and/or wear performance of DM implants through either in-vitro, retrieval, or computational analyses. It is thought that this may be due to a lack of available characterisation and/or experimental testing methodologies suitable for the novel geometry and function of these constructs.

1.7.2 – Aims

The overall aim of this project was to improve the current understanding of the mechanical function and failure mechanisms of DM bearings. This was achieved through the development of novel characterisation and in-vitro testing methodologies, which were later applied in a comprehensive retrieval analysis and in-vitro motion tracking assessment.

1.7.3 – Objectives

The objectives of this project were –

- To develop a non-destructive characterisation methodology to assess damage on the articulating surfaces of retrieved and in-vitro tested DM polyethylene liners (Chapter 2).

- To develop an experimental testing methodology for the assessment of DM liner motion under physiologically relevant loading, displacement, and lubrication conditions (Chapter 4).
- To assess a collection of retrieved DM components using a variety of methods and identify the most prevalent and clinically-relevant modes of surface damage (Chapter 3).
- To conduct an in-vitro motion tracking study to assess the intra- and inter-component repeatability and kinematic function of DM liner motion under standard gait conditions (Chapter 5).
- To compare outputs from the retrieval analysis and in-vitro motion tracking assessment and suggest the possible in-vivo functional mechanisms of DM constructs (Chapter 6).
- To recommend key areas of research which should be considered in the future analysis of DM implants (Chapter 6).

Chapter 2 – Development of a characterisation methodology to assess the wear and deformation at the articulating surfaces of dual mobility liners

2.1 – Introduction

As discussed in Chapter 1, there is a limited understanding of the function and failure mechanisms of DM bearings. Few studies have investigated the wear performance of these types of implants which is likely due, in part, to a lack of appropriate characterisation methodologies suitable for their novel geometry and function. An example of a DM implant is shown in **Figure 2.1**, which features an unconstrained, supra-hemispheric polyethylene liner that sits within an acetabular component (e.g., monobloc or modular shell) and encapsulates a femoral head. Damage characterisation of DM bearings has previously been assessed using semi-quantitative methods, such as a modified Hood system (D'Apuzzo et al., 2016; Spece et al., 2018) or a binary impingement score (Nebergall et al., 2016; Laura, H.S. Hothi, et al., 2017; Scott et al., 2018). Few studies have assessed the damage at these surfaces using geometric measurements. Even in these instances, the measurements either excluded a significant portion of the surface (Geringer et al., 2011; D'Apuzzo et al., 2016) or contained a low number of sampling points e.g., fewer than 100 (Adam et al., 2014). Additionally, sectioned liners have been geometrically assessed (D'Apuzzo et al., 2016) however this is not desirable in circumstances in which the original geometry of the liner aims to be preserved, such as in retrieval analyses (i.e., limited number of available components) or in-vitro simulator studies (i.e., mid-way through a test).

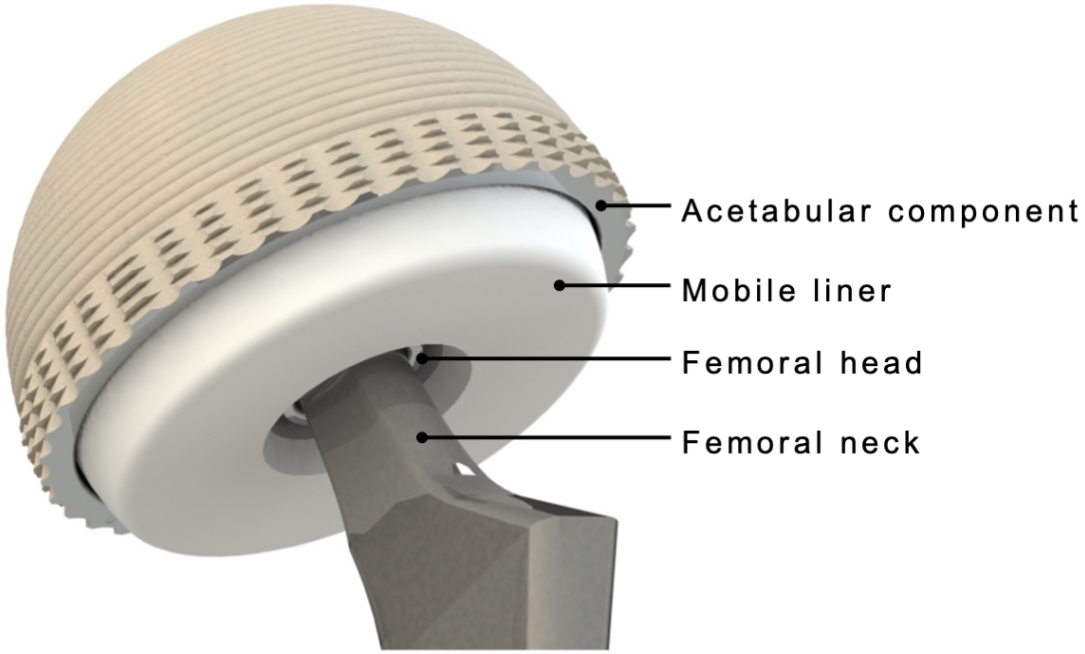

Figure 2.1 – Schematic of a DM implant, which features an unconstrained and supra-hemispheric polyethylene liner. The liner sits within an acetabular component and encapsulates the femoral head.

In summary, there is no published methodology which geometrically assesses both internal and external surfaces of an intact DM liner. Visualisation of the surface damage would provide information about the kinematics and possible failure mechanisms of these bearings. For example, a circumferential wear stripe has been reported as a characteristic trait of retrieved DM bearings with no additional pathologies (e.g., arthrofibrosis), which suggests that the liner may rotate within the acetabular shell when functioning normally (Geringer et al., 2011). Additionally, quantitative outputs (i.e., approximate volume change) would provide information about the wear performance of these bearings.

Therefore, the aim of this study was to develop a geometric characterisation methodology to assess the wear/deformation of the articulating surfaces of DM liners. The development of this methodology was achieved through the following steps –

- Development of a geometric data collection protocol (Section 2.2).
- Development of a data analysis algorithm (Section 2.3).
- Assessment of geometric variance of as-manufactured liners (Section 2.4).

- Assessment of the repeatability of the method (Section 2.5),
- Verification of the method (Section 2.6).

2.2 – Development of the geometric measurement protocol

2.2.1 – Equipment

A coordinate measuring machine (Legex 322 CMM, Mitutoyo, Japan) was used to trace the articulating surfaces of DM liners and collect three-dimensional coordinate data. It is challenging to capture the full geometry of DM liners using vertically positioned scanning probes because these liners are supra-hemispherical thus resulting in re-entrant features. This introduces the risk of the probe shaft coming into contact with the liner, as shown in Figure 2.2A. In this instance, the probe would deflect thus resulting in a false coordinate reading and measurement error which will be referred to as a probe shaft contact error or PSCE. Therefore, it was important that the probe was carefully selected for this application to ensure that all geometric features of DM liners were captured without the introduction of PSCEs.

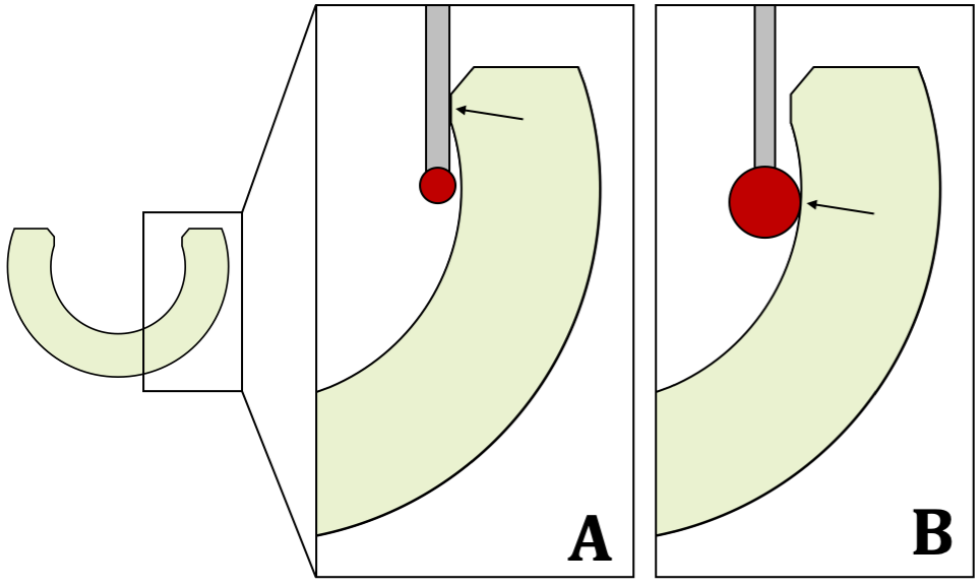

Figure 2.2 – During the CMM measurement process, errors known as PSCEs may be introduced if the probe shaft comes into contact with the liner prior to the probe head (A). These errors can be avoided by using a probe which offers a clearance that is greater than the maximum lateral distance of any re-entrant space (B).

During the selection of the appropriate probe, two key parameters were considered: the probe clearance and the probe head size. The probe clearance is defined as the difference in radii between the probe head and shaft. The probe clearance must be greater than the maximum lateral distance of any re-entrant feature in order to avoid PSCEs (Figure 2.2B). A larger probe head is often used in circumstances where an increased clearance is required. However, the caveat to this approach is that the diameter of the probe head is inversely proportional to its scanning resolution. Therefore, a probe should be selected which offers the required level of clearance and the smallest head size possible.

Initial pilot studies determined that the maximum lateral distance of the internal re-entrant feature of DM liners (28-mm internal diameter) was approximately 1.3-mm and thus a minimum probe clearance of 1.3-mm was required for this methodology. Therefore, a ruby-tipped probe was selected with a head diameter of 6-mm and a probe clearance of 1.75-mm.

2.2.2 – Component fixation

Liners must be securely fixed in place throughout the measurement period to prevent the components from moving, which could introduce error into the data. To achieve this, two separate fixtures were developed: one for measurements of the internal surfaces, and another for measurements of the external surface. Both fixtures were developed against the design criteria specified in Table 2.1.

Table 2.1 – Design criteria for the development of fixtures for geometric measurements of DM liners.

Criteria	Essential = E Desirable = D	Target
Design		
Simple	D	Maximum number of parts 5
	D	Easy geometry to manufacture
	D	Easy to use (<5 minutes set-up time, to be completed by one user without assistance)
Versatile	D	Capable of fixing a range of liner sizes (e.g., 35- to 63-mm outer diameter)
Compatible with CMM	D	Screws directly onto CMM bed
	E	Material does not interfere with ruby-tipped styli (e.g., aluminium)
Performance		
Non-destructive	E	Does not damage (e.g., scratch) or deform the surfaces of the liner
Stable	E	Does not allow component to move more than ±50 microns during any scan
Ease to orientate	D	Built-in alignment mechanism between fixtures so components can be orientated consistently between scans

For measurements of the internal surface, liners were placed within a cylindrical fixture lined with plasticine, as shown in Figure 2.3. The plasticine was used to prevent surface damage and reduce component shift. For measurements of the external surface, liners were placed onto a cylindrical spigot attached to a flat plate (Figure 2.4). Small amounts of plasticine were introduced at the outer edge of the component to prevent rotation. In each case, the component surface was cleaned with isopropanol and sprayed with compressed air to remove any surface contaminants.

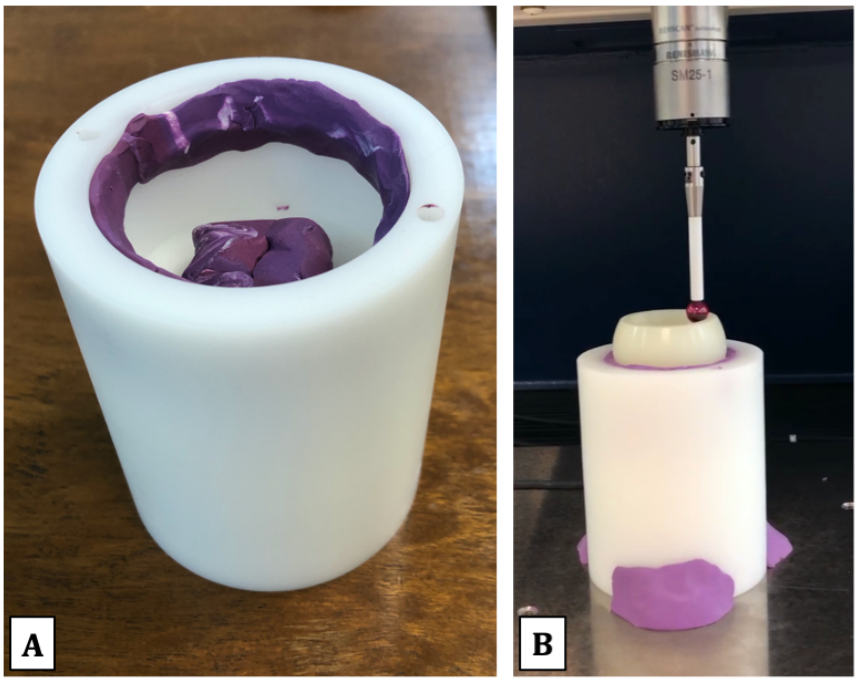

Figure 2.3 – Fixture used during scans of the internal surface of a DM liner. The fixture is cylindrical in shape and contains plasticine at the edges to prevent component damage (A). The fixture is secured onto the CMM bed with additional plasticine (B).

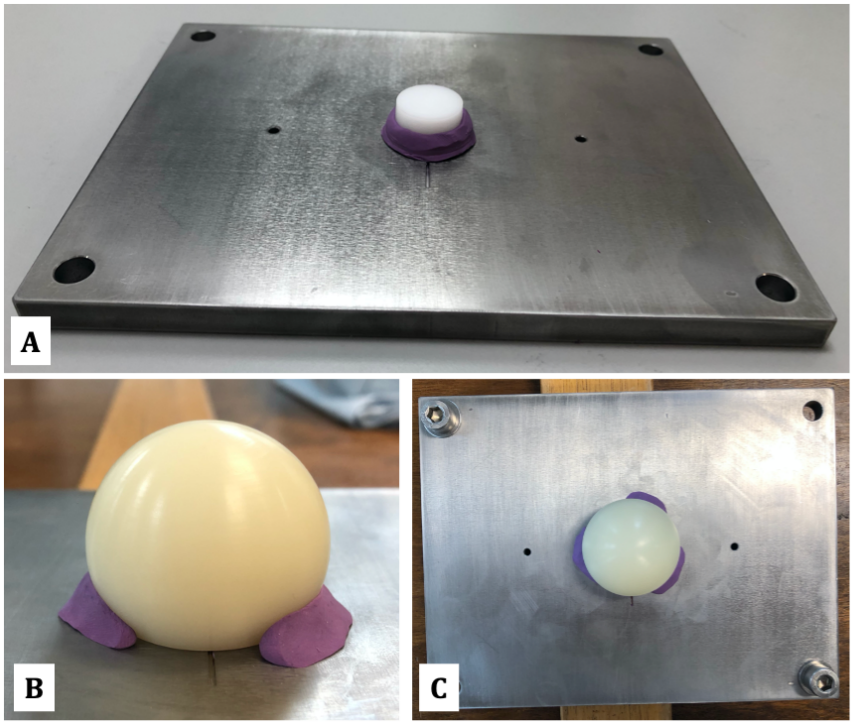

Figure 2.4 – Fixture used during scans of the outer surface of a DM liner. The fixture includes a flat plate with a cylindrical spigot in order to keep the liner in place (A). Small amounts of plasticine were introduced at the outer edge of the sample to prevent component rotation (B). The fixture was secured directly onto the CMM bed with screws (C).

To ensure that the components were consistently orientated between the internal and external surface scans (i.e., for registration of the surfaces), an orientation mark on the liner (e.g., pen mark, etched line) was visually aligned to the 12 o'clock position of the CMM bed. Although this alignment mechanism was done by eye, this was sufficiently accurate for the surfaces to be registered. Additionally, the components were placed within the fixtures for a minimum of 30 minutes prior to collecting any geometric data. This was to ensure the plasticine was able to elastically recover because early measurement data revealed a slight positional shift of the liner when measured directly after fixation thus introducing error into the measurements.

2.2.3 – Data collection

The Legex 322 CMM was manually programmed to instruct the probe to semi-automatically capture coordinate data. The first step involved the user manually moving the stylus to several pre-defined locations along the liner's surface, which were used to define a Cartesian coordinate system in a consistent and repeatable manner amongst all samples. Four points were acquired either along the horizontal surface of the liner's flat rim (for measurements of the internal surface) or on the flat base plate of the fixture (for measurements of the external surface). The four points were used to generate a reference plane. The XY plane of the coordinate system was aligned parallel to the reference plane, which corrected for any malalignment of the component (e.g., if the component was tilted). A further five points were acquired on the spherical surface of the liner (one point per quadrant plus one at the pole) to determine the surface's centre of rotation (COR) and establish the position of the origin. It should be noted that it was possible for the origin to be biased towards the worn or damaged regions of the surface, due to the low number of sampling points. However, five points were selected as this was the minimum number of sampling points required by the CMM to determine an origin of a spherical surface. This was found to be sufficient for the measurement protocol to be completed without the probe unexpectedly colliding into the surface of the sample and therefore no further points were included to ensure the measurement time was minimised. In addition, the true origin of the surface was re-established later in the data analysis process (Section 2.3). The final position of the origin with respect to the liner is shown in Figure 2.5.

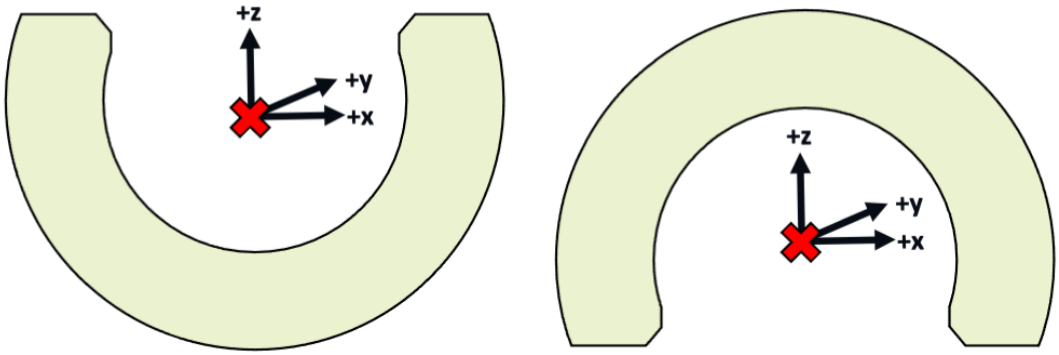

Figure 2.5 – Origin of the coordinate system (denoted by the red X) for measurements of the internal (left) and external (right) surfaces of DM liners using the developed methodology.

Following the generation of a coordinate system, the geometric data of the surface(s) was collected automatically through a series of traces. It is known that the geometry of the trace path influences the measurement time and thus three methods of data collection were considered, and the most efficient method was determined. In summary, 144 traces were taken at 2.5° intervals. For measurements of the internal surface, each trace originated at the pole and terminated at the rim (Figure 2.6A). For measurements of the external surface, each trace originated 3-mm beyond the equator and terminated at the pole (Figure 2.6B). It should be noted that the trace path does not encompass the entirety of the external surface to avoid the probe making contact with the base plate fixture thus introducing measurement error.

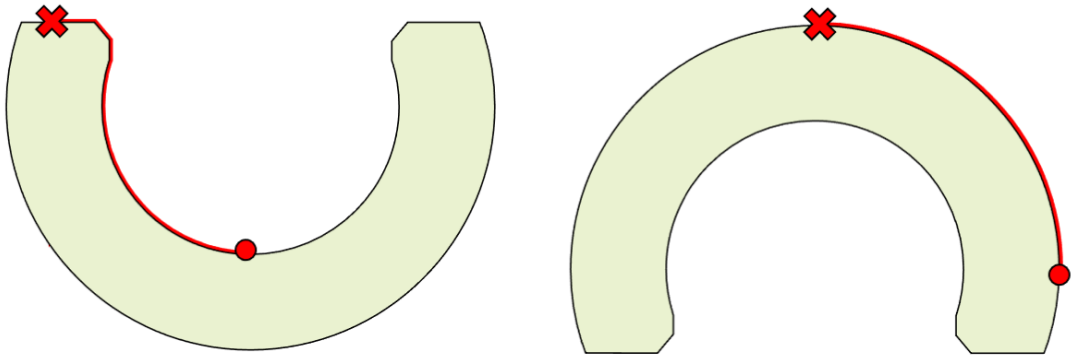

Figure 2.6 – CMM trace paths of the internal (left) and external (right) surfaces of a DM liner. The origin of traces is denoted with a red circle, and the termination point of the traces is denoted with a red cross.

The data acquisition time per liner was assessed using one large-diameter DM liner (69/28-mm BI-MENTUM™), which represents the worst-case scenario because it has

the longest theoretical measurement time due to its large external surface area. The geometric data of the internal and external surfaces was captured in 31 and 62 minutes respectively, resulting in a maximum data acquisition time of 93 minutes per liner. A total of approximately 15,000 and 26,000 coordinate points of the internal and external surfaces were collected respectively.

2.3 – Development of the data analysis protocol

All data was analysed using MATLAB R2020b (MathWorks, United States). The decision to use MATLAB was based on the flexibility it provides to make custom, purpose-built scripts. It was preferred over alternative options such as RedLux software packages (RedLux Ltd, UK), which operate as a 'black box' thus making the individual data manipulation steps difficult for the user to understand.

2.3.1 – Compensation of the probe radius

The data outputted by the CMM was in the form of Cartesian coordinates (x, y, z) relative to the centre of the probe head, and thus it was necessary for the coordinate data to be radially scaled by the probe radius (3-mm) to represent the true geometry of the liner's surface (Figure 2.7). To do this, a sphere was first fit to the coordinate data (see Section 2.3.2 for further details) to determine the true centre of rotation of the bearing surface and thus the desired origin (O') of the coordinate system. This was done to correct for any inaccuracies introduced by the CMM, which could be bias towards the worn regions due to the low number of sampling points. A translation of axes was performed to shift the coordinate data to the true origin O'.

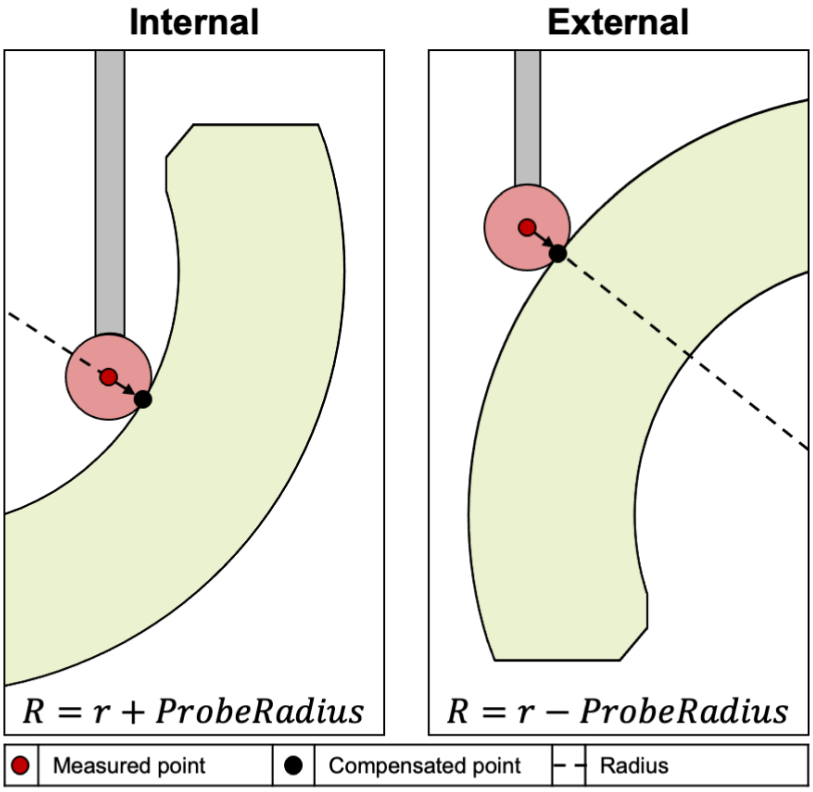

Figure 2.7 – Schematic illustrating the measured geometric data (red points), which is relative to the centre of the scanning probe, versus the compensated geometric data (black points), which accounts for the probe radius and thus reflects the true surface geometry.

Following this, the data was converted into spherical coordinates whereby each point was represented by one radial distance (r) and two angular values: the polar angle (θ) and the azimuthal angle (φ). The 3-mm radius of the probe was either added to (for internal surfaces) or subtracted from (for external surfaces) the radial distance, r, of each point (Figure 2.7).

2.3.2 – Generation of unworn reference surface

The unworn reference surface was approximated using a sphere fitting method similar to the approach described by Hua and Li for the analysis of conventional liners (Hua and Li, 2020). Several other published methodologies to analyse conventional liners also utilise a sphere as an approximation for the unworn reference geometry (Uddin et al., 2016).

To approximate the unworn reference surface, a sphere was fitted to the coordinate data. This was done using an algorithm developed by Alan Jennings, which utilises a least-squares method (Jennings, 2020). At each point, the deviation between the

radius of the sphere and the true radius (i.e., the distance between the point and the centre of the sphere) was calculated. Deviation values below 10 μm were considered to be within the manufacturing tolerance of DM liners (Adam et al., 2014). If the maximum deviation exceeded 10 μm, this indicated that a portion of the coordinate data used to generate the unworn reference geometry belonged to a worn region (i.e., beyond the accepted manufacturing variation) and thus the reference geometry was insufficient. In these circumstances, a threshold equal to 90% of the maximum deviation value was set. Any points with deviation values beyond this threshold were disregarded and a new set of coordinate points was created. A refined sphere was fit to the new set of points, and this process was repeated over several iterations until the maximum deviation of all points was below 10 μm. The final sphere was assumed to be an approximation of the unworn reference surface.

2.3.3 – Calculation of geometric variance

The geometric variance at each point was calculated as its deviation from the reference sphere (i.e., the difference between the true radius and radius of the reference sphere), as shown in Figure 2.8 and Figure 2.9 for the internal and external surfaces, respectively. Geometric variance was calculated using the raw coordinate data; no smoothing algorithms were applied. Positive geometric variance values denote penetration into the surface, whilst negative geometric values represent protrusion. It is important to note that geometric variance may be caused by either material loss (i.e., wear) or deformation; the method cannot distinguish between the two.

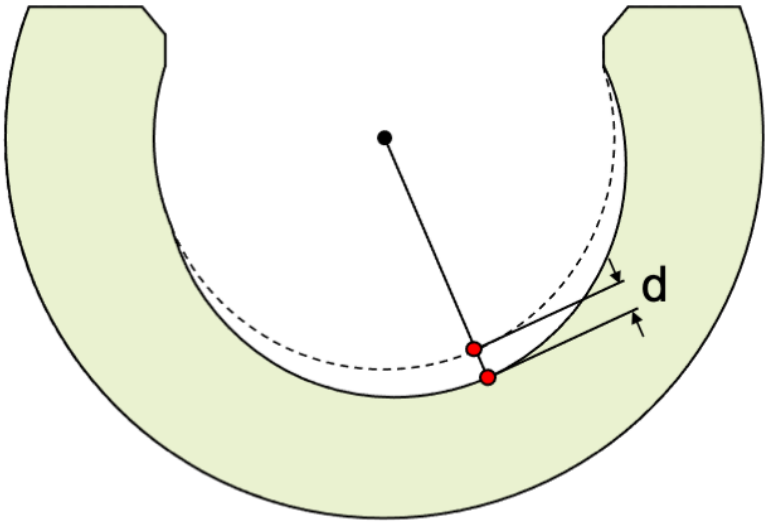

Figure 2.8 – Schematic illustrating how the penetration depth, d, was calculated for points taken along the internal surfaces of DM liners. The solid line represents the worn surface. The dotted line represents the unworn reference geometry.

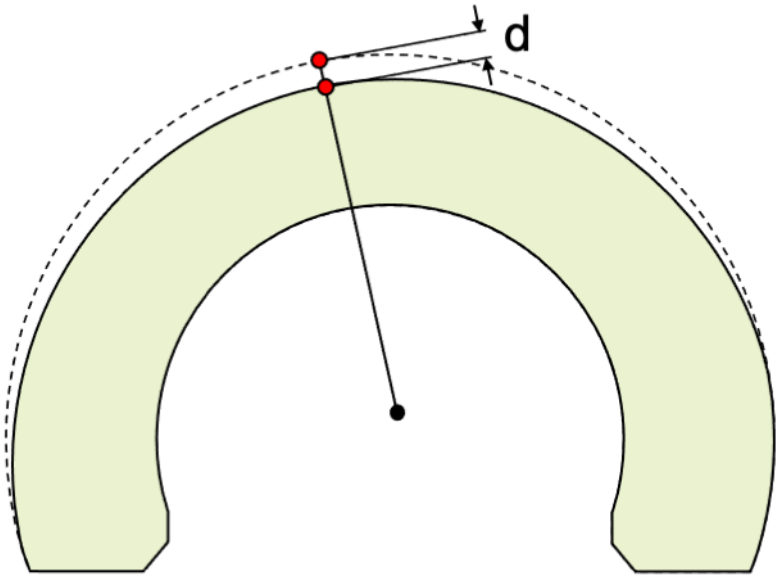

Figure 2.9 – Schematic illustrating how the penetration depth, d, was calculated for points taken along the external surfaces of DM liners. The solid line represents the worn surfaces. The dotted line represents the unworn reference geometry.

2.3.4 – Calculation of volumetric change

For each individual surface, the Delaunay triangulation function in MATLAB (version R2020b) was utilised to apply a triangular mesh to the raw coordinate data. This determined a set of triangular grids connecting each of the raw coordinate points,

referred to as nodes, within a set constraint of edges. For each individual triangular grid, the surface area and mean geometric variance was determined. The surface area was calculated using Heron's formula (Equation 2.1) which determined the area of a triangle using its semi-perimeter (*s*) and individual side lengths (*a, b, c*). The mean geometric variance was determined by the average geometric variance of the triangular grid's three nodes. The volumetric change of the individual grid was calculated by multiplying the grid's surface area by its mean geometric variance. This approach is similar to previously validated methods for the assessment of volume change for retrieved conventional polyethylene liners (Uddin, 2014; Hua and Li, 2020).

$$Area = \sqrt{(s)(s-a)(s-b)(s-c)} \tag{2.1}$$

The volumetric change of a surface was equal to the summation of the volumetric change values from the individual grids within the mesh (Equation 2.2). The volumetric change of a component was determined as the sum of the volumetric change values of both the internal and external surfaces.

$$Volume\ change\ of\ the\ surface = \sum_{i=0}^{n} V_i \tag{2.2}$$

2.3.5 – Generation of surface deviation heatmaps

To visualise areas of wear/deformation, the coordinate data was plotted in two dimensions in the XY-plane, and each point was assigned a colour based on its geometric variance. Due to the liner's supra-hemispheric geometry, there are several points which overlap near the liner's equator (Figure 2.10) thus resulting in some of the geometric data becoming hidden. In order to avoid this, coordinate data from the upper hemisphere was represented in the heatmaps as an exploded view as shown in Figure 2.10. An example of a surface deviation heatmap from an in-vitro tested liner is shown in Figure 2.11.

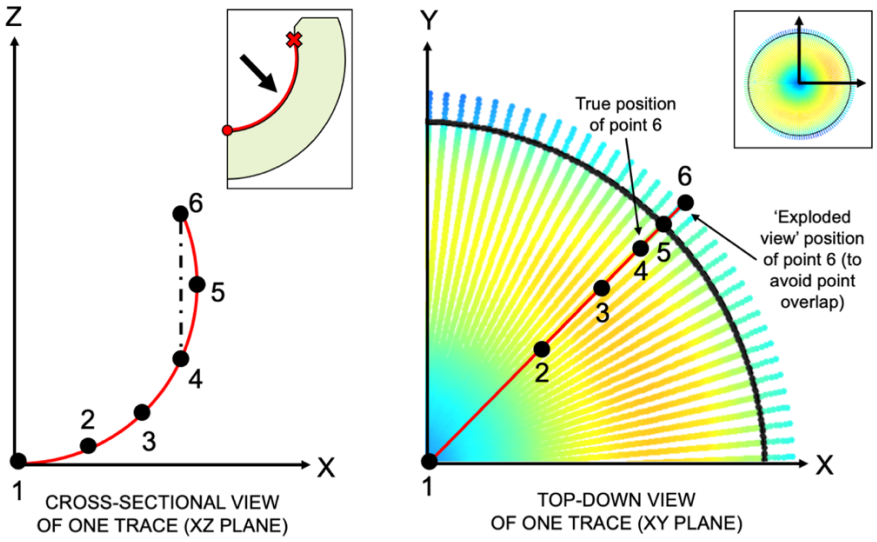

Figure 2.10 – Schematic illustrating the coordinate data from an individual trace in the XZ (left) and XY (right) planes. If coordinates are plotted in their true (X, Y) positions, this results in the upper hemisphere data being hidden due to an overlap of points. In order to avoid this, the upper hemisphere data is plotted as an expanded view as shown in orange.

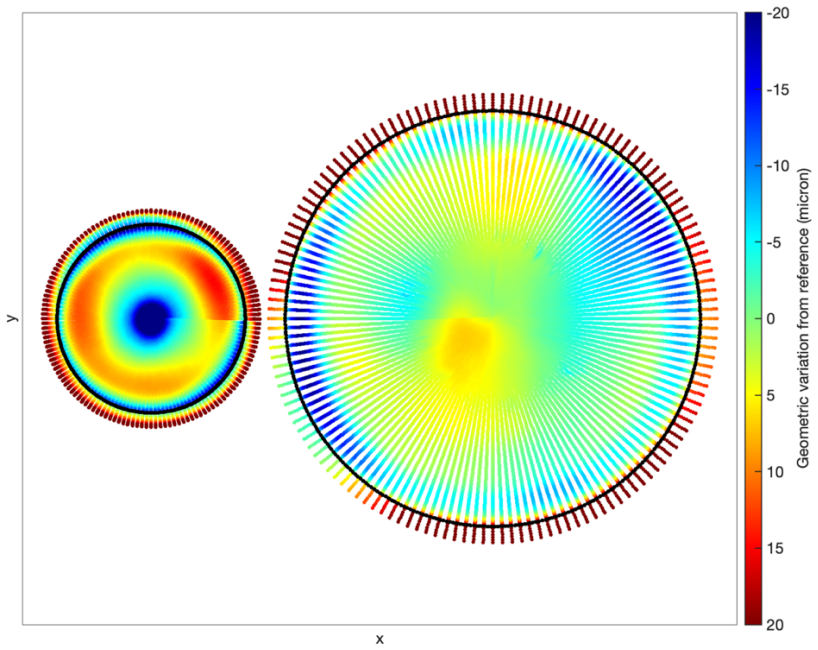

Figure 2.11 – Example of a surface deviation heatmap which depicts the internal (left) and external (right) surfaces of an in-vitro tested 69/28-mm DM liner. The surfaces are scaled proportionally to one another. The black line in each individual heatmap represents the position of the equator, thus separating the lower and upper hemisphere data. Positive geometric variance (i.e., red regions) represent areas of penetration, whilst negative geometric variance (i.e., blue regions) represent areas of protrusion with respect to the reference geometry.

It should be noted that the liner was rotated 180° about the Y-axis between the internal and external measurements. Therefore, to ensure registration of the internal and external surfaces, the external coordinate data was reflected about the Y-axis as shown in Figure 2.12.

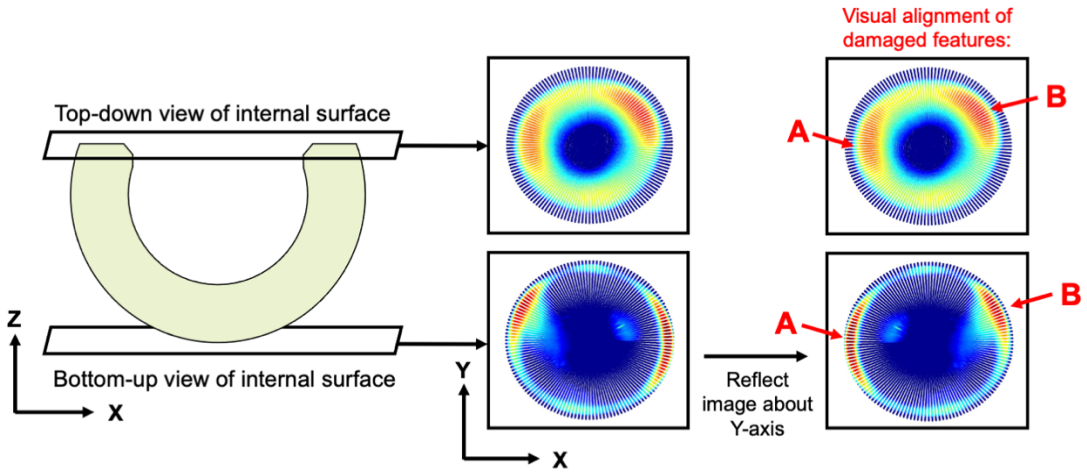

Figure 2.12 – When acquiring geometric data of DM liners, the internal surface was measured from a top-down perspective. The external surface must be rotated 180° however and thus its coordinate data reflects a bottom-up view of the component. Therefore, the external surface heatmap must be reflected about the Y-axis to represent the change in the component's position throughout the measurement process and thus provide appropriate surface registration. This results in a visual alignment of the damaged features, as shown by arrows A and B.

2.4 – Assessment of the geometric variance of unworn liners

As-manufactured DM liners (six 69/28-mm BI-MENTUM™ liners, see Table A1 of Appendix A) were assessed using the developed methodology to identify the geometric variance of components and thus determine a threshold which distinguishes variation due to manufacturing tolerance from wear/deformation of the surface.

The radius of the unworn reference sphere, which approximates the unworn geometry of the liner, had a variation (standard deviation) of ±6 μm (range: 17.3 μm) for the internal surfaces and ±2 μm (range: 4 μm) for the external surfaces. It is clear that the variation is greater for the internal surface, which may be explained by the

increased manufacturing complexity to machine a concave sphere with re-entrant features.

The geometric variance (mean, median, minimum, maximum) of the internal and external surfaces of the liners are reported in Table 2.2 and Table 2.3, respectively.

Table 2.2 – Geometric variance of the internal surface of six as-manufactured 69/28-mm DM liners.

Sample	Geometric variance (μm)			
	Mean	Median	Minimum	Maximum
1	0	0	-14	6
2	0	0	-16	6
3	0	1	-20	7
4	0	0	-18	6
5	0	0	-20	8
6	0	0	-16	6
Mean	0	0	-17	7
Range	0	1	6	2

Table 2.3 – Geometric variance of the external surface of six as-manufactured 69/28-mm liners.

Sample	Geometric variance (μm)			
	Mean	Median	Minimum	Maximum
1	0	0	-21	8
2	0	0	-23	8
3	0	0	-24	8
4	0	0	-22	10
5	0	0	-29	7
6	0	0	-27	10
Mean	0	0	-24	9
Range	0	0	8	3

The mean and median geometric variance of both surfaces was 0 μm, which suggests that the method to generate the reference geometry is appropriate as it closely matches the as-manufactured geometry. The magnitude of the minimum geometric variance was greater than the maximum geometric variance for all liners and surfaces

(internal and external). In all cases, the minimum geometric variance occurred at the pole whereby a small region of protruding material is present (Figure 2.13A) and thus may be considered an artefact of the manufacturing process. Other features on the as-manufactured surface deviation heatmaps include circumferential stripes on both surfaces (Figure 2.13B) and the presence of three penetrating regions on the upper hemisphere of the external surface (Figure 2.13C) which was likely due to the use of a tripod grip during the manufacturing process.

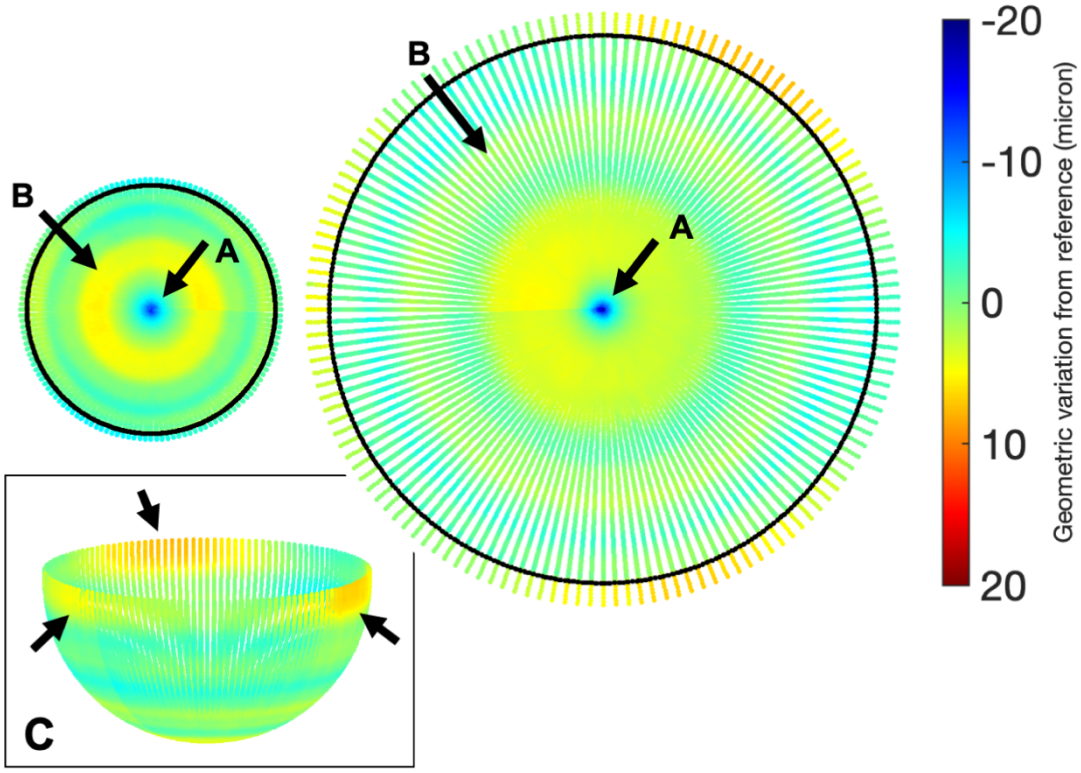

Figure 2.13 – Surface deviation heatmap of Sample 1, depicting a small region of protruding material at the pole (A) and a circumferential stripe (B) on each of the surfaces. Three penetrating regions were also noted on the upper hemisphere of the external surface (C).

2.5 – Method repeatability

2.5.1 – Methods

The articulating surfaces of one in-vitro tested 69/28-mm BI-MENTUM™ DM liner were measured on five separate occasions using the developed method. The liner was provided by DePuy Synthes (Leeds, UK), and further information about the in-vitro testing methodology applied to the liner is described in Section 2.6.1.1. An in-vitro tested liner was chosen for this analysis to ensure the characterisation

methodology was capable of repeatably assessing the surfaces of a damaged component (i.e., in which the reference geometry must be approximated from the unworn regions).

The liner was orientated in the same position during the first three measurements (i.e., 0° position), and then rotated 90° and 180° clockwise from the original starting position for the final two repeats. Several outputs were recorded, including the radius of the unworn reference sphere, geometric variance (mean, median, minimum, maximum) and volumetric change of each surface. Surface deviation heatmaps were also qualitatively assessed for similarity.

2.5.2 – Results

The unworn reference sphere was approximated in a consistent manner throughout the study. The radius of the internal reference sphere varied by a standard deviation of ±0.002 mm (range: 0.004 mm) between the repeats. For the external surface, the standard deviation of the reference sphere radius was ±0.001 mm (range: 0.001 mm).

The geometric variance and volumetric change data for the internal and external surfaces are reported in Table 2.4 and Table 2.5, respectively. The total volumetric change (i.e., the sum of the internal and external volumetric change) was 46.88 ± 0.80 mm^3 (range: 2.00 mm^3).

Table 2.4 – Geometric variance and volumetric change of the internal surface.

Repeat	Geometric variance (µm)				Volumetric change (mm^3)
	Mean	Median	Minimum	Maximum	
0° (Repeat 1)	-3	-2	-42	59	29.24
0° (Repeat 2)	-3	-2	-41	58	30.38
0° (Repeat 3)	-3	-2	-42	58	30.64
90°	-3	-2	-42	58	31.55
180°	-3	-2	-42	57	31.07
Mean	-3	-2	-42	58	30.58
St dev	0	0	0	1	0.87

Table 2.5 – Geometric variance and volumetric change of the external surface.

Repeat	Geometric variance (μm)				Volumetric change (mm^3)
	Mean	Median	Minimum	Maximum	
0° (Repeat 1)	2	0	-20	40	16.84
0° (Repeat 2)	2	0	-19	40	16.70
0° (Repeat 3)	2	0	-19	41	16.29
90°	2	1	-21	42	14.68
180°	2	1	-19	44	17.01
Mean	2	0	-20	41	16.30
St dev	0	1	1	2	0.95

There were no qualitative differences noted in the surface deviation heatmaps between the five repeats, apart from the change in component orientation in the latter two measurements (i.e., rotation of 90° and 180°).

2.5.3 – Discussion

Geometric measurements were collected from the internal and external surfaces of one in-vitro tested DM liner on five separate occasions to assess the repeatability of the developed methodology. The method was shown to repeatably generate the unworn reference geometry over several occasions, with a variation in the reference radius as low as ±2 μm for the internal surface and ±1 μm for the external surface. Additionally, the geometric variance (mean, median, minimum, and maximum) varied by a maximum of ±2 μm and the volumetric change had a variation of less than 1 mm^3. This suggests that the methodology, including the data collection and data analysis protocols, is highly repeatable and robust (i.e., unaffected by orientation of the component).

2.6 – Method verification

To assess the reliability of the developed methodology, two verification studies were performed. The aim of the first, which is described in Section 2.6.1, was to compare the method's quantitative outputs (i.e., volumetric change) against gold-standard gravimetric data from in-vitro tested samples. The aim of the second study (see Section 2.6.2) was to determine whether the methodology was able to detect changes to the surface geometry through the surface deviation heatmaps.

2.6.1 – Verification of the quantitative data

2.6.1.1 – Materials and methods

In-vitro tested DM liners were assessed using the developed method, and the results were compared against known gravimetric data to assess the reliability of the method's quantitative output.

In-vitro tested BI-MENTUM™ DM liners were provided by DePuy Synthes for this analysis. Two material groups were assessed: UHMWPE (n=7) and ALTRX (n=7). The UHMWPE liners were manufactured from GUR 1020 and gamma sterilised in air. The ALTRX samples were manufactured from GUR 1050 and moderately cross-linked at 7.5 megarads. All liners were dimensionally suited for 69/28-mm bearings.

Five components from each material group were subjected to experimental hip simulator testing, following the ISO 14242-1 loading and displacement conditions for eight million cycles (Mc). The remaining components were used as loaded soak controls to correct for any fluid absorption. The components were gravimetrically assessed before testing and after every 0.5 Mc of testing. At each measurement point, the femoral head and liner were disassembled to allow for the polyethylene to be cleaned and weighed. The volume loss of each sample was determined by dividing the gravimetric weight loss by the density of the polyethylene (0.934 g/cm^3). It should be noted that all experimental testing and gravimetric weighing of the components was conducted by DePuy Synthes (Leeds, UK) and therefore is not the direct work of the author.

The articulating surfaces of each liner were then geometrically assessed using the developed methodology. Quantitative outputs including the nominal radius of the reference sphere, maximum geometric variance and volumetric change were recorded for each sample. Additionally, surface deviation heatmaps were qualitatively assessed to identify any obvious signs of wear/deformation.

2.6.1.2 – Results

The mean gravimetric volume loss of the UHMWPE samples was 76.50 ± 30.17 mm^3 (range: 76.40 mm^3). Data was not supplied for the soak controls or for the ALTRX samples which experienced a net increase in weight due to fluid absorption.

The geometric analysis revealed the maximum geometric variance of the UHMWPE samples to be 78 ± 27 μm (range: 71 μm) for the internal surface and 42 ± 8 μm (range: 20 μm) for the external surface. The corresponding values for the ALTRX components were 65 ± 26 μm (range: 62 μm) and 7 ± 2 μm (range: 4 μm), respectively.

The geometric volume change of the UHMWPE and ALTRX samples was 43.28 ± 26.17 mm^3 (range: 72.66 mm^3) and 58.10 ± 4.62 mm^3 (range: 10.77 mm^3), respectively. There was a poor correlation between the gravimetric volume loss and geometric volume change data, with a Pearson correlation coefficient, r, of -0.43 (Figure 2.14).

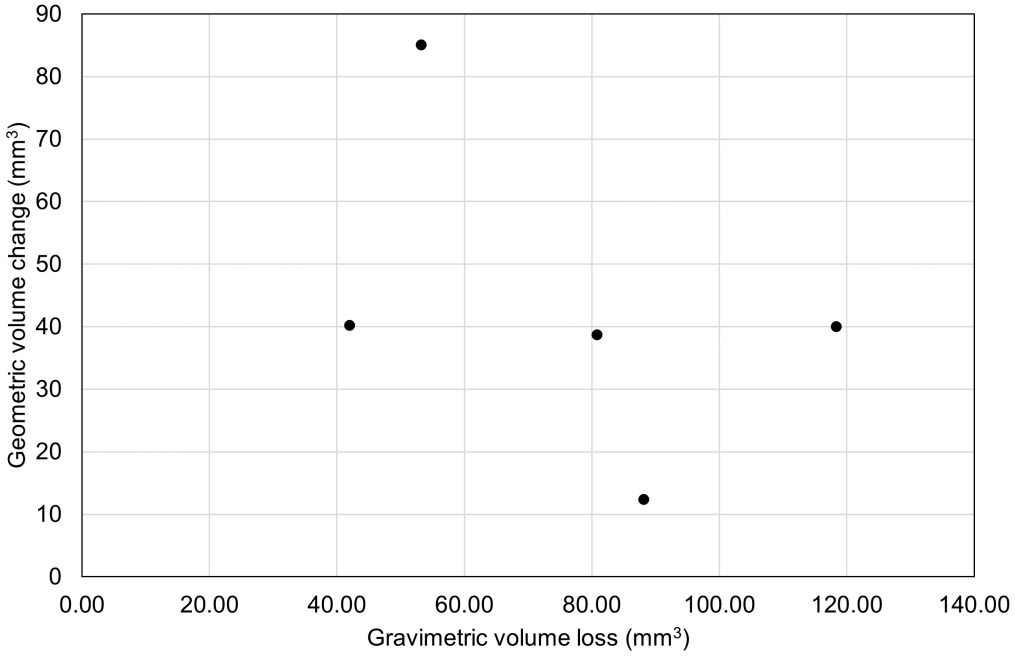

Figure 2.14 – Gravimetric volume loss versus geometric volume change data, which revealed a poor association between the two variables (Pearson correlation coefficient, r, of -0.43).

The surface deviation heatmaps revealed several geometric features on the articulating surfaces of the in-vitro tested liners, including areas of circumferential, crescent-shaped, and circular damage. However, the ALTRX samples displayed less damage than the UHMWPE samples on visual inspection of the heatmaps (Figure 2.15). Additionally, there was a circumferential region of positive geometric variance (i.e., penetration) identified on the internal surface of all samples, including the controls, adjacent to the retentive bore as shown in Figure 2.16.

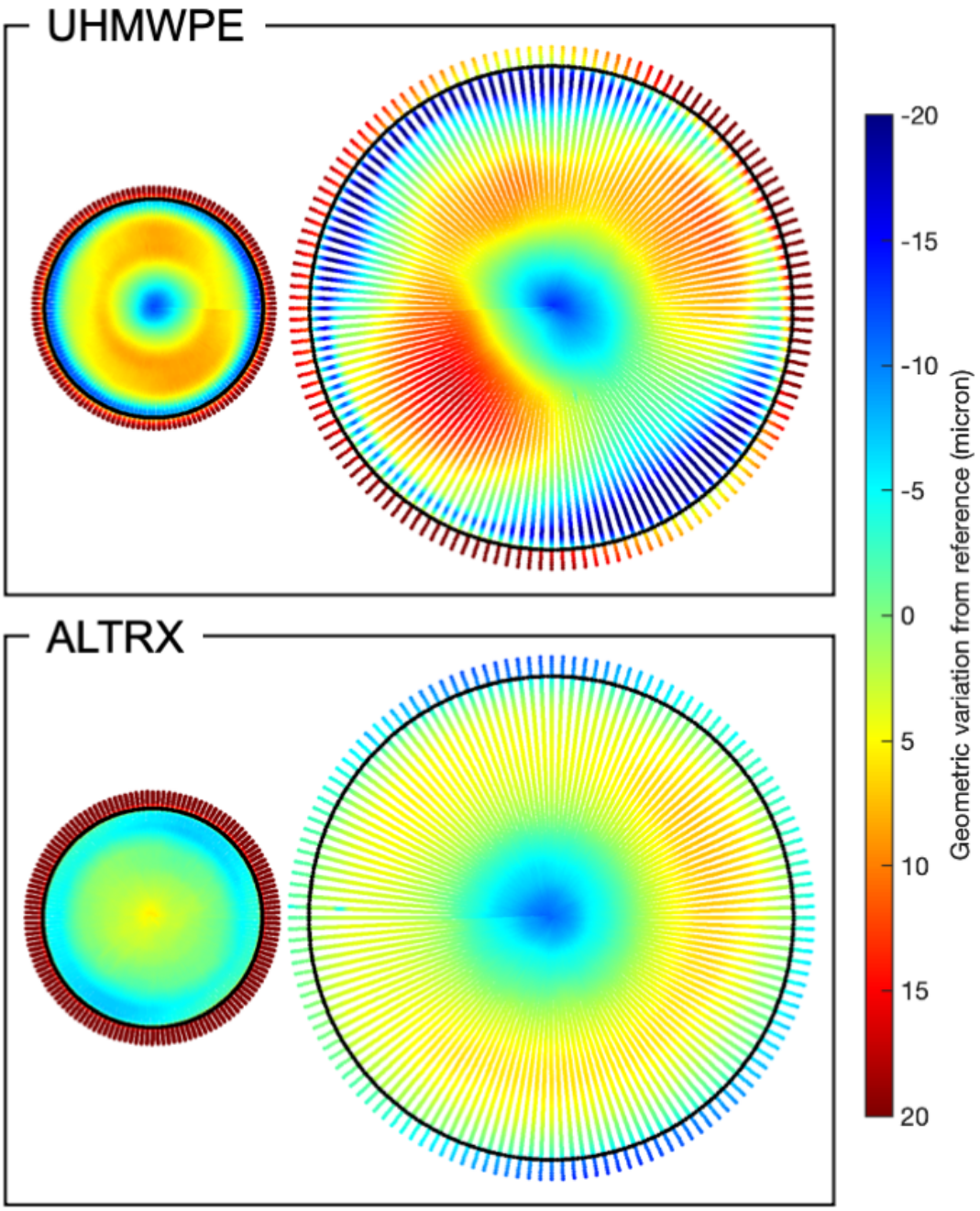

Figure 2.15 – Example of surface deviation heatmaps from the in-vitro tested DM liners, which included two material groups: UHMWPE (top) and ALTRX (bottom). The UHMWPE samples displayed several damage patterns, including circumferential wear stripes (as seen on the internal surface) and asymmetric wear (as seen on the external surface). In general, the ALTRX samples appeared less damaged than the UHMWPE group.

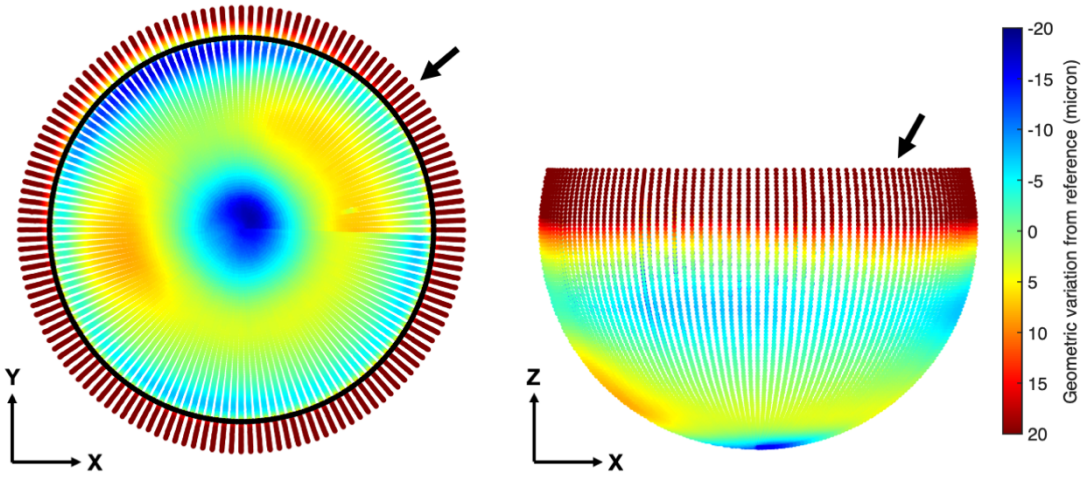

Figure 2.16 – Example of the circumferential region of positive geometric variance (i.e., penetration) noted on the internal surfaces of all samples.

2.6.1.3 – Discussion

A validation study was conducted to determine whether geometric data was a suitable metric for the assessment of liner wear, particularly when alternatives such as the gold-standard gravimetric approach are not possible e.g., a retrievals analysis where no pre-service data is available. The results of the study showed a poor correlation between gravimetric volume loss and geometric volume change (r = -0.43). This may be explained by the difference in what these individual metrics measure; gravimetric volume loss reflects wear (i.e., material loss) whereas geometric volume change also accounts for deformation of the sample. In addition, the gravimetric measurements were taken with the liners in a soaked condition (i.e., after being submerged in deionised water for a minimum of two weeks) whereas the geometric measurements were taken several months later whilst the liners were in a dry state. It is unknown whether measurement of the polyethylene liners in a soaked condition may have increased the reliability of the results due to swelling of the polyethylene.

Additionally, closer inspection of the surface deviation heatmaps revealed a characteristic ring of uniform deformation present on the internal surface of all samples, including the load controls. This feature has not been identified on pristine samples which were previously assessed. Therefore, it is hypothesised that this damage was caused by the successive assembly and disassembly of the femoral head and liner via the snap-fit mechanism. This process was repeated on 17 occasions throughout the duration of the in-vitro testing to facilitate cleaning and gravimetric assessment of the liners. This theory would explain both the location and

morphology of the deformed region. The damage is uniform and located in the upper hemisphere of the internal surface adjacent to the retentive bore, which is consistent with the damage expected when uniaxially removing the femoral head (see Figure 2.17).

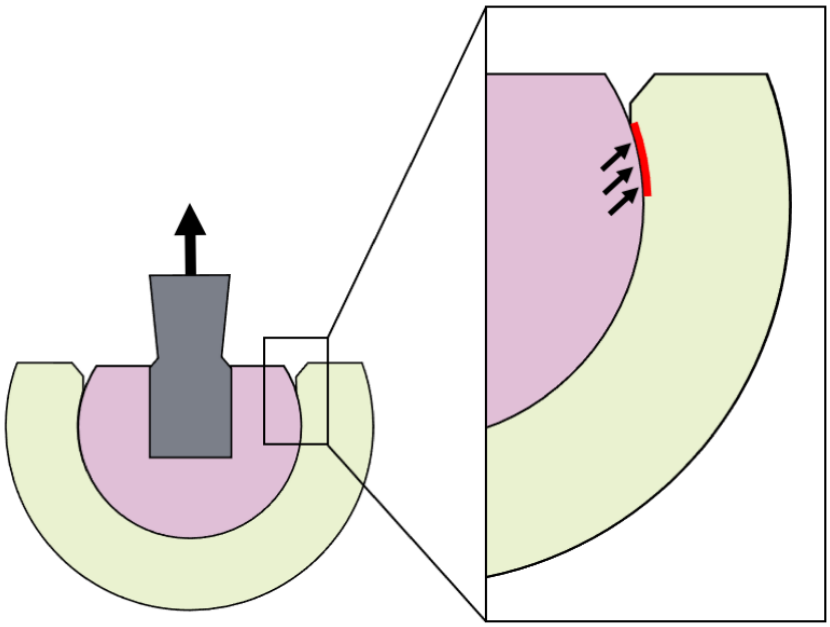

Figure 2.17 – Schematic illustrating the expected damage to a DM polyethylene liner, caused by uniaxially removing the femoral head. The damage is expected to be in the upper hemisphere of the internal surface, adjacent to the retentive bore and should be uniform across the circumference of this region.

Interestingly, the depth of the damaged region varied between samples. However, this variation can be explained by the variation in the nominal radii of the samples as shown in Figure 2.18. Samples with a larger nominal radius had an increased clearance for the femoral head to be introduced and removed and thus displayed a damaged region with a reduced depth. The ALTRX samples appeared to have less variation in this depth, although this can be explained by a sixfold difference in the range of nominal radii between the UHMWPE (range: 0.066 mm) and ALTRX (range: 0.010 mm) samples.

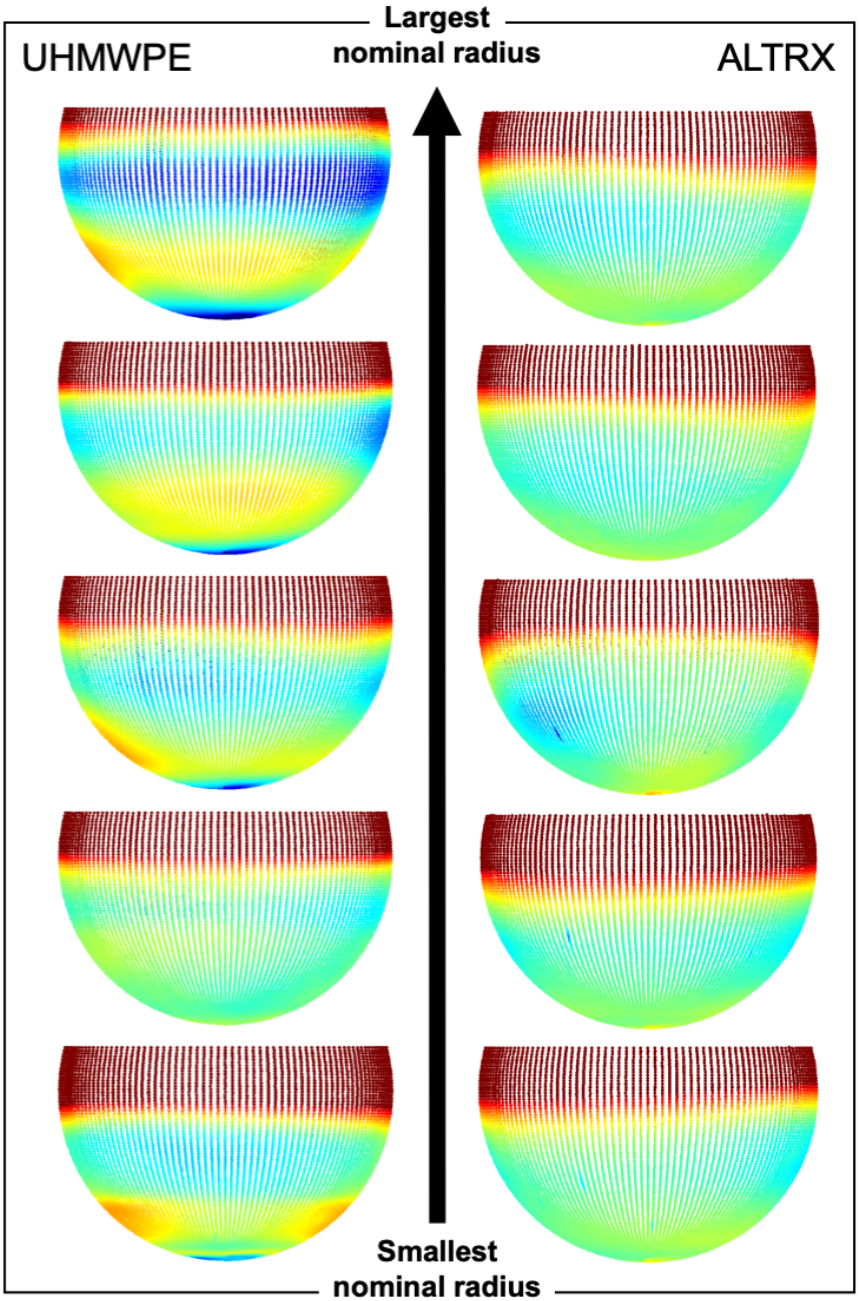

Figure 2.18 – Schematic illustrating the effects of the nominal radius of the internal surface on the extent at which the area adjacent to the retentive bore becomes damaged. All heatmaps are shown as a side-on view (XZ plane) of the liners. Among the UHMWPE group, it is clear that samples with an increased nominal radius display less damage in this region. This relationship is less clear in the ALTRX group however this can be explained by a sixfold decrease in the variation of the nominal radii of this group when compared to the UHMWPE samples.

The ring of damage observed on the internal surface of the samples has an effect on the geometric volume change and thus could be a contributing factor to describe the

poor association between the gravimetric and geometric datasets. In fact, the majority of the internal surface's volume change occurred in the upper hemisphere as seen in Table 2.6. This data also describes minimal volumetric changes to the lower hemisphere, which may be the result of a low degree of damage to the surface. However, a more likely explanation is that any regions of negative geometric variance (i.e., protrusion) are masking the effects of positive geometric variance (i.e., penetration). For instance, it is known that there is a region of protrusion at the pole of these surfaces as described in Section 2.4. It is possible that the volume change algorithm could be modified to exclude such regions so that penetration into the surface, which will most accurately represent wear and thus theoretically yield values closer to the gravimetric data, is solely characterised and this will be discussed in the future work and recommendations of this chapter.

Table 2.6 – Volumetric change data for the internal surface of five in-vitro tested samples assessed in this study.

Sample	Volumetric change (mm^3)		Total volumetric change (mm^3)	% Volume Change due to Upper Hemisphere
	Lower hemisphere	Upper hemisphere		
UHMWPE 1	-3.80	29.73	25.93	115%
UHMWPE 2	3.16	82.56	85.73	96%
UHMWPE 3	-1.10	52.74	51.64	102%
UHMWPE 4	-0.11	28.23	28.12	100%
UHMWPE 5	0.08	61.06	61.14	100%
Mean	-0.35	50.86	50.51	103%

In conclusion, the use of quantitative metrics (i.e., volumetric change) is not recommended for this methodology due to its poor correlation with gravimetric data and thus the difficulty involved in comparing geometric volume change with metrics available in the literature. Instead, the methodology should be used as a semi-quantitative tool to visualise areas of wear/deformation on the articulating surfaces of DM liners. The study has also identified a region of circumferential damage seen consistently across the cohort of samples. This damage was hypothesised to be caused by the frequency of component assembly and disassembly throughout the test. It is critical to understand whether component assembly has a compounding and

damaging effect on DM liners and thus this should be investigated in greater detail in future studies.

2.6.2 – Verification of the qualitative data

In summary, the external surfaces of five DM polyethylene liners were assessed which contained gross regions of surface damage visible by eye. This included one in-vitro tested and four retrieved components. The objective of this study was to visually compare regions of surface damage against the surface deviation heatmaps to verify the methodology was capable of detecting and accurately depicting these regions. The internal surfaces of the components were excluded from this verification analysis due to their poor visibility (i.e., due to their supra-hemispheric geometry) thus making it challenging to visually inspect the surfaces for regions of damage.

2.6.2.1 – Methods

One in-vitro tested liner (53/28-mm Serf Novae®) was used for this testing, which was provided by DePuy Synthes (Leeds, UK). First, the liner was cleaned by being ultrasonicated for 10 minutes in soapy water, rinsed, and then ultrasonicated for a further 10 minutes in 70% isopropanol. The liner was allowed to air dry and transferred to a temperature- and humidity-controlled environment for a minimum period of 48 hours. The pre-test weight of the liner was gravimetrically assessed with a Mettler XP205, by taking an average of five consecutive measurements within ±0.05 mg of one another. In addition, the starting geometry of the component was assessed using the geometric method described in this Chapter. A small amount of material was then artificially removed from the external surface of the in-vitro tested liner using a Dremel rotary tool, in a location approximately 45° from the pole as shown in Figure 2.19. After this, the liner was cleaned, weighed, and geometrically assessed using the methods described previously.

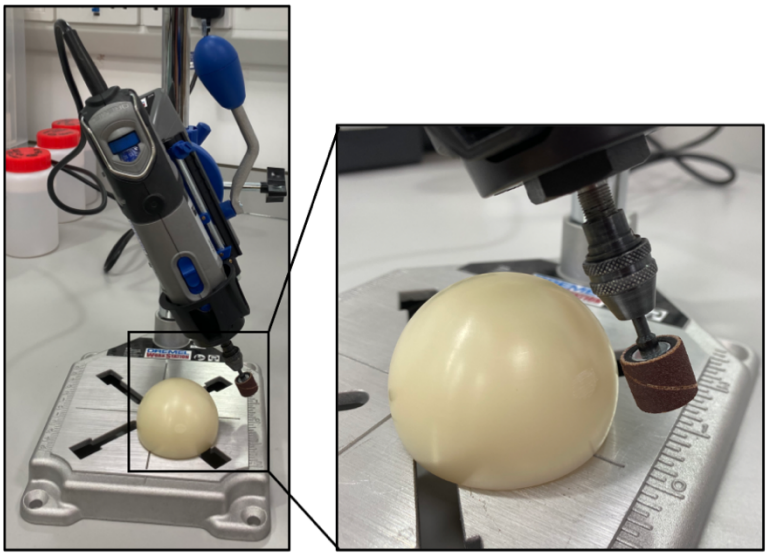

Figure 2.19 – Dremel setup for the removal of material from the external surface of a DM liner.

In addition, four retrieved DM polyethylene liners were assessed. These were sourced from ethically approved retrievals collection programs at Dartmouth College (IRB CPHS: STUDY00022199), which were provided to the University of Leeds on loan following approval from the Faculty Research Ethics Committee (MEEC 20-025), and the University of Leeds (NRES IRAS study number 18/NW/1707). These components were later assessed in a comprehensive retrieval analysis detailed in Chapter 3 (Retrievals 11, 15, 17, and 19), where further details relating to the components and their associated patient information are specified. In summary, two liners (Retrievals 11, 17) presented with deep penetrating regions whilst another (Retrieval 19) had four protruding, circular marks. Finally, Retrieval 15 featured a C-shaped indentation which was the result of contact with the acetabular shell during extra-articular dislocation of the femoral head and liner. The surfaces were geometrically assessed using the described methodology, and the surface deviation heatmaps were inspected for the presence of these damaged regions which were visually compared to the samples.

2.6.2.2 – Results

A total of 1.39 mg (approximately 1.46 mm^3 in volume) was removed from the external surface of the in-vitro tested liner. Pre- and post-surface deviation heatmaps (Figure 2.20) demonstrated the formation of a damaged region which closely resembled the surface damage visually inspected by eye. In addition, damage features observed on

the retrieved DM liners were clearly visible on the surface deviation heatmaps as exampled in Figure 2.21.

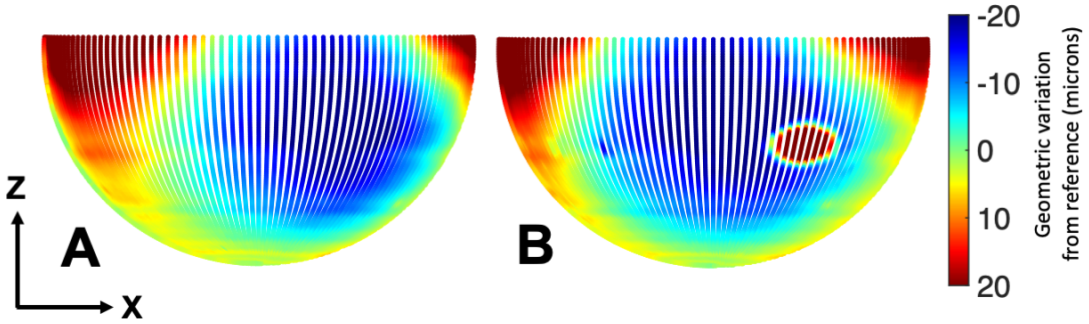

Figure 2.20 – Pre- (A) and post-test (B) surface deviation heatmaps of the external surface of one liner, which depicts the formation of a damaged region following the artificial removal of material using a Dremel.

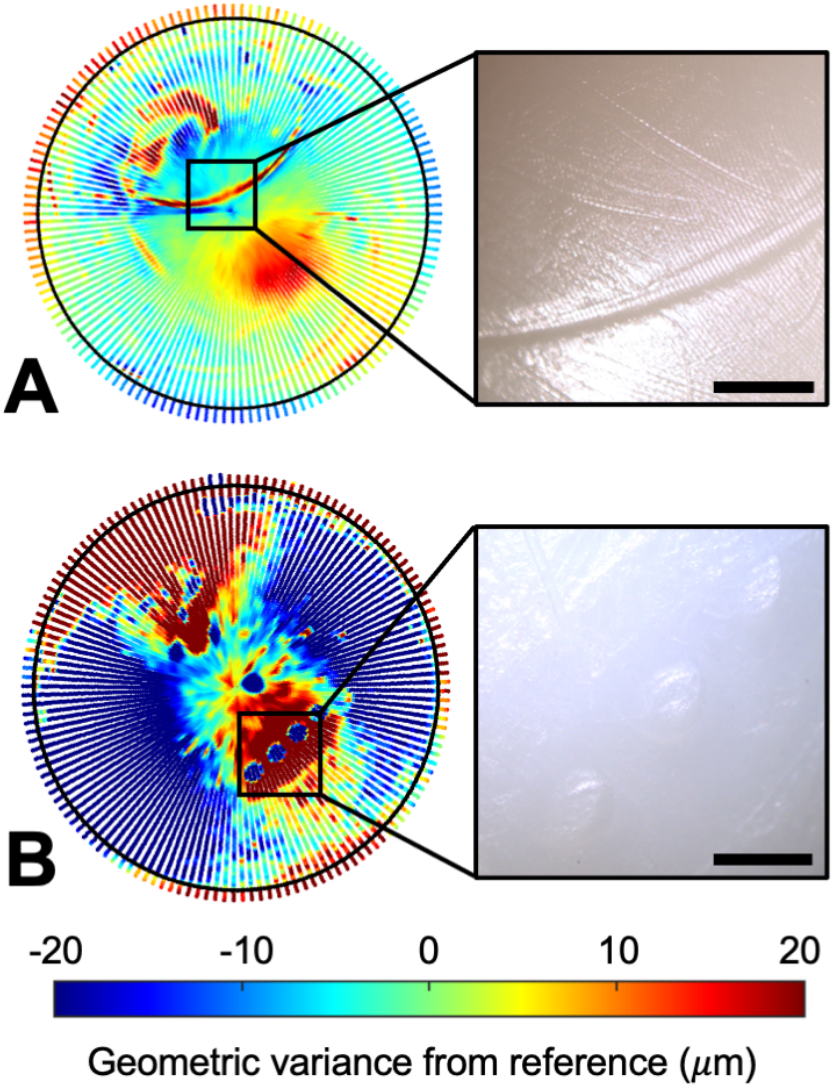

Figure 2.21 – External surface deviation heatmaps of Retrieval 15 (A) and 19 (B), and corresponding microscope images. Scalebar represents a unit of 2 mm.

2.6.2.3 – Discussion

This study assessed the external surfaces of one in-vitro tested and four retrieved DM liners to visually compare regions of gross surface damage to the surface deviation heatmaps produced by the geometric assessment methodology. Agreement between the visual inspection and surface deviation heatmap findings were found. Therefore, this study verified that the methodology could successfully detect changes in the surface geometry of DM liners without the need for pre-service information relating to the original geometry of the components. This suggests that the methodology is able to accurately approximate the pre-service reference geometry of these components using the sphere fitting algorithm described in Section 2.3.2.

2.7 – Method summary

The final CMM-based characterisation methodology developed as part of this thesis is described in Figure 2.22.

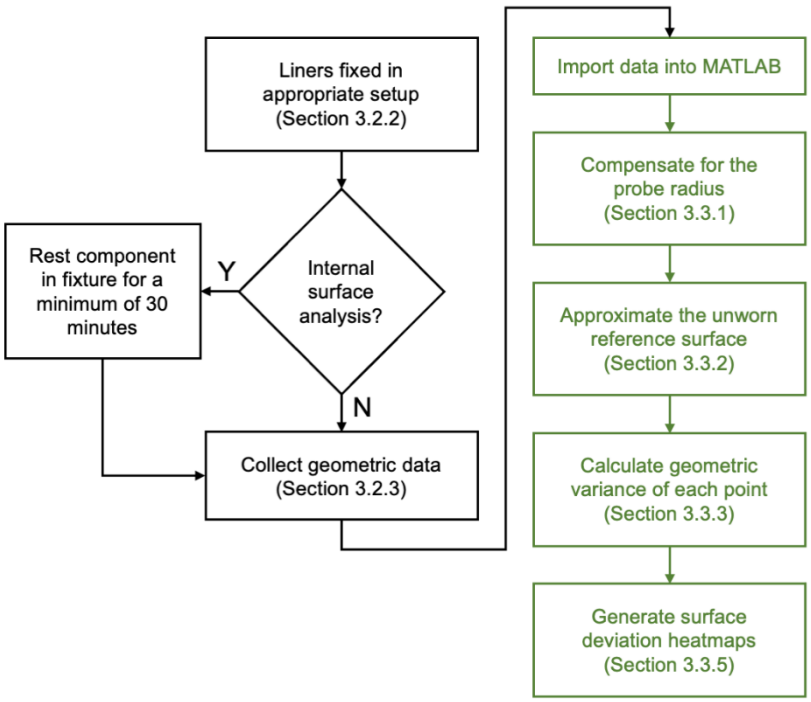

Figure 2.22 – Flowchart describing the final method for the characterisation of DM liners. Steps written in black are part of the data collection process, whilst steps written in green represent steps for the data analysis process.

2.8 – Discussion

Geometric assessment methodologies described in the literature were deemed unsuitable for the novel geometry (i.e., supra-hemispheric, or encapsulating, design) and function (i.e., articulation of both surfaces) of DM liners thus giving rise to the present study. Therefore, this chapter describes the successful development of a characterisation methodology to assess the articulating surfaces of DM liners for wear and/or deformation.

The described methodology has demonstrated an effective way to comprehensively acquire geometric data from both articulating surfaces of DM liners without requiring prior sectioning of the components or exclusions of large regions of the surface, as previously reported in the literature (Geringer et al., 2011; Adam et al., 2014;

D'Apuzzo et al., 2016). It should be noted that the method does exclude a small, circumferential region of the external surface adjacent to the rim (approximately 5-mm in depth), to avoid the probe from contacting the flat fixture plate. However, the majority of the external surface is still possible to measure using this methodology.

Additionally, the method benefits from an automated data analysis process which cannot be influenced by user input. It also does not require any pre-service data and thus is compatible to use with both in-vitro tested and retrieved liners of any size and from any manufacturer.

Due to the supra-hemispheric geometry of DM liners, it can be challenging to visually present the geometric data in a meaningful way. Three-dimensional surface deviation heatmaps provide accurate reflections of the surface geometry, but often require multiple viewpoints in order for the entire surface to be visualised. On the other hand, two-dimensional heatmaps are more simplistic to assess but require an exclusion of the upper hemisphere data in order to avoid point overlap. In this study, a unique two-dimensional heatmap format has been demonstrated which allows the entirety of the surface to be visualised.

The method has demonstrated that it is highly repeatable (Section 2.5) and can reliably generate surface deviation heatmaps (Section 2.6.2). However, verification testing demonstrated that the volume change data was unreliable and poorly correlated to known gravimetric data (Section 2.6.1). Although gravimetric and geometric data do not measure the same outcomes (i.e., gravimetric – wear; geometric – wear and deformation), studies have shown that it is possible to use geometric data to closely approximate gravimetric volume loss for conventional liners (Uddin, 2014; Hua et al., 2014; Hua and Li, 2020) though this was not the case for the developed method. Therefore, it is recommended that the described methodology is used exclusively as a semi-quantitative tool although it may be possible to re-introduce quantitative outcomes through further development and research.

The method has several additional limitations which should be recognised. Most notably, the method cannot distinguish between wear (i.e., material loss) and deformation (i.e., plastic flow). Therefore, the surface deviation heatmaps should be used to identify overall damage rather than wear and deformation as individual components. Additionally, the method cannot approximate volume change as previously discussed and thus is limited as a semi-quantitative tool.

Despite its limitations, the described methodology is a promising tool for the assessment of DM liners both within in-vitro testing and retrieval analyses applications. For in-vitro simulator testing, this method may be used as a complimentary tool alongside the standard gravimetric approach in order to track the development of surface damage throughout the test period. Additionally, this method may be used to assess retrieved liners whereby no pre-service information is available. By investigating the damage patterns observed on these surfaces, the in-vivo mechanics and failure modes of these complex bearings may be further understood.

2.9 – Conclusion

In conclusion, this chapter demonstrates the successful development of a geometric assessment methodology to visualise wear/deformation on the articulating surfaces of retrieved DM polyethylene liners. The method was shown to be repeatable, and its outputs were verified against regions of surface damage which were visibly identified on both retrieved and in-vitro tested components. The method benefits from an automated data analysis protocol which does not require any user input or component information (e.g., manufacturer, dimensions, etc). This methodology will be useful for the analysis of both retrieved and in-vitro tested DM liners. By assessing the development, morphology, and severity of damage regions (i.e., regions of penetrative or protruding geometric variance), the functional mechanisms of DM bearings may be better understood.

Chapter 3 –
Analysis of retrieved dual mobility bearings

3.1 – Introduction

There is a limited understanding about the in-vivo kinematic function and mechanical failure modes of Dual Mobility (DM) Total Hip Replacements (THRs), particularly with regards to the unconstrained polyethylene liner. Current joint registry data suggests that DM implants may exhibit higher failure rates than conventional THRs (National Joint Registry, 2021; American Joint Replacement Registry, 2022), although it is possible these outcomes may be confounded by patient factors such as pre-existing comorbidities and inherent risk of dislocation. In addition, there are concerns about failure modes unique to these bearings such as accelerated polyethylene wear (due to the introduction of a secondary, outer articulation of the liner) and intraprosthetic dislocation. This is in contrast to data from the literature which suggests that DM bearings show good in-vivo survivorship (98% at a mean of 8.5 years follow-up) and comparable wear performance to conventional THRs under both standard and adverse conditions (Saikko and Shen, 2010; Loving et al., 2015; Darrith et al., 2018). The analysis of retrieved (i.e., ex-vivo) implants may provide pertinent information about the biomechanical function and failure of these bearings under true physiological conditions, which cannot be obtained from alternative studies such as long-term survivorship data or in-vitro simulator tests. Retrieval analyses are particularly important as implant design and materials are improved, especially in the context of DM bearings as they are implanted more frequently, and their indications are broadened. Today, only a small percentage (2-3%) of revisions are due to implant failure therefore making it difficult for joint registries to identify these issues early on (Morlock et al., 2022).

Retrieval analyses of conventional THRs have been used to assess the surface damage (Bradford et al., 2004; Shon et al., 2005; Schroder et al., 2011; Pang et al., 2015) and linear or volumetric wear (Teeter, Naudie, et al., 2010; Bowden and Bergström, 2015; Wang et al., 2016; Hua and Li, 2020) of polyethylene liners. Additionally, retrieved femoral heads from conventional THRs have been investigated for signs of surface damage (Jasty et al., 1994) and roughening (Eberhardt et al., 2009; Merola et al., 2016). Whilst a wide range of retrieval analyses are available in the literature, a limited number of studies have assessed DM THRs. These predominantly focus on analysis of the polyethylene liner, which includes visual inspection of the surface to assess for damage (D'Apuzzo et al., 2016; Spece et al., 2018) or impingement (Adam et al., 2014; Nebergall et al., 2016; Laura, H.S. Hothi, et al., 2017; Scott et al., 2018). In addition, surface measurements of the liner have been facilitated using coordinate measuring machines (Adam et al., 2014; D'Apuzzo et al., 2016), microCT (Laura, H.S. Hothi, et al., 2017) and roundness measuring machines (Laura, H.S. Hothi, et al., 2017). There has been limited assessment of the remaining DM components, which includes the femoral head and acetabular shell. One exception to this is the analysis of modular acetabular shells for signs of corrosion, which has been investigated in several studies (Spece et al., 2018; Weitzler et al., 2019; Kolz et al., 2020).

Therefore, the aim of this study was to comprehensively assess retrieved DM components including the polyethylene liner, femoral head and acetabular shell using a variety of methodologies to improve our understanding of their biomechanical function. These included visual inspection techniques, a novel geometric assessment method (as discussed in Chapter 2) and contacting profilometry. This was the first study, to the author's knowledge, which assessed all articulating DM components including the femoral head and outer metal bearing (i.e., modular shell insert, or monobloc acetabular shell).

3.2 – Retrieved dual mobility bearings

A total of 16 implants were sourced by Dartmouth College (New Hampshire, USA) as part of an established IRB-approved retrievals collection program. These were provided to the University of Leeds on loan, following approval from the Faculty Research Ethics Committee (MEEC 20-025). Four additional implants were sourced following a search of an NRES-approved retrieval collection study at the University of

Leeds (18-NW-1707 ‘Study of Retrieved Orthopaedic Implants and Associated Tissues and Data’), resulting in a total of 20 retrieved sets of components available for this study. Further information regarding the retrieved components may be found in Table A2 of Appendix A.

The received components included polyethylene liners (n=20) and, when available, their corresponding femoral heads (n=17) and/or acetabular articulating component in the form of either a monobloc acetabular shell (n=4) or modular shell insert (n=8). Pertinent implant and anonymised patient data were also received including time in-vivo, reason for revision, patient BMI and side (left/right). A summary of the demographic information for each retrieval is described in Table 3.1.

Table 3.1 – Summary of DM retrievals collected for this study. Note – Inner and outer diameters of the polyethylene liners are rounded to the nearest mm. Two types of outer articulation components were received in this study: monobloc acetabular shells (components listed as 'MONO') or modular acetabular shell inserts (components listed as 'MOD').

Retrieval number	Liner device type	Bearing combination	Polyethylene liner		BMI	Time in-vivo (months)	Side (L/R)	Reason for revision	Other available components	
			Inner diameter	Outer diameter					Femoral head	Outer articulation
1	MDM	MoPoM	28-mm	42-mm	27.12	0.9	R	IPD	✓	✓ (MOD)
2	E1	MoPoM	28-mm	56-mm	26.79	3.7	R	Infection	✓	✓ (MONO)
3	MDM	MoPoM	28-mm	42-mm	24.82	12.4	R	Fracture	✓	✓ (MOD)
4	ADM	CoPoM	28-mm	56-mm	N/K	50.7	L	Metal wear	✓	✓ (MONO)
5	MDM	MoPoM	22-mm	38-mm	27.03	26.2	L	Instability	✓	✓ (MOD)
6	ADM	CoPoM	28-mm	46-mm	N/K	N/K	N/K	N/K	✓	
7	ADM	MoPoM	28-mm	46-mm	31.25	7.0	L	Loose	✓	✓ (MONO)
8	E1	N/K	28-mm	40-mm	43.71	1.5	L	Infection		
9	ADM	MoPoM	28-mm	46-mm	38.16	22.5	L	Loose	✓	
10	MDM	MoPoM	28-mm	46-mm	25.97	57.0	R	Loose	✓	✓ (MOD)
11	MDM	CoPoM	28-mm	46-mm	N/K	N/K	N/K	N/K	✓	✓ (MOD)
12	MDM or ADM	CoPoM	28-mm	50-mm	45.84	4.5	L	Loose	✓	✓ (MOD)
13	MDM	N/K	28-mm	42-mm	23.07	28.6	L	Loose		
14	MDM	MoPoM	22-mm	38-mm	21.19	42.9	R	N/K	✓	✓ (MOD)
15	E1	CoPoM	28-mm	54-mm	31.94	2.7	L	Dislocation	✓	

Retrieval number	Liner device type	Bearing combination	Polyethylene liner		BMI	Time in-vivo (months)	Side (L/R)	Reason for revision	Other available components	
			Inner diameter	Outer diameter					Femoral head	Outer articulation
16	MDM	N/K	28-mm	46-mm	27.02	14.7	R	Infection		
17	Novae	CoPoM	28-mm	54-mm	26.83	6.0	R	Pain	✓	
18	ADES	MoPoM	28-mm	42-mm	26.6	46.0	L	Fracture	✓	
19	Novae	MoPoM	28-mm	41-mm	24.9	N/K	L	Loose	✓	✓ (MOD)
20	Avantage	MoPoM	28-mm	48-mm	28.6	13.0	R	IPD	✓	✓ (MONO)

Abbreviations: N/K, Information not known; MDM®, Modular Dual Mobility® (Stryker; Kalamazoo, MI, USA); ADM®, Anatomical Dual Mobility® (Stryker); E1, Active Articulation™ E1® (Zimmer Biomet; Warsaw, IN, USA); Novae® (Serf); ADES (Dedienne Sante); Avantage® (Zimmer Biomet); IPD, intraprosthetic dislocation.

The retrievals were in-vivo for less than two years on average (20.0 ± 18.8 months) although the time in-vivo had a large range amongst the collection (0.9 to 57 months). In summary, half of the implants (n=10) were in-vivo for more than 12 months, seven were in-vivo for less than 12 months and three were unknown. Various reasons for revision were indicated amongst the collection, with the most common indication being 'loose' (n=6). Other reasons for revision included infection (n=3), instability or dislocation (n=2), periprosthetic fracture (n=2), Intraprosthetic Dislocation or IPD (n=2), metal wear (n=1) and pain (n=1). This information was unknown for three implants. Associated clinical notes revealed that two implants were retrieved with fibrous tissue identified at the sleeve (Sample 9) or cup (Sample 13).

The implants received in this study included six device types. The most common in this collection (n=13) was the Modular Dual Mobility® (MDM®) or Anatomic Dual Mobility® (ADM®) from Stryker (Kalamazoo, MI, USA). These consist of a highly cross-linked polyethylene liner (X3®; Stryker) which articulates against either a modular shell (MDM®) or a monobloc shell with integrated notches to prevent psoas impingement (ADM®). Four implants were manufactured by Zimmer Biomet (Warsaw, IN, USA), which included three Active Articulation™ E1® (annealed, vitamin-E infused liner) and one Avantage® implant. Two Serf Novae® and one Dedienne Sante ADES devices were included in the study, which all utilise a UHMWPE liner.

The bearing combinations of the retrieved implants included 11 Metal-on-Polyethylene-on-Metal (MoPoM) and six Ceramic-on-Polyethylene-on-Metal (CoPoM) devices (n=3 unknown). The majority of the implants utilised a head diameter of 28-mm, which articulated against varying thickness of polyethylene (range: 8- to 14-mm liner thickness).

It should be noted that all implants, with the exception of those revised for IPD, were revised with the head and liner intact and thus these components were disassembled in-house via a lever-out mechanism either at Dartmouth College or the University of Leeds. This process generated an observable indentation mark at the liner's chamfer, due to contact with the femoral neck during the lever-out process.

3.3 – Overview of the analysis

A comprehensive analysis of retrieved DM bearings was conducted, which included the assessment of DM polyethylene liners, femoral heads and acetabular shells as

described in Figure 3.1. In summary, the internal and external surfaces of the polyethylene liners were visually inspected (Section 3.4) and geometrically assessed (Section 3.6) to characterise surface damage. Additionally, the material composition of any identified embedded debris was determined using energy-dispersive x-ray analysis (Section 3.5) to determine possible origins of the third body particles. Furthermore, femoral heads and acetabular components were visually inspected for signs of surface scratching (Section 3.7). Please note that the term ‘acetabular components’ in this chapter refers to the outer articulating component which encompasses both monobloc acetabular shells and modular acetabular shell inserts which were received in the present study. In addition, a contacting profilometer was used to characterise the surface roughness of the femoral heads (Section 3.7). This analysis was not completed for the acetabular components due to limitations of the equipment.

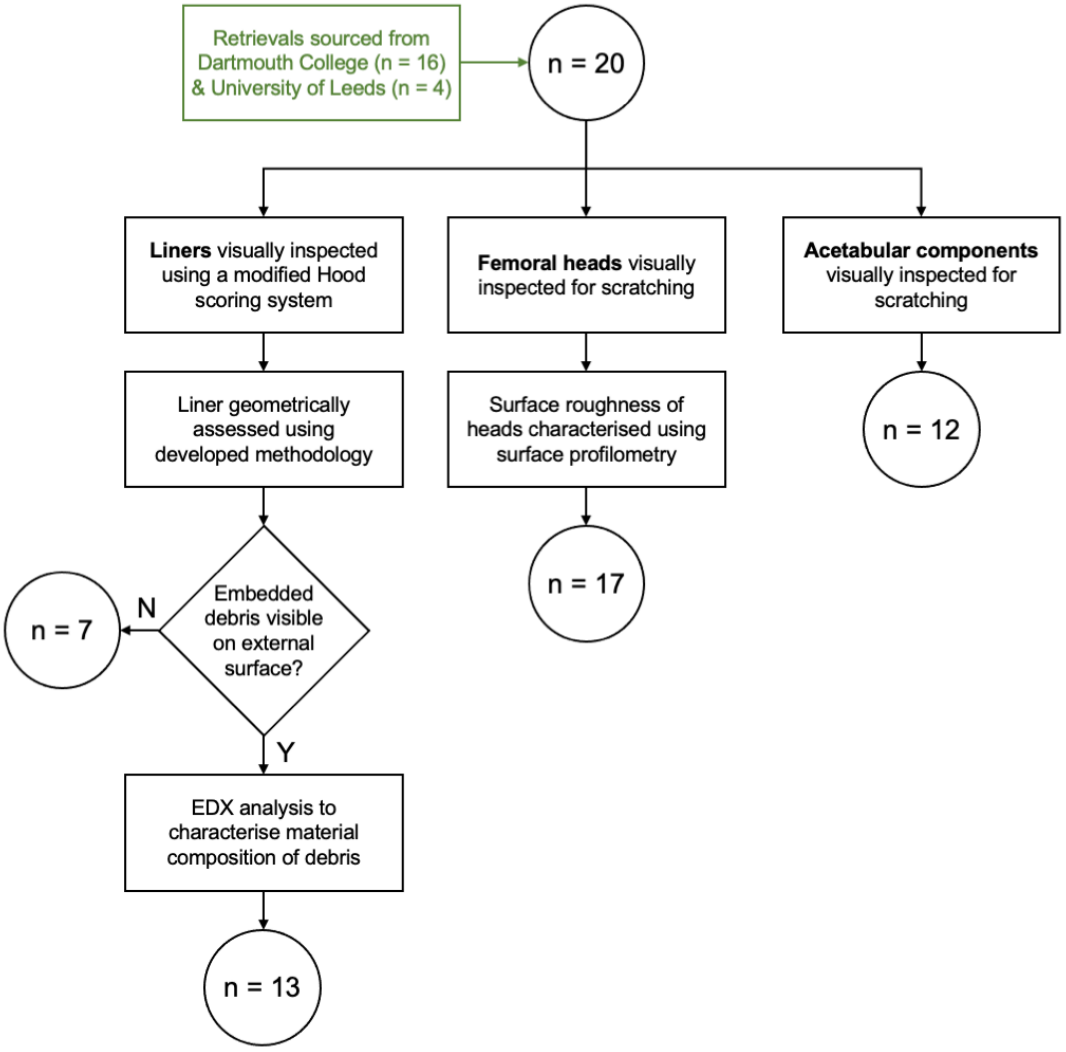

Figure 3.1 – Flowchart illustrating the analysis of retrieved DM bearings. Acetabular components refer to either monobloc acetabular shells (n=4) or modular acetabular shell inserts (n=8) which were received in this study.

3.4 – Visual assessment of retrieved DM liners

3.4.1 – Methods

The retrieved liners were visually inspected for signs of damage with a Nikon optical microscope and the damage was characterised through an adapted scoring system (Hood et al., 1983). Each surface was individually assessed for the presence of seven damage modes which included scratching, pitting, embedded debris, abrasion, delamination, burnishing, and deformation as defined in Table 3.2.

Table 3.2 – Damage modes characterised in the retrievals analysis. Definitions from Hood, Wright and Burstein (1983).

Damage mode	Definition
Scratching	Multi-directional indentations in the surface of the material
Pitting	Depressions (usually circular in shape) in the surface of the material
Embedded debris	Third body particles embedded into the surface of the material
Abrasion	Roughened polyethylene surface with a shredded or tufted appearance
Delamination	Removal of a plane of material due to sub-surface cracking
Burnishing	Highly polished regions on the surface, also denoted by a loss of machining marks
Deformation	Permanent deformation of the surface

For each damage mode, a binary scoring system was applied whereby a score of zero was assigned if the damage mode was not present and a score of one was assigned if the damage mode was identified anywhere on the surface. It's important to note that this scoring system assessed for the presence of damage, but it did not grade for its severity or extent. The assignment of severity scores may be subject to inter-rater variability, particularly for the internal surface which is challenging to visualise due to its supra-hemispheric, concave geometry. Additionally, the surfaces were not sub-divided (e.g., into quadrants) and instead each surface was graded as a whole. This was due to the unknown orientation of the liners in-vivo and their inherent mobility to change orientation throughout the in-vivo service period. The damage score for each surface was equal to the sum of the individual damage scores (range: 0 to 7), and the combined damage score was equal to the sum of the internal and external scores (range: 0 to 14).

Each liner was also assessed for the presence of an impingement-like notch at the chamfer (Figure 3.2) and for the presence of machining marks on each surface.

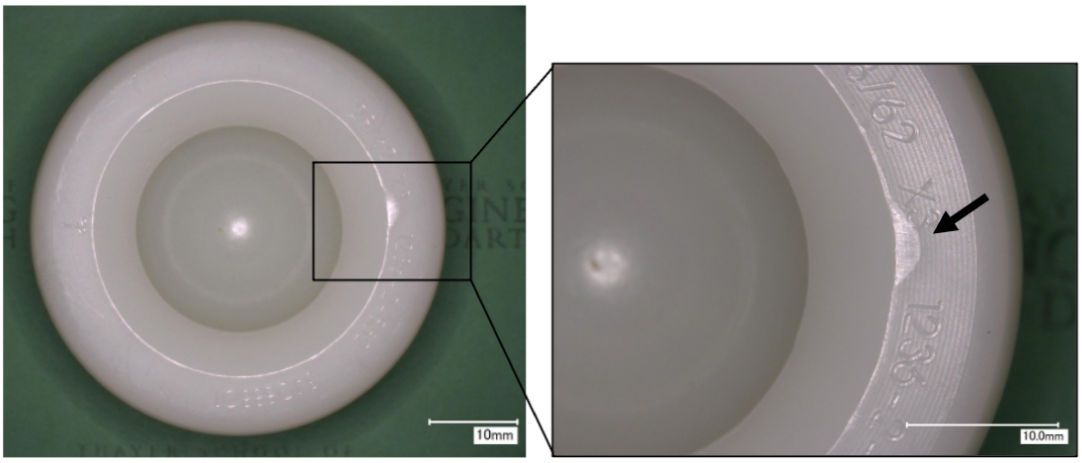

Figure 3.2 – Characteristic notch observed on the chamfer of retrieved DM liners.

3.4.2 – Results

The frequency of each damage mode identified amongst the collection of retrieved liners is described in Table 3.3. Examples of these damage modes are shown in Figure 3.3. The average internal, external, and combined damage scores were 2.7 ± 0.9, 3.7 ± 1.0 and 6.4 ± 1.4, respectively. The internal and external damage scores were compared with a paired t-test (IBM SPSS Statistics, Version 27), which revealed a significant difference between the two groups (p=0.002).

Table 3.3 – Frequency of damage modes observed on the internal and external surfaces of retrieved DM liners (n=20).

Damage mode	Frequency of damage	
	Internal surface	External surface
Scratching	20 (100%)	20 (100%)
Pitting	17 (85%)	18 (90%)
Embedded debris	5 (25%)	13 (65%)
Abrasion	2 (10%)	9 (45%)
Delamination	0 (0%)	2 (10%)
Burnishing	10 (50%)	3 (15%)
Deformation	0 (0%)	9 (45%)

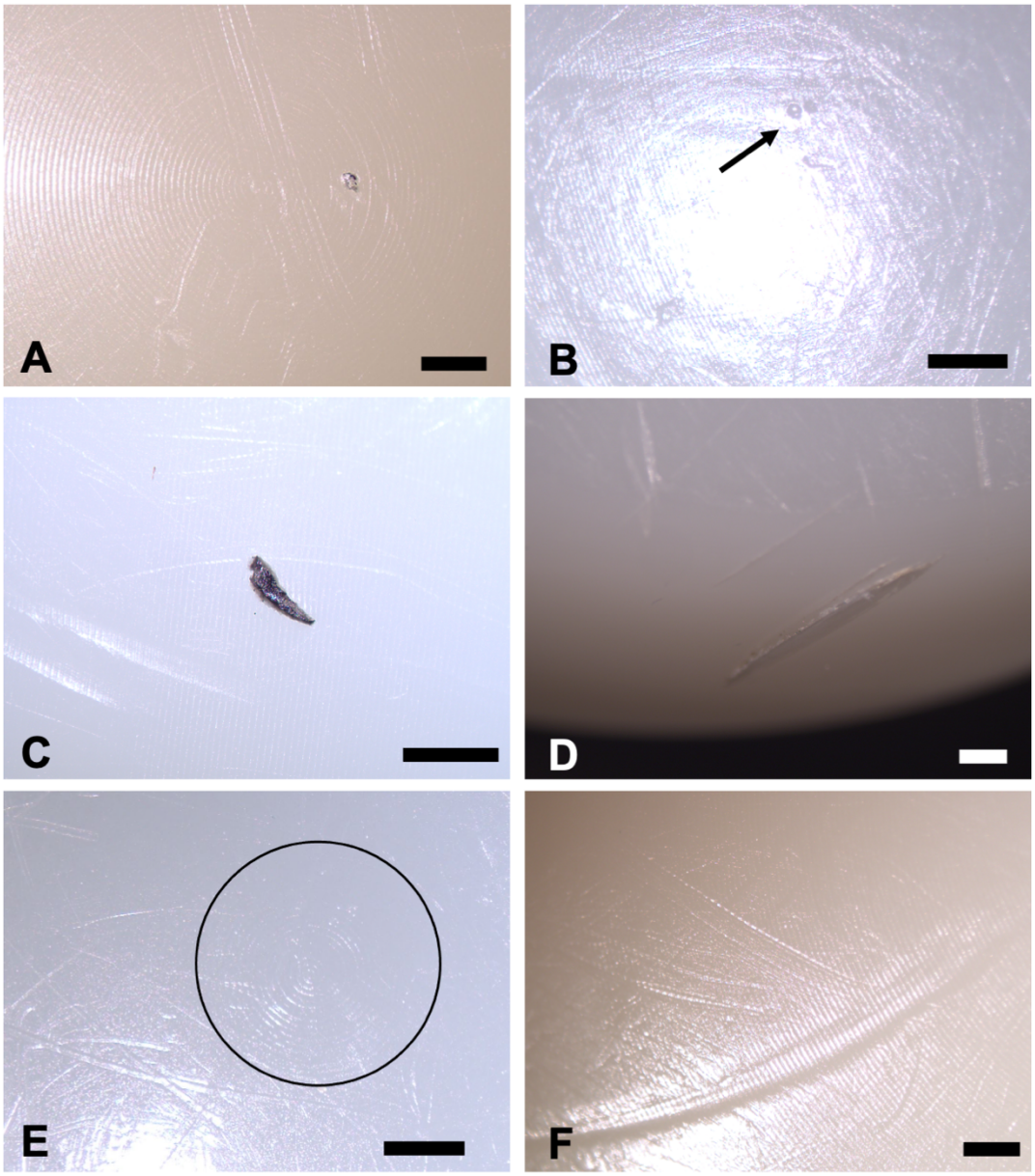

Figure 3.3 – Examples of the damage modes which were identified on the articulating surfaces of retrieved DM liners. This includes scratching (A), pitting (B), embedded debris (C), delamination (D) and deformation (F). Additionally, burnishing was identifiable through the loss of machining marks as shown in E. The black circle represents the only area in which machining marks are present; the area outside of this is representative of burnishing. Scale bar represents a unit of 1 mm.

With regards to the internal surface, the most frequently observed modes of damage were scratching (100%), pitting (85%) and burnishing (50%). Additionally, embedded debris was identified on the internal surface of five liners (25%). This debris appeared to be metallic in composition for three liners and either elliptical (Figure 3.4A) or spherical (Figure 3.4C, D) in shape. Alternatively, white, non-metallic debris particles

were observed on Samples 9 and 19 (Figure 3.4B). Abrasion was observed on two liners (10%), located either at the pole or chamfer. There were no signs of delamination or deformation on the internal surfaces of any samples assessed in this study.

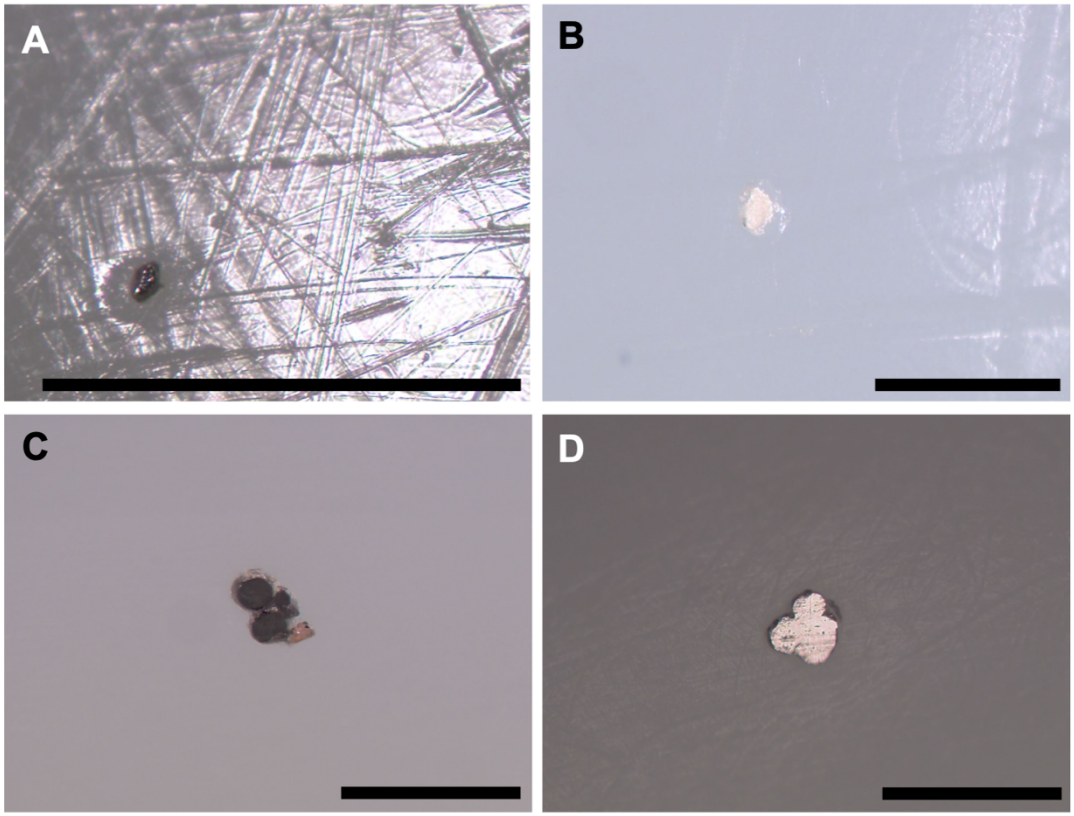

Figure 3.4 – Embedded debris identified on the internal surfaces of Sample 4 (A), 9 (B) and 7 (C, D). Scale bar represents a unit of 1 mm.

For the external surfaces, the most frequently observed modes of damage included scratching (100%), pitting (90%) and embedded debris (65%). The embedded debris was a metallic composition for all liners but presented in a variety of shapes (Figure 3.5). Abrasion and deformation were identified on 45% of samples, whilst burnishing (15%) and delamination (10%) were less common.

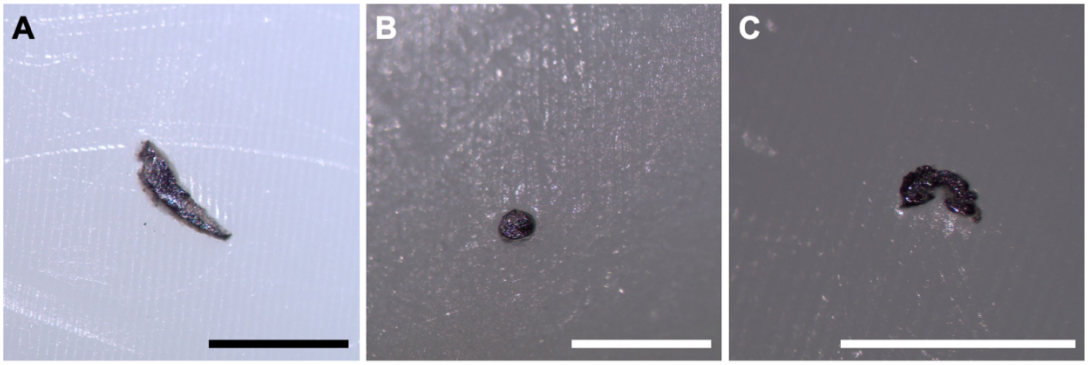

Figure 3.5 – Various geometries of embedded debris identified on the external surfaces of Sample 5 (A), 7 (B) and 12 (C). Scale bar represents a unit of 1 mm.

An impingement-like notch was identified on the chamfer of 19 liners (95%). Additionally, residual machining marks were observed on the internal and external surfaces of 14 (70%) and 19 (95%) liners, respectively.

3.4.3 – Discussion

A collection of retrieved DM liners was visually inspected for signs of damage. Scratching and pitting were observed as the most common modes of damage of both surfaces, which is consistent with previous retrieval analysis conducted on DM bearings (D'Apuzzo et al., 2016; Spece et al., 2018). In addition, burnishing was observed on a high proportion (50%) of the internal surfaces. This incidence was over three times greater than that found on the external surface. This would suggest that the internal surface acts as the primary articulation site thus leading to an increased incidence of surface polishing and loss of machining marks.

Although the severity of the damage was not assessed in this study, it should be noted that the external surfaces visibly appeared more damaged both in terms of severity and extent when compared to the internal surfaces. This is evidenced by an increased incidence of embedded debris, abrasion, delamination, and deformation in comparison to the internal surface scores. It is difficult to theorise a scenario in which the in-vivo conditions would consistently cause such severe damage to the samples, particularly due to their short service period in-vivo (20.0 ± 18.8 months). Therefore, it is hypothesised that the external surface damage was, at least in part, caused by ex-vivo factors (e.g., during the retrieval process or in transit). During implant retrieval, it is likely that surgical instruments make contact and therefore cause damage to the external surface of DM liners and thus is consistent with this theory. However, the

effects of implant retrieval on liner damage have not been previously assessed and therefore no conclusions can be drawn. This information would be useful for visual inspection studies and thus is recommended as future work.

Additionally, this study found that the external surfaces were nearly three times more likely to have embedded debris. The debris may originate from other implant sites (i.e., femoral stem, acetabular shell) or, alternatively, from surgical instruments used during the revision process. The material composition of this debris will be further investigated in Section 3.5.

A notch at the chamfer was noted on the majority (95%) of the liners. Although this type of damage would suggest that an impingement mechanism was frequently occurring in-vivo, it is more likely this damage occurred as a result of the disassembly process required to separate the femoral head and liner post-revision. This is because the formation of this notch was observed with three of the retrieved samples (Samples 17, 18 and 19), which were disassembled by the author via a lever-out mechanism. Prior to disassembly, a notch was not visible anywhere on the chamfer. The remainder of the samples were also disassembled using an identical procedure, with the exception of those revised for IPD, and thus it is hypothesised that the high incidence of notch formation identified in this study was an artefact of the disassembly process, rather than a consequence of in-vivo impingement. It is recommended that for future retrieval analyses of DM bearings, a visual inspection for this type of damage is done prior to component disassembly.

The limitations of this analysis should be acknowledged. Although this study characterised the frequency of damage which occurred on retrieved DM liners, a simplistic methodology was applied thus limiting the results as the severity and extent of the damage was not assessed.

3.5 – Material characterisation of debris embedded on the articulating surfaces of DM liners

3.5.1 – Methods

Energy-dispersive x-ray analysis (EDX) is a useful and well-established analytical method which is conducted on a scanning electron microscope (SEM) to identify the elemental composition of an unknown material. In this study, the material composition of embedded debris identified on the surfaces of retrieved DM liners was

characterised using EDX with a Carl Zeiss EVO MA15 SEM. The output of this analysis produced emission spectrums for each sample (Figure 3.6), whereby the peaks correspond to different elemental compounds within the material. The author would like to acknowledge the help of Stuart Micklethwaite of the LEMAS core facility (University of Leeds) for his assistance in acquiring this data.

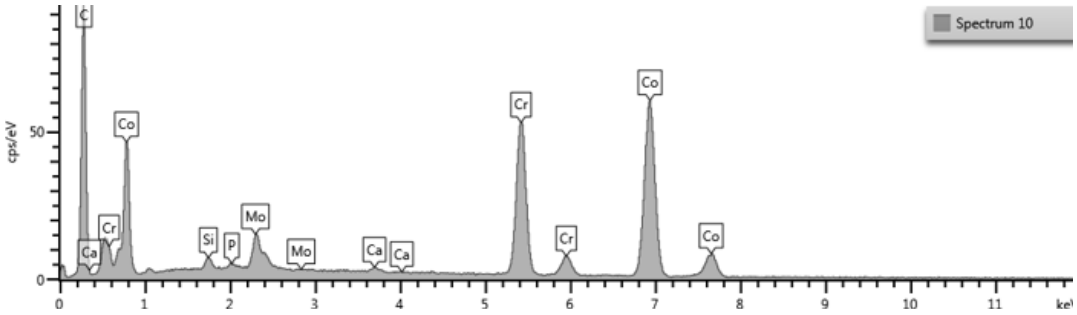

Figure 3.6 – Example of an emission spectrum produced from EDX analysis, which shows elemental peaks for carbon (C), calcium (Ca), chromium (Cr), silicon (Si), phosphorous (P), molybdenum (Mo) and cobalt (Co).

This analysis was only possible for the assessment of debris embedded on the external surfaces of samples due to limitations of the equipment and the complex geometry of DM liners. Therefore, debris identified on the internal surfaces (n=5 samples) was excluded in this analysis.

3.5.2 – Results

One sample was excluded from this analysis due to space constraints in the SEM chamber (Sample 4), and no metallic particles could be located on Sample 3. Therefore, the embedded debris from 11 samples was analysed in this study. Several materials were identified using EDX, including iron (Fe), titanium (Ti), aluminium (Al), cobalt (Co), chromium (Cr), vanadium (V), molybdenum (Mo), tantalum (Ta) and zirconium (Zr). A breakdown of the debris materials identified on each component may be found in Table 3.4.

Table 3.4 – Material composition of embedded debris identified on the external surface of 10 retrieved DM liners. No metallic particles were identified on Sample 3 and therefore this has not been excluded from the results.

Component number	Materials identified	Possible origin of debris
5	Ti, Al, V	Implant
7	Co, Cr, Mo	Implant
8	Fe	Surgical instrument
9	Fe, Ti, Al, V	Implant and/or surgical instrument
10	Fe	Surgical tool
11	Fe, Ti, Al	Implant and/or surgical instrument
12	Ta	Implant
13	Ti, Al, V	Implant
14	Fe, Ti, Co, Cr, Mo	Implant and/or surgical instrument
16	Ti, Fe, Mo, Zr	Implant
20	Fe	Surgical instrument

The size and morphology of the embedded debris varied throughout the samples. The length of the debris was approximately 100 to 200 μm for six (60%) of the assessed samples. This debris was composed of various materials, including titanium alloy (n=2), iron (n=2), cobalt-chrome alloy (n=1) and tantalum (n=1). However, small (<10 μm) metallic particles were also observed on the surfaces of four samples. These particles were often presented in clusters across a portion of the surface (Figure 3.7) and typically composed of several elements including iron, aluminium and titanium. Additionally, a large shard of titanium alloy (Ti-Al-V), approximately 800 μm in length, was identified on Sample 5.

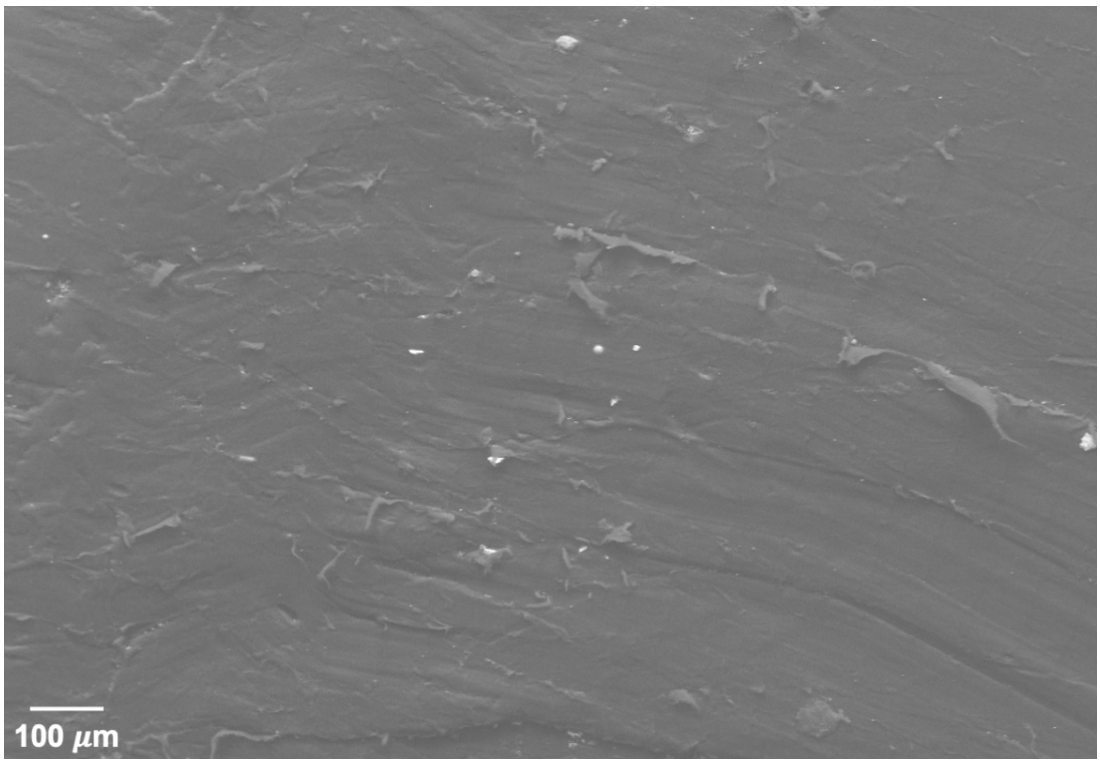

Figure 3.7 – Small (<10 μm) metallic particles observed on the surface of Sample 11. The metallic particles are denoted by the bright white regions on the image.

In terms of the morphology of the debris, larger shards (>100 μm) were usually jagged and asymmetrical in shape (Figure 3.8, A-C, F) however circular or elliptical particles were observed on Samples 7 and 13 (Figure 3.8, D-E). The morphology of the smaller particles (<10 μm) was more challenging to determine, due to the magnification range of the equipment.

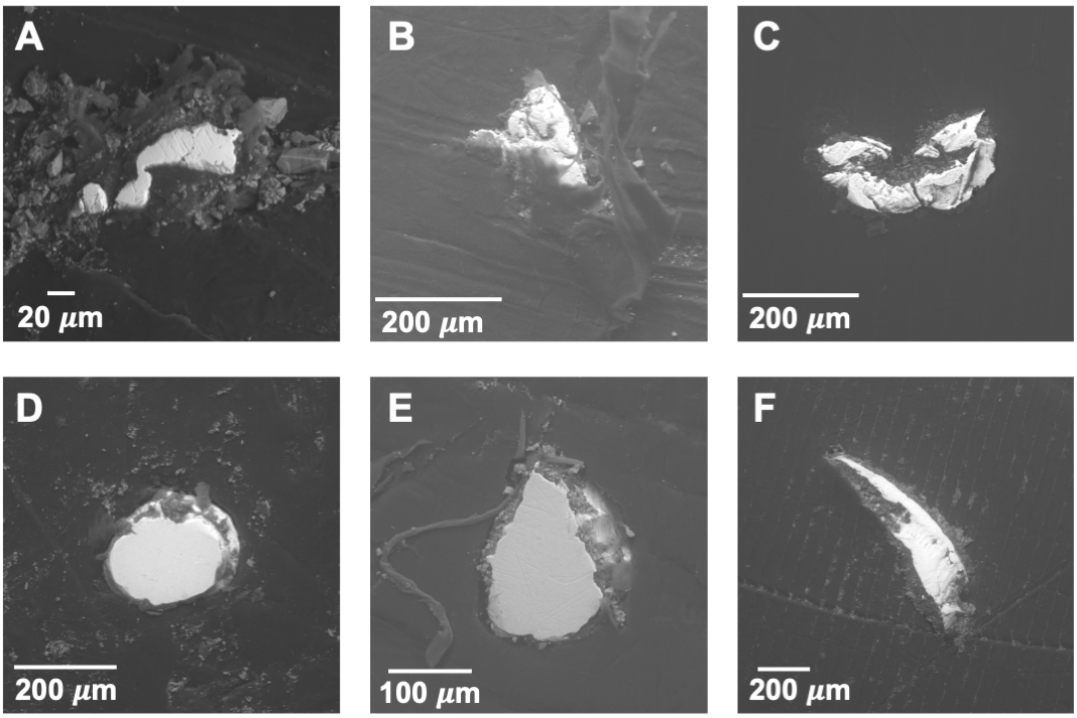

Figure 3.8 – Various morphologies of embedded debris identified on the external surface of retrieved DM liners. This includes jagged, asymmetric particles approximately 100 to 200 μm in length (A-C) or larger particles up to 800 μm in length (F). Circular or elliptical particles were also observed (D-E). Material composition: Fe (A, B), Ta (C), CoCr alloy (D), Ti alloy (E, F).

3.5.3 – Discussion

Debris embedded into the external surfaces of retrieved DM liners was characterised using EDX analysis, and several materials were identified including titanium and cobalt-chrome alloys, iron, and tantalum.

In this study, titanium was identified on six (55%) of the assessed samples. Titanium and titanium alloys are a common orthopaedic biomaterial used to manufacture both femoral stems and acetabular components, but not surgical instruments. These components are often made of a Ti-6Al-4V alloy (Saenz de Viteri and Fuentes, 2013). Indeed, titanium was identified in the presence of aluminium and/or vanadium on four of the assessed samples in this study (Samples 5, 9, 11, 13). Therefore, it may be assumed this debris originated from a Ti-6Al-4V implant although the exact source (i.e., femoral stem or acetabular shell) could not be determined due to a lack of supplemental implant information. Alternatively, one sample (Sample 16) contained debris composed of titanium, molybdenum, zirconium, and iron. It was known this liner was paired with a Rejuvenate® femoral stem (Stryker; Warsaw, IN, USA) which

was manufactured from Ti-12Mo-6Zr-2Fe (TMZF) and thus it is suspected the debris originated from the femoral stem in this case.

Cobalt-based alloys are another common biomaterial used to manufacture hip implants (Aherwar et al., 2016). In this study, debris composed of cobalt, chromium and molybdenum were identified on two implants (Sample 7, 14) which may have originated from the femoral head, femoral stem, or acetabular components. Tantalum debris was also identified on one liner (Sample 12), which likely originated from the tantalum-based Trabecular Metal™ acetabular shell (Zimmer Biomet) which was known to be implanted in-vivo with this liner.

Additionally, debris particles containing iron were found on seven (64%) of liners. In one case, the iron likely originated from the Ti-12Mo-6Zr-2Fe femoral stem as discussed previously. Stainless steels have been used to manufacture femoral stems, although this is uncommon (Hu and Yoon, 2018). Therefore, it is suspected that the iron likely originated from surgical instrumentation used within the revision process. However, this cannot be confirmed without supplemental component information (i.e., comprehensive list of all implanted components for each retrieved set), which was not available for this study.

In summary, titanium, cobalt, and tantalum-based debris particles were identified on approximately 70% of the assessed liners alongside other common alloying materials such as aluminium, vanadium and molybdenum. These are known orthopaedic biomaterials which are commonly used for the manufacture of THR components and therefore this debris is thought to have originated from various implant sites such as the femoral stem or acetabular shell. In contrast, iron-based debris particles were identified on 64% of the liners, which may have originated from the use of surgical instruments within the revision process. If this is true, this would suggest that the revision process does indeed cause damage to DM liners through the introduction of third-body particles thus further warranting a need to investigate these effects.

This study is not without its limitations. First, it was not possible to characterise the debris identified on the internal surfaces (Section 3.4) without destructively sectioning the components and thus they were excluded from the analysis. One further sample (Sample 4) was excluded from the analysis due to space constraints in the SEM chamber. In addition, no embedded particles were identified on the external surface of Sample 3 despite debris being identified in the visual inspection. It is possible that

the debris identified on this sample was non-metallic in composition and thus challenging to locate once in the SEM chamber, particularly due to its highly dimpled and deformed external surface (Figure 3.9). Alternatively, the debris may have been sat loosely within the surface dimples making it difficult to wipe away whilst the sample was being visually inspected but perhaps freed itself prior to SEM analysis.

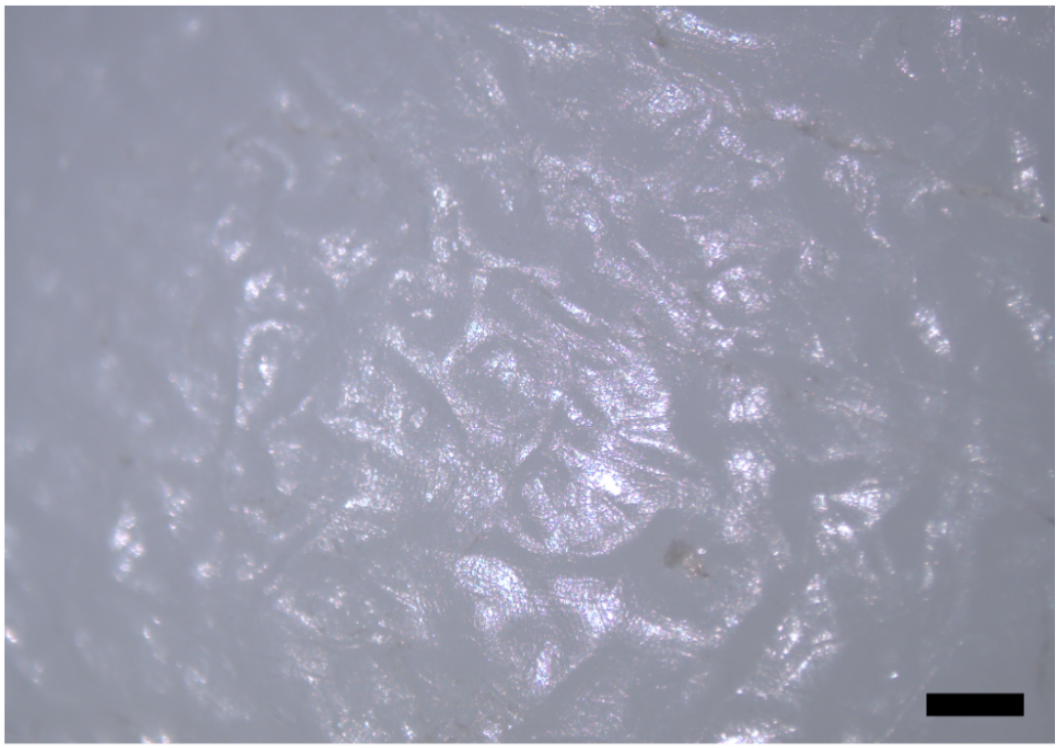

Figure 3.9 – Highly dimpled and deformed external surface of Sample 3. Scalebar represents a unit of 1 mm.

Finally, limited supplemental information (i.e., lack of information about corresponding head, stem and shell used in-vivo with each liner) made it challenging to determine the most likely point of origin of the embedded debris.

3.6 – Geometric analysis of retrieved DM liners

3.6.1 – Methods

The retrieved polyethylene liners were semi-quantitatively assessed using the geometric characterisation methodology described in Chapter 2 (see Section 2.7). Additionally, the liners were stratified into sub-groups based on various patient and implant factors including reason for revision, implant type, implant size, material combination (i.e., MoPoM, CoPoM), femoral head size and time in-vivo. The surface

deviation heatmaps were inspected for signs of common or repeated patterns within the individual groupings.

3.6.2 – Results

Various geometric features were observed on the surfaces of retrieved DM liners. The surface deviation heatmaps for all samples are available in Appendix B.

3.6.2.1 – Internal surfaces

The most common damage pattern observed on the internal surfaces was asymmetric, crescent-shaped regions of penetrative geometric variation (Figure 3.10A) which was observed on eight samples (40%). Additionally, circumferential stripes were identified on the internal surfaces of four liners (20%; Figure 3.10B) whilst circular or elliptical regions of geometric variation were observed on three samples (15%; Figure 3.10C). No obvious damage was present on the remaining six samples (30%) with the exception of a notable flattening effect observed on Samples 3, 7, 8, 13 and 14 which will be discussed in greater detail later in this section.

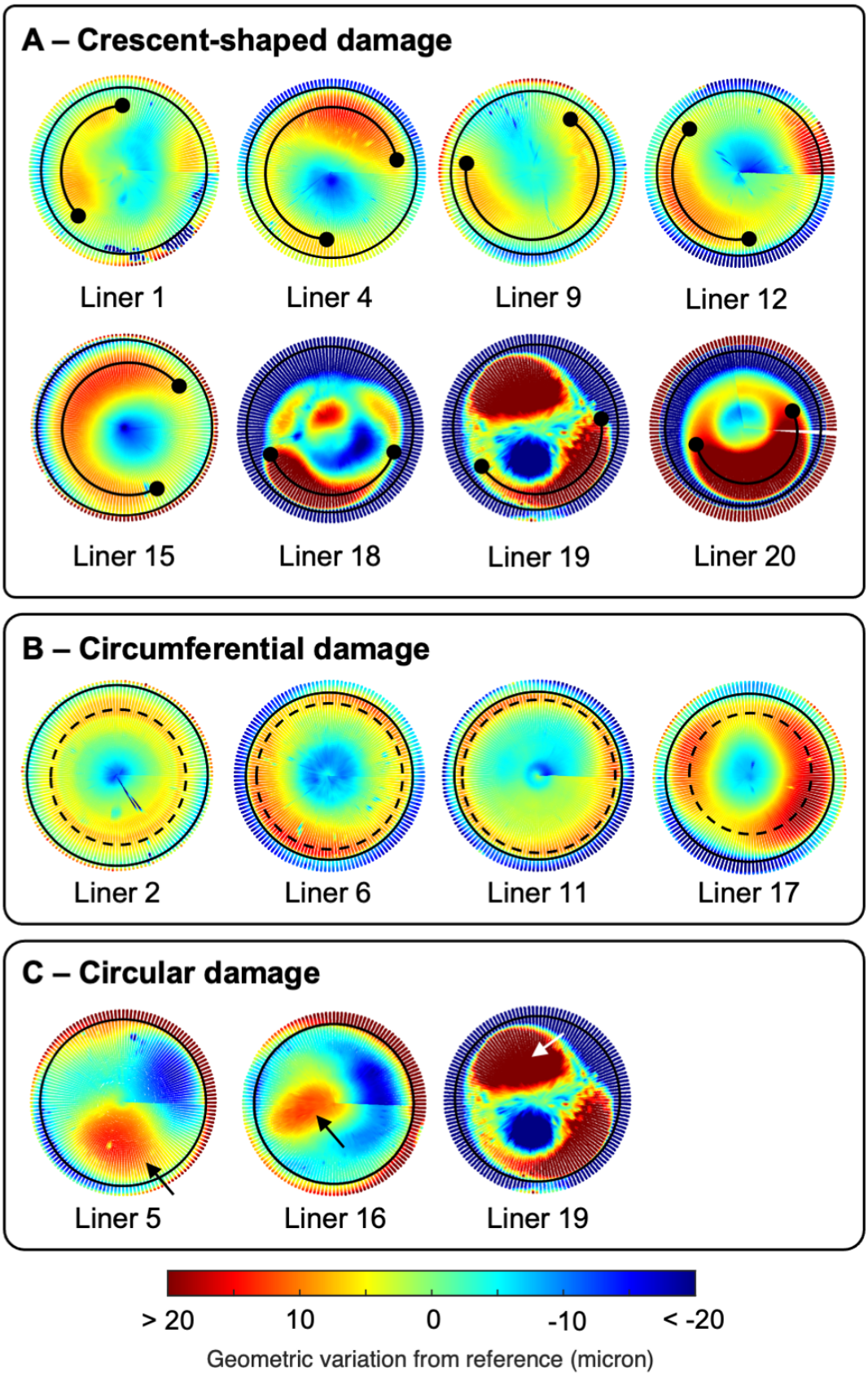

Figure 3.10 – Damage patterns visible on the internal surfaces of retrieved DM bearings, which includes crescent-shaped (A), circumferential (B) and circular (C) regions of positive geometric variance.

3.6.2.2 – External surfaces

With regards to the external surfaces, moderate to deep pitting was observed on 15 samples (75%), as exampled in Figure 3.11. The shape, location and severity of the damage varied, although a similar elliptical gouge appeared in the equatorial region of four samples (Figure 3.11 D, E, F). Additionally, circumferential stripes of positive (n=3; 15%) and negative (n=2; 10%) geometric variation was observed among this group (Figure 3.12). A C-shaped indentation was observed on Sample 15 (Figure 3.13), and minimal damage was identified on four liners.

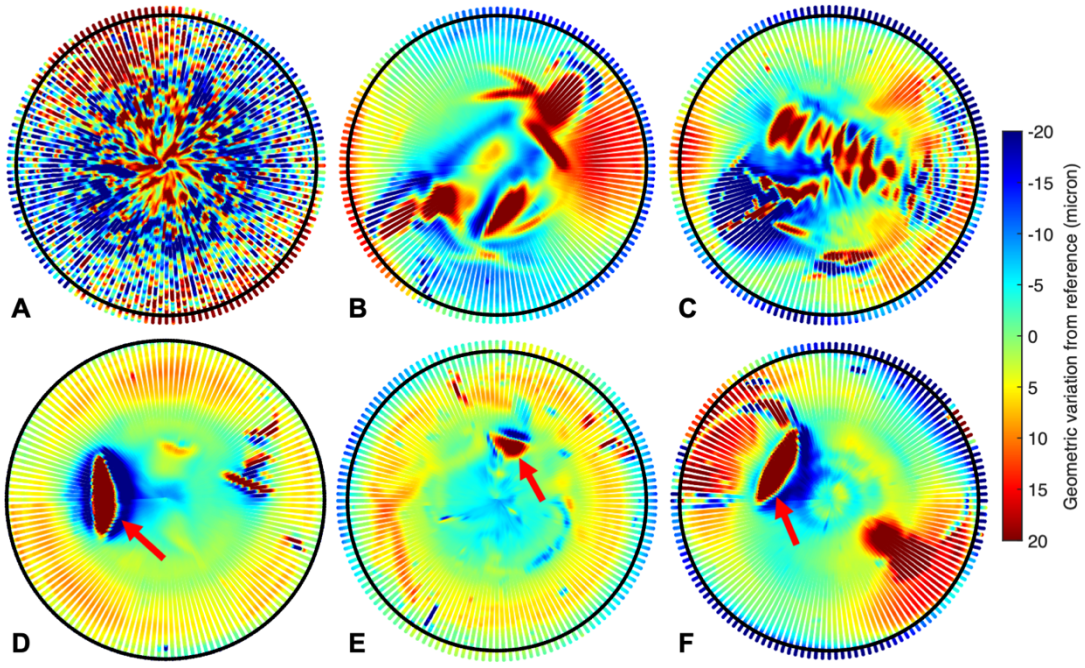

Figure 3.11 – Examples of deep pitting found on the external surfaces of six retrieved DM liners, including samples 3 (A), 5 (B), 16 (C), 11 (D), 12 (E) and 14 (F).

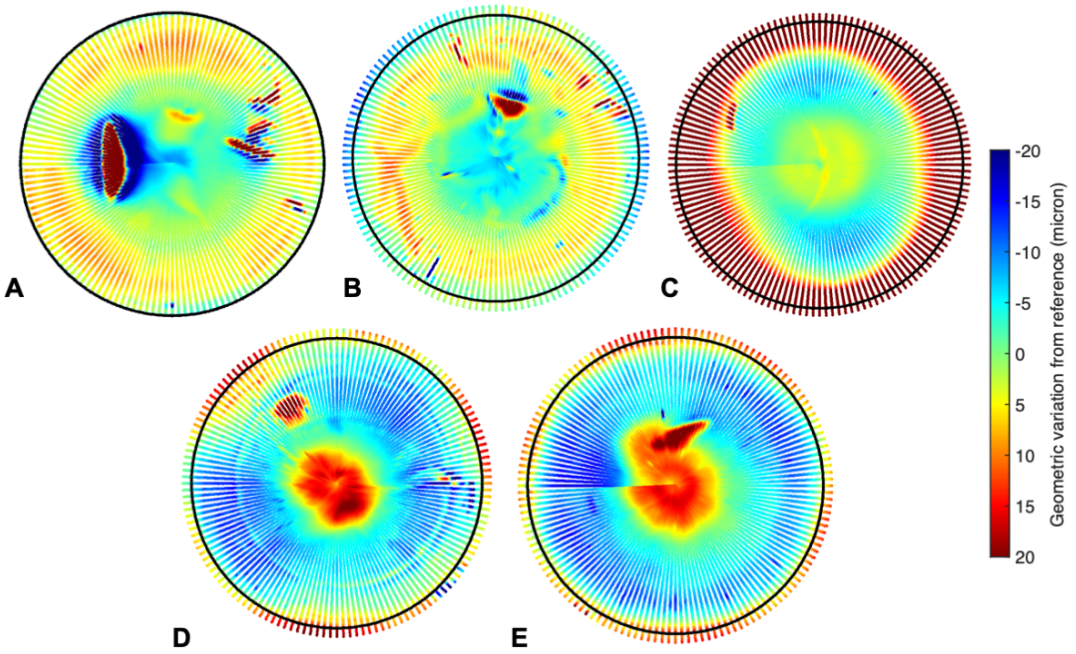

Figure 3.12 – Faint circumferential stripes of positive (A, B, C) and negative (D, E) geometric variation noted on the external surfaces of four liners (A – Sample 11; B – Sample 12; C – Sample 20; D – Sample 9; D – Sample 10).

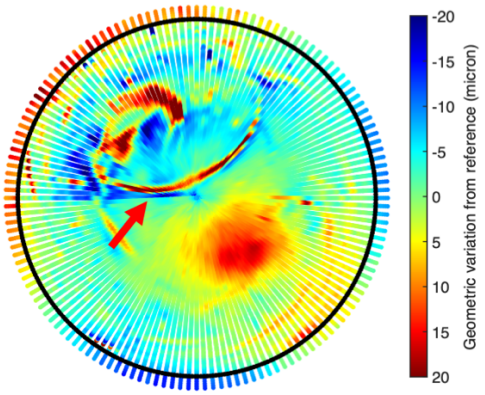

Figure 3.13 – External surface of Sample 15, whereby a C-shaped indentation was apparent.

3.6.2.3 – General trends

The surfaces of seven (35%) liners showed a similar pattern of geometric variation, which included two diametrically opposed regions of positive geometric variation, which were normal to two diametrically opposed regions of negative geometric variation, as shown in Figure 3.14. This pattern was reflected across the internal and external surfaces, although the location of positive and negative geometric variation was inverted between the two. This pattern was more recognisable on some liners

than others although, in all cases, would suggest the liner had become more elliptical in its shape.

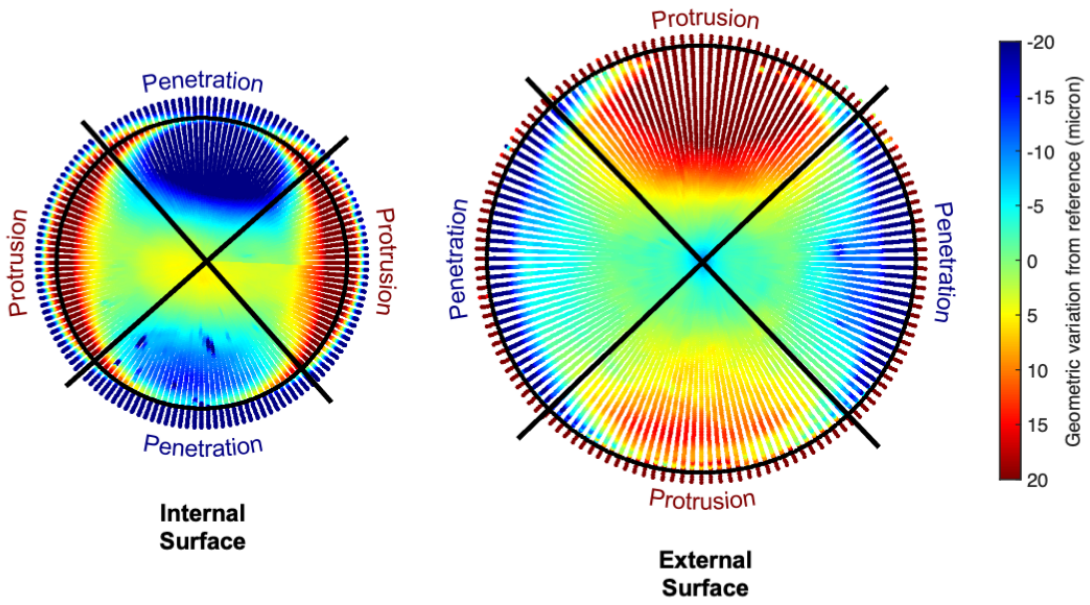

Figure 3.14 – Example of the liner flattening effect, observed on the internal (left) and external (right) surfaces of Sample 13.

There were no obvious trends or similarities in the damage patterns when the heatmaps were stratified into patient- and implant-specific sub-groups including reason for revision, implant manufacturer, femoral head size, femoral head material and liner size. Additionally, there appeared to be no temporal progression of damage when the liner heatmaps were sorted by their time in-vivo.

3.6.3 – Discussion

The geometric assessment methodology described in Chapter 2 was successfully able to detect changes to the surface geometry of retrieved DM liners, and several geometric features were observed in this analysis.

On the internal surfaces, several damage patterns presented on the surface deviation heatmaps including circular (n=2), crescent (n=8) and circumferential (n=4) regions of penetration. The circular damage, denoted by a concentrated region of penetration, is similar to that observed on conventional liners (Wang et al., 2016; Hua and Li, 2020) and thus would suggest the liner became fixed in one orientation (e.g., due to fibrotic tissue) whereby the region of penetration corresponds to the superior position of the liner. In contrast, the circumferential stripes suggest a free and uniform

precession of the mobilised liner throughout its service period. However, faint circumferential stripes were also observed on pristine samples (see Section 2.4) and therefore may be an artefact of the manufacturing process. The latter is the most likely explanation for this geometric feature for Samples 2 and 17, due to their short in-vivo service periods for these particular implants (3.7 months for Sample 2; 6 months for Sample 17). The time in-vivo is unknown for the remaining two samples (Samples 6 and 11) and therefore conclusions cannot be drawn about which mechanism is responsible for the formation of these circumferential damage stripes. Interestingly, asymmetric crescent-shaped regions of penetration were observed on approximately one third of the internal surfaces. This would suggest the liners behaved somewhere in between the first two cohorts described (i.e., circular and circumferential damage), whereby the liner was able to ratchet but only within a limited region. In summary, the range of damage patterns observed on the internal surfaces suggest that the biomechanical function of DM bearings is varied.

The most common damage pattern observed on the external surfaces was deep pitting, which was identified on 75% of the samples. Interestingly, four of these samples displayed a similarly shaped gouged region (Figure 3.11 D-F) which resembled stripe wear patterns previously observed on edge-loaded femoral heads from hard-on-hard (e.g., CoC) bearings (Esposito et al., 2012; Sariali et al., 2014). This suggests that DM implants may be prone to damage as a result of edge loading, particularly at the outer surface of the polyethylene liner which acts as an effective large-diameter femoral head. It should be noted that the in-vivo orientation of these components could not be established due to a lack of suitable supplemental information (e.g., radiographs) and therefore it is not possible to confirm whether these components were, indeed, subjected to edge loading in-vivo. However, these findings warrant further investigation into the performance of DM implants under such conditions.

Additionally, a C-shaped indentation was visible across the external surface of Sample 15 (Figure 3.13). This sample failed due to extra-articular dislocation of the head/liner from the acetabular shell, and thus the indentation may be explained by contact of the external surface of the liner against the rim of the acetabular shell.

The heatmaps suggest that over one third of the liners (n=7) experienced a flattening effect, whereby the components became more elliptical in their shape. It is possible that this is the result of the levering out process used to remove the femoral head

from the liner. During this process, the components were clamped into a vice for stability which may elicit a flattening effect if over-tightened. However, these effects have not been directly investigated and thus no conclusions can be drawn. A damage characterisation study to better understand these effects and to develop effective, non-destructive methodologies for disarticulating the femoral head and liner of retrieved DM bearings is therefore recommended as future work.

In summary, highly variable damage patterns were observed amongst a collection of 20 retrieved DM liners. It is acknowledged that this variation may be due to the limited number of samples available for this study, in conjunction with the numerous implant designs, sizes and materials across the collection. However, the results of this study provide preliminary information about the in-vivo biomechanical function of DM bearings. For example, the data suggests that the internal articulation between the femoral head and polyethylene liner acts as the primary and preferential articulation site. Additionally, the data suggests that the liners rotate within the acetabular shell although the extent to which this occurs may vary between implants. This variability may be explained by patient and surgical factors such as component positioning, the presence of soft tissue fibrosis or patient activities (i.e., how often the outer articulation becomes engaged) and therefore warrants further research.

3.7 – Surface characterisation of retrieved DM femoral heads and acetabular shells

3.7.1 – Methods

3.7.1.1 – Visual inspection

The surfaces of retrieved femoral heads and acetabular articulating components were visually inspected for signs of damage. Unlike the liners, these components generally only showed one mode of damage: scratching of the metallic components or metal transfer patches on the ceramic heads. Therefore, the damage scoring system applied to the liners was not appropriate for use in this analysis; the binary scoring system would yield little valuable information as all components in this cohort exhibited some degree of damage. Alternatively, a complex grading system to rank the extent, location and severity of the damage was not desirable as these are susceptible to intra- and inter-rater variability.

Therefore, a simplistic scoring system was employed for this analysis so that the damage was semi-quantitatively characterised. For each component, the surface was

separated into three zones: the pole, equator, and rim. Each zone was visually assessed and assigned a score between zero and two. A score of zero was assigned if no damage was observable. For the metallic components, a score of one was assigned in the presence of light scratching; these features were often observed but could not be felt when running a fingernail across the surface. A score of two was assigned if moderate to severe scratching was identified. In these circumstances, the scratching was both visible and could be detected by tactile means. Examples of light and moderate/severe scratching are shown in Figure 3.15. For the ceramic components, a score of one was assigned if minor (<1 cm in length) metal transfer patches were observed, whilst a score of two was assigned in the presence of larger (>1 cm in length) metal transfer patches. The sum of the individual zone scores yielded the total damage score for the component (maximum of 6).

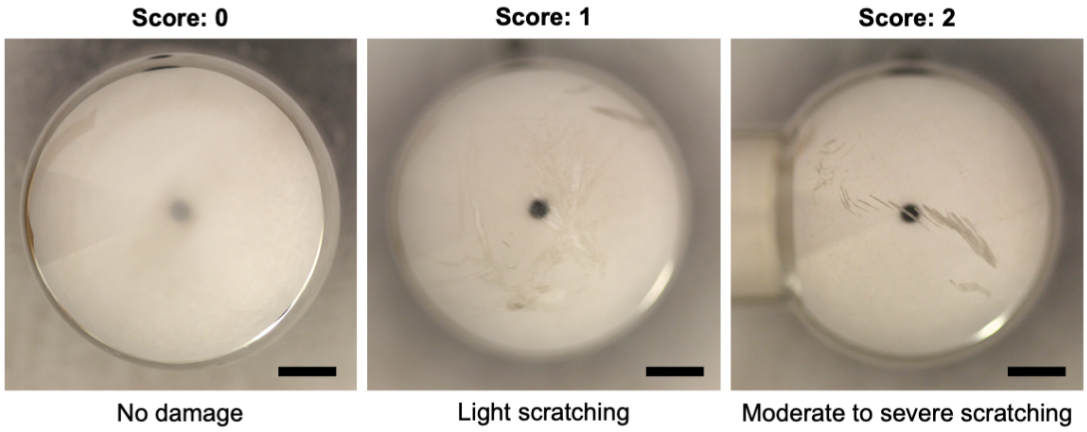

Figure 3.15 – Examples of how the damage scoring system was applied. Each zone (i.e., pole, equator, rim) was assigned a score of zero (no damage, left), one (light scratching, middle) or two (moderate to severe scratching, right). Scale bar represents a unit of 5 mm.

3.7.1.2 – Surface roughness assessment

The surface roughness of the retrieved femoral heads was assessed using a contacting profilometer (Form Talysurf series; Taylor Hobson, UK). It was not possible for the acetabular shells to be measured due to the configuration of the equipment which featured a vertically oriented stylus. The position and length of the stylus made it impossible to reach the acetabular shell's concave surface, particularly in areas of interest (i.e., at the pole or equator), without the horizontal shaft of the stylus contacting the sample in error. Although the use of a longer stylus would provide a solution, these were not available to the author and would compromise the accuracy of the data. Therefore, all acetabular shells were excluded from this analysis.

To characterise the roughness of the femoral heads, six traces were acquired per sample and the data was averaged to provide an estimate of its overall roughness. The traces included two perpendicular measurements at the pole and one measurement in each quadrant, located approximately 30° from the pole. This is similar to the methodology described in ISO 7206-2:2011, which describes the requirements for the articulating surfaces of THR components and how to characterise their surface roughness.

For each trace, the stylus was crested in the X and Y planes to locate the highest point on the sample which was used as the midpoint of the trace. Each trace had a length of 8-mm. The data was analysed with a Gaussian filter with varying bandwidth and cut-off settings dependent on the roughness of the sample (Table 3.5), as specified by ISO 21920-3:2022.

Table 3.5 – Settings used to analyse surface roughness data, including the specified cut-off and bandwidth which are dependent on the roughness of the sample (Ra).

Ra (µm)	Cut-off, Lc (mm)	Bandwidth
>0.02	0.08	30:1
0.02 – 0.1	0.25	100:1
0.1 – 2	0.8	100:1

Several parameters were recorded, including the surface roughness (Ra) and skewness (Rsk). The skewness gives an indication of whether the trace predominantly consists of peaks or valleys, with positive values being associated with a surface mainly consisting of peaks and negative values being associated with a surface mainly consisting of valleys. Additional parameters, including Rp (maximum peak height) and Rv (maximum valley height), were also collected. Rp was of particular interest for this analysis, as it is the formation of peaks which may result in an abrasive mechanism whilst articulating against the polyethylene liner thus leading to wear (i.e., loss of material).

Severe femoral head damage was also characterised in this study. Samples with severe damage were identified from the visual inspection assessment (Section 3.7.1.1) as those with a damage score of two in at least one zone. One additional

trace was acquired in the region of the severe damage, using the previously described methods, in order to characterise its roughness.

3.7.2 – Results

3.7.2.1 – Femoral heads

All available femoral heads (n=17) were visually inspected in this study which comprised of two 22-mm metal, nine 28-mm metal and six 28-mm ceramic heads. On inspection, it was noted the metal heads appeared more damaged than those made of ceramic. The damage scores for the metal and ceramic femoral heads were 3.3 ± 1.0 and 1.0 ± 0.6, respectively. A significant difference ($p<0.001$) in these damage scores was found using an independent t-test (IBM SPSS Statistics, Version 27). Damage to the femoral heads did not appear to dominate within a particulate zone.

For the metal femoral heads, light scratching (i.e., a score of one) was the most common damage mode noted in any zone. Moderate to severe damage was noted on only four metal heads (Samples 1, 3, 5, and 20) in locations near either the equator or rim as shown in Figure 3.16. Among these, similar gouged regions were observed on two samples (Samples 1 and 5), which may have been caused by contact with surgical instrumentation due to the local and discrete nature of the scratching. Alternatively, the most common score assigned to the ceramic heads was a zero indicating that no damage was identified; this was true for all three zones. Five of the six ceramic heads had a score of one (i.e., small metal transfer patches) assigned in one or more zones, and no heads were identified with moderate or severe metal transfer.

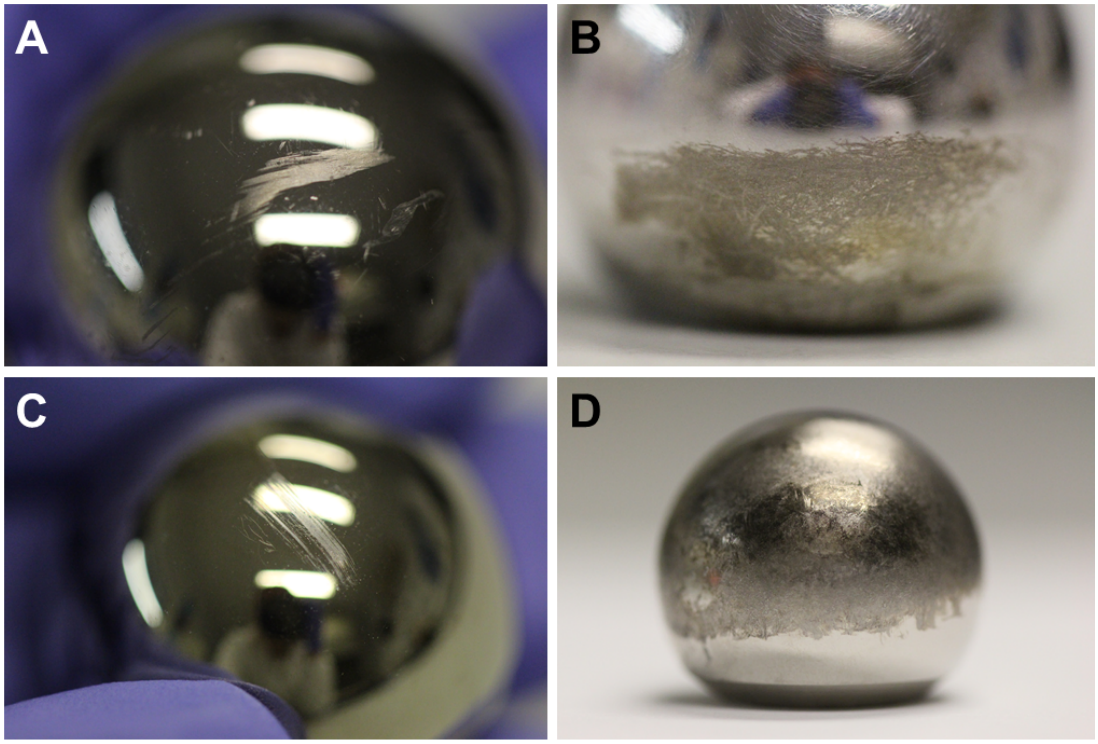

Figure 3.16 – Severe damage observed on the femoral heads of Samples 1 (A), 3 (B), 5 (C) and 20 (D).

The surface roughness of the femoral heads was also assessed. One of the heads (Sample 18) was affixed to a femoral stem and thus only five of the six traces were possible to collect due to limitations of the equipment and setup. Therefore, the overall roughness of this sample was determined using the average of five traces, whilst the sixth was excluded. The results of the surface roughness analysis are specified in Table 3.6, which stratifies the data by material type. The surface roughness was compared between the two material groups using independent t-tests (IBM SPSS Statistics, Version 27) which found no significant differences between the Ra, Rsk, Rp or Rv values. However, all relationships became significant when outliers were excluded as shown in Table 3.6.

Table 3.6 – Mean surface roughness of retrieved femoral heads from DM bearings, stratified into metal and ceramic sub-groups. The surface roughness metrics were statistically compared between the two material groups using independent t-tests; the results of this analysis are listed in the final column (P-value). Results denoted with an asterisk imply there was a statistically significant difference found at an alpha of 0.05. The adjusted P-values were determined by repeating the statistical analysis once outliers were excluded. Samples which were identified as outliers are specified.

Material	n	Surface roughness			
		Ra (µm)	Rsk	Rp (µm)	Rv (µm)
Metal	11	0.0346	-1.5434	0.0996	0.1296
Ceramic	6	0.0040	0.5338	0.0114	0.0134
P-value	-	0.304	0.087	0.266	0.172
Outliers	-	15, 20	5	15, 20	15, 20
Adjusted P-value	-	0.007*	0.020*	0.007*	0.009*

There appeared to be an association between the surface roughness (Ra) and peak height (Rp) of the components, with rougher components being associated with higher peaks (r=0.996). In contrast, there was no association between the head roughness (Ra) or peak height (Rp) and time in-vivo of the femoral heads, with Pearson correlation coefficients of -0.199 and -0.210, respectively.

Regions of severe damage were also characterised in this analysis. Four femoral heads (Samples 1, 3, 5, and 20) met the specified criteria, whereby moderate to severe damage was identified from the visual inspection. All components were either 22- or 28-mm diameter metallic femoral heads. The surface roughness of these regions was varied (Table 3.7), with Ra values ranging from 0.3543 µm to 1.3267 µm and Rp values ranging from 1.7468 µm to 3.4139 µm. The maximum Ra and Rp identified from this collection of samples was 1.3267 µm and 3.4139 µm, respectively. This was from Sample 20, which was revised for IPD and had clear evidence of metal-on-metal articulation between the femoral head and acetabular shell as shown in Figure 3.17.

Table 3.7 – Surface roughness of moderate to severe regions of damage, from retrieved dual mobility MoPoM femoral heads. The location where the most severe damage was observed (e.g., pole, equator, rim) is described in the table.

Sample	Location of damage	Surface Roughness (µm)			
		Ra	Rsk	Rp	Rv
1	Equator	0.4574	1.3283	2.3639	1.0238
3	Rim	0.4169	1.5247	2.0415	0.9211
5	Equator	0.3543	3.2214	1.7468	0.6331
20	Equator	1.3267	-0.0287	3.4139	3.6048
	Mean	**0.6388**	**1.5114**	**2.3915**	**1.5457**

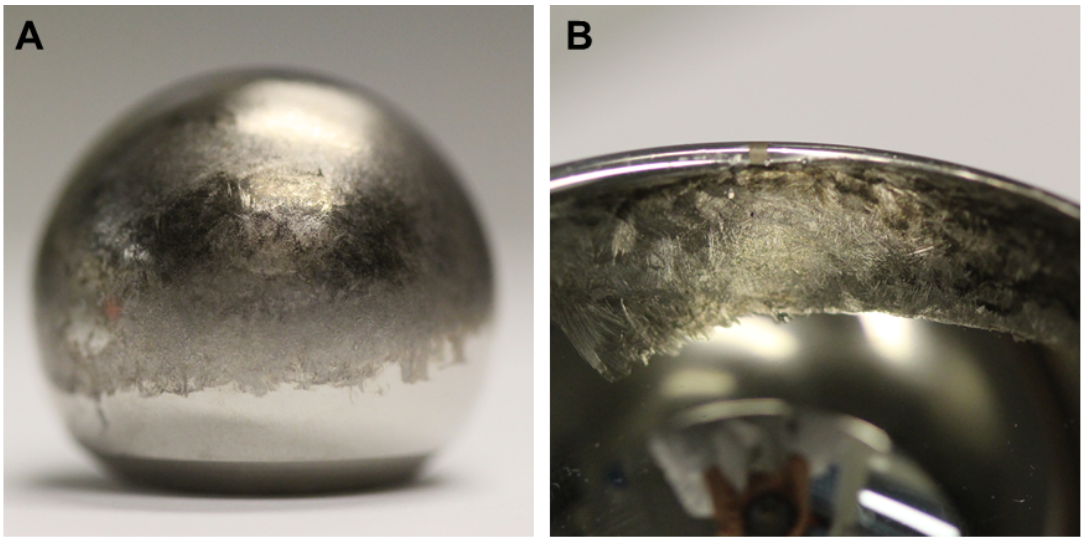

Figure 3.17 – Severe damage observed on the femoral head (A) and acetabular shell (B) of Sample 20. Evidence of metal-on-metal articulation, secondary to IPD, was observable.

3.7.2.2 – Acetabular components

All available acetabular components (eight modular inserts and four monobloc shells) were visually inspected, which included nine MoPoM bearings and three CoPoM bearings. The combined damage score for the acetabular components was 3.7 ± 0.7. When compared with an independent t-test (IBM SPSS Statistics, Version 27), no significant difference was observed in the combined damage scores between modular and monobloc samples ($p=0.226$) at an alpha of 0.05. However, acetabular components from MoPoM bearings appeared to have significantly higher combined damage scores than those from CoPoM bearings ($p=0.033$).

Light scratching was the most common damage mode identified within any region, and a fine layer of surface scratching was observed on the majority of samples. Moderate to severe damage was identified on nine acetabular components. For the majority of these samples (78%), this damage was located at the rim and consisted of small (<1 cm) scratches over a small portion of the component's edge. The most severe damage was observed on Sample 20, which was revised for IPD. As a result of this, evidence of metal-on-metal articulation between the femoral head and acetabular shell was observable as shown in Figure 3.17. Interestingly, this type of damage could not be seen on the other component revised for IPD (Sample 1).

3.7.3 – Discussion

To the author's knowledge, the present study was the first to assess retrieved femoral heads (n=17) and articulating acetabular components (n=12) from DM bearings.

3.7.3.1 – Femoral heads

A total of 11 metallic and six ceramic components were analysed. In summary, the metallic heads appeared to sustain more damage than those manufactured from ceramic, as evidenced by a significant different in the damage scores and surface roughness parameters (namely Ra and Rp) between the material groups.

Interestingly, the average roughness Ra for both the metallic (0.0346 μm) and ceramic (0.0040 μm) femoral heads was noted to be below the maximum surface roughness threshold required for as-manufactured femoral heads, as described by ISO 7206-2:2011. This effect has been previously observed for retrieved heads from conventional THRs (Wong, MD et al., 2013; Laurent et al., 2014). However, it should be noted that these standards only specify a maximum threshold but do not necessarily reflect the true manufacturing specification of the implants. Therefore, the surface roughness of three as-manufactured CoCr femoral heads were characterised to provide some baseline data (see Table 3.8). This revealed a tenfold increase in the average roughness Ra and maximum peak height Rp between the pristine and retrieved metallic heads. In addition, the skewness Rsk increased from -15.2724 μm to -1.5434 μm between the pristine and retrieved samples, respectively. This signifies a tendency for the retrieved heads to contain more peaks and asperities than the pristine samples, thus negatively impacting the wear performance of the implant. Regions of moderate to severe surface damage were locally characterised in this analysis, which also revealed a further increase in the surface roughness parameters.

Therefore, it can be concluded that the retrieved metallic femoral heads experienced some degree of roughening and damage whilst in-vivo. This is also evidenced by the visual inspection assessment which identified signs of light damage on all samples, and the presence of moderate to severe damage on 36% of samples.

Table 3.8 – Surface roughness of three pristine CoCr femoral heads. All components were 28-mm CoCr ARTICUL/EZE® femoral heads supplied by DePuy Synthes (Leeds, UK). The average roughness parameters for the retrieved metallic femoral heads, including those which were locally assessed in regions of moderate to severe damage, have also been specified as a comparison.

Sample	Surface Roughness (μm)			
	Ra	Rsk	Rp	Rv
1	0.0032	-18.0099	0.0093	0.0281
2	0.0033	-13.5455	0.0097	0.0230
3	0.0039	-14.2619	0.0106	0.0291
Mean	**0.0034**	**-15.2724**	**0.0098**	**0.0267**
Retrieved	**0.0346**	**-1.5434**	**0.0996**	**0.1296**
Retrieved (Severe)	**0.6388**	**1.5114**	**2.3915**	**1.5457**

Published studies have previously reported the average roughness Ra of retrieved femoral heads from conventional THRs, as shown in Table 3.9. In summary, these studies have reported an average roughness Ra of 0.0105 μm to 0.0250 μm for metallic components (Wong, MD et al., 2013; Laurent et al., 2014; Taddei et al., 2016) and 0.0035 μm to 0.0078 μm for ceramic components (Kim, 2007; Nogiwa-Valdez et al., 2014; Elpers et al., 2014). The results of this analysis suggests a comparable in-vivo roughening of ceramic femoral heads from both conventional and DM implants. However, there appears to be an increased roughening of metallic femoral heads from DM bearings in comparison to conventional THRs. The cause of this roughening is unknown however the introduction of modular acetabular shells, which acts as an additional origination site for third body debris, may have some influence on this. Additionally, these results may provide some insight into the increased revision rates observed for DM bearings in comparison to conventional implants as reported in early National Joint Registry data (National Joint Registry, 2021).

Table 3.9 – Mean surface roughness (Ra) of retrieved femoral heads from conventional THRs as reported in the literature. Mean roughness of DM femoral heads reported in the present study have been included as a comparison.

Material	Study	Ra (μm)
CoCr	(Wong, MD et al., 2013)	0.0105
	(Laurent et al., 2014)	0.0177
	(Taddei et al., 2016)	0.0250
	Present	**0.0346**
Ceramic	(Kim, 2007)	0.0078
	(Nogiwa-Valdez et al., 2014)	0.0012 to 0.0040
	(Elpers et al., 2014)	0.0035
	Present	**0.0040**

It is known that the roughness of femoral heads may be increased in the presence of metal transfer patches (Eberhardt et al., 2009; Merola et al., 2016) or following dislocation of the joint (Mai et al., 2010; Ito et al., 2010). In the present study, no metal transfer was observed on the metallic heads and only minor metal transfer marks (i.e., thin streaks <1 cm in length) were identified on a portion of the ceramic heads. Additionally, only a small proportion of the femoral heads (one metal and one ceramic) failed due to instability or dislocation.

3.7.3.2 – Acetabular components

With respect to the acetabular components, a visual inspection was carried out on all 12 components which included eight modular inserts and four monobloc shells. Visual inspection of the components revealed light scratching to the most common mode of damage. In fact, a high proportion of samples were covered in fine, multi-directional scratches. Moderate to severe damage was observed on nine samples (75%) which usually consisted of small (<1 cm), deep scratches localised on a small portion of the component's rim. It is thought that this type of damage may be the result of contact with surgical instrumentation due to its localised and discrete nature.

It was not possible to characterise the surface roughness of these components due to limitations of the available equipment. To the author's knowledge, this type of analysis has not yet been conducted on DM acetabular components and would be advantageous in order to better understand the tribological and functional properties of DM implants. Optical methods are typically not suitable for these types of components due to their concavity and requirements for optical lenses to sit close to

the sample's surface. However, advancements in profilometry equipment including angled or lengthened styli may facilitate this type of study in the future.

3.8 – Discussion

The aim of this study was to characterise surface damage on a collection of retrieved DM bearings so that their in-vivo biomechanical function may be better understood. In summary, a total of 20 sets of DM retrievals were assessed using a range of methodologies which included visual inspection techniques, a novel geometric assessment method (developed in Chapter 2), energy dispersive x-ray analysis and contacting profilometry. To the author's knowledge, this is the first instance in which all articulating DM components (i.e., liner, head, shell) were comprehensively and non-destructively characterised in one study.

The implants assessed in this study consisted of six device types which were in-vivo for an average of 20.0 ± 18.8 months. Half of the implants were in-vivo for less than 12 months and therefore represent early failures. Despite the enhanced stability provided by DM THRs, two (10%) of the implants failed due to dislocation (Sample 15) or instability (Sample 5) at 2.7 and 26.2 months, respectively. Additionally, two (10%) of the implants failed due to IPD. This is a long-term failure mechanism unique to DM bearings which occurs due to degradation of the liner's retentive bore thus allowing the femoral head to disassociate. However, in the present study, two implants presented with short-term IPD failures i.e., at 0.9-and 13-months post-implantation. In one case (Sample 20), there was also clear evidence of metal-on-metal articulation between the femoral head and acetabular shell (Figure 3.17). This was not evident in the second sample (Sample 1). Both implants were manufactured from modern DM devices. This contradicts the current literature which reports no incidence of IPD after primary THR with 8.5 years follow-up for new-generation DM bearings or for those with a 28-mm femoral head (Darrith et al., 2018). Due to the small sample size of this study, it is difficult to conclude that IPD remains a prevalent complication of DM THRs. However, this highlights the need for long-term survivorship studies with large sample sizes to identify and better understand the pertinent failure modes of these types of implants.

This study has successfully provided some insight into the in-vivo mechanisms of DM constructs, particularly with regards to the unconstrained polyethylene liner. More specifically, the results of this study suggest that the internal articulation between the

femoral head and liner is the primary and preferential articulation site. This is evidenced by a high incidence of burnishing observed at the internal surface of retrieved DM liners (50%), in comparison to the external surfaces (15%). Additionally, geometric analysis of the liners demonstrated larger, more concentrated regions of positive geometric variation across the internal surfaces, which is consistent with frequent articulation and therefore wear/deformation of the surface. Interestingly, the morphology of these damaged regions varied between samples. In this study, crescent-shaped, circumferential, and circular regions of positive geometric variation were observed. This suggests that rotation of a DM liner within the acetabular component is possible, although the extent at which this occurs may vary implant to implant. This variation may be explained by a number of implant, patient, and surgical factors although further research is necessary to better understand these relationships.

Furthermore, the results of this analysis provide some evidence that DM implants may be susceptible to damage as a result of edge loading, which occurs when the loaded region shifts towards the rim of the acetabular component. This may be caused by a steep cup inclination angle or a dynamic separation between the head and liner, and is known to adversely affect the wear performance of conventional THRs (Leslie et al., 2009). In this study, four samples (20%) presented with a similarly-shaped, discrete region of damage on the external surface of their polyethylene liners as exampled in Figure 3.11 (D-F). These damaged features resemble a characteristic wear stripe previously observed on edge-loaded femoral heads from hard-on-hard (e.g., CoC) bearings (Esposito et al., 2012; Sariali et al., 2014). The external surface of a DM polyethylene liner acts as an effective large-diameter femoral head situated within the acetabular component, and therefore it is unsurprising that these implants may present with similar damage patterns to conventional femoral heads if subjected to the same conditions. Limited studies have assessed the performance of DM bearings under edge loading, although one in-vitro simulation study reports no significant difference in the volumetric wear rate of these devices when subjected to standard gait and varying cup inclination angles of 50° and 65° (Loving et al., 2015). To the author's knowledge, this is the first study which suggests that DM devices may be adversely affected by edge loading and therefore warrants further investigation into the performance of these devices under such conditions.

In addition, analysis of the retrieved liners revealed significantly more damage at the external surfaces in comparison to the internal surfaces. This is evidenced by both the visual inspection (i.e., increased incidence of abrasion, delamination, and deformation) and geometric assessment (i.e., increased incidence of deep pitting) studies. Due to the unexplainable nature of this damage, it is hypothesised that this was caused, at least in part, due to ex-vivo factors. For example, contact with surgical instrumentation may explain why a high proportion (50%) of the embedded debris found on the external liner surfaces contained traces of iron. Additionally, this may explain why localised and discrete regions of deep scratching were identified on a portion of the femoral heads and acetabular rims in Section 3.7.

Ex-vivo component damage was also observed via the levering out process required to disarticulate the femoral head and liner. This resulted in the formation of a notch at the liner's chamfer, a feature which was observed on 95% of the samples. Additionally, geometric assessment of the liner revealed a flattening effect on seven samples, which is believed to have occurred due to the use of a vice clamp (to stabilise the component during disassembly of the head and liner).

In summary, there is evidence to suggest that a portion of the damage observed on the retrieved components may be contributed to ex-vivo factors. No studies have characterised the damage caused to DM liners, heads and acetabular inserts/shells as a result of the retrieval collection, transit and preparation process. It is recommended that this type of study is considered as future work to improve future retrieval collection protocols and retrieval analyses specific to these types of implants.

In addition to polyethylene liners, retrieved femoral heads and acetabular components were also assessed in this study. It was difficult to assess the relationship in damage progression between the components (e.g., how femoral head roughness is associated with damage to the liner or acetabular component) due to a limited sample size, lack of full component sets and methodological limitations. For example, previous in-vitro testing and retrieval analyses of conventional THRs have shown a positive correlation between femoral head roughness and volumetric change of the liner (Barbour et al., 2000; Laurent et al., 2014). Unfortunately, it was not possible to assess this type of relationship in the present study due to limitations of the geometric assessment methodology (i.e., no quantitative outputs such as volumetric change). Instead, the head roughness (Ra, Rp) was compared against the internal and combined damage scores of the liner. No correlation between head

roughness and liner damage score was apparent within any of the groupings (Figure 3.18), although this may be an artefact of the damage scoring methodology whereby the severity and extent of damage was not assessed. In addition, the femoral head roughness (Ra, Rp) did not appear to be associated with the damage observed on the internal surfaces of the liners (e.g., increased Ra associated with larger regions of geometric variance).

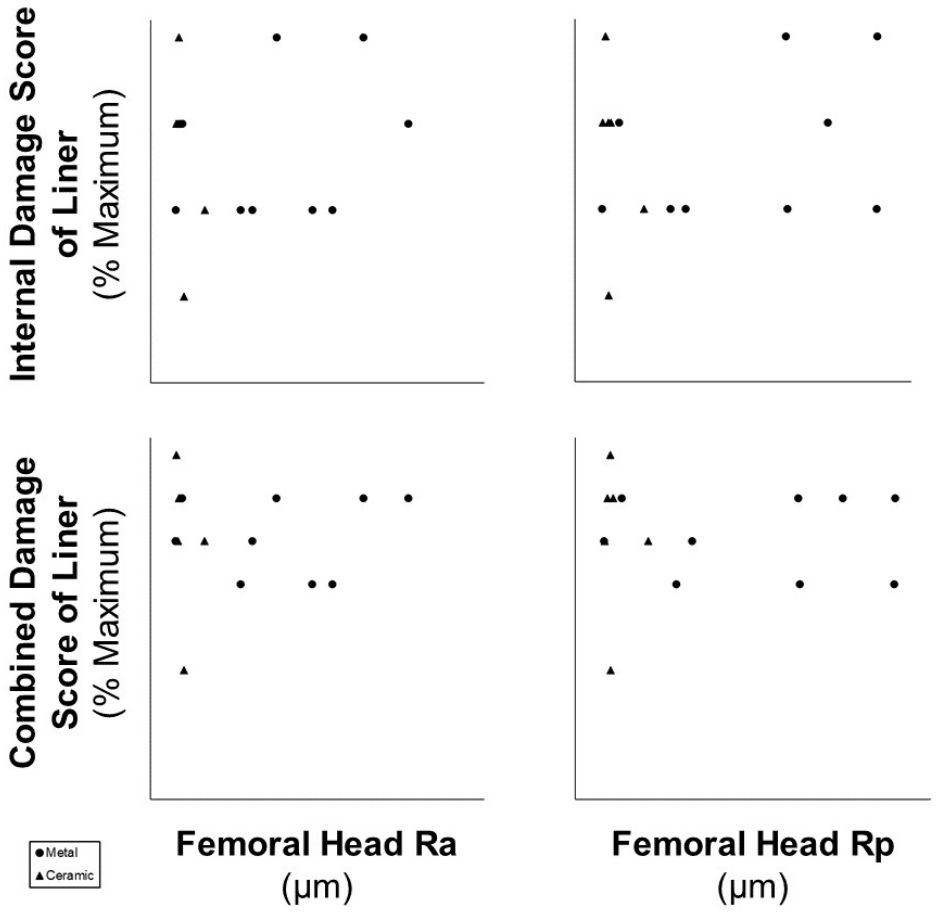

Figure 3.18 – No association between femoral head roughness (Ra, Rp) and liner damage (internal, combined damage score) was apparent in any of the groupings.

The limitations of this study should be acknowledged. All components included in this analysis were retrieved and thus are not necessarily representative of well-functioning implants. Additionally, the components had a mean time in-vivo of 20 months (range: 0.9 to 57) and thus lack long-term service periods under physiological conditions. The limited supplemental information made it challenging to stratify the components into sub-groups based on various patient and/or surgical factors, and thus restricted the scope of the analyses. Finally, it was not possible to distinguish component damage

caused in-vivo versus ex-vivo although it was suspected that all components, including the liners, femoral heads, and acetabular components, did sustain some degree of damage as a result of the revision process.

3.9 - Conclusion

Despite its limitations, this study has provided some insight into the in-vivo mechanics of DM bearings through the multi-method analysis of 20 retrieved DM component sets. Data from this study suggests that the internal articulation between the femoral head and liner is the primary and preferential articulation site for these bearings. In addition, there is evidence to suggest there is an ability for DM liners to rotate within the acetabular component. However, a variation in this ability was observed within the collection and future research is recommended to better understand the effects of surgical, patient and implant factors on DM kinematic behaviour. Furthermore, the results of this analysis have provided some evidence to suggest that DM implants may be adversely affected by edge loading although further research is required to confirm this finding. This study has also highlighted the importance and utility of retrieval analyses, although an increased sample size and more complete supplemental information would have strengthened this study.

Chapter 4 –
Development of an in-vitro methodology for motion tracking of dual mobility liners

4.1 – Introduction

The in-vivo kinematics of Dual Mobility (DM) bearings are not well understood. The mechanics of DM liner motion have been inferred from studies such as retrieval analysis however few studies have directly investigated these behaviours. Direct assessment of DM kinematics has previously been facilitated through computational, experimental, cadaveric or Radiostereometric Analysis (RSA). For example, Fabry and colleagues have developed experimental protocols and mathematical models to assess the self-centering motions of eccentric DM designs (Fabry, Kaehler, et al., 2014; Fabry, Woernle, et al., 2014). The experimental protocol utilised a six-axis robot arm to load and displace the implants and video capture systems to monitor the position of the liner under various motion profiles. However, the loads were reduced by 75% to prevent damage to the equipment, the tests were limited to 100 cycles and the implants were not fully submerged in lubricant. Additionally, the components were oriented in a horizontal position and therefore the setup of the test did not represent in-vivo physiological conditions. Alternatively, mathematical models were developed and validated against the experimental protocol but could only consider two-dimensional rotations of the liner. The findings of these studies will be later discussed in Section 5.1.

The behaviour of DM liners has also been assessed in-vivo through cadaveric models or RSA. Cadaveric models have been used to assess the interaction between DM implants and their surrounding soft tissues (Nebergall et al., 2016; Logishetty et al., 2019). The motions of DM liners were also assessed through static and dynamic RSA

whereby tantalum beads were placed into the liners although only non-weight bearing activities were possible to investigate (Jørgensen et al., 2022). Cadaveric and in-vivo motion analyses provide useful insights into the mechanics of DM implants under physiologically relevant conditions and soft tissue constraints although data from these studies are patient-specific and often involve small sample sizes.

In-vitro simulator testing is an established methodology to assess Total Hip Replacements (THRs) under controlled and physiologically relevant conditions. Simulator testing has been widely utilised in the literature to characterise the wear performance of conventional implants (Wroblewski et al., 1996; Brockett et al., 2007; Leslie et al., 2009; Al-Hajjar et al., 2013). More recently, DM bearings have also been analysed with in-vitro tests, but these studies are limited in their numbers (Saikko and Shen, 2010; Loving et al., 2013; Loving et al., 2015; Gaudin et al., 2017). These studies have investigated the performance of DM THRs under standard and adverse (e.g., high cup inclination angle, impingement) conditions. However, there are no published studies which have investigated the functional behaviour of DM bearings, particularly relating to the mobile liner. It is hypothesised that this is due to a lack of available and suitable methodologies to facilitate this type of analysis.

One of the main challenges in monitoring the position and behaviour of DM bearings arises from the requirement to submerge the implants into lubricant during testing. This is to ensure the in-vitro tribological conditions mimic those found in the body. This removes line-of-sight of the implants therefore making it challenging to track the position of a mobile DM liner, which can move freely and independently of the simulator axes. It is possible to omit the use of the lubricant container so the implant can be visually or optically monitored however, alterations to the tribological environment may influence function of the implant. Instead, the orientation of the liner may be compared pre- and post-test, but this only provides a crude measure of motion and does not provide information about the temporal behaviour of the component. Advancements in laboratory technology may provide a solution to this challenge. A novel, non-destructive positional tracker was developed for DM liners at the University of Leeds by Dr Matthew P. Shuttleworth (Shuttleworth et al., 2021).

Therefore, the aim of this study was to develop an in-vitro testing methodology for the motion tracking of DM liners under physiologically relevant loading, displacement, and lubrication conditions using the novel tracker.

4.2 – Overview of the analysis

In line with the aim of the study, two pilot studies were performed: an intra- and inter-liner repeatability analysis to assess DM liner motion under standard conditions, and a sensitivity study to determine whether the simulator input conditions influenced the observed motion (Table 4.1). The results of this study will provide rudimentary information about the mechanics of DM bearings. In addition, outputs of this analysis will be used to further inform in-vitro motion tracking methodologies for DM bearings which will later be applied in a larger, more robust study as described in Chapter 5.

Table 4.1 – Description of the test conditions used for the repeatability and sensitivity analyses described in this chapter for the assessment of DM liner motion. Note – Standard gait refers to the conditions described by ISO 14242-1 with a cup inclination angle of 45°, which are further detailed in Section 4.3.2.3. In each test repeat, the components were subjected to 3,600 cycles of standard or modified gait conditions.

Test		Description	Repeats
Intra-liner repeatability		Standard gait	1 Liner x 10 Repeats
Inter-liner repeatability		Standard gait	3 Liners x 3 Repeats
Sensitivity testing (i.e., altered or adverse test conditions)	High cup angle	Standard gait with an increased cup inclination angle of 65°	1 Liner x 3 Repeats
	Low swing phase	Standard gait with a decreased swing phase load of 100N	1 Liner x 3 Repeats
	Abrasion	Standard gait against an artificially scratched femoral head	1 Liner x 3 Repeats
	Increased gait speed	Standard gait	1 Liner x 3 Repeats

4.3 – Materials and methods

4.3.1 – Materials

All liners used in this testing were 69/28-mm BI-MENTUM™ DM liners manufactured from moderately cross-linked polyethylene (ALTRX®). Each of these were articulated against a 69-mm monobloc BI-MENTUM™ Press-Fit acetabular shell, and a 28-mm CoCr femoral head (ARTICUL/EZE®) mounted onto a Corail® femoral stem. A femoral stem was utilised for this testing, in contrast to less realistic options such as in-house manufactured spigots which are often used for in-vitro simulator tests. This was to ensure the femoral neck geometry and surface roughness was reflective of true THR components, as this affects how the outer articulation is engaged and thus influences motion of the liner. Additionally, the femoral neck geometry is known to

influence how damage progresses at the retentive bore (Laura, H.S. Hothi, et al., 2017). Therefore, the use of femoral stems was thought to be essential for the in-vitro testing of DM bearings in both wear/damage progression and motion tracking studies.

It should be noted that all liners were articulated against the same femoral head, femoral stem, and acetabular shell, with the exception of one sensitivity test condition of increased cup inclination angle (Section 4.3.5.1) whereby an identical, duplicate femoral head and acetabular shell were utilised due to the altered setup of the simulator and fixtures. Therefore, independent component sets were not used in this testing. This made the testing more economical and time efficient. The use of independent component sets was not considered to be an important factor for the purposes of methodological development and pilot data collection. The femoral head and acetabular shell were routinely inspected throughout testing to ensure no significant damage had occurred which would bias the results of the study. If scratching was identified on either the head or shell, the damaged component was switched out for a pristine sample. This only occurred on one occasion whereby a new femoral head was required for the high cup inclination angle testing (see Section 4.3.5.1).

All components were supplied by DePuy Synthes (Leeds, UK). Further component information can be found in Table A3 of Appendix A.

4.3.2 – In-vitro testing methodology

4.3.2.1 – Anatomical Hip Simulator

A ProSim electromechanical single-station hip joint simulator, known as the Anatomical Hip Simulator (Simulation Solutions Ltd, UK), was used to apply physiologically relevant loading and displacement conditions to DM THRs for the analyses described in this chapter. It is a six-axis machine which can apply axial loading, translational displacement in the medial-lateral axis, and rotational displacements in flexion/extension, adduction/abduction, and internal/external rotation as shown in Figure 4.1. The simulator was setup to recreate the motions of a right hip.

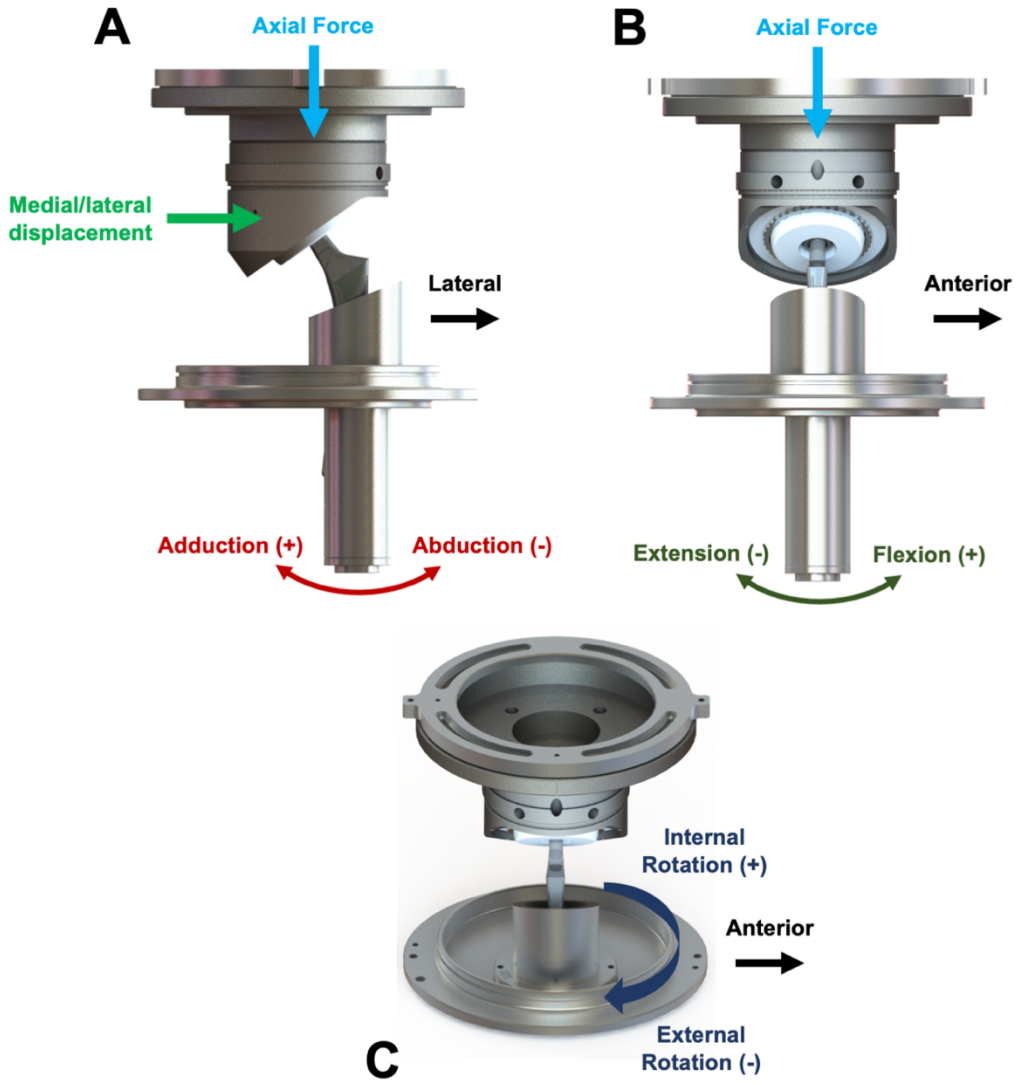

Figure 4.1 – Setup of the Anatomical Hip Simulator, viewed from the coronal (A) and sagittal (B, C) planes. The fixturing includes an acetabular cup holder (top component) and femoral stem holder (base component). The schematic also illustrates how the axial loading, translation and rotational displacements were applied to the components. The simulator was setup to recreate the motions of a right hip.

4.3.2.2 – Simulator setup

Implants were mounted into the simulator using bespoke fixtures (Figure 4.1) which included an acetabular cup holder and femoral stem holder. Two iterations of the acetabular cup holder were manufactured to represent standard (45° in-vivo) and high (65° in-vivo) cup inclination angles. The axial loading is applied vertically in the simulator although this force vector is estimated to be approximately 10° medialised in the body. Therefore, the cup holders were manufactured with inclination angles of 35° and 55° to represent in-vivo inclinations of 45° and 65°, respectively. The 45° in-

vivo acetabular cup holder was used for all tests described in this chapter, with the exception of the high cup angle testing detailed in Section 4.3.5.1.

Acetabular shells and femoral stems were secured into the fixtures with PMMA bone cement and bespoke cementing jigs which ensured the centre of rotation (COR) of the components were aligned to the COR of the simulator. Femoral heads were securely mounted onto the femoral stem with an impactor, and liners were then assembled onto the femoral heads with a handheld vice clamp. Both instruments were designed as intra-operative surgical tools and therefore do not cause damage to the components.

Once the components and associated fixturing were seated within the simulator, the liner was placed into a neutral position prior to testing whereby the flat face of the liner was parallel to the flat face of the shell. Additionally, the liner was rotated so that a marker on the tracking device (see Section 4.3.3) was positioned at the most superior point.

4.3.2.3 – Standard gait conditions

The implants were enclosed in a flexible silicone casing (referred to as a gaiter) which was filled with lubricating fluid. The lubricant comprised of 25% newborn calf serum (Thermo Fisher Scientific, USA) in deionised water. The lubricant was supplemented with 0.03% (v/v) sodium azide to inhibit bacterial growth. The protein concentration of the lubricant was approximately 15 g/L. Prior to testing, a small amount of serum (~1 mL) was injected directly in between the femoral head and liner, to ensure the inner articulation was sufficiently lubricated at the start of each test.

The simulator was programmed to apply standard gait conditions at a frequency of 1 Hz as recommended by ISO 14242-1. This included a twin-peak axial loading profile with a maximum load of 3 kN and a swing phase load of 300 N, as shown in Figure 4.2. Rotational displacements of the femoral component were applied in three axes: flexion (+25°) / extension (-18°), adduction (+7°) / abduction (-4°) and internal (+2) / external (-10°) rotation (Figure 4.2).

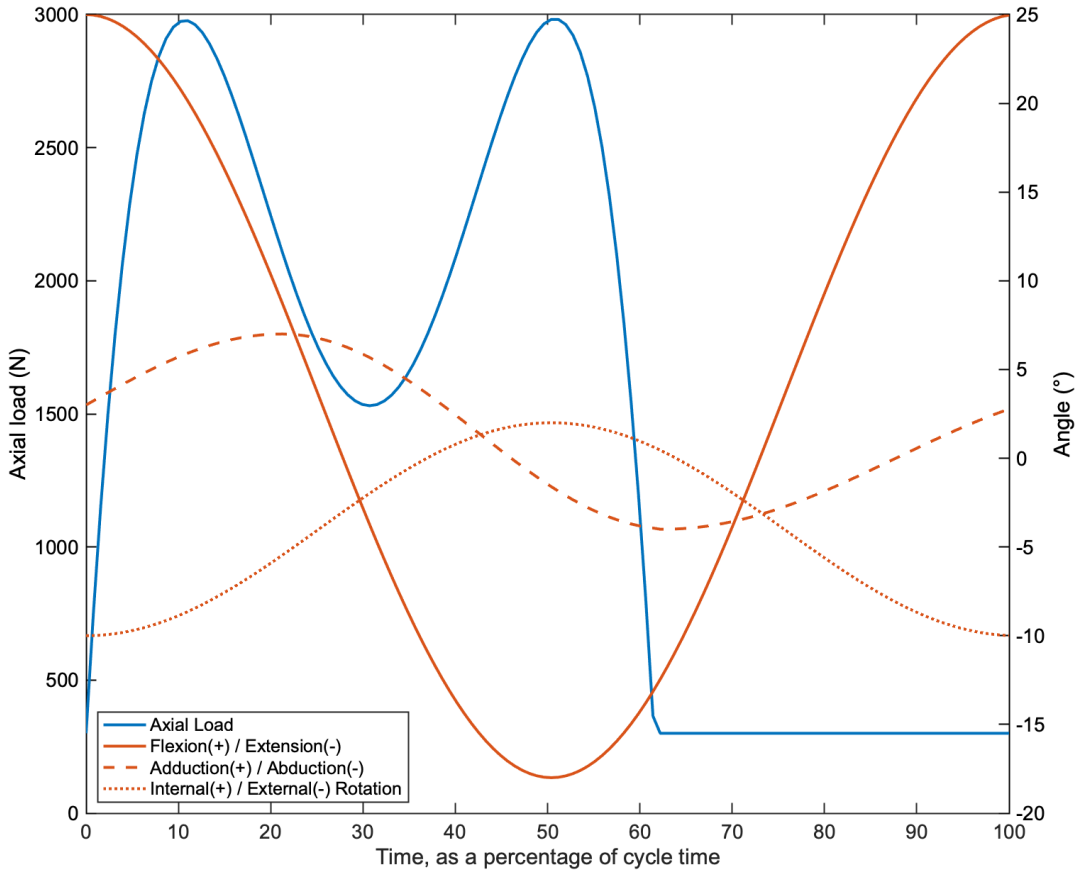

Figure 4.2 – Axial loading and rotational displacement profiles for standard gait, as recommended by ISO 14242-1.

As part of the simulator's initialisation process, the first 10 cycles of gait applied the rotational displacements to the components with incrementally increasing axial forces until these met the specified profile. This is known as the simulator ramp-up period.

4.3.3 – Measurement method

It is challenging to visualise the orientation of DM liners throughout in-vitro simulation studies due to the use of an enclosed, lubricant-filled gaiter. Therefore, a bespoke tracker was used to monitor the position of DM liners for the purposes of this study (Shuttleworth et al., 2023). It is important to note that the tracker was prototyped and developed by Dr Matthew P Shuttleworth and was not the direct work of the author.

Prior to testing, the tracker was mounted to the flat face of the liner using double-sided adhesive tape as shown in Figure 4.3, which reliably secured the tracker without damaging the liner. Additionally, the tracker did not interfere with the liner's articulating surfaces or the femoral neck-liner junction (i.e., the 'third' bearing

surface). The tracker was connected to a microcontroller via a thin tether which was threaded through a hole in the acetabular cup holder. The hole was then sealed with reusable engineering putty. A portion of the tether was left free-floating in the gaiter to ensure it was not taut and thus interfering with the liner's position.

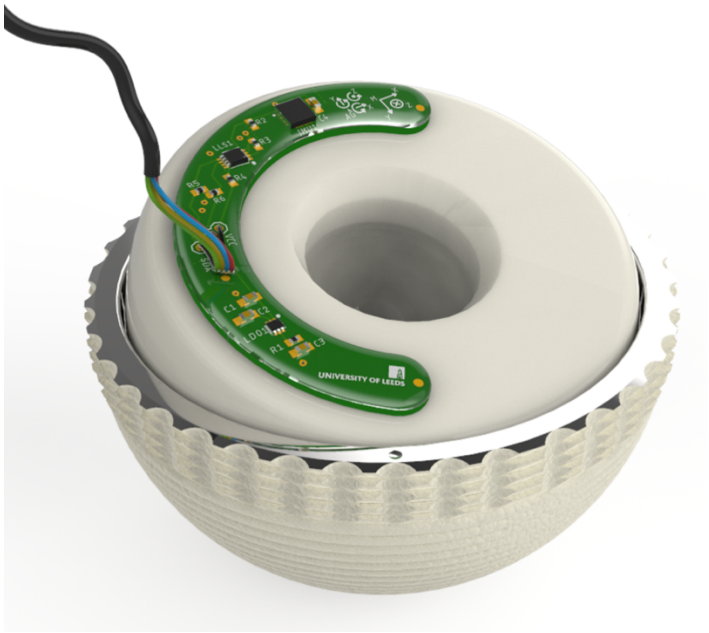

Figure 4.3 – Dual mobility liner tracker, which is attached to the flat face of the liner with double-sided adhesive tape. Image produced by Dr Matthew P Shuttleworth and reproduced with permission to include in this thesis.

The tracker relied on a multi-sensing fusion algorithm, whereby the rotation of the liner was deduced by combining information from several individual sensors (i.e., accelerometer, gyroscope, magnetometer) to improve reliability of the data. In addition, a coil of copper wire was mounted to the acetabular cup holder (see Figure 4.4) to ensure the tracker was positioned within a stable and well understood magnetic field. This did not impede liner motion, and significantly improved the performance of the magnetometers within the disruptive magnetic environment of the simulator and thus the quality of the data. The tracker's outputs were validated and calibrated against a six-axis robot arm (UR3, Universal Robots GmbH) which demonstrated it could reliably produce orientation measurements within 3.9º of the true value under the described setup (i.e., in a hip joint simulator with the copper coil affixed) and with negligible drift (Shuttleworth et al., 2023).

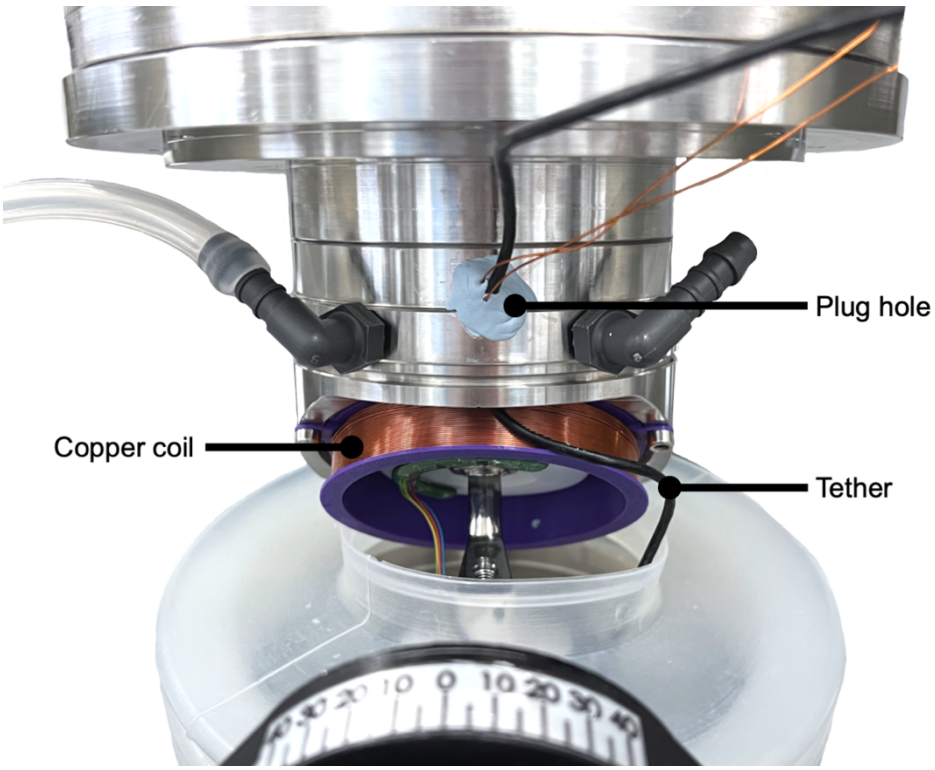

Figure 4.4 – Setup of the tracker, including a tether which is threaded out of a small hole in the acetabular cup holder (i.e., plug hole) and connected to a microcontroller. A coil of copper wire was also mounted to the cup holder to position the tracker within a stable and well understood magnetic field throughout testing.

The tracker recorded rotation of the liner about the X-axis (roll), Y-axis (pitch) and Z-axis (yaw), with respect to an origin positioned at the COR of the liner. The X- and Y-axes of the coordinate system were parallel to the liner's flat face as shown in Figure 4.5, with the X-axis passing through the inertial measurement unit (IMU) of the tracker. Therefore, rotations in pitch and roll referred to a tilting of the liner within the shell. In contrast, the Z-axis was defined as being normal to the flat face of the liner and thus yaw represented precession of the component within the shell. The axes were fixed to the liner and therefore the orientation of the coordinate system changed with each elemental rotation of the component as exampled in Figure 4.5. These types of rotations are known as intrinsic rotations with a Z-Y'-X'' sequence (i.e., the order in which the rotations must be applied to determine the component's final position). This is in contrast to extrinsic rotations which are always referenced against a global (unchanging) coordinate system.

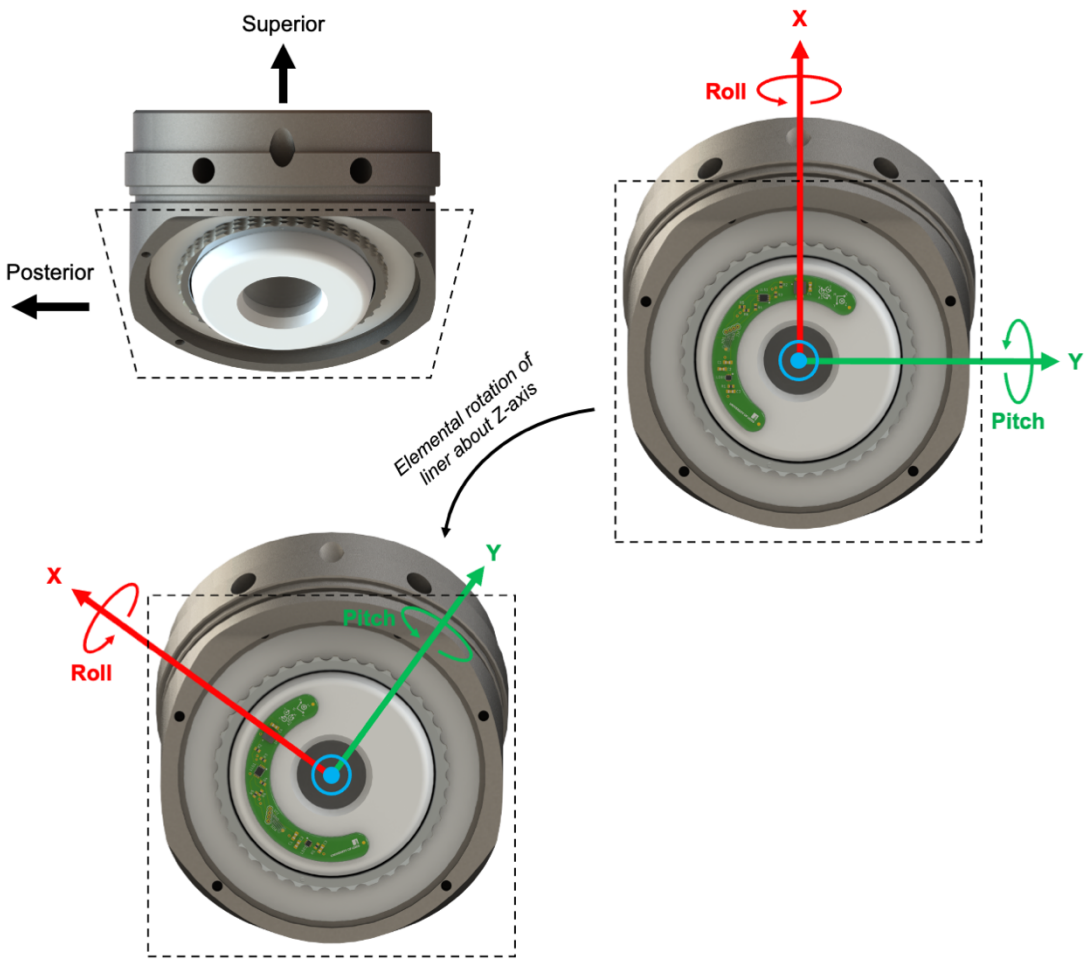

Figure 4.5 – Schematic illustrating the three axes of liner rotation which are recorded by the tracker: roll (i.e., rotations about the X-axis), pitch (i.e., rotations about the Y-axis), and yaw (i.e., rotations about the Z-axis). The rotations are intrinsic and therefore the orientation of the coordinate system changes with each elemental rotation of the liner, as exampled in the figure whereby a rotation about the Z-axis was applied.

Initial pilot testing revealed that the roll-pitch-yaw notation of describing liner orientation was unintuitive and undesirable. Therefore, a bespoke MATLAB (version R2020b) script was developed to convert the roll-pitch-yaw orientations into new and more easily understood parameters. These described orientation of the liner in terms of its inclination relative to the shell, and its azimuth. Within this thesis, these angles will be referred to as inclination* and azimuth* respectively, whereby an asterisk will be used to denote orientation of the polyethylene liner relative to the acetabular shell.

In summary, inclination relative to the shell, or inclination*, is a directionless parameter which describes how tilted the liner's flat face is from its neutral position as shown in Figure 4.6. Inclination* is a useful metric to monitor DM liner motion as

this may be used to identify the occurrence of impingement events between the femoral neck and liner. This would result in an activation of the outer articulation thus causing a sudden change in inclination*. Alternatively, azimuth* refers to the clockface direction in which the inclined plane is facing (Figure 4.7), which can range from 0° to 360°. Several examples of liner orientation, with associated inclination* and azimuth* values, are presented in Figure 4.8. Appendix C details the mathematical calculations required to determine inclination* and azimuth*.

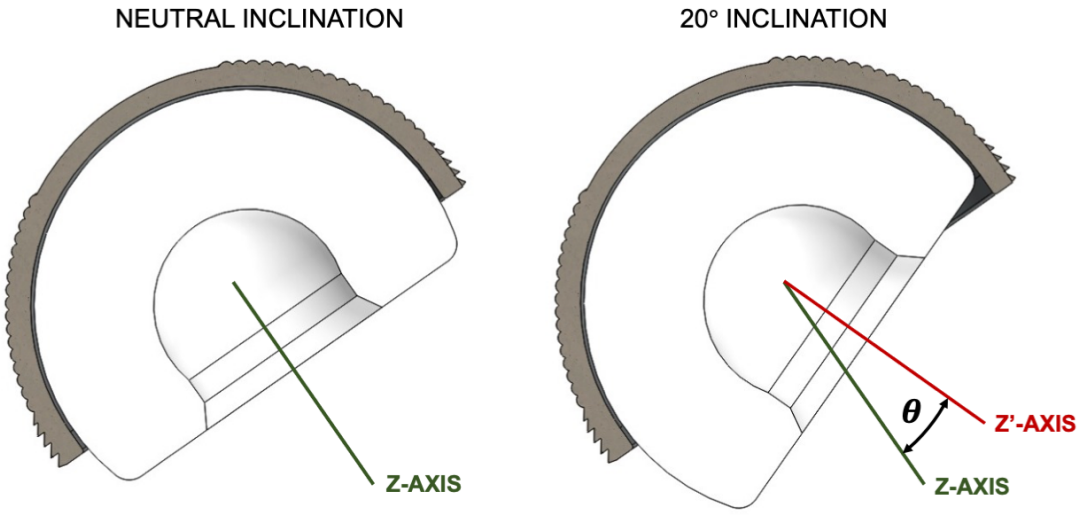

Figure 4.6 – Schematic illustrating the inclination* of the liner, which refers to the tilt of its flat surface irrespective of direction. A neutral inclination* of the liner (i.e., 0°) refers to when the flat face of the liner is parallel to the flat surface of the acetabular shell, as shown in the image on the left. As the liner tilts, as shown on the right, the position of the Z-axis changes. The inclination* is determined as the angle between the original Z-axis and the new Z-axis, also known as Z'.

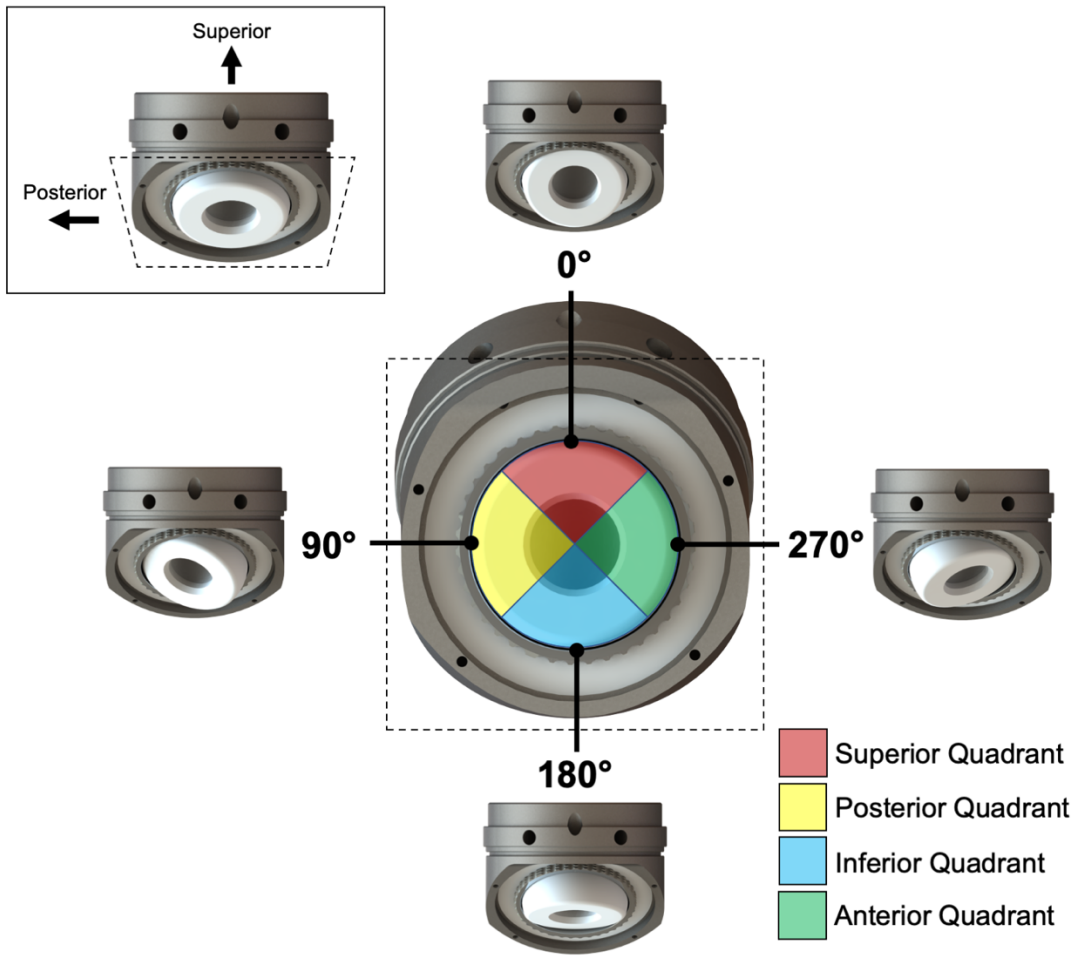

Figure 4.7 – Schematic illustrating how the azimuth* of the liner is calculated. The azimuth* refers to the direction in which the liner's flat face is oriented, whereby positions of 0°, 90°, 180° and 270° refer to superior, posterior, inferior and anterior directions, respectively.

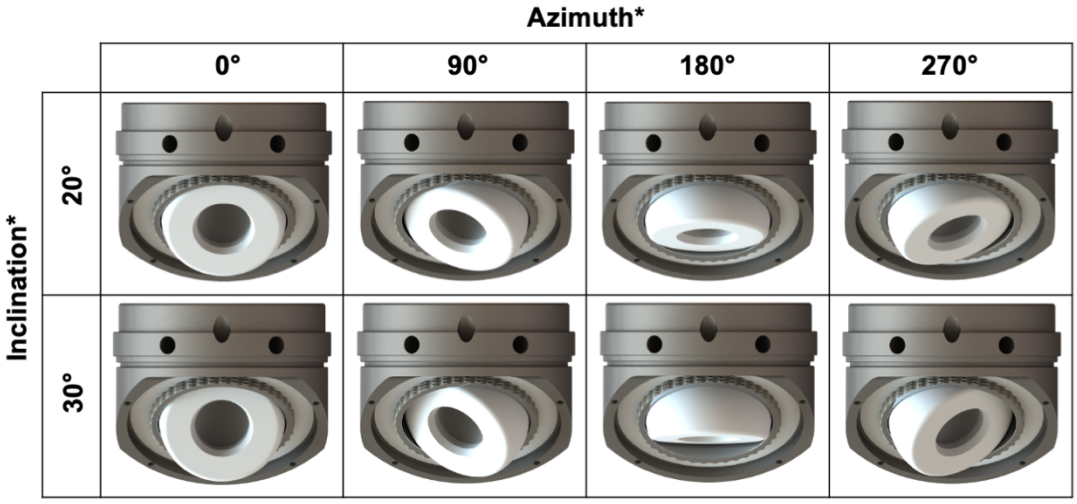

Figure 4.8 – Schematic illustrating several cases of liner orientation, including inclination* angles of 20° and 30° and an azimuth* of 0°, 90°, 180° and 270°.

One limitation to describing orientation of the liner in terms of its inclination* and azimuth* is that it does not consider the rotation of the liner within the shell, as shown in Figure 4.9. However, this behaviour is captured by the original yaw data (i.e., rotation about the Z-axis). Of the three intrinsic angles reported by the raw sensor data (i.e., roll, pitch, yaw), yaw is the first angle in the rotation sequence and therefore continues to represent rotation of the liner about an axis perpendicular to its flat face (i.e., Z-axis) regardless of any elemental rotations in the X-, Y- or Z-axes. Therefore, rotation of the liner can be assessed in a separate analysis. This angle will be referred to as precession*. Positive precession* was defined as a counter-clockwise rotation of the liner about its Z-axis, or the axis perpendicular to the flat face of the liner, as shown in Figure 4.10. Precession* of the liner was defined by the setup of the tracker's inertial measurement unit and was independent from the type of hip analysed (i.e., left versus right). However, the clinical implications of positive precession* differed between left and right hip setups. For the simulator setup specified in this methodology, which represents a right hip, a positive precession* (i.e., counter-clockwise rotation) represents a rotation of the tracker's inertial measurement unit from the superior, to posterior, to inferior, to anterior quadrants in this order.

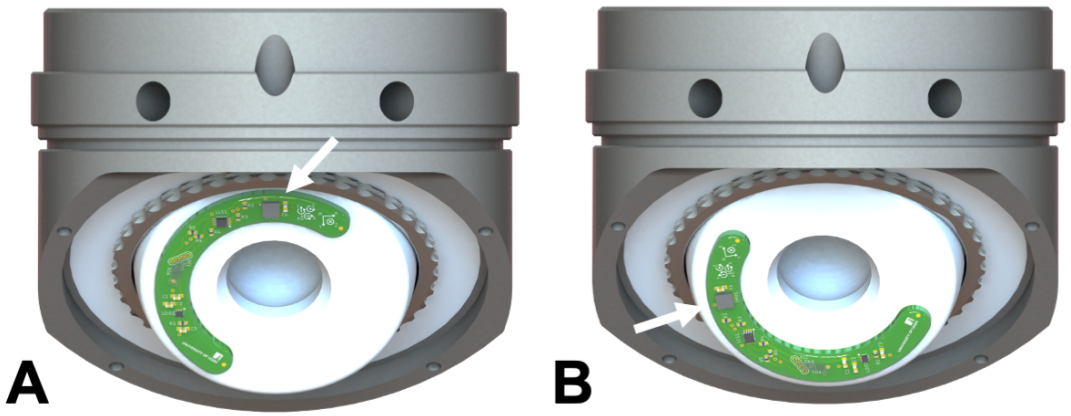

Figure 4.9 – Schematic illustrating that the inclination* and azimuth* metrics do not capture the rotational behaviour of the liner. Both images depict a liner orientated at an inclination* of 20° and azimuth* of 0°. However, the precession* of the liner differs between the two examples as denoted by the position of the tracker's IMU chip (white arrow).

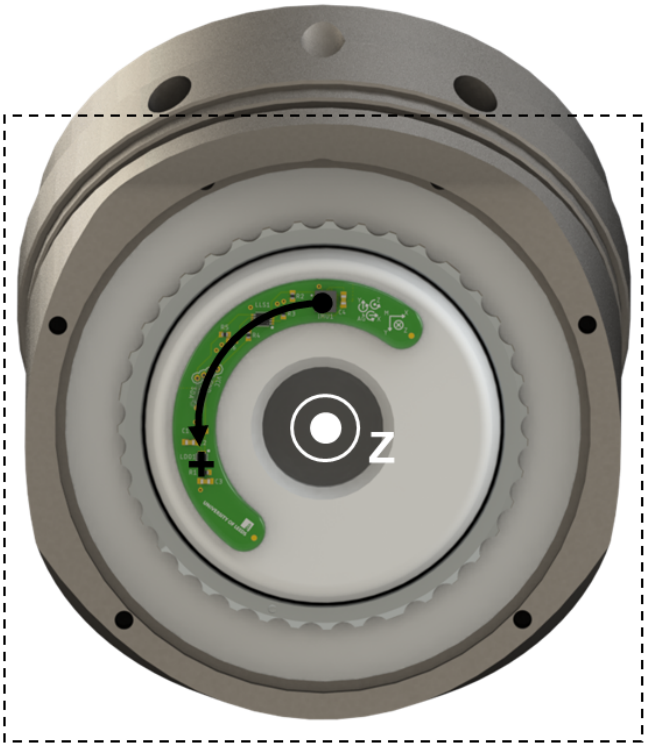

Figure 4.10 – Schematic illustrating a positive precession* of the liner, which is defined as a counter-clockwise rotation of the liner about its Z-axis.

4.3.4 – Intra- and inter-liner repeatability of DM liner motion

The aim of this pilot study was to assess the intra- and inter-liner repeatability of DM liner motion under standard gait conditions.

4.3.4.1 – Intra-liner repeatability assessment

One 69/28-mm DM liner (Liner 1) was subjected to standard gait conditions (Section 4.3.2.3) for 3600 cycles (i.e., 1 hour) on ten separate occasions. The position of the liner, including its inclination*, azimuth* and precession*, was monitored at a frequency of 50 Hz throughout each of the tests using the tracker (Section 4.3.3).

4.3.4.2 – Inter-liner repeatability assessment

A further two 69/28-mm DM liners (Liners 2 and 3) were subjected to standard gait (Section 4.3.2.3) for 3600 cycles (i.e., 1 hour) on three separate occasions each. The inclination*, azimuth* and precession* of each liner was monitored throughout all tests with the tracker (Section 4.3.3).

4.3.5 – Sensitivity analysis under altered test conditions

In order to assess whether the simulator input conditions have an effect on DM liner behaviour, a sensitivity analysis was performed whereby four samples (Liners 3, 4, 5, 6) were subjected to gait conditions modified from the standard described in Section 4.3.2 for 3600 cycles on three separate occasions each. The input conditions were modified to reflect various adverse conditions which DM bearings may be subjected to in-vivo, such as increased cup inclination angle (Section 4.3.5.1), reduced swing phase loading (Section 4.3.5.2), scratching of the femoral head (Section 4.3.5.3) and increased gait frequency (Section 4.3.5.4). Details regarding these modified conditions are discussed in the following sections.

4.3.5.1 – High cup inclination angle

Increasing the inclination of the acetabular shell is known to adversely affect the wear performance of conventional THRs (Leslie et al., 2009; Al-Hajjar et al., 2013). This is due to a condition known as edge loading, whereby the wear region is displaced closer to the edge of the sample therefore reducing the contact patch and increasing local stresses. Interestingly, DM bearings have shown either reduced (Loving et al., 2015) or similar wear rates (Saikko and Shen, 2010) to conventional bearings at high cup angles, suggesting that these bearings may have superior wear properties under conditions with high cup inclinations. However, results from the retrieval analysis (Chapter 3) suggests that DM implants may be susceptible to damage as a result of edge loading. Therefore, one 69/28-mm DM liner (Liner 4) was subjected to standard gait (Section 4.3.2) against an acetabular shell which was positioned at an inclination angle of 55° in-vitro of 65° in-vivo. It is important to note that a new acetabular shell was used for this test condition (see Table A3 of Appendix A) so that it could be cemented into simulator fixtures with the increased angle of inclination.

4.3.5.2 – Reduced swing phase load

In-house computational data suggests that a reduction in the swing phase load could result in increased articulation of the outer bearing of DM implants. The in-vivo swing phase load may be influenced by variations in patient anatomy (e.g., laxity of soft tissues), surgical approach and component positioning. Therefore, one 69/28-mm DM liner (Liner 5) was subjected to identical gait conditions described in Section 4.3.2 with the exception of the swing phase load which was reduced threefold from 300 N to 100 N. In particular, a swing phase load of 100 N was selected for this testing as

this was the lowest threshold allowable by the simulator before the load cells began reporting safety errors thus resulting in simulator faults.

4.3.5.3 – Scratched femoral head

Scratching of the femoral head is known to increase its surface roughness and lead to increased polyethylene wear. It is hypothesised that an increase in the friction of the internal articulation (e.g., introduction of scratches) could drive the outer articulation to be engaged more frequently. Therefore, one 69/28-mm DM liner (Liner 6) was subjected to standard gait (Section 4.3.2) against an artificially scratched femoral head.

One femoral head (28-mm CoCr ARTICUL/EZE™) was scratched using a mechanical indentation rig. The aim was to generate scratches which reproduced physiologically relevant peak heights identified from the retrieved femoral heads assessed in Chapter 3 (Section 3.7). Retrieved femoral heads which were identified to have regions of moderate to severe damage were used as the target group for this testing to represent the worst-case scenario and therefore increase the probability of inducing a change in liner motion through this testing. Therefore, the target peak height (Rp) of the artificially generated scratches was approximately 2.4 μm, as determined from Section 3.7.

The femoral head was scratched with a 200 μm diamond indenter applied at a constant load of approximately 27 N. In total, eight equally spaced scratches were generated in an asterisk formation. Each scratch originated at the pole and extended 6-mm towards the equator of the head. Scratches were characterised using a contacting profilometer and previously described methods (Section 3.7.1), prior to simulator testing.

4.3.5.4 – Increased gait frequency

In-vitro simulator testing of THR implants is most commonly performed at a gait frequency of 1 Hz as recommended by ISO 14242-1. No studies have investigated the effects of gait frequency on DM liner mechanics or wear performance to the author's knowledge. By increasing the gait frequency, this test condition would also allow the limitations of the motion tracking methodology to be assessed (i.e., to assess whether the tracker was capable of reliably performing at increased frequencies of rotational movement). Therefore, one 69/28-mm DM liner (Liner 3) was

subjected to standard gait (Section 4.3.2) at an increased frequency of 2 Hz. It is important to note that this testing was completed with Liner 3, which was used as part of the inter-liner repeatability assessment, due to a lack of available components. This naturally confounded the results of the study, and the results should be interpreted accordingly.

4.3.5.5 – Alternative conditions

Other relevant, adverse test conditions were considered for this sensitivity analysis, but several were not possible due to limitations of either the tracker setup or simulator. For example, dynamic separation between the liner and femoral head is known to increase the wear rate of conventional THRs (Al-Hajjar et al., 2013; Partridge et al., 2018), but its effect on DM THRs is not well understood. It is caused by a lateral mismatch in the centres of rotation of the femoral head and liner, which results in a dynamic separation (<1 mm) of the components during the swing phase of gait. Due to the possible lateral motion of the DM liner, it was not possible to reliably assess the effects of dynamic separation on DM liner motion in the present study. This was due to a limitation of the tracker, which was positioned within an established and well understood magnetic environment created by the copper coil. The tracker was not designed or calibrated to withstand lateral motion within the copper coil fixture and therefore the accuracy of the tracker's output data could not be established.

Combined gait cycles (i.e., intermittent walking amongst other activities such as sit-stand) were considered. High flexion activities (e.g., sit) were thought to increase the possibility of impingement events between the femoral neck and liner therefore engaging the outer articulation. However, these activities could not be investigated under the current simulator setup due to limited ranges of motion in each of the simulator axes and hence were beyond the scope of this study.

4.4 – Results

4.4.1 – General observations

The position of the DM liners was monitored in real-time throughout the duration of each test using the tracker's graphical user interface to ensure any faults with the simulator or tracker could be detected immediately. At the start of each test, a sudden change in the liner orientation was observed. This was characterised by a small shift in inclination* (i.e., less than 5°), sharp fluctuations in the azimuth*, and no notable changes in precession* (i.e., less than 1°) which occurred during the simulator ramp-

up period (i.e., the first 10 gait cycles). This is reflected in some of the outputted data, whereby the liner's start position does not appear to be at a neutral orientation of 0° inclination*, 0° azimuth*, and 0° precession*. This shift could not be reasonably controlled due at the start of each test due to the liner's inherent mobility. However, the magnitude of these changes was small and does not distract from the results of these types of analyses whereby overall trends in behaviour over time are observed.

In addition, spontaneous and frequent spikes were observed in the inclination*, azimuth* and precession* data across all tests, as exampled in Figure 4.11. Further testing confirmed that these were an artefact of the tracker whilst seated within the magnetic environment of the simulator and thus should be ignored. Therefore, a Matlab script was used to identify peaks and exclude their datapoints from the presentation of all figures presented in this thesis to make them more easily interpreted (Figure 4.11). Small, residual peaks in the modified data should be ignored as these are remanent artefacts of magnetic interference with the tracker and thus are not representative of true changes in liner orientation.

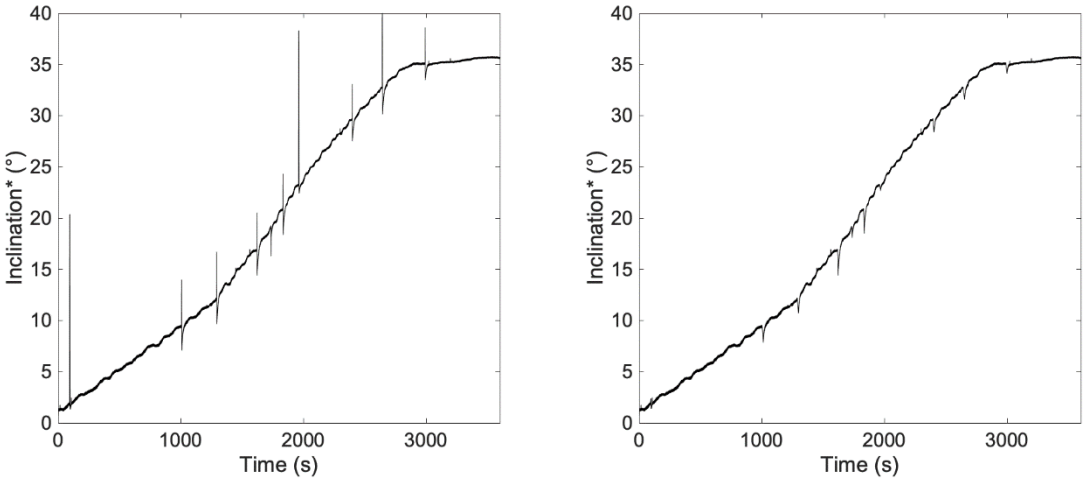

Figure 4.11 – Example of the spontaneous peaks identified in the tracker data (left). A peak removal algorithm was applied to remove a majority of the peaks and make the figures more easily interpreted (right).

4.4.2 – Repeatability assessment

4.4.2.1 – Intra-liner repeatability

The inclination*, azimuth* and precession* of one liner over 10 repeated tests are shown in Figure 4.12. The final resting position of the liner after each test is detailed in Table 4.2. On average, the final inclination*, azimuth* and precession* of the liner

was 28° ± 8° (range: 19°), 271°± 26° (range: 88°) and -47° ± 38° (range: 125°), respectively.

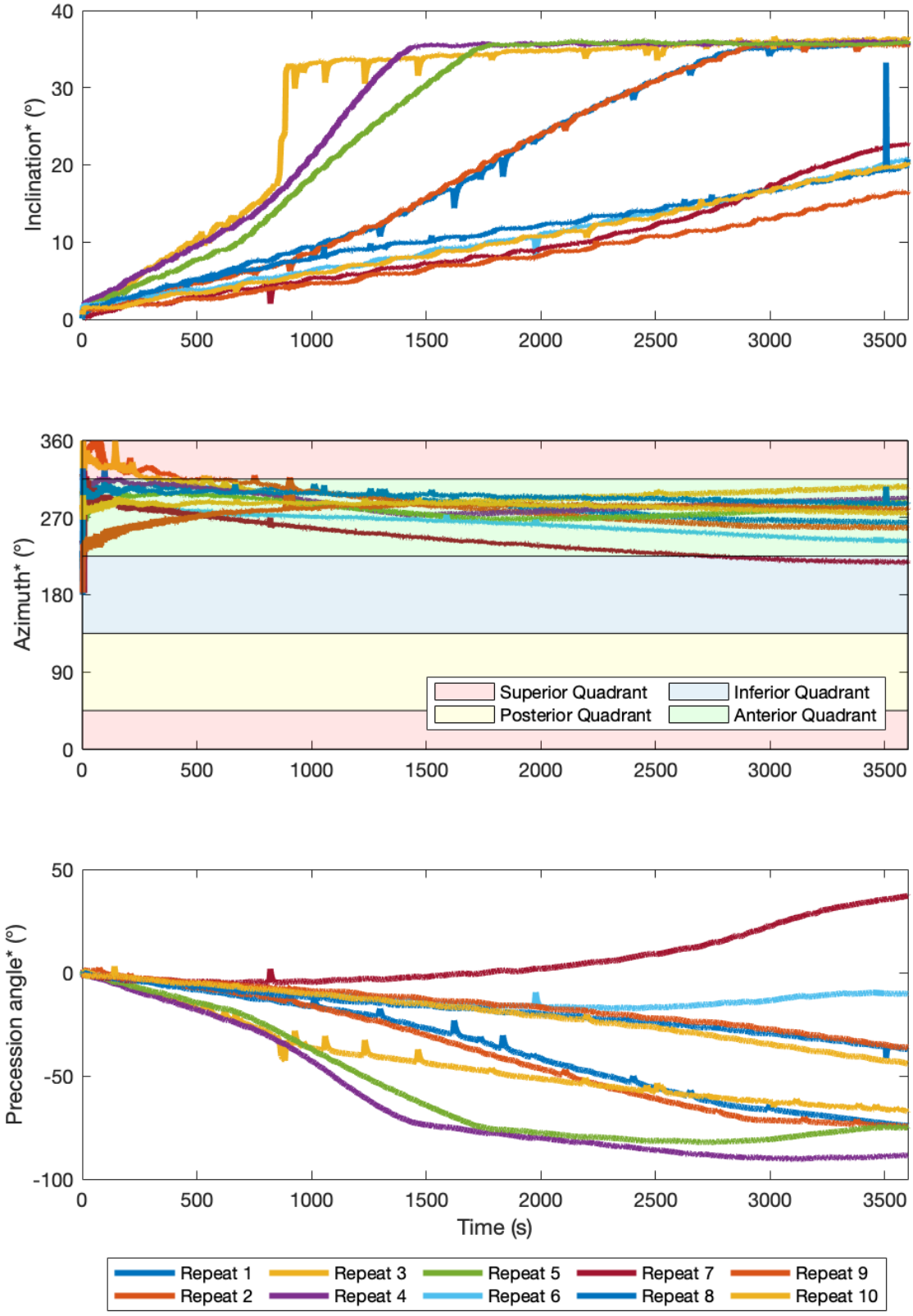

Figure 4.12 – Inclination*, azimuth* and precession angle* of one DM liner over ten repeated tests, whereby the liner was subjected to 3,600 cycles of standard gait as defined by ISO 14242-1.

Table 4.2 – Final resting positions of one DM liner after ten repeated tests.

Repeat	Final resting position		
	Inclination*	**Azimuth***	**Precession***
1	36°	264°	-74°
2	36°	258°	-75°
3	36°	306°	-67°
4	36°	293°	-88°
5	36°	288°	-75°
6	21°	243°	-10°
7	23°	218°	37°
8	20°	286°	-37°
9	17°	281°	-36°
10	20°	275°	-44°
Mean	28°	271°	-47°
St dev	8°	26°	38°
Range	19°	88°	125°

In general, there was a consistent tendency for the liner inclination* to increase over the duration of each test until a threshold of approximately 36° was reached after which the inclination* plateaued. This threshold represents the maximum possible inclination* of the liner in the test setup (i.e., when the liner's chamfer was contacting the femoral neck). This threshold was reached within the first five repeats, after which point the rate of change of the liner's inclination* notably decreased as seen in Figure 4.12. This was also observed in Table 4.2, whereby the final resting inclination* of the liner was 36° and 20° on average for the first and final five repeats, respectively.

The azimuth* of the liner tended towards a mean value of 271° although this ranged by 88° between repeats. In all cases, the azimuth* of the liner was positioned within the anterior quadrant.

The precession* of the liner generally rotated in the clockwise direction with the exception of one test. The magnitude of precession* was variable between repeats with a 125° range in the final resting position. Interestingly, the magnitude of the precession* appeared to be larger in the first five repeats (mean 76° of rotation) in comparison to the latter five (mean 33° of rotation), similar to the trends observed for the liner's inclination*.

4.4.2.2 – Inter-liner repeatability

During testing of the final component (i.e., Liner 3), the first repeat was successfully obtained. After this point, the tracker unexpectedly began to fault. Because of this, a further three repeats were attempted but all were prematurely terminated due to the tracker. To ensure three complete (i.e., 3,600-cycle) repeats were obtained, an alternative tracker was mounted onto the sample and a further two repeats were successfully completed. Therefore, this sample was tested on a total of six occasions which included three successful repeats and three incomplete repeat attempts, which resulted in approximately 3,000 additional gait cycles being applied to the component between successful repeats one and two.

The inclination*, azimuth* and precession* of three liners across three repeated tests are shown in Figure 4.13. The first three repeats of the intra-liner repeatability assessment (Section 4.4.2.1), referred to as ‘Liner 1,’ have been included in this dataset. The final inclination*, azimuth* and precession* of the three liners after three repeated tests are summarised in Table 4.3.

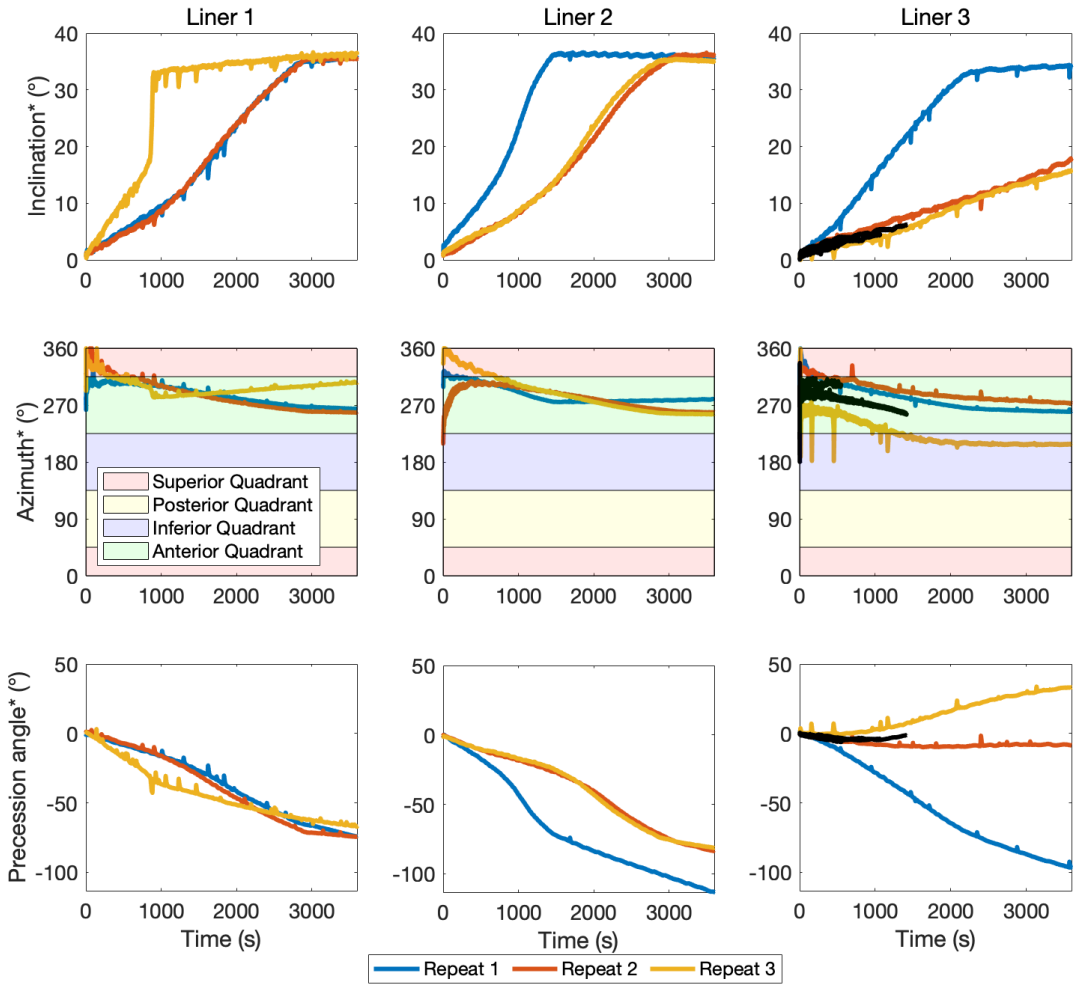

Figure 4.13 – Inclination*, azimuth* and precession angle* of three DM liners subjected to standard gait conditions on three separate occasions each. During testing of Liner 3, three repeats were prematurely terminated due to a tracker fault. This occurred after the first repeat and, for completeness, are illustrated as black lines in the figure.

Table 4.3 – Final position of three DM liners after being subject to standard gait conditions for 3600 cycles. Data presented as mean ± SD (range), in degrees.

Liner	Final resting position		
	Inclination*	Azimuth*	Precession angle*
1	36° ± 0° (0°)	276° ± 26° (48°)	-72° ± 5° (8°)
2	36° ± 1° (1°)	265 ± 13° (24°)	-93° ± 18° (32°)
3	23° ± 10° (19°)	247° ± 34° (64°)	-24° ± 67° (130°)

In general, the inclination* of each liner behaved similarly to the trends observed in the intra-liner repeatability testing whereby it would increase throughout each test and plateau if a maximum value of approximately 36° was reached. As seen in Figure

4.13, the first and second liner reached this maximum in all three repeats. In contrast, the third liner only reached the maximum inclination* on the first repeat. However, it was after the first repeat that the three prematurely terminated tests were conducted and therefore it is unknown whether these additional tests, which resulted in an approximately 3,000 additional gait cycles being applied to the liner, was the cause for this change in behaviour.

The azimuth* of the liners all trended towards a similar position whereby the final rest position was within the anterior quadrant (mean 247° to 276°).

The precession* of the liner was generally in the clockwise direction and the temporal motion appeared similar between liners one and two, but not three. However, it was more difficult to discern trends in the precession* behaviour between samples.

4.4.3 – Sensitivity analysis under altered test conditions

The inclination*, azimuth* and precession* of four liners subjected to various adverse testing conditions across three repeated tests are shown in Figure 4.14. Standard gait data collected in the intra-liner repeatability analysis has been included in the presentation of data as a control.

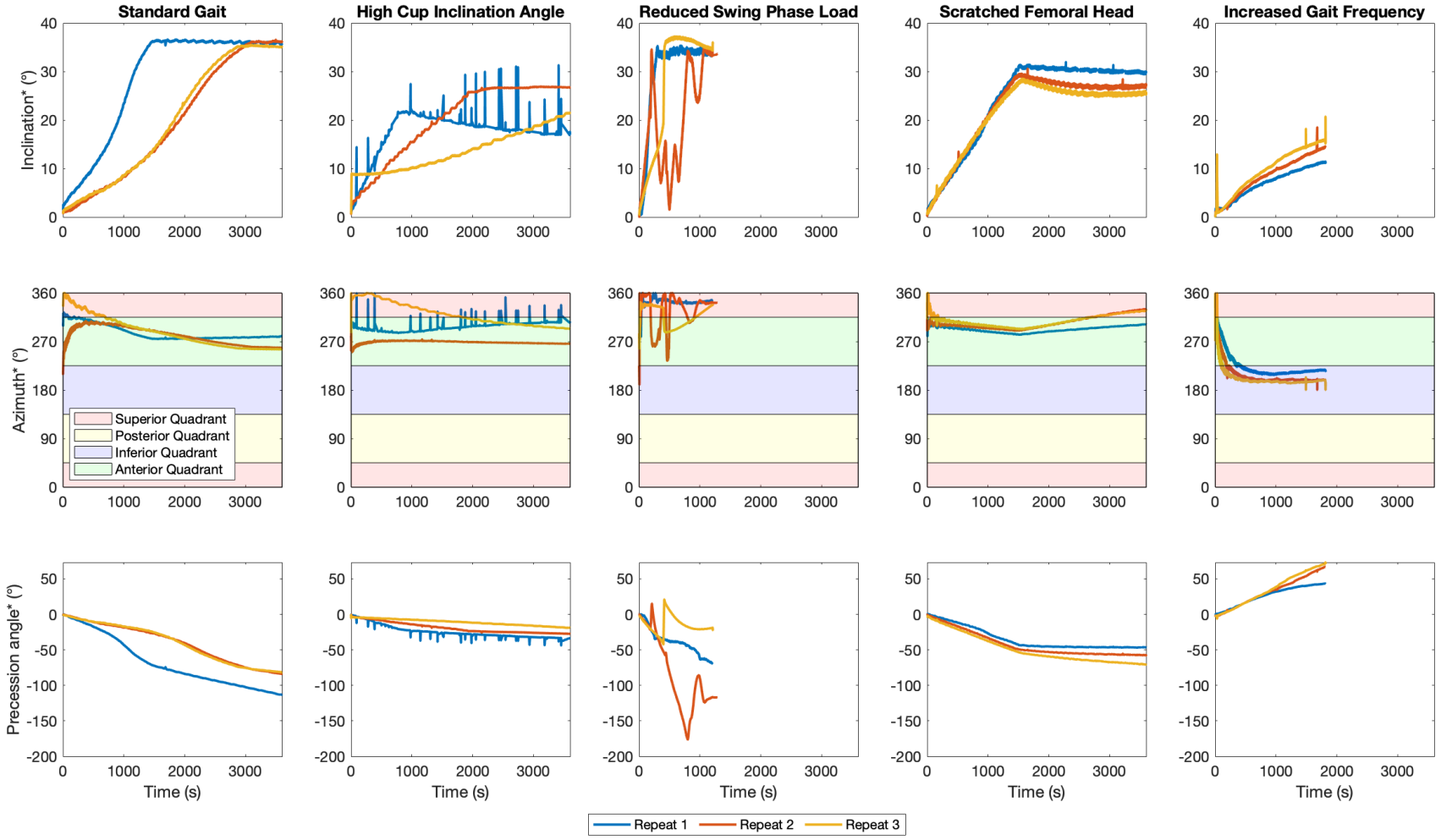

Figure 4.14 - Inclination*, azimuth* and precession* of four DM liners subjected to various adverse test conditions across three repeated tests.

4.4.3.1 – High cup inclination angle

The final resting position of one DM liner, following three repeated tests at an increased cup inclination angle of 65° in-vivo, are specified in Table 4.4. In general, increasing the cup inclination angle yielded inconsistent trends in inclination* and azimuth* whilst the precession* was more repeatable.

Table 4.4 – Final resting position of one DM liner following three repeated tests under increased cup inclination angle conditions.

Repeat	Final resting position		
	Inclination*	**Azimuth***	**Precession***
1	17°	306°	-34°
2	27°	266°	-27°
3	21°	294°	-19°
Mean	22°	289°	-27°
St dev	5°	21°	7°
Range	10°	40°	15°

The inclination* of the liner increased at the start of all three repeats but began decreasing approximately a quarter of the way through the first repeat or plateauing at a maximum inclination of 27° in the second repeat. The azimuth* generally settled in the anterior quadrant for all repeats, with a final resting position between 226° and 306°. This was similar to the trends observed in the standard gait testing. Interestingly, precession* of the liner was consistent between all repeats. The liner precessed* in a clockwise direction, similar to trends observed in the standard gait condition, but the magnitude of this rotation was less (27° on average).

4.4.3.2 – Reduced swing phase loading

The final resting position of one liner, following three repeated tests with a reduced swing phase load of 100 N, is reported in Table 4.5. In summary, reducing the swing phase loading resulted in more erratic and less predictable behaviour of the DM liner. In fact, this motion was so great that it caused the tether to become taut during testing, resulting in permanent and irreversible damage to the tracker. Therefore, a new tracker was fitted, and all tests were limited to 1,200 cycles to prevent further tracker damage or the tether from becoming taut (which could influence the behaviour of the DM liner).

Table 4.5 - Final resting position of one DM liner following three repeated tests under reduced swing phase loading. Each repeat was limited to 1,200 cycles to prevent tracker damage.

Repeat	Final resting position		
	Inclination*	**Azimuth***	**Precession***
1	34°	346°	-67°
2	34°	342°	-117°
3	35°	337°	-19°
Mean	34°	342°	-67°
St dev	0°	4°	49°
Range	1°	9°	97°

The inclination* of the liner rapidly increased for two repeats and subsequently plateauing at a maximum inclination* by approximately cycle 100. In contrast, the inclination* did not reach a maximum during the standard gait condition until much later in the testing (cycles 1,500 to 3,000). Alternatively, the second repeat showed erratic changes in the inclination* throughout the duration of the test. This suggests that the outer articulation was frequently being engaged in this repeat. The azimuth* of the liner was also variable between tests but generally settled in a similar position in the superior quadrant with a final resting position ranging from 337° to 346°. The precession* of the liner was seemingly random with no discernible trends in its behaviour between tests and a wide range in the final resting position (-19° to -117°).

4.4.3.3 – Scratched femoral head

The artificially generated scratches had an average Ra and Rp of 0.4784 μm and 2.5013 μm, respectively. Therefore, these scratches closely approximated those identified on the worst-case retrieved femoral heads, which had an average Ra and Rp of 0.6388 μm and 2.3915 μm, respectively.

The final resting position of one liner, following three repeated tests with a reduced swing phase load of 100 N, is reported in Table 4.6. In summary, repeatable trends in motion were observed when a DM liner was articulated against a scratched femoral head. Interestingly, there appeared to be a notable change in the behaviour of the liner after the first 1,500 cycles of testing. This was observed across all three repeated tests.

Table 4.6 – Final resting position of one DM liner following three repeated tests with an artificially scratched femoral head.

Repeat	Final resting position		
	Inclination*	**Azimuth***	**Precession***
1	30	302	-46
2	27	330	-57
3	26	327	-70
Mean	28	320	-58
St dev	2	15	12
Range	4	28	24

The inclination* of the liner increased throughout the start of the test and, after approximately 1,500 cycles, appeared to either plateau at a maximum of 30° (Repeat 1) or steadily begin decreasing (Repeats 2 and 3). No sudden changes were observed in the inclination* data which would be indicative of articulation at the outer bearing surface as predicted. However, the inclination* of the liner appeared to increase more rapidly at the start of the test in comparison to the standard gait data. This suggests that the increased friction of the internal articulation resulted in more motion of the outer articulation. The azimuth* generally remained within the anterior quadrant throughout each of the repeats, as seen in Figure 4.14. However, the azimuth* appeared to shift towards a more inferior position after the 1,500-cycle mark. Overall, the average final resting position was an interiorly facing liner which was inclined at approximately 28°. In addition, the liner precessed* an average of 58° clockwise until the test reached 1,500 cycles after which this behaviour stabilised.

4.4.3.4 – Increased gait frequency

The final testing position of one liner, following three repeated tests with an increased gait frequency of 2 Hz, is reported in Table 4.7. In summary, an increase in the gait frequency resulted in more repeatable trends in all three angles. However, the behaviour was notably different from those observed in all other test conditions particularly relating to azimuth* and precession*. It should be noted that this testing was completed with Liner 3, which was also used in the inter-liner repeatability testing, due to a lack of available components. Therefore, this test condition is confounded by this factor and the results should be interpreted accordingly.

Table 4.7 – Final resting position of one DM liner following three repeated tests at an increased gait frequency of 2 Hz.

Repeat	Final resting position		
	Inclination*	Azimuth*	Precession*
1	11°	217°	43°
2	14°	199°	67°
3	16°	195°	71°
Mean	14°	205°	60°
St dev	2°	10°	15°
Range	5°	18°	28°

Interestingly, there was a notable change in the liner's behaviour between the standard and increased gait frequency conditions. The inclination* appeared to increase throughout the duration of the test, reaching an average final resting position of 14°, however this could be attributed to the pre-conditions of the sample as observed in the intra-liner repeatability results (Section 4.4.2.1). The azimuth* rapidly settled into a stable position within the inferior quadrant, for which it remained for the duration of the test (final resting position between 195° and 217°). This is in contrast to the previous inter-liner repeatability results whereby the liner settled into a position in the anterior quadrant (final resting position between 209° and 273°). In addition, the precession* of the liner rotated in a counter-clockwise direction and continued to increase throughout the duration of the test, reaching a final resting position between 43° and 71°. This is the only test condition which resulted in a counter-clockwise precession* of the liner and is markedly different from the liner's behaviour under the previous standard gait conditions.

4.5 – Discussion

This study showed the successful development of a novel in-vitro motion tracking methodology for the assessment of DM bearings and demonstrated that it is possible to assess DM liner motion under physiologically relevant loading, displacement, and lubrication conditions within a hip joint simulator.

4.5.1 – Repeatability assessment

The motion of three DM liners was observed under repeated in-vitro tests simulating standard gait. In general, the liners displayed similar and repeated trends in motion

over consecutive tests (i.e., intra-liner repeatability) and between components (i.e., inter-liner repeatability).

For example, the inclination* of the liner increased throughout the test period and plateaued if a threshold of approximately 36° was reached, which was the maximum possible inclination* of the liner in the specified test setup. This behaviour was observed across all liners and in all repeats. Interestingly, the rate at which the inclination* increased appeared to slow after the first five rounds of testing (i.e., 18,000 gait cycles) as seen from the intra-liner repeatability testing (Section 4.4.2.1). After this point, the liner's temporal behaviour was more stable and repeatable as seen in Figure 4.12. This change in behaviour is also evidenced in the final resting inclination* of the liner, which was significantly different between the first five (mean 36° ± 0°) and final five (mean 20° ± 2°) repeats ($p<0.001$). In fact, a significant difference in the final resting position between the first five and final five repeats was evident for all measured outputs i.e., inclination*, azimuth* and precession* as shown in Table 4.8. Therefore, it is hypothesised that the initial bedding-in of the polyethylene (i.e., within the first 18,000 cycles) may influence the motion of DM liners. Pre-conditioning samples with a suitable number of gait cycles prior to in-vitro motion tracking studies may be a vital consideration to ensure DM liner behaviour reflection of true in-vivo motion is captured.

Table 4.8 – Final resting position of one DM liner in the first and final five repeats of the intra-liner repeatability assessment, which resulted in an observable change in the liner's behaviour. The final resting positions were compared with a paired t-test (IBM SPSS Statistics, Version 27), which revealed a significant different between repeats 1-5 and repeats 6-10 at an alpha of 0.05.

Test Variable	Final Resting Position		
	Repeats 1-5	Repeats 6-10	p
Inclination*	36° ± 0°	20° ± 2°	<0.001
Azimuth*	281° ± 20°	260° ± 29°	0.014
Precession*	-75° ± 8°	-18° ± 33°	0.018

No sudden or rapid changes in the liner inclination* were observed in any of the repeatability tests. This would suggest that there was minimal movement at the outer articulation and therefore provides further evidence that the inner articulation between the femoral head and polyethylene liner is the primary and preferential articulation site for DM implants under idealised conditions specified by ISO 14242-1. This aligns

with the outputs of the retrieval analysis described in Chapter 3 and therefore supports the idea that the described in-vitro motion tracking methodology accurately reproduces and monitors DM liner motion.

With regards to the liner's azimuth*, a significant difference in the final resting position between the first and final five repeats of the intra-liner repeatability test was observed (Table 4.8), further strengthening the need to pre-condition DM implants prior to motion tracking studies. However, in all cases, the liner settled into a similar position whereby the flat face of the liner was anteriorly facing. This trend was observed in all intra- and inter-liner repeatability tests conducted, whereby the average resting position ranged between 247° and 276°.

There were less discernible trends in the precession* of the DM liners assessed in this study. Typically, the liners would rotate in a clockwise direction throughout the duration of the test, which represents a rotation of the tracker's IMU from the superior, to anterior, to inferior, to posterior quadrants in this order for the specified test setup (i.e., right hip). However the rate at which it precessed* varied between tests and components. This suggests that the precession* of DM liners may be more erratic in nature, or perhaps is a more sensitive or complex motion which requires further research to better understand.

In summary, the preliminary repeatability assessment described in this Chapter provides some evidence to suggest that DM liners behave repeatably when subjected to the idealised operating conditions suggested by ISO 14242-1. However, the intra-liner repeatability assessment identified a change in the temporal behaviour of the liner as the number of repeats progressed therefore suggesting that the use of as-manufactured samples for these types of analysis are not suitable. Further studies are required to assess the effects of pre-conditioning on DM liner behaviour and to investigate the repeatability of these motions under these conditions.

4.5.2 – Sensitivity analysis under altered test conditions

DM liners were subjected to several adverse or altered gait conditions, and their motion was observed to assess whether DM liner motion was sensitive to changes in implant, patient and/or surgical factors. This study was conducted with a limited number of samples and repeats, and therefore the results of this study should be interpreted as pilot data. However, data from the repeatability assessment described

in Section 4.4.2 suggest that DM liners may behave repeatably and therefore it is predicted that changes observed in DM liner motion in this sensitivity analysis are more likely to be an artefact of the changing input conditions rather than a change in the components (i.e., due to manufacturing variations and/or poor inter-liner repeatability). Overall, this study provided some evidence to suggest that DM liner motion may be influenced by a change in the in-vitro input conditions.

For example, the inclination* of the liner generally appeared to steadily increase throughout each test or until a maximum threshold was reached. This trend was visible in the standard gait, scratched femoral head and increased gait frequency conditions. In addition, this behaviour was observed in two of three repeated tests in the high cup inclination angle and reduced swing phase conditions. However, the rate at which inclination* increased varied between conditions. Additionally, more erratic behaviour in the liner* inclination was observed when the swing phase loading was decreased suggesting more frequent activation of the outer articulation (i.e., between the liner and acetabular shell). This was the only test condition whereby the articulation site appeared to switch between the inner and outer bearings. In all other test cases, the inner articulation appeared to be the primary articulation site amongst all repeated tests.

The trends in azimuth* were more variable, with final resting positions observed in the anterior (i.e., standard gait, high cup inclination angle), superior (i.e., low swing phase loading) and inferior (i.e., increased gait frequency) quadrants.

The precession* of the liner also appeared to be variable, although this variability was also present in the repeatability analysis under standard gait conditions. Generally, liners rotated in a clockwise direction (i.e., superior to anterior rotation of the tracker's IMU) but interestingly an increase in the gait frequency resulted in a counter-clockwise precession* (i.e., superior to posterior rotation of the tracker's IMU). The average precession* of the liner was -24° to -72° under standard gait conditions, -27° with an increased cup inclination angle, -67° with a reduced swing phase load and 60° with increased gait frequency.

In summary, the results of this study suggest that DM liner motion may be sensitive to changes in input conditions and therefore in-vitro motion tracking studies should investigate a wide range of operating conditions. Understanding how DM liner motion changes in response to various implant, patient and/or surgical factors may provide

information about how these implants are likely to perform in the long-term. For example, a decrease in the swing phase loading resulted in more erratic motion of the liner and more frequent engagement of the outer articulation in this pilot study. This could have adverse effects on the long-term wear performance of these implants. For example, joint laxity could leave to increased use of the outer articulation, whereby the large-diameter polyethylene liner acts as an effective femoral head articulating against the acetabular shell, leading to an increased sliding distance and thus increased opportunity for polyethylene wear.

4.5.3 – Strengths and limitations of the methodology

This Chapter describes the successful development of an in-vitro motion tracking methodology suitable for DM bearings. The method benefits from the use of a novel positional tracker which allows DM liner motion to be observed in-vitro without line-of-sight. In addition, the method allows for the functional behaviour of these constructs to be rapidly assessed under a variety of conditions through short-term (i.e., less than one hour) and economical tests. Therefore, there is an opportunity for these types of analyses to provide an alternative to long-term wear simulation studies, which are more expensive and time consuming, in predicting long-term performance and function of these implants.

However, the tracker currently requires the use of a tether to transmit data. The tether becoming taut may influence the behaviour of the liner or cause irreparable damage to the tracker. In the sensitivity analysis described in Section 4.3.5, the use of a tether caused premature termination of several tests (i.e., reduced swing phase loading) due to increased liner motion. Therefore, it should be noted that the use of a tether is a current limitation of the methodology. This is particularly challenging under circumstances which yield increased motion or more erratic behaviour, as these conditions may be of heightened interest in the analysis of DM bearings so to understand their worst-case operating conditions. However, the identification of early and rapid liner movement still provides useful information about DM function and possible long-term consequences on implant performance despite the reduced tests lengths. Further development of the tracker to provide tether-free motion analysis is possible although this would require both wireless data transmission and power supply methods and is beyond the scope of this project.

The tracker was also sensitive to changes in the local magnetic field. The use of the copper coil provided a workaround for this problem in variable and inconsistent magnetic environments (e.g., electromechanical hip joint simulators). However, this may restrict the possible range of motion of the tests depending on fixture setup and does not allow for conditions such as dynamic separation, whereby the COR of the tracker would be displaced from the COR of the copper coil, to be assessed.

4.6 – Conclusion

In summary, this study demonstrated the successful development of an in-vitro simulator testing methodology for the motion tracking of DM liners. Results from this initial pilot study suggest that DM liners behave repeatably and that their motion may be influenced by a change in input conditions (e.g., reflective of various patient, surgical and/or implant factors). In addition, there is evidence to suggest that the motion of pristine versus serviced DM liners may differ therefore highlighting that pre-conditioning may be an important consideration for future motion tracking analyses. In light of this, it is recommended that DM liner motion is assessed through motion tracking studies using the described methodology, pre-conditioned samples, an increased sample size and a wide range of operating conditions as future work.

Chapter 5 -
In-vitro assessment of dual mobility liner kinematics

5.1 – Introduction

The in-vivo kinematic function of Dual Mobility (DM) bearings is not well understood. It is important that these mechanisms are investigated as these bearings are increasingly used in a more diverse population of patients. The lack of available long-term survivorship data and early National Joint Registry evidence which suggests these implants do not perform as well as conventional THRs in the first five years further highlights the need for adequate and comprehensive pre-clinical testing of DM constructs.

The in-vivo motion of DM liners has previously been inferred through retrieval analyses or directly investigated through experimental or cadaveric studies, mathematical or computational models, and in-vivo Radiostereometric Analysis (RSA). Current evidence suggests that DM bearings operate with a primary articulating surface between the femoral head and liner and that the liner has an ability to rotate within the acetabular shell over time (Geringer et al., 2011; Jørgensen et al., 2022). Interestingly, a study by Jørgensen et al (2022) suggests that femoral neck-liner contact is not necessary to activate the outer bearing although this may be an artefact of the liner's design (i.e., concentric versus eccentric) as previously investigated by Fabry et al (2014). For example, eccentric liners were found to shift into a valgus position under most activity profiles therefore aligning their symmetry axis with the force vector. In contrast, concentric designs did not articulate at the outer bearing surface without femoral neck contact. The role of the surrounding soft tissues

was also investigated in cadaveric studies (Nebergall et al., 2016; Logishetty et al., 2019).

However, these studies are limited in their numbers, and none have investigated the motion of DM constructs under physiologically relevant loading, displacement, lubrication, and setup conditions. Instead, the motions have been indirectly assumed through retrieval analyses, or directly observed using methodologies which did not suitably represent the in-vivo environment as previously discussed in Chapter 4.

Therefore, the aim of this study was to directly investigate DM liner motion using a novel in-vitro tracking methodology (Chapter 4) which allows the implant motion to be assessed under physiologically representative conditions. The study has two primary objectives. The first was to assess the effects of pre-conditioning on DM liner motion, in light of the pilot data generated in Chapter 4. The study provided some evidence that the motion of DM liners may change as the liner shifts from an as-manufactured to a pre-conditioned state. The second objective of the study was to assess the intra- and inter-liner repeatability of DM liner motion under standard gait conditions specified by ISO 14242-1. It is important to establish whether these motions are repeatable prior to assessing how the mechanics are influenced by a change in patient, surgical and/or implant factors.

5.2 – Material and methods

5.2.1 – Overview

An in-vitro assessment of DM liner motion was conducted to investigate the effects of implant conditioning and to assess the intra- and inter-liner repeatability of these behaviours under idealised conditions as illustrated in Figure 5.1. In summary, three independent BI-MENTUM™ component sets (DePuy Synthes; Leeds, UK) were subjected to two stages of in-vitro hip simulation to investigate the motion of DM liners in their as-manufactured (i.e., pristine) and conditioned states (Section 5.2.3.1). In each of the motion tracking phases, the components were subjected to 3,600 cycles of standard gait on three separate occasions. The implants were conditioned with 20,000 cycles of standard gait in between the two motion tracking phases (Section 5.2.3.2).

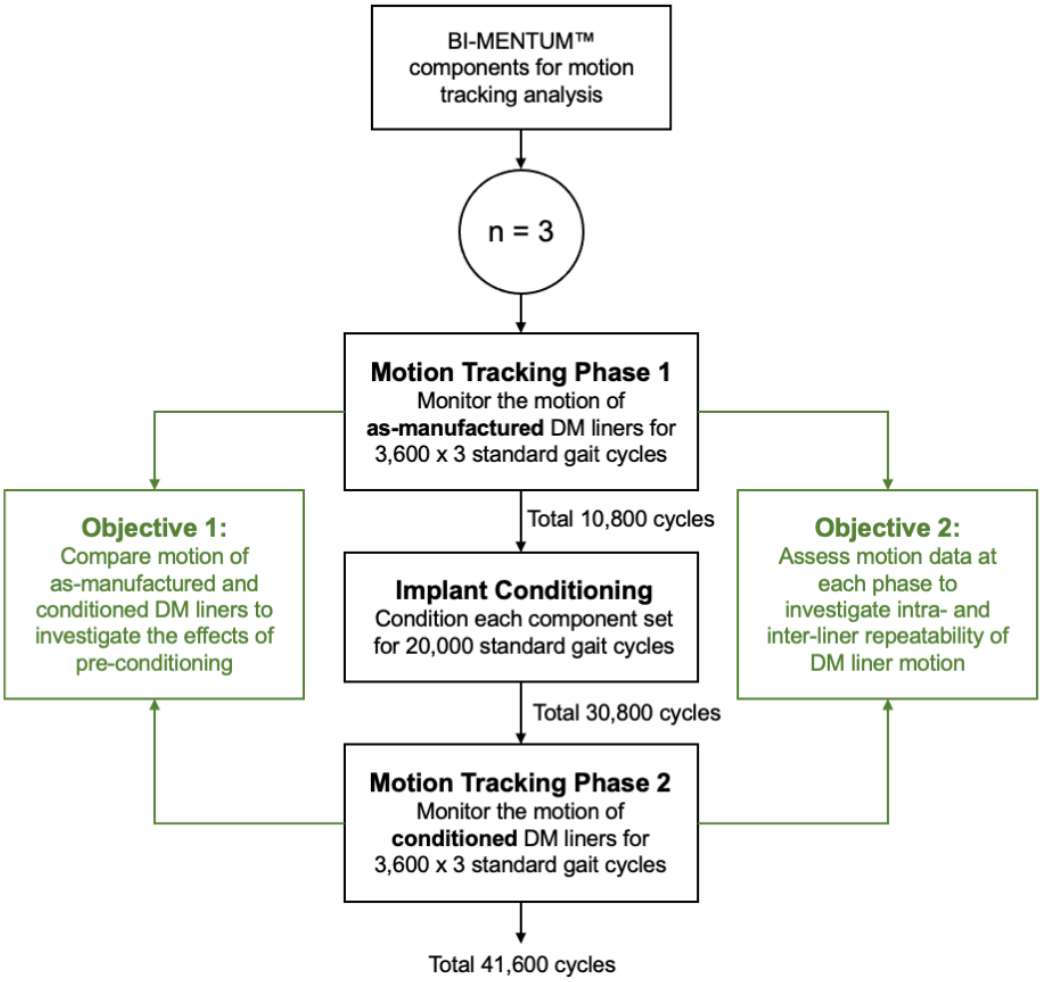

Figure 5.1 – Flowchart illustrating the in-vitro motion tracking assessment described in this Chapter.

In line with the objectives of this study, data from the two motion tracking phases was compared to assess the effects of pre-conditioning on DM liner motion (Objective 1). In addition, the data from each phase was separately assessed to investigate the intra- and inter-liner repeatability of DM liner motion under standard gait conditions. A pilot repeatability study was previously conducted in Chapter 4, although independent component sets were not utilised and therefore no conclusions could be drawn from that data about these behaviours.

5.2.2 – Materials

A total of three independent component sets were used for this testing, all of which were 69/28-mm Metal-on-Polyethylene-on-Metal (MoPoM) DM bearings. The liners were BI-MENTUM™ DM liners manufactured from a moderately cross-linked polyethylene (Marathon™, DePuy Synthes) with a 28-mm internal and 63-mm

external diameter. These were articulated against 69-mm monobloc BI-MENTUM™ PressFit acetabular shells and 28-mm CoCr femoral heads (ARTICULEZE®) mounted onto Corail® femoral stems. All component sets were supplied by DePuy Synthes (Leeds, UK). Further component information is available in Table A4 of Appendix A.

5.2.3 – Methods

5.2.3.1 – Motion tracking assessment

Motion tracking was performed in this study on two occasions. The first (i.e., Phase 1) monitored the motion of as-manufactured DM components. The second (i.e., Phase 2) monitored the motion of conditioned components which had been subjected to a total of 30,800 cycles of standard gait prior to testing (see Section 5.2.3.2).

In each motion tracking phase, each liner was mounted into the Anatomical Hip Simulator (AHS) which has previously been detailed in Section 4.3.2.1 using bespoke fixtures and a standard cup inclination angle of 45°. Each liner was subjected to standardised gait condition described by ISO 14242-1 (see Section 4.3.2.3) at a frequency of 1 Hz for 3,600 cycles (i.e., one hour) in three separate tests.

Liner orientation was monitored throughout all tests using the bespoke tracker described in Section 4.3.3. In summary, the tracker was mounted onto the flat face of the DM liner using double sided adhesive tape. This captured rotational displacements of the liner in the X-, Y- and Z-axes (i.e., roll, pitch, yaw) at a frequency of 50 Hz. The roll-pitch-yaw output of the tracker was transformed into inclination*, azimuth* and precession* angles (see Section 4.3.3).

5.2.3.2 – Implant conditioning

To condition the implants, each component set was fixed into the AHS and subjected to 20,000 cycles of standard gait conditions identical to those used in the motion tracking assessment (see Section 4.3.2.3). The number of conditioning cycles was set at 20,000 due to the data generated from the pilot intra-liner repeatability assessment described in Section 4.4.2.1. This identified a significant change in the final resting position of the liner after the first 18,000 gait cycles (i.e., first five test repeats). The rate of change of the liner inclination* and the magnitude of the precession* appeared to decrease after this threshold. This provided some evidence that pre-conditioning may affect the behaviour of DM implants and therefore a

threshold above that identified in the pilot study was selected (i.e., 20,000 cycles). The motion of the liners was not recorded during this phase.

5.3 – Results

5.3.1 – Motion of as-manufactured liners

The inclination*, azimuth* and precession* of three as-manufactured liners across three repeated tests are shown in Figure 5.2. The final resting positions of each liner are specified in Table 5.1. One observation which was consistent across all liners and repeated tests in Phase 1 was an immediate and rapid change in the liner orientation within the simulator ramp-up period (i.e., first 10 cycles of applied gait) whereby the axial loading was gradually increased over the 10 cycles to facilitate the start of the simulation process. This explains why the liners do not appear to start at a neutral orientation of 0° inclination* and 0° precession* at the start of each test (Figure 5.2), despite the test setup accounting for this. It was noted that the liners felt looser and easier to articulate against the femoral head and within the acetabular shell than those previously assessed in Chapter 4, which may explain why this phenomenon was not previously observed.

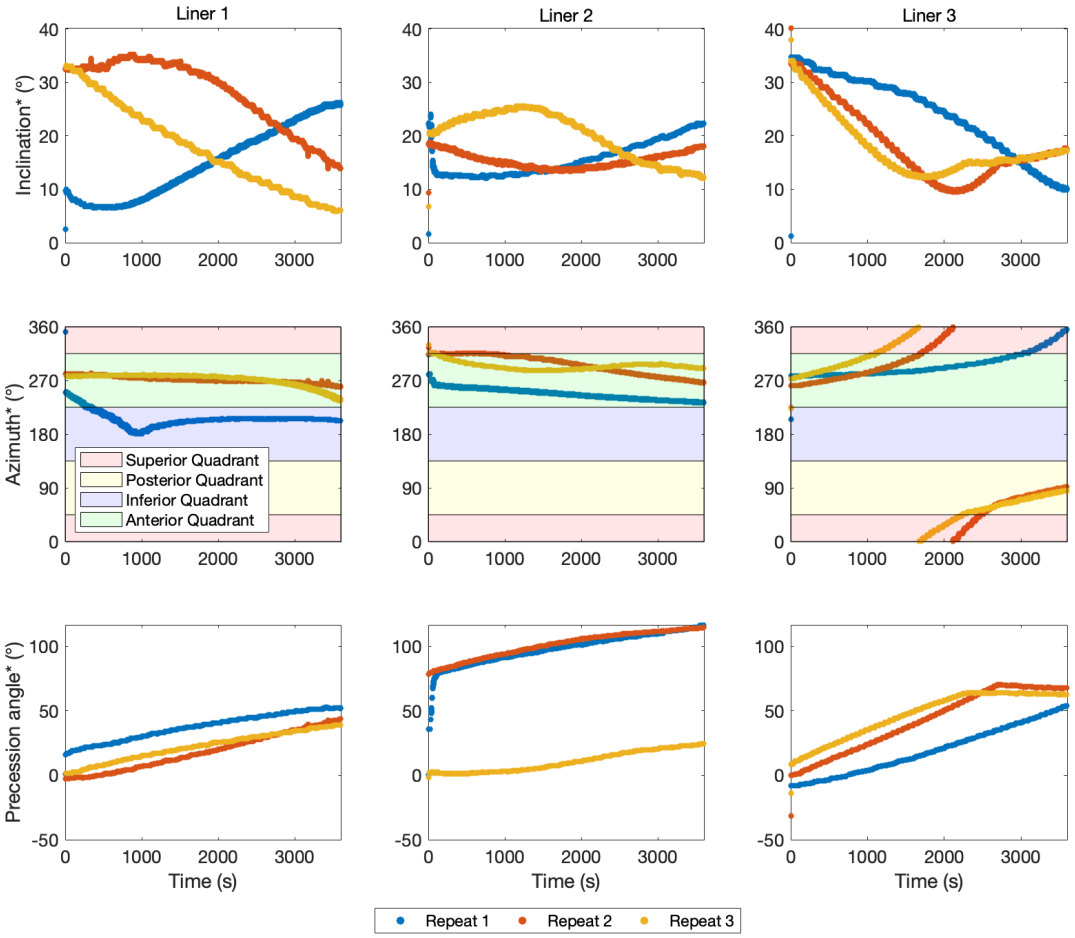

Figure 5.2 – Inclination*, azimuth* and precession* of three as-manufactured DM liners which were subjected to standard gait conditions on three separate occasions each.

Table 5.1 – Final resting position of three as-manufactured DM liners after being subjected to 3,600 cycles of standard gait on three separate occasions. Data presented as mean ± standard deviation.

Liner	Final Resting Position		
	Inclination*	Azimuth*	Precession *
1	15° ± 10°	234° ± 29°	45° ± 6°
2	18° ± 5°	264° ± 29°	85° ± 53°
3	15° ± 4°	177° ± 154°	61° ± 7°

In summary, there were no discernible trends in inclination* both within repeated tests of the same component set (i.e., high intra-component variability) or between component sets (i.e., high inter-component variability). At the start of each test, the liner inclination* appeared to immediately increase by approximately 10° to 35° for all liners. In general, the inclination* steadily decreased throughout the test period for

Liners 1 and 3 although the rate of this change varied between components and individual repeats. For example, the inclination* of Liners 1 and 3 decreased by 10° and 19° on average although their motion over time varied. In contrast, the inclination* of Liner 2 displayed inconsistent trends in motion with two repeated tests showing a gradual increase in inclination* and another containing both increasing and decreasing phases of inclination* change.

The azimuth* data revealed that the liners immediately oriented themselves to face anteriorly at the start of each test. Minimal motion was observed throughout the test period for Liners 1 and 2 and therefore the azimuth* of these components generally remained within the anterior quadrant until test completion. However, a steady decrease in the azimuth* was observed for these components throughout the test period (i.e., 36° and 40° decrease on average for Liners 1 and 2, respectively) thus representing a tendency towards an inferior-facing position if the test had continued in length. In contrast, an increase in the azimuth* of Liner 3 was observed across each of its repeated tests thus resulting in final resting positions in the superior and inferior quadrants. In summary, the azimuth* of the liners appeared to have some degree of intra-component repeatability as evidenced by similar trends in motion and final resting positions within individual component sets. However, these motions were not generalised across all component sets and thus no evidence of inter-component repeatability was present.

The precession* of the liners was more repeatable both within and between component sets i.e., intra- and inter-component repeatability. The precession* rapidly increased at the start of two repeats of Liner 2. This represented a counter-clockwise rotation of the liner within the acetabular shell, which appeared to orient the tracker at the most inferior position of the liner and thus it is thought that the weight of the tracker may have influenced this change in position under low loading conditions (i.e., simulator ramp-up period). Despite the variation in initial start positions, the precession* of the liners appeared to steadily increase in a counter-clockwise direction with similar rates of change observed across component sets and test repeats. The precession* of Liners 1, 2 and 3 increased by an average of 40°, 47° and 61°, respectively. If a distinct marking was placed at the most superior position of the liner, a counter-clockwise rotation in this simulation setup would represent the mark moving towards the posterior quadrant as shown in Figure 5.3.

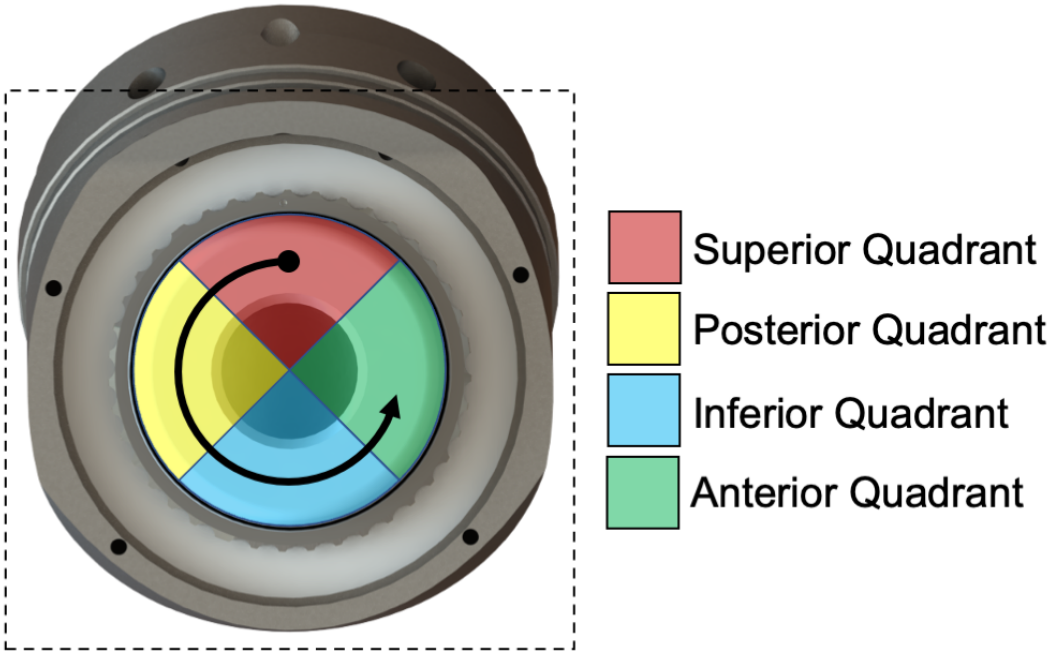

Figure 5.3 – Schematic illustrating a counter-clockwise precession* of a DM liner in the specified simulator setup, which represents a right hip. If a distinct mark is placed on the most superior position of the liner, a counter-clockwise rotation represents the mark moving towards the posterior, then inferior, then anterior quadrants in this order.

5.3.2 – Motion of conditioned liners

Each component set was successfully conditioned on a single-station simulator (AHS) for 20,000 cycles of standard gait following the first phase of motion tracking. Therefore, data presented in this Section represents motion of DM liners which were conditioned with a total of 30,800 cycles of standard gait prior to motion analysis (i.e., 10,800 cycles applied in the first phase of motion tracking plus 20,000 cycles of implant conditioning).

The inclination*, azimuth* and precession* of three conditioned liners across three repeated tests are shown in Figure 5.4. The final resting positions of the liners are detailed in Table 5.2. An immediate and rapid shift in the liner orientation was observed within the ramp-up period of the simulator as previously described the Section 5.3.1. In addition, two tracker-related faults occurred during this phase of testing. A failure in the tracker's adhesive occurred at approximately cycle 3,300 in the first repeat of Liner 1. Therefore, the final 300 cycles of data were considered unreliable and thus excluded from the results detailed in this Section. Additionally, the integrity of the tracker's tether was compromised in the second repeat of Liner 3. This

occurred at approximately cycle 1,000 and therefore data beyond this point was excluded from the results.

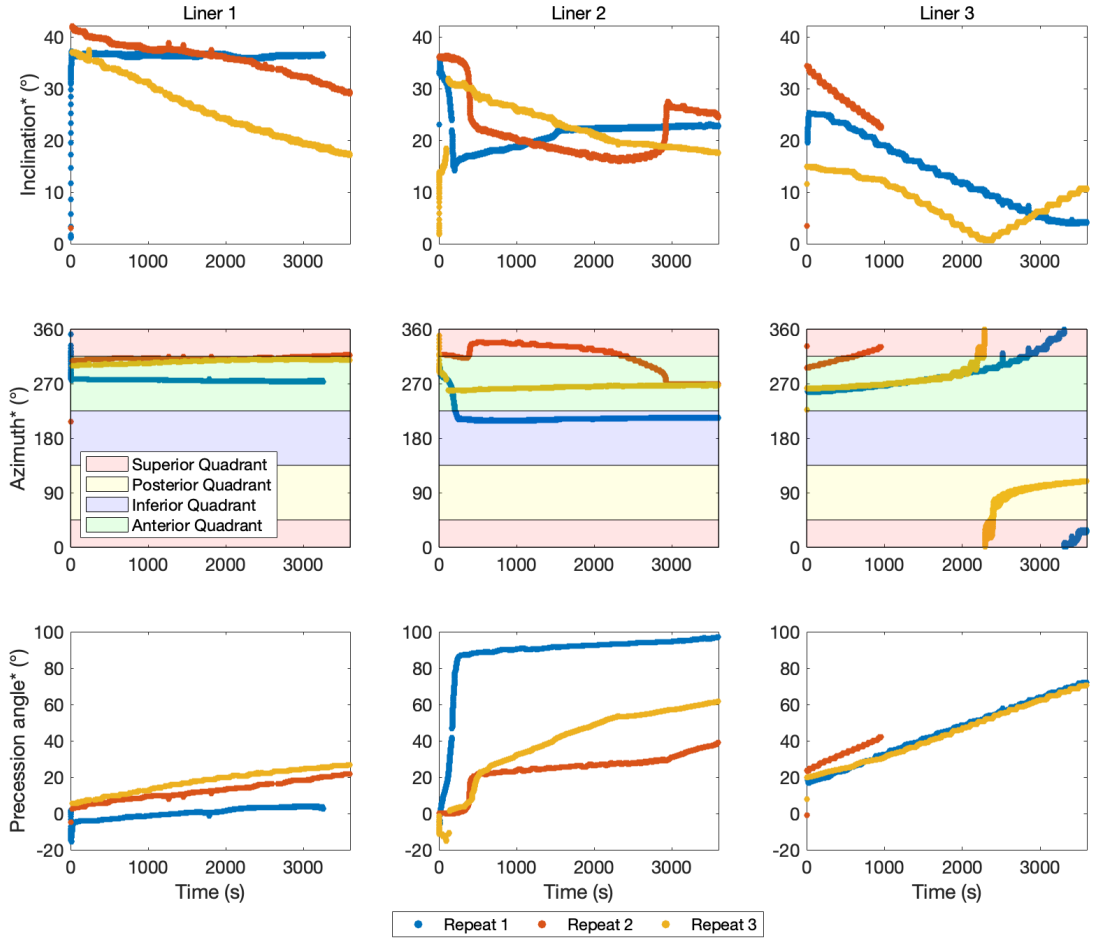

Figure 5.4 – Inclination*, azimuth* and precession* of three pre-conditioned DM liners which were subjected to standard gait conditions on three separate occasions each.

Table 5.2 – Final resting position of three pre-conditioned DM liners after being subjected to standard gait conditions on three separate occasions each. Data from the two tests which were prematurely terminated due to tracker-related faults were excluded from this dataset. Data presented as the mean final resting position.

Liner	Final Resting Position		
	Inclination*	Azimuth*	Precession *
1	23°	314°	24°
2	22°	250°	66°
3	7°	67°	71°

With respect to the liner inclination*, this appeared to rapidly increase at the start of each test by approximately 15° to 40°. In general, the inclination* of the liners decreased throughout the test period although the temporal motion and rate of change varied between individual components and tests. Rapid changes in inclination* were observed throughout the second repeated test of Liner 2. These sudden changes may suggest activation of the outer articulation at multiple points throughout the test period although the cause of this is unknown. In summary, the inclination* data from three conditioned DM liners revealed some similarities in their behaviours such as a rapid increase in the start inclination* during the simulator's ramp-up period and a tendency for the inclination* to decrease throughout the test. These trends suggest there may be some degree of intra- and inter-component repeatability in the inclination* of conditioned liners although a high variation in the motions over time were observed and therefore no conclusions can be drawn. Further studies should be conducted to confirm this finding.

Similar to the motion of as-manufactured liners, the azimuth* data revealed that the liners generally oriented themselves to face the anterior direction during the ramp-up phase of the simulator test. However, a range of temporal trends in motion were observed. For example, the azimuth* of Liners 1 and 2 remained stable throughout the duration of the test. In contrast, the azimuth* of Liner 3 appeared to increase throughout the test period. A range of final resting positions were observed in all four quadrants as evidenced by Figure 5.4. In summary, some similarities were observed in the trends in azimuth* within individual component sets (i.e., intra-component repeatability) although no inter-component repeatability was identified.

The precession* of the liners showed evidence of both intra- and inter-component repeatability. The precession* of the liners was noted to rapidly increase within the simulator ramp-up period although this was not observed in all test repeats. Despite the initial shift in orientation, the precession* of each liner appeared to steadily rotate in a counter-clockwise (posterior) direction as illustrated in Figure 5.3. The magnitude of this rotation was approximately 20°, 70° and 50° for Liners 1, 2, and 3, respectively.

5.4 – Discussion

5.4.1 – Repeatability of DM liner motion

*5.4.1.1 – Trends in inclination**

In general, a rapid 10° to 40° increase in liner inclination* was observed during the simulator ramp-up period for each liner in both their as-manufactured and conditioned states. Beyond this, no repeatable or discernible trends in inclination* were observed for the as-manufactured liners. In the conditioned state, a gradual reduction in the inclination* was observed throughout the test period for each of the liners. This trend suggests there may be some degree of intra- and inter-component repeatability although further testing is required to confirm this finding due to the high variation in the motions observed throughout each test.

*5.4.1.2 – Trends in azimuth**

The temporal orientation of the liner's flat face, as denoted by the liner azimuth*, demonstrated some evidence of intra-component repeatability, but not inter-component repeatability, in the present study. At the start of each test (i.e., within the first or second cycle of simulator ramp-up period), liners consistently shifted into a position whereby the flat face was oriented towards the anterior direction as denoted by an initial azimuth* ranging between 225° and 315° (i.e., the anterior quadrant). The behaviour of the liner after this point varied between individual component sets.

For each individual component set, the orientation of the liner's flat face generally settled into a similar location (i.e., the same azimuth* quadrant) by the end of each repeated test. Interestingly, there was a degree of consistency in these final positions between the as-manufactured and conditioned states of each liner. Therefore, some evidence of intra-component repeatability was observed in relation to the liner's azimuth*. However, the final resting positions were not consistent between component sets thus there was no evidence of inter-component repeatability. For example, the final resting azimuth* of Liners 1 and 2 remained within the anterior quadrant whereas Liner 3 generally settled within the superior or posterior quadrants. It is unclear why these final orientations would have such a high degree of inter-component variability although it is possible this was an artefact of the variations in individual component setup (e.g., variations in femoral stem and acetabular shell positions due to the cementing process).

*5.4.1.3 – Trends in precession**

The rotation of the liner within the acetabular shell (i.e., precession*) demonstrated consistent trends within individual component sets (i.e., intra-component repeatability) and between component sets (i.e., inter-component repeatability). This was true in both the as-manufactured and conditioned liner states, which identified similar trends in motion. In general, the liners linearly precessed* approximately 45° counter-clockwise throughout the duration of the test. If a discrete mark was placed on the flat surface of the liner, a counter-clockwise rotation would represent a shift in this mark from the superior, to posterior, to inferior, to anterior quadrant in the described test setup which represents a right hip, as shown in Figure 5.3.

Interestingly, a rapid increase in the liner precession* was observed during the simulator ramp-up period in a small number of tests. This phenomenon was also observed during the test setup whilst positioning the liners in a neutral orientation (i.e., 0° inclination*, 0° precession*). During the setup of the test, small vibrations or disturbances to the implant or gaiter would cause the liner to rapidly precess* counter-clockwise by approximately 80°. It was clear the liner was unstable when positioned in a neutral orientation thus making it challenging to repeatably setup each test. Rotations in the counter-clockwise direction provided the most direct route to position the tracker at the inferior position of the liner and therefore it is thought that under low loads, the weight of the tracker (4 g) may have been the cause of this instability. It is unclear whether its weight also influenced the precession* of the liner to move in a counter-clockwise direction during testing.

5.4.1.4 – Discussion and general observations

The primary objective of this study was to assess the repeatability of DM liner motion. In summary, loose intra- and inter-component trends in inclination* were observed for the conditioned liners and a degree of intra-component repeatability was observed for the azimuthal* orientation in both the as-manufactured and conditioned liner states. However, a high variability in the temporal motions were observed in both the inclination* and azimuth* axes and therefore no conclusions can be drawn about the repeatability of these motions. Further studies should be conducted to confirm these findings. Alternatively, the rotation of the liner within the acetabular shell (i.e., precession*) was consistent and demonstrated both intra- and inter-component repeatability in both the as-manufactured and conditioned liner states.

The results of this study hint at the complexity and sensitivity of DM liner kinematics which may be influenced by various implant, patient and/or surgical factors thus resulting in the unpredictable motions observed in this analysis. This complexity may also explain the high variability in the surface damage observed previously in the retrievals analysis (Chapter 3).

Interestingly, the motions observed in this study varied from those previously identified in the pilot study described in Chapter 4 which demonstrated a higher degree of intra- and inter-liner repeatability, despite using the same methodology and components across the two tests. Independent component sets were not utilised in the pilot testing and thus provide an explanation for the differences in motion observed. For example, independent component sets require each femoral stem and acetabular shell to be individually setup and cemented within the simulator fixtures. Small changes in the component position, due to limitations in the accuracy of the cementing process, may result in small offsets in the Centre of Rotation (COR) of the components in relation to the COR of the simulator. The effects of this misalignment on liner motion would not be observed in the pilot testing described in Chapter 4 due to the use of a single femoral stem and acetabular shell. Therefore, the increased variation in liner motion observed in the present study may be an artefact of the cementing process which was individually performed for each component set. In a clinical setting, this may suggest that relatively small variations in the in-vivo component position may also have an effect on the behaviour of the component.

In addition, the implant material of the liners varied between the two tests. In the pilot testing described previously in Chapter 4, the liners were manufactured from an remelted, moderately cross-linked (7.5 MRad) polyethylene known as AltrX™ (DePuy Synthes). Alternatively, liners utilised in the current study featured the same design but were manufactured from Marathon™ (DePuy Synthes), a moderately cross-linked (5 MRad) and remelted polyethylene. Although changes to the polyethylene composition is unlikely to affect liner motion, it is possible the liners were subjected to different manufacturing processes and thus varied in their radial dimensions. Therefore, the as-manufactured diameters (internal and external) were compared between the AltrX™ and Marathon™ liners using a two-tailed t-test. No significant difference in the internal diameters was identified ($p=0.157$). However, there was a significant difference between the external diameters ($p=0.025$). It is possible that differences in the radial clearances between the liners may have contributed to the increased variations in motion observed.

Despite the poor repeatability of these motions, some general trends were observed which were similar between all component sets, repeats and condition phases (i.e., as-manufactured and conditioned). The data suggests that DM bearings operate with a primary articulation site between the femoral head and liner. Rapid changes in the liner inclination* at a frequency of approximately 1 Hz (i.e., the gait cycle frequency) would suggest an activation of the outer bearings surface. In general, this was not observed throughout the testing performed in this chapter and thus provides evidence of a primary articulation site at the internal bearing surface between the femoral head and liner. Additionally, the precession* data provides clear evidence of an ability for DM liners to rotate within the acetabular shell. These general behaviours of DM bearings have been previously hypothesised in the literature and indeed in the retrieval analysis conducted in Chapter 3 but, until now, have not been directly observed. In addition, the directionality of liner precession* was assessed in the present study which, to the author's knowledge, has not been previously reported.

5.4.2 – The influence of pre-conditioning on DM liner motion

The second objective of this study was to assess the effects of preconditioning on DM liner motion. The purpose of this investigation was in response to pilot data described in Chapter 4, which suggested a potential change in the liner motion after some level of implant pre-conditioning, possibly due to plastic flow of the polyethylene. Therefore, the motion of three 69/28-mm BI-MENTUM™ DM bearings was assessed under standard gait. This was done in their as-manufactured or pristine condition and once again after being conditioned with a total of 30,800 gait cycles.

In summary, pre-conditioning of the implants to 30,800 gait cycles did not appear to cause a change in liner motion. Most notably, the precession* of the liners to repeatably rotate in a counter-clockwise direction with similar rates of change between the two implant states. Therefore, it is clear that the rotational behaviour of the liner was not influenced by pre-conditioning of the implants. In addition, the azimuth* of each individual component set appeared to settle into similar final resting quadrants in both the as-manufactured and conditioned liner states and thus it is thought that this behaviour was not influenced by implant conditioning. In contrast, the effects of pre-conditioning on the behaviours in inclination* were more difficult to discern due to the inherent randomness of these motions and thus no conclusions could be drawn.

In addition, the sudden change in liner orientation observed during the simulator ramp-up period, which was characterised by an increase in inclination*, anterior-facing azimuth*, and occasional increase in precession*, was still observed once the implants had been conditioned.

It is possible that further implant conditioning (e.g., to one million cycles) would reveal a change in behaviours although further studies would be required to investigate these effects.

5.4.3 – Challenges in in-vitro motion tracking of DM liners and future recommendations

There are a number of challenges which should be considered during the design and planning of in-vitro experimental testing to track the motion of DM liners.

For example, it was difficult to set the liners into a neutral orientation (i.e., 0° inclination*, 0° precession*) at the start of each test due to their inherent mobility and instability which may have been caused by the weight of the tracker. These components had a tendency to rapidly shift into a new orientation, characterised by an increase in inclination* and, in some cases, precession*, under load loads and within the first or second cycle of the simulator ramp-up period. This ultimately made the data more challenging to analyse because the start positions were not controlled or consistent across repeats by the time full axial loading was applied (i.e., at the 11th gait cycle). Interestingly, this phenomenon was not previously observed in the pilot testing conducted previously in Chapter 4.

Additionally, the motion data captured in this study demonstrated variability within individual components (i.e., intra-component variability) and between component sets (i.e., inter-component variability). The motions observed in this study were more variable than those previously observed in the pilot study described in Chapter 4 despite using identical test methodologies and component designs. This was likely due to the individual variations in component position (e.g., due to the accuracy of the component cementing process) and highlights the importance of using independent component sets during these types of analyses. To improve the accuracy of component position with respect to the simulator's COR, new fixtures could be developed for the femoral stems and acetabular shells which do not rely on bone

cement but instead mechanically lock the components into place. Alternatively, the use of femoral stems could be excluded and replaced with spigots which are easy to manufacture and precisely control the position of the femoral head. However, it is important to maintain a clinically relevant femoral neck geometry and angle in the context of DM THRs. This is because the femoral neck plays an important role as part of the 'third' bearing surface of DM implants (i.e., between the femoral neck and liner) thus activating motion at the outer articulation between the liner and acetabular shell.

The intra- and inter-component variability in liner motion observed in this Chapter highlights the complexity of DM mechanics, which may be affected by various in-vitro testing factors such as liner design (e.g., size, manufacturer), implant position or input activity profiles (e.g., ISO 14242-1 standard gait, adverse conditions). It is recommended that the component details, activity profiles and test setup protocols are transparently defined in these types of studies in the future, as they may influence the observed motion.

Further research is required to better understand the influence of various patient, implant, and/or surgical factors on DM liner motion. The study presented in this Chapter suggests liners may perform with high intra- and inter-component variability despite being subjected to identical test conditions. Therefore, it is recommended that future in-vitro motion tracking analyses also consider the repeatability of the motions to exclude intra- and inter-component variability from obscuring the results. Recommendations for future in-vitro motion tracking analyses of these bearings include –

- A comparison of the motion of various DM implant designs (e.g., variations in size or manufacturer) to assess whether DM liner motion is implant-specific or whether their mechanics can be generalised across several design types.
- To further assess the motion of DM bearings under standard and adverse activity profiles (e.g., high cup inclination angle, reduced swing phase loading) and identify whether DM liner motions are sensitive to changes in input conditions.

5.4.4 – Limitations

The study was limited by its small sample size (n=3) and two tracker faults which resulted in the premature termination of two tests during Phase 2 (i.e., motion of

conditioned liners). These faults were caused by a failure of the double-sided adhesive and a breakage of the tether. In addition, it is thought that the weight of the tracker may have influenced the precession* of the liner to preferentially rotate in a counter-clockwise direction although further analyses would be required to confirm this hypothesis.

5.5 – Conclusion

In summary, the motions of three 69/28-mm BI-MENTUM™ DM component sets were assessed under standard gait conditions as specified by ISO 14242-1. The motions of these components were assessed when the liners were in both as-manufactured (i.e., pristine) and conditioned states (i.e., after 30,800 cycles). This is the first study, to the author's knowledge, which directly observed the behaviour of DM liners under physiologically relevant loading, displacement, and lubrication conditions. The study confirmed several hypotheses in the literature which suggests DM bearings have a primary articulation site between the femoral head and liner and an ability for the liner to rotate within the acetabular shell.

This study identified a high intra- and inter-component variability in the motion of DM liners in both their as-manufactured and conditioned states, apart from liner precession* (i.e., rotation within the acetabular shell) which repeatably and steadily precessed* in a counter-clockwise direction throughout testing. It was noted that implant pre-conditioning to 30,800 gait cycles did not influence the motion of these implants although the high variability in the data made it challenging to draw conclusions about its effect on liner motion. The variability observed in this testing suggests that DM motion is not influenced solely by the design of the implant but instead may be sensitive to other factors such as component position or patient anatomy thus highlighting the complexity of DM mechanics. This study is a promising first step towards improving our understanding of the complex DM mechanics and has highlighted some challenges and limitations associated with this type of testing.

Chapter 6 –
Overall discussion and conclusion

6.1 – Introduction

One of the most common causes of early (<2 year) total hip replacement revision is dislocation (National Joint Registry, 2022). The prevalence of prosthetic hip dislocation is likely underestimated because joint registries only capture those with result in a revision procedure and thus exclude those successfully treated with a closed reduction (Devane et al., 2012). In addition, dislocation-associated revision procedures are associated with poorer patient outcomes and increased re-revision rates (Kärrholm et al., 2017). The financial burden of dislocations (i.e., treatment costs of closed reductions and dislocation-associated revisions) are particularly challenging for the NHS under the current clinical landscape whereby there are unprecedented orthopaedic waiting lists and tight economical budgets (Sanchez-Sotelo et al., 2006; Clement et al., 2021).

To combat the complex challenge of hip dislocation, dual mobility implants were introduced in the 1970s in France as a highly stable hip replacement option. Initially, these implants performed poorly and were associated with high rates of failure, but next-generation design modifications have improved the performance of these implants and thus have contributed to their recent resurgence in the elective and acute orthopaedic settings (National Joint Registry, 2022). Dual mobility bearings are characterised by an unconstrained polyethylene liner which introduces a secondary articulating surface between the liner and acetabular component. Due to the encapsulation of the femoral head within the liner, the effective head size of the bearing is increased thus increasing the jump distance (i.e., distance the head must travel to dislocation) and overall stability of the implant. Dual mobility devices have been used to treat at-risk patients, including elderly populations and those with

neuromuscular conditions, abductor deficiencies, spinal fusions, or skeletal cancers (Philippeau et al., 2010; Adam et al., 2012; Sanders et al., 2013; Mudrick et al., 2015; Ozden et al., 2018). In addition, these implants have been increasingly used to treat patients with a fractured neck of femur (National Joint Registry, 2022).

The National Joint Registry highlights the emerging use of dual mobility constructs in the UK since 2013 in both elective and acute trauma settings (National Joint Registry, 2022). Although the literature suggests dual mobility devices have good overall survivorship and low rates of dislocation (Darrith et al., 2018; Reina et al., 2019), early joint registry data suggest that these bearings have higher revision rates in comparison to conventional implants (National Joint Registry, 2022; American Joint Replacement Registry, 2022). In addition, there is evidence that the revision rate of cemented dual mobility bearings remain higher than conventional implants even in the longer-term. However, a small number of DM THRs have been recorded within the NJR at present and patients receiving these types of implants may not match the demographical characteristics of those receiving a conventional THR. Therefore, further monitoring of DM survivorship and revision rates is essential over the coming years.

Complications unique to dual mobility devices also remain a concern. These include accelerated polyethylene wear, due to the use of a large-diameter polyethylene liner which articulates at both surfaces, and a unique failure mechanism known as intraprosthetic dislocation. Although the incidence of intraprosthetic dislocation is reportedly low for new-generation dual mobility bearings or those with a 28-mm femoral head (Darrith et al., 2018), it is unclear whether the timeframe in which this failure mechanism occurs has simply been lengthened as a result of new-generation design features (e.g., cross-linked polyethylene, added chamfers). In addition, few studies have assessed the performance of dual mobility constructs and therefore the function and failure mechanisms of these bearings are not well understood. It is important to understand these mechanisms as dual mobility implants are implanted more frequently, their indications are broadened, and in light of joint registry data, which suggests possible unfavourable performance of these bearings in comparison to conventional bearings.

Therefore, the aim of this project was to advance the current understanding of dual mobility function and failure mechanisms. This was achieved through the development of characterisation and in-vitro testing methodologies suitable for the

novel geometry and function of dual mobility constructs (Chapter 2 and Chapter 4), which were later applied within a comprehensive retrievals analysis (Chapter 3) and in-vitro motion tracking assessment (Chapter 5).

6.2 – Methodological advancements for the characterisation and in-vitro testing of dual mobility implants

In this thesis, the successful development of two novel methodologies was presented which enabled the geometric characterisation and in-vitro motion tracking of dual mobility polyethylene liners. The following sections will discuss each of these methods in detail including their impact, strengths, limitations, and recommendations for further development.

6.2.1 – Geometric assessment methodology

Geometric assessment methods have been widely used and reported in the literature to characterise the surface damage and functional performance of conventional polyethylene liners (Goldvasser et al., 2014; Trommer et al., 2015; Holdcroft and Van Citters, 2018). These methods can provide valuable semi-quantitative information about the morphology, extent, and severity of damage on the surface of an implant which may be used to assess their function and failure mechanisms. In addition, these methods can be further developed to provide quantitative outputs such as volumetric change which have shown to reliably correlate to gold-standard gravimetric data (Uddin, 2014; Hua and Li, 2020) for the assessment of polyethylene wear (i.e., material loss).

However, there have been no reports of characterisation methodologies suitable for dual mobility constructs due to their novel geometry (e.g., supra-hemispheric design) and function (e.g., two articulating surfaces). Previous attempts to geometrically assess dual mobility liners have been limited by their measurement protocols which were unable to collect data from all regions of the articulating surfaces. In response to this, these studies either destructively sectioned the samples or excluded portions of the pole and/or rim from the analysis (Geringer et al., 2011; D'Apuzzo et al., 2016). Therefore, the aim of the study described in Chapter 2 was to develop a non-destructive and comprehensive geometric assessment methodology which could characterise the articulating surfaces (i.e., internal and external) of dual mobility polyethylene liners for wear and/or deformation. To increase utility of the method, the aim was to develop a protocol which was suitable for both retrieved and in-vitro tested

samples. Retrieved liners are particularly challenging to characterise because no adequate pre-service information relating to their surface geometry is available.

In summary, a semi-quantitative geometric characterisation methodology was successfully developed which met the aims of the study. The method benefits from fully automated measurement and data analysis protocols and is the first to non-destructively capture all regions of the articulating surfaces (i.e., pole, equator, rim) from these components. No information about the implant (e.g., dimensions, manufacturer) is required and therefore the method is suitable for use with retrieved and in-vitro tested dual mobility liners of any design, size, or specification. This highlights the utility of the method, which may be utilised in future research to enhance the current understanding of how these devices function and fail.

The method was shown to be repeatable (Section 2.5) and the quality of the generated surface deviation heatmaps was verified against samples with visible regions of surface damage. The sensitivity of the method was demonstrated through the assessment of as-manufactured dual mobility liners (Section 2.4) which identified artefacts of the manufacturing process at geometric variance below 25 μm. This confirmed the methodology could identify regions of geometric variance and surface damage beyond what is visible by eye and therefore unable to be captured through alternative methods such as visual inspection.

In conclusion, the method developed in Chapter 2 provides an advanced mechanism for assessing surface damage on the articulating surfaces of dual mobility liners and overcomes the limitations previously described by alternative attempts in the literature. The method has scope within a number of applications including both orthopaedic retrieval and in-vitro testing analyses. For example, the method was utilised in the analysis of 20 retrieved dual mobility liners (Chapter 3). This provided information about the possible in-vivo function of these components and may be applied within future retrieval analyses to enhance the outputs of the study. In addition, geometric assessment of dual mobility liners may be used to monitor the progression of damage throughout in-vitro simulator tests.

The method is limited by its inability to distinguish between wear (i.e., material loss) and deformation (i.e., plastic flow) of the polyethylene, which is a common limitation for geometric characterisation methodologies of this type. In addition, the method was unable to reliably determine volumetric change of the component. This was

demonstrated in Section 2.6 where a poor correlation between measured gravimetric data and the geometric volume change data was identified. No methodologies have been identified in the literature which can approximate the volume change of dual mobility liners through a geometric approach and therefore future research should consider improving the reliability of this algorithm to increase utility of the method. In addition, the method could be adapted to identify geometric changes at the retentive bore and chamfer. Identifying degradation in this region could be a precursor for intraprosthetic dislocation and therefore should be considered in future projects.

6.2.2 – In-vitro motion tracking of the polyethylene liner

At present, the in-vivo functional mechanisms of dual mobility bearings are poorly understood. The behaviour of dual mobility liners has previously been assessed using cadaveric models (Nebergall et al., 2016; Logishetty et al., 2019), in-vivo radiostereometric analysis (Jørgensen et al., 2022), computational models (Fabry, Woernle, et al., 2014) and in-vitro testing (Fabry, Kaehler, et al., 2014). However, each methodology has several limitations. For example, cadaveric and in-vivo radiostereometric analyses account for the interaction of surrounding soft tissues but yield patient-specific data and often involve small sample sizes due to economical- or recruitment-related challenges. Computational analyses are more cost effective but rely on suitable experimental methods as a validation tool although these are not available in the context of dual mobility bearings.

Alternatively, in-vitro studies could facilitate the rapid functional assessment of dual mobility implants under controlled conditions which can be modified to reflect a variety of typical, atypical, and adverse operating conditions. However, previous attempts to develop this type of methodology utilised inverted component orientations, reduced axial loads, and non-physiological lubrication conditions (Fabry, Kaehler, et al., 2014). Therefore, an in-vitro motion tracking methodology was successfully developed in Chapter 4 which is the only known method to allow direct observation of dual mobility liners under physiologically relevant loading, displacement, setup, and lubrication conditions.

The method benefits from the use of a bespoke positional sensor, developed by Dr Matthew P Shuttleworth (University of Leeds), which is non-destructive, easy to install and does not require component line-of-sight. The method is easily transferrable to a variety of in-vitro setups (e.g., simulators) and can be used to generate new findings

relating to the mechanics of dual mobility bearings and how this may be influenced by a variety of patient, implant, or surgical factors. This information may be used to improve next-generation implant designs, provide surgeons with improved guidelines relating to suitable patient demographics and optimal component orientations, and ultimately improve patient outcomes in the long-term. In addition, this method may be used to validate computational models or streamline in-vitro simulator tests by rapidly identifying conditions of interest (i.e., conditions which are likely to represent the best- or worst-case operating conditions).

6.3 – In-vivo function and failure mechanisms of dual mobility bearings

It is important to characterise the functional mechanisms of dual mobility bearings due to their emerging use so that their best- and worst-case operating conditions may be assessed. For example, conditions that result in excessive motion of the outer bearing (i.e., between the liner and acetabular shell) may increase wear of the implant as the liner effectively functions as a large-diameter polyethylene head. Alternatively, conditions which cause frequent contact at the third articulation site (i.e., between the femoral head and liner) may increase wear of the liner's retentive features therefore increasing the risk of intraprosthetic dislocation. By investigating the performance of dual mobility bearings, optimal component orientations and suitable patient populations may be identified.

In this thesis, the motions of one dual mobility liner design were directly observed through a novel in-vitro tracking methodology (Chapter 5). This study was the first to directly assess dual mobility liner motion under physiologically relevant loading, displacement, and lubrication conditions and thus has generated new findings in relation to the mechanics of these implants. In addition, a collection of 20 retrieved dual mobility implants were assessed in Chapter 3 which yielded information about the in-vivo function and potential failure mechanisms of these constructs in a more generalised collection of samples (i.e., a variety of implant designs and sizes). The functional mechanisms of dual mobility implants are discussed in the following sections.

6.3.1 – Primary articulation site

This thesis provides evidence to strengthen an ongoing hypothesis that dual mobility bearings operate with a primary articulation site at the inner bearing surface (i.e.,

between the femoral head and liner). In-vitro simulation of three dual mobility component sets (Chapter 5) confirmed this theory through direct observation of the liner motion under standard gait conditions although only one implant type and size (i.e., 69/28-mm BI-MENTUM™, DePuy Synthes) was assessed. In addition, a wider collection of implants containing various device types and sizes was assessed in a comprehensive retrievals analysis detailed in Chapter 3. This identified an increased incidence of surface polishing and larger, more concentrated regions of penetrative geometric variance on the internal surfaces of the polyethylene liners therefore suggesting this was the primary site for in-vivo articulation. In theory, the bearing surface with the lowest frictional torque will act as the primary articulation site which is proportional to its radius and coefficient of friction. Therefore, assuming each bearing surface has comparable frictional coefficients, the inner bearing will have a reduced frictional torque under normal operating conditions due to its reduced radial dimensions and thus explains why it acts as the primary mover of dual mobility bearings.

However, it is possible that the outer articulation could become the primary mover for dual mobility constructs which would cause the polyethylene liner to act as an effective large-diameter femoral head. This would dispose the implant to accelerated levels of polyethylene wear and thus adversely affect its long-term performance. Several factors relating to the implant, patient, or surgery may encourage motion at the outer articulation site. Implant factors relating to the condition and/or design of the implant could change the tribological properties at each articulation site and thus negatively influence its mechanics. For example, this could occur if the implant's radial clearances are altered or if inner bearing surface becomes significantly damaged (i.e., increasing its coefficient of friction and frictional torque) although this effect was not observed in the pilot study described in Chapter 4. Additionally, the concentricity of the liner may also influence the primary articulation site. In theory, concentric designs should only move in response to contact between the femoral neck and liner (i.e., at the 'third' articulation site). However, motion at the outer bearing of concentric dual mobility devices was observed in Chapter 5 under standard gait (i.e., without extremes of motion) therefore suggesting that implant design is not the only factor which drives dual mobility mechanics. Other factors which may encourage motion of the outer articulation site include a reduction in the swing phase load, a change in the component position, or a build-up of fibrotic soft tissue around the implant in-vivo (i.e., arthrofibrosis).

In theory, these conditions would have a negative impact on the performance of dual mobility implants although these effects have not been directly investigated in the literature. It is recommended that these are investigated in future analyses using the novel in-vitro tracking method described in Chapter 4 so that worst-case operating conditions may be identified for these implants.

6.3.2 – Rotational capabilities of the polyethylene liners

Dual mobility bearings are characterised by a polyethylene liner which is unconstrained and thus freely mobile. Therefore, it has been hypothesised in the literature that these components rotate within the acetabular shell over time (Geringer et al., 2011) although this behaviour has not yet been directly observed.

The in-vitro motion tracking analysis described in Chapter 5 directly monitored the orientation of three 69/28-mm BI-MENTUM™ DM liners (DePuy Synthes) under standard gait conditions which identified a steady and repeatable internal rotation of the liners. It is unclear why the liners preferentially rotated in a counter-clockwise direction (i.e., internally) although it is possible the weight of the positional tracker influenced the directionality of this motion. In addition, geometric assessment of retrieved polyethylene liners (Chapter 3) identified crescent-shaped and circumferential regions of penetrative geometric variance on the internal surfaces of approximately 40% and 20% of the collection, respectively. This suggests the majority of the liners were able to rotate in-vivo although, in the presence of crescent-shaped damaged regions, this motion may have been restricted within a limited region. In summary, this is the first study to directly observe the rotational behaviour of dual mobility liners under physiologically-relevant conditions and to suggest that these implants may perform with varying degrees of mobility in-vivo.

6.3.3 – Repeatability and sensitivity of dual mobility liner kinematics

The motion of three 69/28-mm BI-MENTUM™ dual mobility liners was assessed in Chapter 5. The study suggests that these liners do not behave repeatably under standard gait conditions, with the exception of liner precession* (i.e., rotation of the liner within the acetabular shell), and that their motions are not influenced by implant pre-conditioning to approximately 30,000 gait cycles as previously hypothesised in Chapter 4. Similar, gross trends in behaviour were observed across the collection of implants such as a gradual reduction in inclination* throughout the test period although this evidence was not strong enough to suggest the motion over time was

repeatable. In consideration of the significant differences observed in liner motion between Chapter 4 and Chapter 5, it is unknown whether the repeatability of dual mobility liner motion is influenced by device design, size, and setup. Therefore, further studies are recommended to comprehensively assess these motions using an increased sample size and various implant designs. In particular, it would be interesting to assess whether the repeatability of dual mobility motion is influenced by the concentricity of the liner (i.e., concentric versus eccentric). In this Thesis, only the motions of concentric dual mobility devices were directly investigated (Chapter 5), which identified poor trends in both intra- and inter-component repeatability. Alternatively, eccentric designs provide a self-centering mechanism under force application which is introduced through an axial offset of the centres of rotation of the inner and outer bearing surfaces. Theoretically, this should lead to more predictable behavioural patterns and component orientations as these types of devices are designed to align the liner's axis of symmetry with the applied force vector. By improving the predictability of these motions, it is possible to make more informed conclusions about the long-term wear performance of dual mobility devices through pre-clinical tests. Furthermore, it may be possible to introduce a secondary, radial offset between the centres of rotation to further improve the predictability of these motions with regards to the liner precession*. However, no studies at present have directly investigated the effects of liner concentricity in dual mobility bearings under physiologically relevant conditions. This has been made possible through the development of a novel in-vitro motion tracking methodology (Chapter 4). This would lead to an improved understanding of how dual mobility design influences the mechanics of these devices and thus aid in the development of next-generation implants.

In addition, this is the first study to suggest that dual mobility liner motion may be sensitive to changes in the input conditions (e.g., component orientation, axial load profiles) as detailed in Chapter 4. For example, increased activation of the outer bearing was identified when the swing phase loading was reduced from 300 N to 100 N. However, further research with increased sample sizes and independent component sets is required to confirm this hypothesis. If dual mobility liner motions are indeed sensitive to changes in these input condition, it is important that the results of in-vitro motion tracking analyses are transparent about the conditions utilised and refrain from generalising the observed behaviours to alternative implant designs, setups, or activity profiles. Further work is recommended to investigate the behaviour

of dual mobility implants under a variety of operating conditions, which may provide some information about their long-term performance in these situations.

6.3.4 – Failure mechanisms

Early dual mobility designs performed poorly with approximately 4% of these implants failing due to a unique complication known as intraprosthetic dislocation (Philippot et al., 2009). Intraprosthetic dislocation is characterised by a disarticulation of the femoral head and polyethylene liner following degradation of the liner's retentive features. This is a serious complication which results in metal-on-metal or ceramic-on-metal articulation between the femoral head and acetabular component and metal ion release in the body. It is thought that the incidence of intraprosthetic dislocation has been reduced through new-generation implants which feature modified designs (e.g., addition of a chamfer) and improved biomaterials. However, it is unclear whether the timeframe in which this failure mechanism occurs has instead been lengthened due to the limited available survivorship data for these implants. One systematic review reports no incidence of intraprosthetic dislocation for new-generation dual mobility devices which were implanted after 2007 or featured a 28-mm femoral head (Darrith et al., 2018). However, two dual mobility retrievals assessed in Chapter 3 (20%) failed due to intraprosthetic dislocation despite their new-generation designs. In the case of Retrieval 20, this resulted in clear evidence of severe metal-on-metal articulation between the femoral head and acetabular shell as shown in Figure 6.1. In addition, a further two dual mobility retrievals (20%) failed due to instability or dislocation of the hip. Therefore, the retrieved implants assessed in Chapter 3 reflect increased intraprosthetic dislocation and instability rates in comparison to those reported in the literature (Darrith et al., 2018; Reina et al., 2019). Further monitoring of implant survivorship and in-vitro testing are required to better assess the failure mechanisms of these bearings.

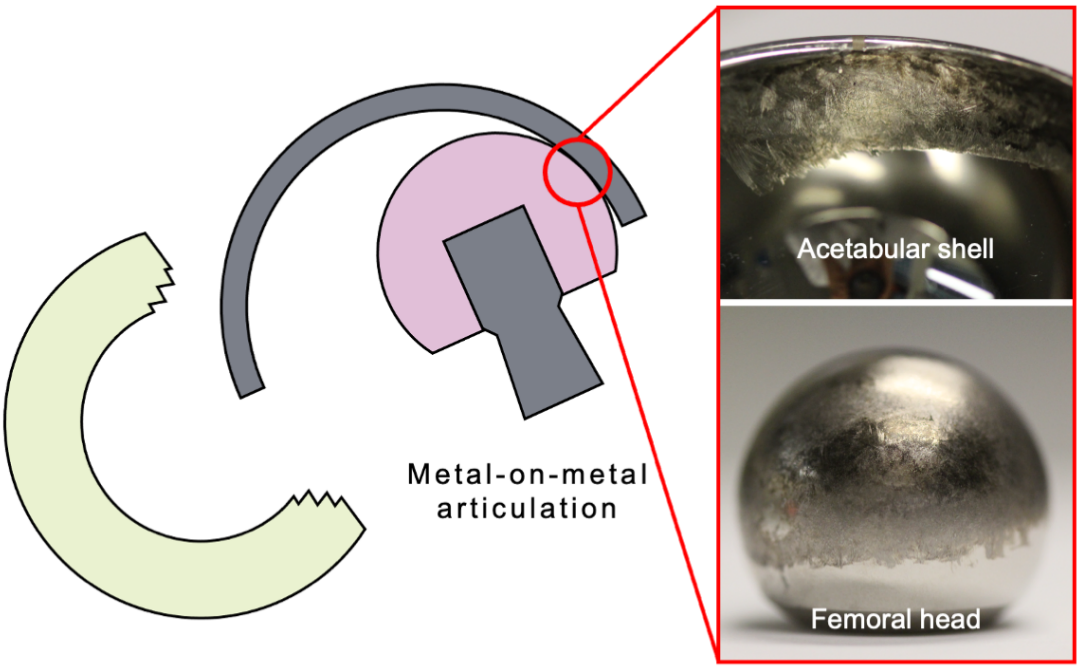

Figure 6.1 – Evidence of metal-on-metal articulation between the femoral head and acetabular shell of Retrieval 20 as a result of intraprosthetic dislocation.

In addition, this Thesis suggests that DM implants may be adversely affected by edge loading despite a previous in-vitro simulation study by Loving et al (2015) reporting comparable wear rates of these devices when subjected to both standard (50°) and increased (65°) cup inclination angles. This was evidenced by a region of stripe wear present on the external surface of four retrieved polyethylene liners (Section 3.6), which is similar to those previously observed on edge-loaded femoral heads from hard-on-hard (e.g., CoC) bearings (Esposito et al., 2012; Sariali et al., 2014). At the outer articulation site of a DM implant, the polyethylene liner acts as an effective large-diameter polyethylene femoral head which articulates against a hard (metallic) counterface shell thus explaining why these components have comparable damage patterns to those identified on femoral heads from conventional THRs. Although it was not possible to determine the in-vivo orientation of the DM retrievals due to a lack of supplemental information (e.g., radiographs), this Thesis provides evidence that this type of damage may be possible in the context of DM devices and thus warrants further investigation. At present, few studies have investigated the effects of edge loading on DM implants although this type of analysis will be made possible in future research through the geometric assessment methodology developed in Chapter 2.

6.4 – Challenges in analysing dual mobility bearings

Several challenges were observed in this thesis which should be considered in the experimental design of future studies investigating dual mobility implants. For example, retrieval analyses of dual mobility liners may be confounded by significant ex-vivo damage present on the external (i.e., convex) surfaces. It is thought that this may have been caused during the surgical revision process whereby the external liner surfaces are exposed to contact with surgical instruments and would explain why a high proportion of the embedded debris on these surfaces was iron-based (Section 3.5). At present, it is not possible to objectively distinguish between in-vivo and ex-vivo surface damage and therefore further research is recommended which characterises ex-vivo damage mechanisms to improve future retrieval analyses of this type.

In-vitro testing of dual mobility bearings is also challenging. For example, it is difficult to maintain a consistent or controlled orientation of the polyethylene liners at the start of simulator testing as observed in Chapter 5. This makes orientation data more challenging to assess in motion tracking analyses and may have a more profound effect on long-term wear simulation studies. This is because these studies must be intermittently paused to facilitate component cleaning and measurement and a change of the lubricant. If the starting orientation of these components cannot be controlled, it is possible the surface damage will not progressively worsen over the course of a test but instead present with multiple, discrete wear areas as an artefact of these intermittent test suspensions. It is unclear whether this would also have an effect on the gravimetric volume loss of the implants. The effects of this could be characterised through an in-vitro simulation study which combines the motion tracking methodology developed in Chapter 4, to assess the component's start position, with the geometric characterisation methodology developed in Chapter 2, to assess the progression of damage and identify whether this results in the production of discrete wear areas. It is recommended that long-term in-vitro simulation studies assessing dual mobility bearings carefully consider the effects of liner orientation and minimise disruptions throughout testing.

In addition, in-vitro motion tracking of dual mobility bearings is challenging due to the complexity of their liner motions which do not always display intra- or inter-component repeatability as observed in Chapter 5. Orientation of the liners is also difficult to describe due to a lack of standardised notations to describe dual mobility liner position

therefore making it difficult to compare results between studies with differing methodologies. In this thesis, the orientation of the liner was described in terms of its inclination*, azimuth*, and precession*. These angles are simple to calculate and correlate to important functions of the dual mobility liner. For example, inclination* describes the tilt of the liner and provides information about which articulating surface is moving (i.e., inner versus outer) and precession* describes the liner's unique ability to rotate within the acetabular shell. It is recommended that these angles are considered in future motion tracking analyses as a consistent and standardised system of describing dual mobility liner orientation.

Finally, it is challenging to disarticulate the femoral head from the polyethylene liner due to the liner's snap-fit mechanism. In a clinical scenario, these components should not become disassembled except in extraordinary and adverse circumstances such as intraprosthetic dislocation. Alternatively, it is necessary to disarticulate the head and liner during in-vitro tests to facilitate adequate cleaning and analysis (e.g., gravimetric or geometric measurement) of the components. However, methods to separate these components may cause permanent damage to the liner. This includes either uniaxial removal of the femoral head, which causes uniform deformation underneath the retentive bore as previously observed in Chapter 2 (Section 2.6.1), or a levering-out process which results in the formation of a deep impingement notch on the liner's chamfer and rim (Chapter 3), as shown in Figure 6.2. The method of disarticulation should be well documented for retrieved dual mobility implants, so the resultant damage is not mistaken for in-vivo damage. In addition, components should be disarticulated as few times as possible throughout in-vitro simulation testing to ensure the collective damage does not become excessive. It is unclear whether this process would cause additional and compounding damage to the mobile liner and thus result in the degree of wear/deformation being overestimated in these types of analyses as an artefact of component disassembly. Therefore, further research should be conducted to assess the effects of repeated implant assembly and disassembly on liner damage.

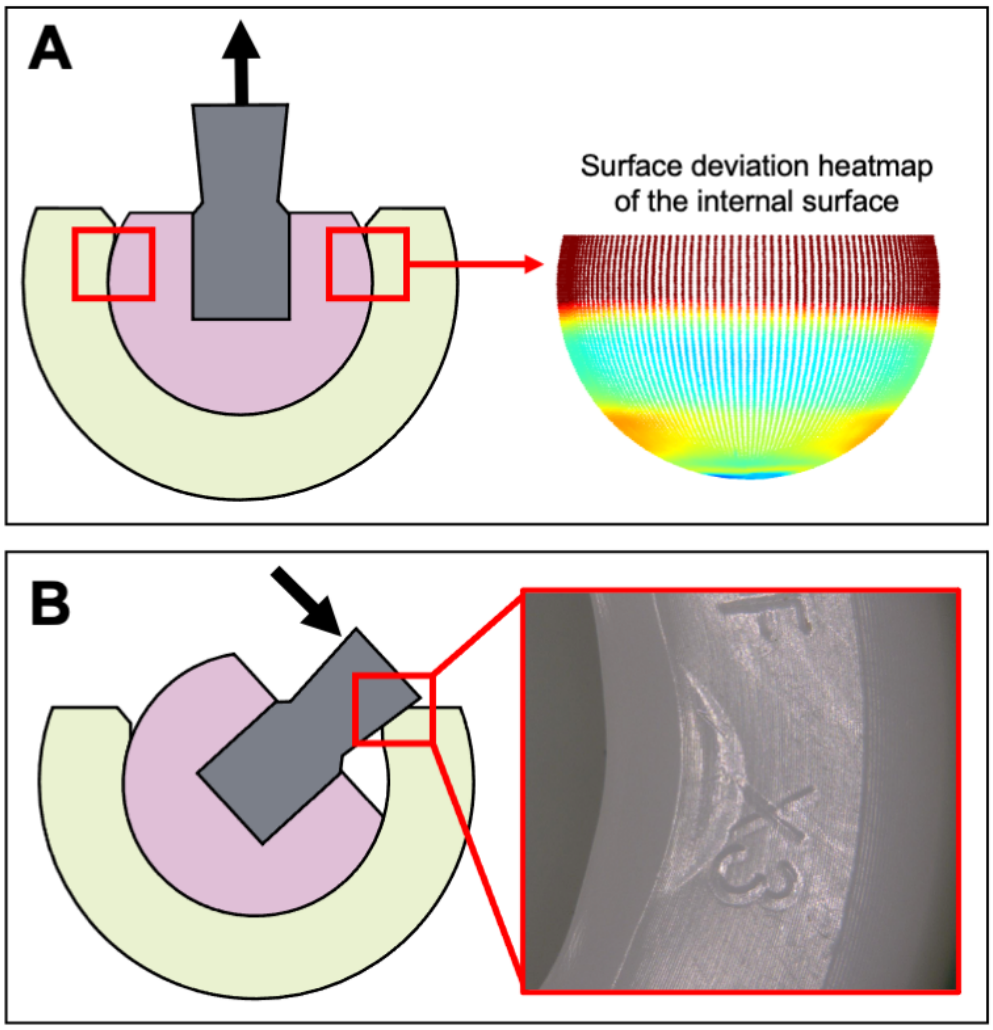

Figure 6.2 – Schematic illustrating the two methods of disarticulating the femoral head from a dual mobility liner, including uniaxial removal (A) and levering out (B), and associated damage mechanisms resulting from these processes.

6.5 – Conclusions

Despite their increasing use, Chapter 1 highlights the lack of available information relating to the in-vivo function of dual mobility implants. There is an absence of suitable methodologies to characterise and test these bearings, and few studies have investigated their performance. In this thesis, several novel methodologies were developed which address this unmet need and may be used to enhance the assessment of dual mobility implants in future studies. These methods have the potential to aid in the assessment of best- and worst-case operating conditions, the identification of optimal component orientations and patient populations, and the optimisation of implant design to improve longevity. In addition, a multi-method retrieval analysis and in-vitro motion tracking simulation were conducted to improve

the current understanding of dual mobility kinematic function. The following conclusions were made as a result of the work presented in this Thesis –

- The current understanding of in-vivo dual mobility function is poor, and available in-vitro testing and assessment methodologies in the literature are not suitable for the novel geometry and function of these implants.
- The developed geometric characterisation methodology is the first known method to repeatably and reliably identify regions of surface damage (i.e., geometric variance) across the articulating surfaces of dual mobility polyethylene liners in a non-destructive manner and without excluding large portions of the bearing surfaces.
- The developed in-vitro motion tracking methodology is a useful tool for investigating the real-time behaviour of dual mobility liners, and is the first to allow direct observation of these components under physiologically relevant loading, displacement, and lubrication conditions without implant line-of-sight.
- Dual mobility bearings primarily articulate at their inner bearing surface between the femoral head and liner, although it is possible for the outer bearing to become engaged at extreme ranges of motion or under the right operating conditions.
- Dual mobility liners can rotate within the acetabular shell. This is the first study to directly observe such motions, although the factors which influence the angular velocity and directionality of this behaviour remain unclear.
- Dual mobility bearings may remain susceptible to failure mechanisms such as intraprosthetic dislocation and edge loading. This is the first study to report such failure mechanisms in relation to new-generation dual mobility retrievals, in contrast to current literature which suggests these failure mechanisms are no longer relevant for these device types.
- Retrieved dual mobility liners may be susceptible to ex-vivo damage (i.e., during the surgical revision process or in transport), particularly at their external (i.e., convex) surfaces.

- It is likely that dual mobility bearings do not behave repeatably (intra- or inter-component) under standard gait conditions, which suggests their motions are sensitive, complex, and influenced by various patient, surgical and/or implant factors. Further research is required to better understand these behaviours.

6.6 – Publication strategy

At present, the contents of this Thesis have been accepted for presentation at several national and international orthopaedic conferences, as detailed in Appendix D. These have detailed the development of a novel geometric assessment method for dual mobility liners (Chapter 2) and the comprehensive retrievals analysis of dual mobility implants (Chapter 3). At the time of submission, several conference abstracts and papers were planned which include –

- Submitted conference abstract to present the results of the retrieval analysis to a clinical audience at the British Hip Society 2023 Annual Meeting.
- Planned technical note to report the development of a novel geometric assessment method for dual mobility liners in an appropriate journal (e.g., Proceedings of the Institution of Mechanical Engineers, Part H: Journal of Engineering in Medicine).
- Planned manuscript to report the results of the comprehensive retrieval analysis of dual mobility implants in an appropriate journal (e.g., Journal of Arthroplasty). This manuscript will be submitted once the technical note detailing the geometric method is accepted and published, so it can be referenced in the methods section.
- Planned manuscript to report the results of the in-vitro motion tracking study described in Chapter 5 in an appropriate journal (e.g., Medical Engineering and Physics). This manuscript will be submitted once a separate paper detailing the development and working principles of the motion tracker is accepted and published, so it can be referenced in the methods. This paper is authored by Dr Matthew P Shuttleworth and co-authored by the author of this Thesis.

6.7 – Future work

The following are recommendations for future work which should be completed in light of the research conducted in this Thesis –

- Enhanced monitoring of dual mobility implant performance is essential in the coming years (i.e., through joint registries) to assess the long-term survivorship, revision rates, and incidence of intraprosthetic dislocation in new-generation dual mobility designs and compare this against the performance of conventional, unipolar hip implants.

- Further refinement of the geometric assessment methodology described in Chapter 2 is recommended to increase the utility of the method. This includes further development of the volumetric change algorithm, which would be the first known method to assess the volume change of retrieved dual mobility polyethylene liners, and an extension of the method to assess geometric changes at the retentive bore and chamfer. Damage in this region is a precursor to intraprosthetic dislocation and thus is pertinent in the assessment of dual mobility implants.

- It would be advantageous to complete a study characterising the effects of ex-vivo damage on retrieved dual mobility polyethylene liners (e.g., during the revision process, contact with surgical instruments, transport). This would yield a catalogue of known ex-vivo damage mechanisms for these implants thus improving future retrieval analyses.

- It is recommended that an investigation into the effects of the head-liner assembly and disassembly mechanism on dual mobility liner damage is performed. The results of this type of study would inform the design of future in-vitro experimental studies by providing researchers with insights into the efficacy and effects of various disassembly mechanisms so the resultant liner damage can be minimised.

- Further in-vitro assessment of dual mobility liner motion is recommended with increased sample sizes, varying implant designs (i.e., concentric, eccentric, and radially-offset liners) and a broader range of operating conditions, including standard gait and adverse conditions (e.g., high cup inclination angle, reduced swing phase loads, scratched femoral head) so

that the complexity and sensitivity of dual mobility liner motion may be better understood.

References

Adam, P., Farizon, F. and Fessy, M.H. 2014. Dual mobility retentive acetabular liners and wear: Surface analysis of 40 retrieved polyethylene implants. *Orthopaedics and Traumatology: Surgery and Research*. **100**, pp.85–91.

Adam, P., Philippe, R., Ehlinger, M., Roche, O., Bonnomet, F., Molé, D. and Fessy, M.H. 2012. Dual mobility cups hip arthroplasty as a treatment for displaced fracture of the femoral neck in the elderly. A prospective, systematic, multicenter study with specific focus on postoperative dislocation. *Orthopaedics and Traumatology: Surgery and Research*. **98**(3), pp.296–300.

Affatato, S., Modena, E., Toni, A. and Taddei, P. 2012. Retrieval analysis of three generations of Biolox® femoral heads: Spectroscopic and SEM characterisation. *Journal of the Mechanical Behavior of Biomedical Materials*. **13**, pp.118–128.

Agarwala, S., Shetty, V., Taywade, S., Vijayvargiya, M. and Bhingraj, M. 2020. Dual mobility THR: Resolving instability and providing near normal range of movement. *Journal of Clinical Orthopaedics and Trauma*.

Aherwar, A., Singh, A.K. and Patnaik, A. 2016. Cobalt based alloy: A better choice biomaterial for hip implants. *Trends in Biomaterials and Artificial Organs*. **30**(1), pp.50–55.

Akbari, A., Roy, M.E., Whiteside, L.A., Katerberg, B.J. and Schnettgoecke, D.J. 2011. Minimal Backside Surface Changes Observed in Retrieved Acetabular Liners. *Journal of Arthroplasty*. **26**(5), pp.686–692.

Al-Hajjar, M., Fisher, J., Williams, S., Tipper, J.L. and Jennings, L.M. 2013. Effect of femoral head size on the wear of metal on metal bearings in total hip replacements under adverse edge-loading conditions. *Journal of Biomedical Materials Research - Part B Applied Biomaterials*. **101B**(2), pp.213–222.

American Academy of Orthopaedic Surgeons 2019. Sixth Annual AJRR Annual Report on Hip and Knee Arthroplasty Data 2019. *American Joint Replacement Registry*.

American Joint Replacement Registry 2022. *The Ninth Annual Report of the AJRR on Hip and Knee Arthroplasty*.

Arnholt, C.M., MacDonald, D.W., Malkani, A.L., Klein, G.R., Rimnac, C.M., Kurtz, S.M., Kocagoz, S.B. and Gilbert, J.L. 2016. Corrosion Damage and Wear Mechanisms in Long-Term Retrieved CoCr Femoral Components for Total Knee Arthroplasty. *J Arthroplasty*. **31**(2), pp.2900–2906.

Atwood, S.A., Van Citters, D.W., Patten, E.W., Furmanski, J., Ries, M.D. and Pruitt,

L.A. 2011. Tradeoffs amongst fatigue, wear, and oxidation resistance of cross-linked ultra-high molecular weight polyethylene. *Journal of the Mechanical Behavior of Biomedical Materials*. **4**(7), pp.1033–1045.

Australian Orthopaedic Association 2018. *National Joint Replacement Registry: Hip, Knee & Shoulder Arthroplasty Annual Report*.

Bah, M.T., Nair, P.B., Taylor, M. and Browne, M. 2011. Efficient computational method for assessing the effects of implant positioning in cementless total hip replacements. *Journal of Biomechanics*. **44**(7), pp.1417–1422.

Barbour, P.S.M., Stone, M.H. and Fisher, J. 2000. A hip joint simulator study using new and physiologically scratched femoral heads with ultra-high molecular weight polyethylene acetabular cups. *Proceedings of the Institution of Mechanical Engineers, Part H: Journal of Engineering in Medicine*. **214**(6), pp.569–576.

Barrack, R.L., Sawhney, J., Hsu, J. and Cofield, R.H. 1999. Cost Analysis of Revision Total Hip Arthroplasty: A 5-Year Followup Study. *Clinical Orthopaedics and Related Research*. (369), pp.175–178.

Bergiers, S., Hothi, H., Richards, R., Henckel, J. and Hart, A. 2019. Quantifying the bearing surface wear of retrieved hip replacements. *Biosurface and Biotribology*. **5**(1), pp.28–33.

Bergmann, G., Deuretzbacher, G., Heller, M., Graichen, F. and Rohlmann, A. 2001. Hip contact and gait patterns from routine activities. *Journal of Biomechanics*. **34**, pp.859–871.

Blunt, L. and Jiang, X.Q. 2000. Three dimensional measurement of the surface topography of ceramic and metallic orthopaedic joint prostheses. *Journal of Materials Science: Materials in Medicine*. **11**(4), pp.235–246.

Bowden, A.E. and Bergström, J. 2015. Chapter 35: Computer Modeling and Simulation of UHMWPE. *UHMWPE Biomaterials Handbook: Ultra High Molecular Weight Polyethylene in Total Joint Replacement and Medical Devices: Third Edition*., pp.753–771.

Bowden, A.E., Kurtz, S.M. and Edidin, A.A. 2005. Validation of a micro-CT technique for measuring volumetric wear in retrieved acetabular liners. *Journal of Biomedical Materials Research - Part B Applied Biomaterials*. **75**(1), pp.205–209.

Bowman, K.F., Fox, J. and Sekiya, J.K. 2010. A Clinically Relevant Review of Hip Biomechanics. *Arthroscopy: The Journal of Arthroscopic and Related Surgery*. **26**(8), pp.1118–1129.

Bradford, L., Baker, D.A., Graham, J., Chawan, A., Ries, M.D. and Pruitt, L.A. 2004.

Wear and surface cracking in early retrieved highly cross-linked polyethylene acetabular liners. *Journal of Bone and Joint Surgery - Series A*. **86**(6), pp.1271–1282.

Bragdon, C.R., Jasty, M., Muratoglu, O.K. and Harris, W.H. 2005. Third-body wear testing of a highly cross-linked acetabular liner: The effect of large femoral head size in the presence of particulate poly(methyl-methacrylate) debris. *Journal of Arthroplasty*. **20**(3), pp.379–385.

Brockett, C., Williams, S., Jin, Z., Isaac, G. and Fisher, J. 2007. Friction of total hip replacements with different bearings and loading conditions. *Journal of Biomedical Materials Research - Part B Applied Biomaterials*. **81**(2), pp.508–515.

Buckland, A.J., Puvanesarajah, V., Vigdorchik, J., Schwarzkopf, R., Jain, A., Klineberg, E.O., Hart, R.A., Callaghan, J.J. and Hassanzadeh, H. 2017. Dislocation of a primary total hip arthroplasty is more common in patients with a lumbar spinal fusion. *Bone and Joint Journal*. **99B**(5), pp.585–591.

Buckwalter, J.A., Mankin, H.J. and Grodzinsky, A.J. 2005. Articular Cartilage and Osteoarthritis. *Instr Course Lect*. **54**, pp.465–480.

Byrne, D.P., Mulhall, K.J. and Baker, J.F. 2010. Anatomy & Biomechanics of the Hip. *The Open Sports Medicine Journal*. **4**, pp.51–57.

Canton, G., Moghnie, A., Cleva, M., Kostoris, F.M. and Murena, L. 2019. Dual mobility total hip arthroplasty in the treatment of femoral neck fractures: a retrospective evaluation at mid-term follow-up. *Acta Biomed*. **90**(S-1), pp.98–103.

Choudhury, D., Ranuša, M., Fleming, R.A., Vrbka, M., Křupka, I., Teeter, M.G., Goss, J. and Zou, M. 2018. Mechanical wear and oxidative degradation analysis of retrieved ultra high molecular weight polyethylene acetabular cups. *Journal of the Mechanical Behavior of Biomedical Materials*. **79**, pp.314–323.

Clement, N.D., Scott, C.E.H., Murray, J.R.D., Howie, C.R. and Deehan, D.J. 2021. The number of patients “worse than death” while waiting for a hip or knee arthroplasty has nearly doubled during the COVID-19 pandemic: A UK nationwide survey. *The Bone & Joint Journal*. **103-B**(4).

Combes, A., Migaud, H., Girard, J., Duhamel, A. and Fessy, M.H. 2013. Low rate of dislocation of dual-mobility cups in primary total hip arthroplasty. *Clinical Orthopaedics and Related Research*. **471**(12), pp.3891–3900.

Cooper, J.R., Dowson, D. and Fisher, J. 1993. The effect of transfer film and surface roughness on the ear of lubricated ultra-high molecular weight polyethylene. *Clinical Materials*. **14**(4), pp.295–302.

Cuthbert, R., Wong, J., Mitchell, P. and Jaiswal, P.K. 2019. Dual mobility in primary

total hip arthroplasty: Current concepts. *EFORT Open Reviews*. **4**(11), pp.640–646.

D'Apuzzo, M.R., Koch, C.N., Esposito, C.I., Elpers, M.E., Wright, T.M. and Westrich, G.H. 2016. Assessment of Damage on a Dual Mobility Acetabular System. *Journal of Arthroplasty*. **31**, pp.1828–1835.

Dall'Ava, L., Hothi, H., Henckel, J., Di Laura, A., Shearing, P. and Hart, A. 2020. Characterization of dimensional, morphological and morphometric features of retrieved 3D-printed acetabular cups for hip arthroplasty. *Journal of Orthopaedic Surgery and Research*. **15**(157).

Darrith, B., Courtney, P.M. and Della Valle, C.J. 2018. Outcomes of dual mobility components in total hip arthroplasty: A systematic review of the literature. *Bone Joint J*. **100-B**(1), pp.11–19.

Devane, P.A., Wraighte, P.J., Ong, D.C.G. and Horne, J.G. 2012. Do joint registries report true rates of hip dislocation? *Clinical Orthopaedics and Related Research*. **470**(11), pp.3003–3006.

Dowd, J.E., Sychterz, C.J., Young, A.M. and Engh, C.A. 2000. Characterization of Long-Term Femoral-Head-Penetration Rates. *Journal of Bone and Joint Surgery*. **82-A**(8), pp.1102–1107.

Dowson, D., Diab, M.M.E., Gillis, B.J. and Atkinson, J.R. 1985. Influence of Counterface Topography on the Wear of Ultra High Molecular Weight Polyethylene Under Wet or Dry Conditions. *Polymer Wear and Its Control*. **12**, pp.171–187.

Dumbleton, J.H., Manley, M.T. and Edidin, A.A. 2002. A literature review of the association between wear rate and osteolysis in total hip arthroplasty. *Journal of Arthroplasty*. **17**(5), pp.649–661.

Eberhardt, A.W., McKee, R.T., Cuckler, J.M., Peterson, D.W., Beck, P.R. and Lemons, J.E. 2009. Surface Roughness of CoCr and ZrO 2 Femoral Heads with Metal Transfer: A Retrieval and Wear Simulator Study . *International Journal of Biomaterials*. **2009**, pp.1–6.

Elpers, M., Nam, D., Boydston-White, S., Ast, M.P., Wright, T.M. and Padgett, D.E. 2014. Zirconia phase transformation, metal transfer, and surface roughness in retrieved ceramic composite femoral heads in total hip arthroplasty. *Journal of Arthroplasty*. **29**(11), pp.2219–2223.

Engh, C.A., Bobyn, J.D. and Glassman, A.H. 1987. Porous-coated hip replacement. The factors governing bone ingrowth, stress shielding, and clinical results. *Journal of Bone and Joint Surgery*. **69B**(1), pp.45–55.

Esposito, C.I., Walter, W.L., Roques, A., Tuke, M.A., Zicat, B.A., Walsh, W.R. and

Walter, W.K. 2012. Wear in alumina-on-alumina ceramic total hip replacements: A retrieval analysis of edge loading. *Journal of Bone and Joint Surgery - Series B*. **94 B**(7), pp.901–907.

Estok, D.M., Bragdon, C.R., Plank, G.R., Huang, A., Muratoglu, O.K. and Harris, W.H. 2005. The measurement of creep in ultrahigh molecular weight polyethylene: A comparison of conventional versus highly cross-linked polyethylene. *Journal of Arthroplasty*. **20**(2), pp.239–243.

Etchels, L., Wang, L., Al-Hajjar, M., Williams, S., Thompson, J., Isaac, G., Wilcox, R. and Jones, A. 2019. Computationally efficient modelling of hip replacement separation due to small mismatches in component centres of rotation. *Journal of Biomechanics*. **95**.

Evans, R.P. 2001. Rotations and rotation matrices. *Acta Cryst*. **D57**, pp.1355–1359.

Fabry, C., Kaehler, M., Herrmann, S., Woernle, C. and Bader, R. 2014. Dynamic behavior of tripolar hip endoprostheses under physiological conditions and their effect on stability. *Medical Engineering and Physics*. **36**(1), pp.65–71.

Fabry, C., Woernle, C. and Bader, R. 2014. Self-centering dual-mobility total hip systems: Prediction of relative movements and realignment of different intermediate components. *Proc IMechE Part H: J Engineering in Medicine*. **228**(5), pp.477–485.

Firkins, P.J., Tipper, J.L., Ingham, E., Stone, M.H., Farrar, R. and Fisher, J. 2001. A novel low wearing differential hardness, ceramic-on-metal hip joint prosthesis. *Journal of Biomechanics*. **34**(10), pp.1291–1298.

Fisher, J. 1994. Wear of ultra high molecular weight polyethylene in total artificial joints. *Current Orthopaedics*. **8**(3), pp.164–169.

Fisher, J. and Dowson, D. 1991. Tribology of total artificial joints. *Proc Inst Mech Eng H*. **205**(2), pp.73–9.

Fisher, J., Hu, X.Q., Tipper, J.L., Stewart, T.D., Williams, S., Stone, M.H., Davies, C., Hatto, P., Bolton, J., Riley, M., Hardaker, C., Isaac, G.H., Berry, G. and Ingham, E. 2002. An in vitro study of the reduction in wear of metal-on-metal hip prostheses using surface-engineered femoral heads. *Proceedings of the Institution of Mechanical Engineers, Part H: Journal of Engineering in Medicine*. **216**(4), pp.219–230.

Fredette, E.K., MacDonald, D.W., Underwood, R.J., Chen, A.F., Mont, M.A., Lee, G.C., Klein, G.R., Rimnac, C.M. and Kurtz, S.M. 2015. Does metal transfer differ on retrieved ceramic and CoCr femoral heads? *BioMed Research International*. **2015**.

Gaudin, G., Ferreira, A., Gaillard, R., Prudhon, J.L., Caton, J.H. and Lustig, S. 2017.

Equivalent wear performance of dual mobility bearing compared with standard bearing in total hip arthroplasty: in vitro study. *International Orthopaedics*. **41**(3), pp.521–527.

Geringer, J., Boyer, B. and Farizon, F. 2011. Understanding the dual mobility concept for total hip arthroplasty. Investigations on a multiscale analysis-highlighting the role of arthrofibrosis. *Wear*. **271**(9–10), pp.2379–2385.

Glyn-Jones, S., McLardy-Smith, P., Gill, H.S. and Murray, D.W. 2008. The creep and wear of highly cross-linked polyethylene: A three-year randomised, controlled trial using radiostereometric analysis. *J Bone Joint Surg (Br)*. **90**-**B**, pp.556–561.

Goldsmith, A.A.J., Dowson, D., Isaac, G.H. and Lancaster, J.G. 2000. A comparative joint simulator study of the wear of metal-on-metal and alternative material combinations in hip replacements. *Proceedings of the Institution of Mechanical Engineers, Part H: Journal of Engineering in Medicine*. **214**(1), pp.39–47.

Goldvasser, D., Hansen, V.J., Noz, M.E., Maguire, G.Q., Zeleznik, M.P., Olivecrona, H., Bragdon, C.R., Weidenhielm, L. and Malchau, H. 2014. In vivo and ex vivo measurement of polyethylene wear in total hip arthroplasty. *Acta Orthopaedica*. **85**(3), pp.271–275.

Gomoll, A., Wanich, T. and Bellare, A. 2002. J-integral fracture toughness and tearing modulus measurement of radiation cross-linked UHMWPE. *Journal of Orthopaedic Research*. **20**(6), pp.1152–1156.

Grochowsky, J.C., Alaways, L.W., Siskey, R., Most, E. and Kurtz, S.M. 2006. Digital Photogrammetry for Quantitative Wear Analysis of Retrieved TKA Components. *Journal of Biomedical Materials Research Part B: Applied Biomaterials*. **79B**(2), pp.263–267.

Hall, R.M., Siney, P., Unsworth, A. and Wroblewski, B.M. 1997. The effect of surface topography of retrieved femoral heads on the wear of UHMWPE sockets. *Medical Engineering and Physics*. **19**(8), pp.711–719.

Hall, R.M., Unsworth, A., Craig, P.S., Hardaker, C., Siney, P. and Wroblewski, B.M. 1995. Measurement of wear in retrieved acetabular sockets. *Proceedings of the Institution of Mechanical Engineers, Part H: Journal of Engineering in Medicine*. **209**(4), pp.233–242.

Haraguchi, K., Sugano, N., Nishii, T., Sakai, T., Yoshikawa, H. and Ohzono, K. 2001. Influence of polyethylene and femoral head surface quality on wear: A retrieval study. *International Orthopaedics*. **25**(1), pp.29–34.

Heffernan, C., Banerjee, S., Nevelos, J., Macintyre, J., Issa, K., Markel, D.C. and Mont, M.A. 2014. Does dual-mobility cup geometry affect posterior horizontal dislocation distance? *Clinical Orthopaedics and Related Research*. **472**(5),

pp.1535–1544.

Heiner, A.D., Kruger, K.M., Baer, T.E. and Brown, T.D. 2013. Enhancing Damage Visibility on Metallic Bearing Surfaces. A Simple Technique for Photography and Viewing. *Journal of Arthroplasty*. **28**(3), 543.e9-543.e12.

Holdcroft, L.A. and Van Citters, D. 2018. Comparison of Wear in Highly Cross-linked and Conventional Polyethylene Hip Retrievals. *Orthopaedic Proceedings*. **99-B**(SUPP_4).

Hood, R.W., Wright, T.M. and Burstein, A.H. 1983. Retrieval analysis of total knee prostheses: A method and its application to 48 total condylar prostheses. *Journal of Biomedical Materials Research*. **17**, pp.829–842.

Hu, C.Y. and Yoon, T. 2018. Recent updates for biomaterials used in total hip arthroplasty. *Biomaterials Research*. **22**(33).

Hua, X. and Li, J. 2020. CMM-based method for assessing the volume change of retrieved polyethylene cups in MoP total hip replacements. *Biosurface and Biotribology*. **6**(2), pp.37–42.

Hua, X., Wang, L., Jin, Z., Wilcox, R. and Fisher, J. 2014. The Application of a CMM-based Technique for the Assessment of the Volume Change on Retrieved Cups *In*: *Orthopaedic Research Society*.

Isaac, G.H., Atkinson, J.R., Dowson, D. and Wroblewski, B.M. 1986. The role of cement in the long term performance and premature failure of Charnley low friction arthroplasties. *Engineering in Medicine*. **15**(1), pp.19–22.

Ito, H., Maloney, C.M., Crowninshield, R.D., Clohisy, J.C., McDonald, D.J. and Maloney, W.J. 2010. In Vivo Femoral Head Damage and Its Effect on Polyethylene Wear. *Journal of Arthroplasty*. **25**(2), pp.302–308.

Ito, H., Minami, A., Matsuno, T., Tanino, H., Yuhta, T. and Nishimura, I. 2001. The sphericity of the bearing surface in total hip arthroplasty. *Journal of Arthroplasty*. **16**(8), pp.1024–1029.

Jasty, M., Bragdon, C.R., Lee, K., Hanson, A. and Harris, W.H. 1994. Surface damage to cobalt-chrome femoral head prostheses. *Journal of Bone and Joint Surgery - Series B*. **76**(1), pp.73–77.

Jeffers, J.R.T., Browne, M., Lennon, A.B., Prendergast, P.J. and Taylor, M. 2007. Cement mantle fatigue failure in total hip replacement: Experimental and computational testing. *Journal of Biomechanics*. **40**(7), pp.1525–1533.

Jennings, A. 2020. Sphere Fit (least squared).

Jørgensen, P.B., Kaptein, B.L., Søballe, K., Jakobsen, S.S. and Stilling, M. 2022. Polyethylene liner motion in dual-mobility hip prostheses: static and dynamic radiostereometry in 16 patients 1 year after operation. *Acta Orthopaedica*. **93**(2),

pp.375–381.

Kabo, J.M., Gebhard, J.S., Loren, G. and Amstutz, H.C. 1991. In Vivo Wear of Polyethylene Acetabular Components. *The Journal of Bone and Joint Surgery. British volume*. **75-B**(2), pp.254–258.

Kärrholm, J., Mohaddes, M., Odin, D., Vinblad, J., Rogmark, C. and Rolfson, O. 2017. *Swedish Hip Arthroplasty Register Annual Report 2017*.

Kim, Y.H. 2007. Surface roughness of ceramic femoral heads after in-vivo transfer of metal correlation to polyethylene wear *In*: *Ceramics in Orthopaedics: Bioceramics and Alternative Bearings in Joint Arthroplasty - 12th International BIOLOX Symposium, Proceedings*., pp.49–57.

Klemt, C., Smith, E.J., Oganesyan, R., Limmahakhun, S., Fitz, D. and Kwon, Y.M. 2020. Outcome of Dual Mobility Constructs for Adverse Local Tissue Reaction Associated Abductor Deficiency in Revision Total Hip Arthroplasty. *Journal of Arthroplasty*. **35**(12), pp.3689–3691.

Klingenstein, G.G., Yeager, A.M., Lipman, J.D. and Westrich, G.H. 2013. Computerized range of motion analysis following dual mobility total hip arthroplasty, traditional total hip arthroplasty, and hip resurfacing. *Journal of Arthroplasty*. **28**(7), pp.1173–1176.

Kluess, D., Martin, H., Mittelmeier, W., Schmitz, K.P. and Bader, R. 2007. Influence of femoral head size on impingement, dislocation and stress distribution in total hip replacement. *Medical Engineering and Physics*. **29**(4), pp.465–471.

Kolz, J.M., Wyles, C.C., Van Citters, D.W., Chapman, R.M., Trousdale, R.T. and Berry, D.J. 2020. In Vivo Corrosion of Modular Dual-Mobility Implants: A Retrieval Study. *Journal of Arthroplasty*. **35**(11), pp.3326–3329.

Kurtz, S.M. 2015a. *Chapter 1: A Primer on UHMWPE* Second Edi. Elsevier Inc.

Kurtz, S.M. 2015b. *Chapter 2: From Ethylene Gas to UHMWPE Component: The Process of Producing Orthopedic Implants* [Online] Second Edi. Elsevier Inc. Available from: http://dx.doi.org/10.1016/B978-0-12-374721-1.00002-X.

Kurtz, S.M. 2015c. *Chapter 3: Packaging and Sterilization of UHMWPE* Second Edi. Elsevier Inc.

Kurtz, S.M., Gawel, H.A. and Patel, J.D. 2011. History and systematic review of wear and osteolysis outcomes for first-generation highly crosslinked polyethylene. *Clin Orthop Relat Res*. **469**(8), pp.2262–77.

Laura, A. Di, Hothi, H., Battisti, C., Cerquiglini, A., Henckel, J., Skinner, J. and Hart, A. 2017. Wear of dual-mobility cups: a review article. *International Orthopaedics*. **41**(3), pp.625–633.

Laura, A. Di, Hothi, H.S., Henckel, J., Cerquiglini, A., Liow, M.H.L., Kwon, Y.-M.,

Skinner, J.A. and Hart, A.J. 2017. Retrieval evidence of impingement at the third articulation in contemporary dual mobility cups for total hip arthroplasty. *International Orthopaedics*. **41**(12), pp.2495–2501.

Laurent, M.P., Hall, D.J., Urban, R.M., Wimmer, M.A. and Ph, D. 2014. Effect of Femoral Head Surface Roughness on Acetabular Liner Polyethylene Wear - A Postmortem Retrieval Study *In*: *Orthopaedic Research Society*.

Leslie, I.J., Williams, S., Isaac, G., Ingham, E. and Fisher, J. 2009. High cup angle and microseparation increase the wear of hip surface replacements. *Clinical Orthopaedics and Related Research*. **467**(9), pp.2259–2265.

Liu, F., Feng, L. and Wang, J. 2018. A computational parametric study on edge loading in ceramic-on-ceramic total hip joint replacements. *Journal of the Mechanical Behavior of Biomedical Materials*. **83**, pp.135–142.

Logishetty, K., van Arkel, R.J., Ng, K.C.G., Muirhead-Allwood, S.K., Cobb, J.P. and Jeffers, J.R.T. 2019. Hip capsule biomechanics after arthroplasty: the effect of implant, approach, and surgical repair. *The Bone & Joint Journal*. **101**-**B**(4), pp.426–434.

Loving, L., Herrera, L., Banerjee, S., Heffernan, C., Nevelos, J., Markel, D.C. and Mont, M.A. 2015. Dual mobility bearings withstand loading from steeper cup-inclinations without substantial wear. *Journal of Orthopaedic Research*. **33**(3), pp.398–404.

Loving, L.Q., Lee, R.K.F., Herrera, L., Essner, A.P. and Nevelos, J.E. 2013. Wear performance evaluation of a contemporary dual mobility hip bearing using multiple hip simulator testing conditions. *Journal of Arthroplasty*. **28**, pp.1041–1046.

Mai, K.T., Verioti, C., D'Lima, D., Colwell, C.W. and Ezzet, K.A. 2010. Surface roughness of femoral head prostheses after dislocation. *American Journal of Orthopedics*. **39**(10), pp.495–500.

Malatray, M., Roux, J.P., Gunst, S., Pibarot, V. and Wegrzyn, J. 2017. Highly crosslinked polyethylene: a safe alternative to conventional polyethylene for dual mobility cup mobile component. A biomechanical validation. *International Orthopaedics*. **41**(3), pp.507–512.

Malik, A., Maheshwari, A. and Dorr, L.D. 2007. Impingement with total hip replacement. *Journal of Bone and Joint Surgery - Series A*. **89**(8), pp.1832–1842.

Manley, M.T. 2015. *Chapter 14: Highly Cross-Linked and Annealed UHMWPE* Second Edi. Elsevier Inc.

McCarthy, T.F., Alipit, V., Nevelos, J., Elmallah, R.K. and Mont, M.A. 2016.

Acetabular Cup Anteversion and Inclination in Hip Range of Motion to Impingement. *Journal of Arthroplasty*. **31**(9), pp.264–268.

McKellop, H., Shen, F.W., Lu, B., Campbell, P. and Salovey, R. 1999. Development of an extremely wear-resistant ultra high molecular weight polyethylene for total hip replacements. *Journal of Orthopaedic Research*. **17**(2), pp.157–167.

Merola, M., Ruggiero, A., De Mattia, J.S. and Affatato, S. 2016. On the tribological behavior of retrieved hip femoral heads affected by metallic debris. A comparative investigation by stylus and optical profilometer for a new roughness measurement protocol. *Measurement: Journal of the International Measurement Confederation*. **90**, pp.365–371.

Moon, N.H., Shin, W.C., Do, M.U., Kang, S.W., Lee, S.M. and Suh, K.T. 2021. Wear and osteolysis outcomes for highly cross-linked polyethylene in primary total hip arthroplasty compared with conventional polyethylene: a 15- to 18-year single-centre follow-up study. *HIP International*. **31**(4), pp.526–532.

Morlock, M.M., Bishop, N. and Huber, G. 2011. Biomechanics of Hip Arthroplasty *In*: *Tribology in Total Hip Arthroplasty*., pp.11–24.

Morlock, M.M., Gomez-Barrena, E., Wirtz, D.C., Hart, A. and Kretzer, J.P. 2022. Explant analysis and implant registries are both needed to further improve patient safety. *EFORT Open Reviews*. **7**(6), pp.344–348.

Mudrick, C.A., Melvin, J.S. and Springer, B.D. 2015. Late posterior hip instability after lumbar spinopelvic fusion. *Arthroplasty Today*. **1**, pp.25–29.

Muratoglu, O.K. 2009. *Chapter 13: Highly Crosslinked and Melted UHMWPE* Second Edi. Elsevier Inc.

National Joint Registry 2021. *18th Annual Report 2021*.

National Joint Registry 2022. *19th Annual Report*.

Nebergall, A.K., Freiberg, A.A., Greene, M.E., Malchau, H., Muratoglu, O., Rowell, S., Zumbrunn, T. and Varadarajan, K.M. 2016. Analysis of Dual Mobility Liner Rim Damage Using Retrieved Components and Cadaver Models. *Journal of Arthroplasty*. **31**(7), pp.1595–1602.

Neri, T., Boyer, B., Geringer, J., Di Iorio, A., Caton, J.H., Philippot, R. and Farizon, F. 2019. Intraprosthetic dislocation of dual mobility total hip arthroplasty: still occurring? *International Orthopaedics*. **43**(5), pp.1097–1105.

Nessler, J.M., Malkani, A.L., Sachdeva, S., Nessler, J.P., Westrich, G., Harwin, S.F., Mayman, D. and Jerabek, S. 2020. Use of dual mobility cups in patients undergoing primary total hip arthroplasty with prior lumbar spine fusion. *International Orthopaedics*. **44**(5), pp.857–862.

Netter, J.D., Hermida, J.C., Chen, P.C., Nevelos, J.E. and D'Lima, D.D. 2014. Effect

of microseparation and third-body particles on dual-mobility crosslinked hip liner wear. *Journal of Arthroplasty*. **29**(9), pp.1849–1853.

Nogiwa-Valdez, A.A., Rainforth, W.M. and Stewart, T.D. 2014. Wear and degradation on retrieved zirconia femoral heads. *Journal of the Mechanical Behavior of Biomedical Materials*. **31**, pp.145–151.

Ozden, V.E., Dikmen, G., Beksac, B. and Tozun, R. 2018. Dual-mobility bearings for patients with abductor-trochanteric complex insufficiency. *HIP International*. **28**(5), pp.491–497.

Pang, H.N., Naudie, D.D.R., McCalden, R.W., MacDonald, S.J. and Teeter, M.G. 2015. Highly Crosslinked Polyethylene Improves Wear But Not Surface Damage in Retrieved Acetabular Liners. *Clinical Orthopaedics and Related Research*. **473**(2), pp.463–468.

Partridge, S., Buckley, P., de Boer, G. and Williams, S. 2018. A novel method to measure rim deformation in UHMWPE acetabular liners. *Medical Engineering and Physics*. **59**, pp.56–62.

Philippeau, J.-M., Durand, J.-M., Carret, J.-P., Leclercq, S., Waast, D. and Gouin, F. 2010. Dual mobility design socket use in preventing total hip replacement dislocation following tumor resection. *Orthopaedics & Traumatology: Surgery & Research*. **96**(1), pp.2–8.

Philippot, R., Boyer, B. and Farizon, F. 2013. Intraprosthetic dislocation: A specific complication of the dual-mobility system hip. *Clinical Orthopaedics and Related Research*. **471**, pp.965–970.

Philippot, R., Camilleri, J.P., Boyer, B., Adam, P. and Farizon, F. 2009. The use of a dual-articulation acetabular cup system to prevent dislocation after primary total hip arthroplasty: Analysis of 384 cases at a mean follow-up of 15 years. *International Orthopaedics*. **33**, pp.927–932.

Prudhon, J.L., Ferreira, A. and Verdier, R. 2013. Dual mobility cup: Dislocation rate and survivorship at ten years of follow-up. *International Orthopaedics*. **37**(12), pp.2345–2350.

Pryce, G.M. 2019. *Polyethylene acetabular liner rim damage in total hip replacements*. University of Leeds.

Rames, R.D., Stambough, J.B., Pashos, G.E., Maloney, W.J., Martell, J.M. and Clohisy, J.C. 2019. Fifteen-Year Results of Total Hip Arthroplasty With Cobalt-Chromium Femoral Heads on Highly Cross-Linked Polyethylene in Patients 50 Years and Less. *Journal of Arthroplasty*. **34**(6), pp.1143–1149.

Reina, N., Pareek, A., Krych, A.J., Pagnano, M.W., Berry, D.J. and Abdel, M.P. 2019. Dual-Mobility Constructs in Primary and Revision Total Hip Arthroplasty: A

Systematic Review of Comparative Studies. *Journal of Arthroplasty*. **34**(3), pp.594–603.

Reyna, A.L.P., Jäger, M., Floerkemeier, T., Frecher, S., Delank, K.S., Schilling, C. and Grupp, T.M. 2016. Backside Wear Analysis of Retrieved Acetabular Liners with a Press-Fit Locking Mechanism in Comparison to Wear Simulation in Vitro. *BioMed Research International*. **2016**.

Saenz de Viteri, V. and Fuentes, E. 2013. Titanium and Titanium Alloys as Biomaterials. *Tribology - Fundamentals and Advancements*., pp.137–144.

Saikko, V. and Shen, M. 2010. Wear comparison between a dual mobility total hip prosthesis and a typical modular design using a hip joint simulator. *Wear*. **268**, pp.617–621.

Sanchez-Sotelo, J., Haidukewych, G.J. and Boberg, C.J. 2006. Hospital cost of dislocation after primary total hip arthroplasty. *Journal of Bone and Joint Surgery*. **88**-**A**(2), pp.290–294.

Sanders, R.J.M., Swierstra, B.A. and Goosen, J.H.M. 2013. The use of a dual-mobility concept in total hip arthroplasty patients with spastic disorders: No dislocations in a series of ten cases at midterm follow-up. *Archives of Orthopaedic and Trauma Surgery*. **133**(7), pp.1011–1016.

Sandiford, N.A. and Skinner, J.A. 2014. Biomechanics of the Hip *In*: *The Young Adult Hip in Sport*., p.40.

Sariali, E., Klouche, S. and Mamoudy, P. 2014. Ceramic-on-ceramic total hip arthroplasty: Is squeaking related to an inaccurate three-dimensional hip anatomy reconstruction? *Orthopaedics & Traumatology: Surgery & Research*. **100**, pp.437–440.

Schmalzried, T.P., Shepherd, E.F., Dorey, F.J., Jackson, W.O., Dela Rosa, M., Fa'vae, F., McKellop, H.A., McClung, C.D., Martell, J., Moreland, J.R. and Amstutz, H.C. 2000. Wear is a Function of Use, Not Time. *Clinical Orthopaedics and Related Research*. **381**, pp.36–46.

Schroder, D.T., Kelly, N.H., Wright, T.M. and Parks, M.L. 2011. Retrieved highly crosslinked UHMWPE acetabular liners have similar wear damage as conventional UHMWPE. *Clinical Orthopaedics and Related Research*. **469**(2), pp.387–394.

Scifert, C.F., Brown, T.D., Pedersen, D.R., Heiner, A.D. and Callaghan, J.J. 1999. Development and physical validation of a finite element model of total hip dislocation. *Computer Methods in Biomechanics and Biomedical Engineering*. **2**(2), pp.139–147.

Scott, T.P., Weitzler, L., Salvatore, A., Wright, T.M. and Westrich, G.H. 2018. A

Retrieval Analysis of Impingement in Dual-Mobility Liners. *Journal of Arthroplasty*. **33**(8), pp.2660–2665.

Shon, W.Y., Baldini, T., Peterson, M.G., Wright, T.M. and Salvati, E.A. 2005. Impingement in total hip arthroplasty: A study of retrieved acetabular components. *Journal of Arthroplasty*. **20**(4), pp.427–435.

Shuttleworth, M., Vickers, O., Isaac, G., Culmer, P., Williams, S. and Kay, R. 2021. Development of a system for tracking liner orientation in dual mobility hip arthroplasties *In*: *Orthopaedic Proceedings, Vol. 103-B, No. SUPP_16*.

Shuttleworth, M.P., Vickers, O., Smeeton, M., Board, T., Isaac, G., Culmer, P., Williams, S. and Kay, R.W. 2023. Inertial Tracking System for Monitoring Dual Mobility Hip Implants In Vitro. *Sensors*. **23**(904).

Smith, S.L., Dowson, D. and Goldsmith, A.A.J. 2001. The effect of femoral head diameter upon lubrication and wear of metal-on-metal total hip replacements. *Proceedings of the Institution of Mechanical Engineers, Part H: Journal of Engineering in Medicine*. **215**(2), pp.161–170.

Smith, S.L. and Joyce, T.J. 2017. A hop, skip, and a jump: Towards better wear testing of hip implants *In*: *Mechanical Testing of Orthopaedic Implants*., pp.183–206.

Spece, H., MacDonald, D.W., Mont, M.A., Lee, G.-C. and Kurtz, S.M. 2018. Fretting Corrosion and Polyethylene Damage Mechanisms in Modular Dual Mobility Total Hip Arthroplasty. *Beyond the Implant: Retrieval Analysis Methods for Implant Surveillance*., pp.106–117.

Stratton-Powell, A.A. 2018. *On the Failure of Total Ankle Replacement: A Retrieval Analysis*. University of Leeds.

Taddei, P., Tozzi, S., Carmignato, S. and Affatato, S. 2016. May the surface roughness of the retrieved femoral head influence the wear behavior of the polyethylene liner? *Journal of Biomedical Materials Research - Part B Applied Biomaterials*. **104**(7), pp.1374–1385.

Teeter, M.G., Naudie, D.D.R., Charron, K.D. and Holdsworth, D.W. 2010. Three-Dimensional Surface Deviation Maps for Analysis of Retrieved Polyethylene Acetabular Liners Using Micro-Computed Tomography. *Journal of Arthroplasty*. **25**(2), pp.330–332.

Teeter, M.G., Yuan, X., Naudie, D.D.R. and Holdsworth, D.W. 2010. Technique to quantify subsurface cracks in retrieved polyethylene components using micro-CT. *Journal of Long-Term Effects of Medical Implants*. **20**(1), pp.27–34.

Terrier, A., Latypova, A., Guillemin, M., Parvex, V. and Guyen, O. 2017. Dual mobility cups provide biomechanical advantages in situations at risk for dislocation: a

finite element analysis. *International Orthopaedics*. **41**(3), pp.551–556.

Tipper, J.L., Ingham, E., Hailey, J.L., Besong, A.A., Fisher, J., Wroblewski, B.M. and Stone, M.H. 2000. Quantitative analysis of polyethylene wear debris, wear rate and head damage in retrieved Charnley hip prostheses. *Journal of Materials Science: Materials in Medicine*. **11**(2), pp.117–124.

Trommer, R.M., Maru, M.M., Oliveira Filho, W.L., Nykanen, V.P.S., Gouvea, C.P., Archanjo, B.S., Martins Ferreira, E.H., Silva, R.F. and Achete, C.A. 2015. Multi-Scale Evaluation of Wear in UHMWPE-Metal Hip Implants Tested in a hip Joint Simulator. *Biotribology*. **4**, pp.1–11.

Uddin, M.S. 2015. Contact of dual mobility implants: effects of cup wear and inclination. *Computer Methods in Biomechanics and Biomedical Engineering*. **18**(15), pp.1611–1621.

Uddin, M.S. 2014. Wear Measurement and Assessment of Explanted Cross-Linked PE Acetabular Cups Using a CMM. *Tribology Transactions*. **57**(5), pp.767–777.

Uddin, M.S., Mak, C.Y.E. and Callary, S.A. 2016. Evaluating hip implant wear measurements by CMM technique. *Wear*. **364**–**365**, pp.193–200.

Udgata, S. 2014. Osteoarthritis: An Overview. *IOSR Journal of Pharmacy and Biological Sciences*. **9**(5), pp.7–15.

Vielpeau, C., Lebel, B., Ardouin, L., Burdin, G. and Lautridou, C. 2011. The dual mobility socket concept: Experience with 668 cases. *International Orthopaedics*. **35**(2), pp.225–230.

Waddell, B.S., Koch, C., Trivellas, M., Burket, J.C., Wright, T. and Padgett, D. 2019. Have large femoral heads reduced prosthetic impingement in total hip arthroplasty? *HIP International*. **29**(1), pp.83–88.

Wang, A., Essner, A., Polineni, V.K., Stark, C. and Dumbleton, J.H. 1998. Lubrication and wear of ultra-high molecular weight polyethylene in total joint replacements. *Tribology International*. **31**(1–3), pp.17–33.

Wang, L., Peng, X., Sun, C., Wang, H., Li, D., Zhu, J., Jin, Z., Mihcin, S. and Liu, C. 2016. THE DETERMINATION of the VOLUMETRIC WEAR for SURGICALLY RETRIEVED HIP IMPLANTS BASED on CMM. *Journal of Mechanics in Medicine and Biology*. **16**(4).

Weitzler, L., Hemmerling, K., Baral, E., Wright, T.M. and Padgett, D.E. 2019. Corrosion in retrieved metal liners of modular dual mobility systems for THA *In*: *Orthopaedic Research Society*.

Wera, G.D., Ting, N.T., Moric, M., Paprosky, W.G., Sporer, S.M. and Della Valle, C.J. 2012. Classification and Management of the Unstable Total Hip Arthroplasty. *Journal of Arthroplasty*. **27**(5), pp.710–715.

Wimmer, M.A., Sprecher, C., Hauert, R., Täger, G. and Fischer, A. 2003. Tribochemical reaction on metal-on-metal hip joint bearings A comparison between in-vitro and in-vivo results. *Wear*. **255**(7–12), pp.1007–1014.

Wong, MD, W., Clarke, PhD, I., Donaldson, MD, T. and Burgett, M. 2013. Surface roughness of retrieved femoral heads in CoCr-Polyethylene Hip Bearings – A retrieval assessment with 11-17 years follow-up. *Reconstructive Review*. **3**(1), pp.45–48.

Wroblewski, B.M., Siney, P.D., Dowson, D. and Collins, S.N. 1996. Prospective clinical and joint simulator studies of a new total hip arthroplasty using alumina ceramic heads and cross-linked polyethylene cups. *The Journal of bone and joint surgery. British volume*. **78**(2), pp.280–5.

Yamaguchi, M., Akisue, T., Bauer, T.W. and Hashimoto, Y. 2000. The spatial location of impingement in total hip arthroplasty. *Journal of Arthroplasty*. **15**(3), pp.305–313.

Zahar, A., Rastogi, A. and Kendoff, D. 2013. Dislocation after total hip arthroplasty. *Current Reviews in Musculoskeletal Medicine*. **6**(4), pp.350–356.

Zoccali, C., Attala, D., Scotto di Uccio, A., Rossi, B., Scotto, G. and Biagini, R. 2017. The dual mobility cup in muscular skeletal oncology: rationale and indications. *International Orthopaedics*. **41**(3), pp.447–453.

Appendix A – Component numbers

Table A1 - 69/28-mm BI-MENTUM™ DM liners used in Chapter 2 for the assessment of as-manufactured geometric variation. All samples were provided by DePuy Synthes (Leeds, UK) and were manufactured from ALTRX®.

Sample number	iMBE part number	Reference number	Lot number
1	2251	122128069	9729919
2	2252	122128069	9729919
3	2253	122128069	9729919
4	2254	122128069	9729919
5	2255	122128069	9729919
6	2256	122128069	9729919

Table A2 – Retrieved DM components assessed in Chapter 3, including their original retrieval code and source (i.e., Dartmouth College or University of Leeds).

Sample number	Source	Retrieval code
1	Dartmouth	12 03 16 18,28
2	Dartmouth	12 10 23 12,22
3	Dartmouth	14 10 31 14,24
4	Dartmouth	15 08 11 12,22
5	Dartmouth	15 12 09 15,25
6	Dartmouth	16 08 02 11,21
7	Dartmouth	16 08 02 12,22
8	Dartmouth	16 08 06 12,22
9	Dartmouth	16 10 28 11,21
10	Dartmouth	16 10 31 13,23
11	Dartmouth	16 11 28 15,25
12	Dartmouth	17 01 18 13,23
13	Dartmouth	17 05 04 11,21
14	Dartmouth	17 10 24 13,23
15	Dartmouth	19 02 22 12,22
16	Dartmouth	19 06 03 14,24
17	Leeds	HWGT0196B
18	Leeds	HWGT0230
19	Leeds	HWGT0253
20	Leeds	HMPH0287

Table A3 – Samples used for the repeatability and sensitivity analyses described in Chapter 4.

Test		Liner[1]	Head[2]	Shell[3]	Stem[4]
Intra-liner repeatability		iMBE 2255	iMBE 2259 (D15112099)	iMBE 2262	iMBE 2079
Inter-liner repeatability		iMBE 2253			
		iMBE 2254			
		iMBE 2255			
Sensitivity analysis	Reduced swing phase load	iMBE 2256			
	Increased gait frequency	iMBE 2253			
	Scratched femoral head	iMBE 2249			
	High cup inclination angle	iMBE 2248	iMBE 2260 (D1510097)	iMBE 2261	

[1] All liners were 69/28-mm ALTRX BI-MENTUM liners (REF: DEVELOPMENT108).
[2] All heads were 28-mm (+8.5) CoCr Articul/eze heads (REF: 1365-13-000). Lot number specified in the table.
[3] All shells were 69-mm BI-MENTUM PressFit cups (REF: DS45320069; LOT: 2001373A).
[4] Stem was a KS size 12 Corail cementless femoral stem (REF: 3L92512; LOT: 9032785).

Table A4 – Component details for samples used in the motion tracking analysis of DM liners described in Chapter 5.

Component set	Head[1]	Liner[2]	Shell[3]	Stem[4]
1	iMBE 2277	iMBE 2297	iMBE 2284	iMBE 2291
2	iMBE 2278	iMBE 2298	iMBE 2285	iMBE 2292
3	iMBE 2279	iMBE 2299	iMBE 2286	iMBE 2293

[1] All heads were 28-mm (+8.5) CoCr Articul/eze™ heads (REF: 1365-13-000; LOT: D21114002).
[2] All liners were 69/28-mm Marathon™ BI-MENTUM™ prototype liners (REF: n/a; LOT: WR 7499 PN0X, where X is the component set number specified in the table).
[3] All shells were 69-mm BI-MENTUM™ PressFit cups (REF: DS45320069; LOT: 1911125A).
[4] All stems were a KS size 12 Corail cementless femoral stem (REF: 3L92512; LOT: 9804452).

Appendix B – Surface deviation heatmaps of retrieved dual mobility polyethylene liners

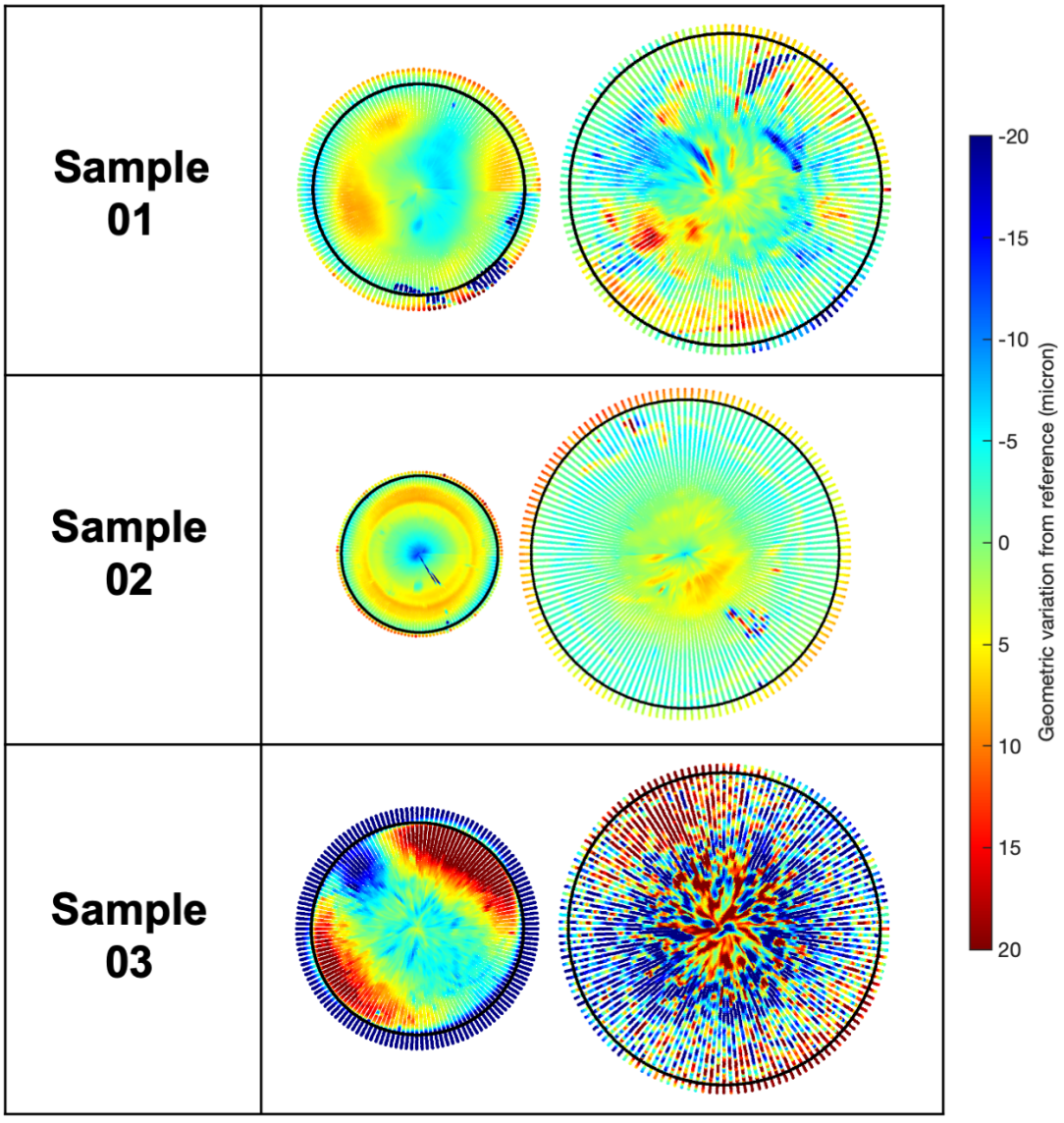

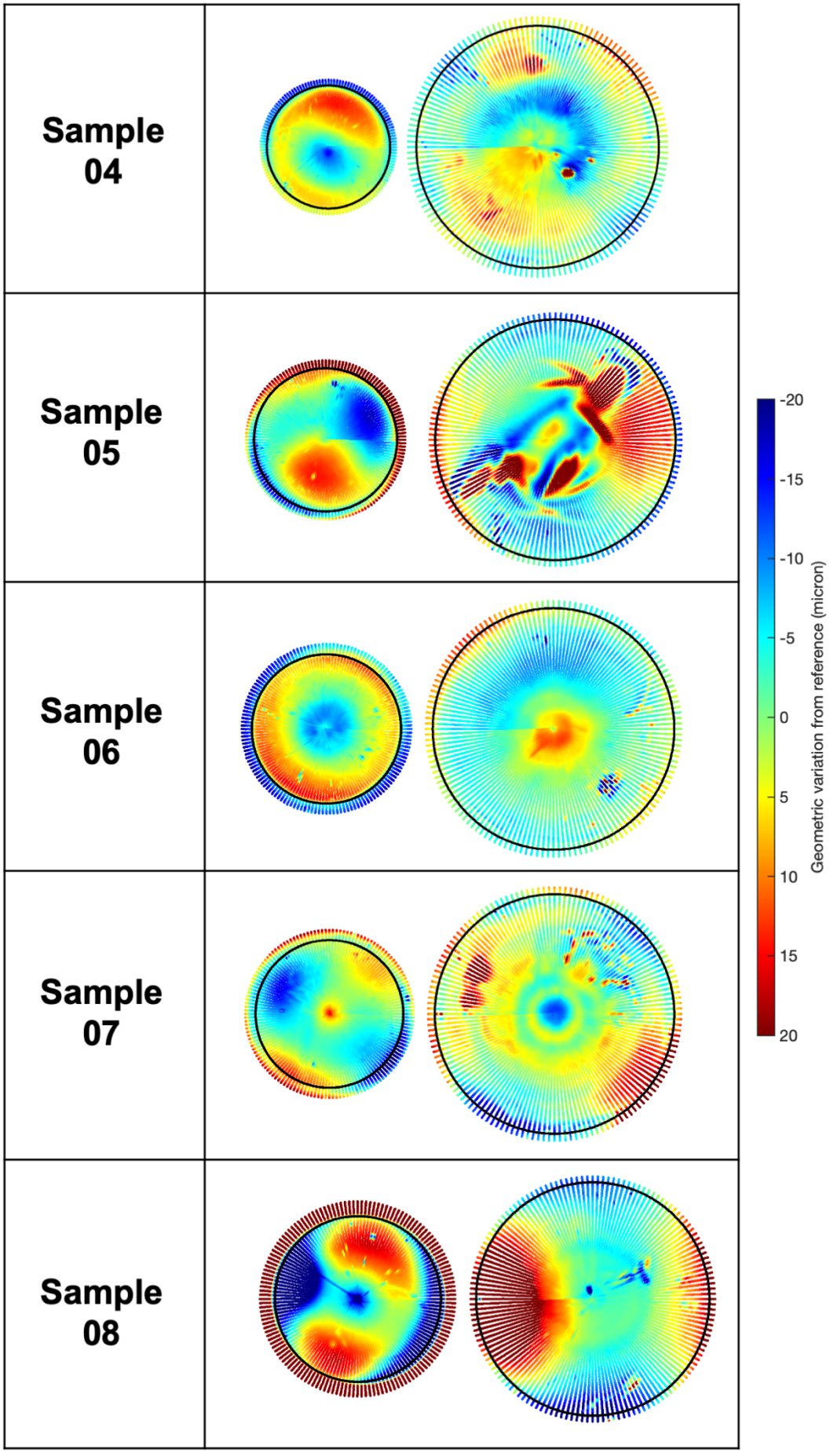
Sample 04
Sample 05
Sample 06
Sample 07
Sample 08
-20
-15
-10
-5
0
5
10
15
20
Geometric variation from reference (micron)

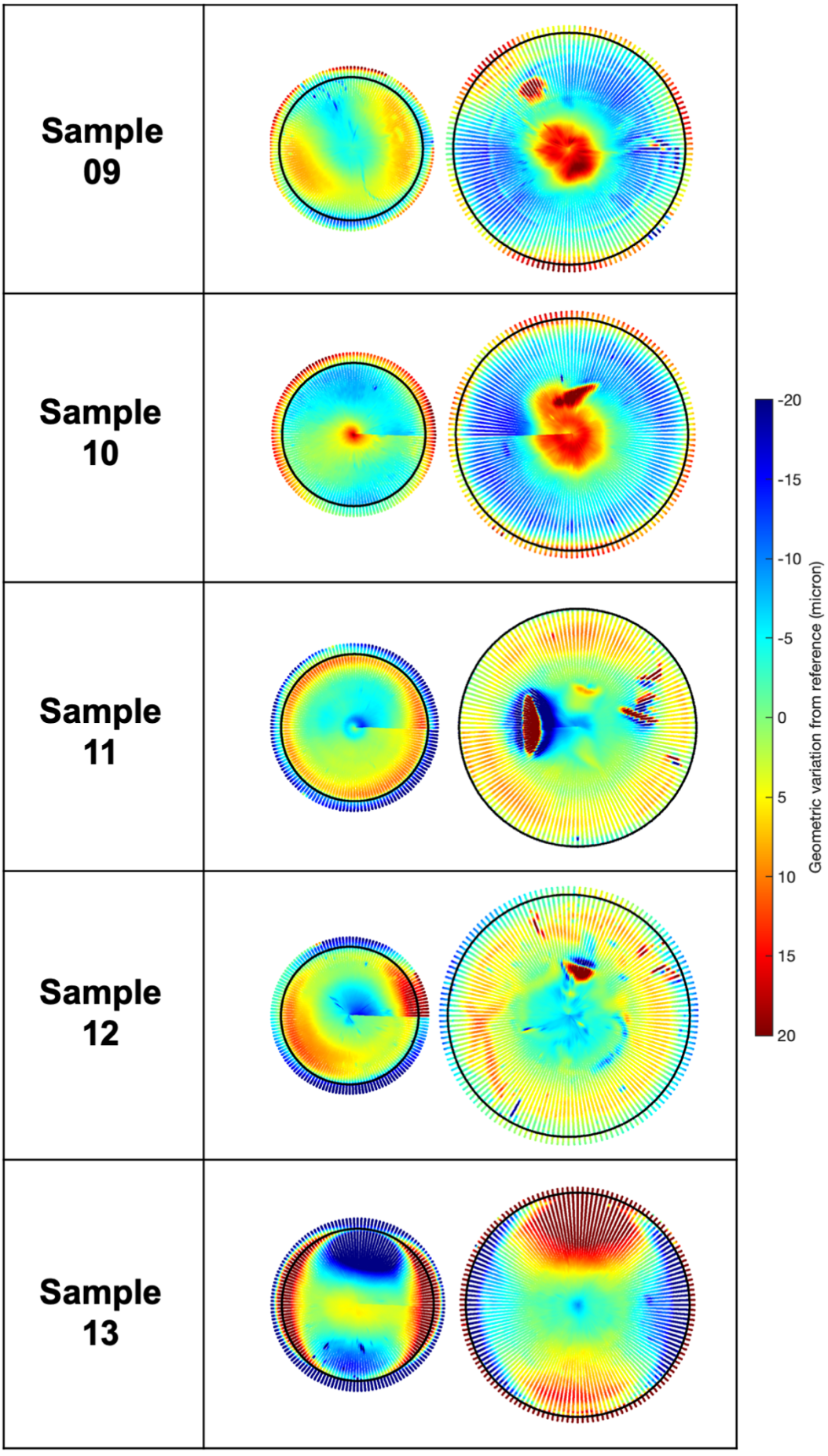
Sample 09
Sample 10
Sample 11
Sample 12
Sample 13
-20
-15
-10
-5
0
5
10
15
20
Geometric variation from reference (micron)

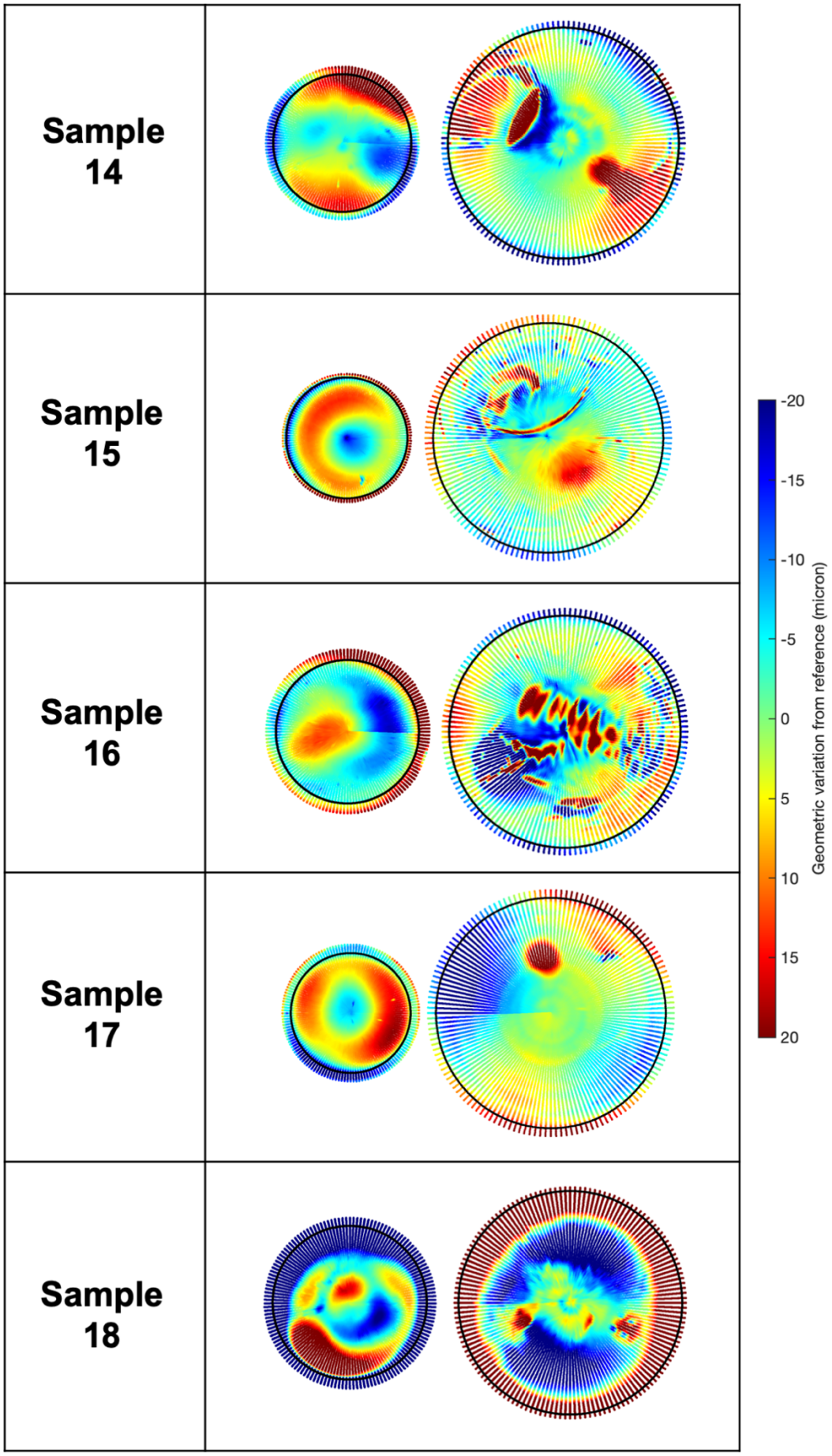
Sample 14
Sample 15
Sample 16
Sample 17
Sample 18
-20
-15
-10
-5
0
5
10
15
20
Geometric variation from reference (micron)

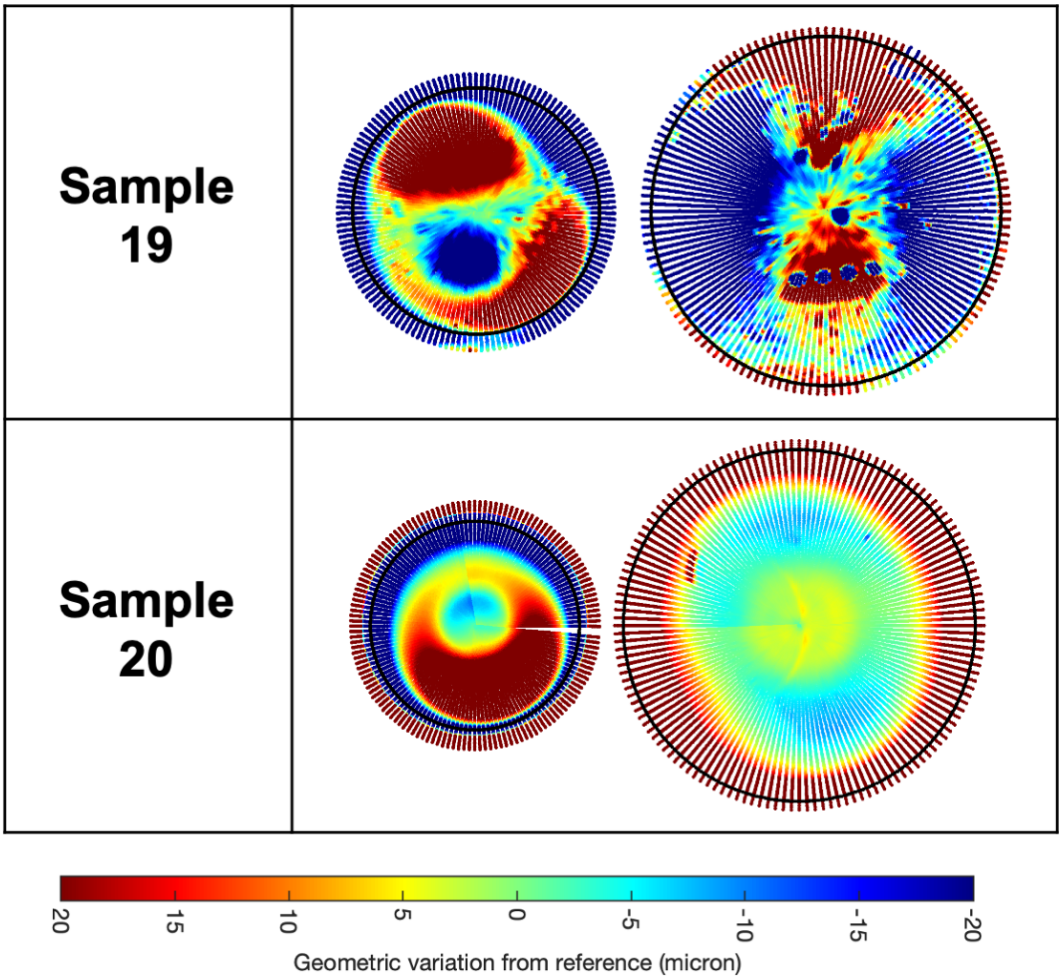
Sample 19
Sample 20
20
15
10
5
0
-5
-10
-15
-20
Geometric variation from reference (micron)

Appendix C – Calculation of inclination* and azimuth* angles

The positional tracker recorded rotation of a dual mobility liner about three axes, which included –

- Roll, which represents an anticlockwise rotation of γ about the X-axis
- Pitch, which represents an anticlockwise rotation of β about the Y-axis
- Yaw, which represents an anticlockwise rotation of α about the Z-axis

The combined rotation of the liner was transformed into a rotation matrix. For context, rotation matrices are used to transform coordinates about two or three axes whilst maintaining the original properties (i.e., shape, size) of the object (Evans, 2001). An example of a three-dimensional rotation matrix is shown in. Equation C.1. The corresponding matrix for a combined rotation in roll, pitch and yaw is shown in Equation C.2. This matrix is determined by multiplying the individual rotation matrices for yaw, pitch and roll in this order (i.e., the sequence for intrinsic rotations of this system).

$$R = \begin{bmatrix} R_{1,1} & R_{1,2} & R_{1,3} \\ R_{2,1} & R_{2,2} & R_{2,3} \\ R_{3,1} & R_{3,2} & R_{3,3} \end{bmatrix} \qquad (\boldsymbol{C.1})$$

$$R(\gamma, \beta, \alpha) = R_z(\alpha) R_y(\beta) R_x(\gamma) \qquad (\boldsymbol{C.2})$$

$$= \begin{bmatrix} \cos(\alpha) & -\sin(\alpha) & 0 \\ \sin(\alpha) & \cos(\alpha) & 0 \\ 0 & 0 & 1 \end{bmatrix} \begin{bmatrix} \cos(\beta) & 0 & \sin(\beta) \\ 0 & 1 & 0 \\ -\sin(\beta) & 0 & \cos(\beta) \end{bmatrix} \begin{bmatrix} 1 & 0 & 0 \\ 0 & \cos(\gamma) & -\sin(\gamma) \\ 0 & \sin(\gamma) & \cos(\gamma) \end{bmatrix}$$

$$= \begin{bmatrix} \cos(\alpha)\cos(\beta) & \cos(\alpha)\sin(\beta)\sin(\gamma) - \sin(\alpha)\cos(\gamma) & \cos(\alpha)\sin(\beta)\cos(\gamma) + \sin(\alpha)\sin(\gamma) \\ \sin(\alpha)\cos(\beta) & \sin(\alpha)\sin(\beta)\sin(\gamma) + \cos(\alpha)\cos(\gamma) & \sin(\alpha)\sin(\beta)\cos(\gamma) - \cos(\alpha)\sin(\gamma) \\ -\sin(\beta) & \cos(\beta)\sin(\gamma) & \cos(\beta)\cos(\gamma) \end{bmatrix}$$

One property of rotation matrices is that their columns represent orthogonal unit vectors (Evans, 2001). Therefore, the inclination* and azimuth* of the liner were calculated using the Equation C.3 and C.4, respectively. Azimuth* returned a value between -180° and 180°, which was then transformed into scale from 0° to 360°.

$$Inclination^{*} = cos^{-1}\left(R_{3,3}\right) = cos^{-1}[\cos(\beta)\cos(\gamma)] \quad (\boldsymbol{C.3})$$

$$Azimuth^{*} = tan^{-1}\left(\frac{R_{1,3}}{R_{2,3}}\right) = tan^{-1}\left(\frac{\cos(\alpha)\sin(\beta)\cos(\gamma) + \sin(\alpha)\sin(\gamma)}{\sin(\alpha)\sin(\beta)\cos(\gamma) - \cos(\alpha)\sin(\gamma)}\right) \quad (\boldsymbol{C.4})$$

Appendix D – Conference proceedings

Mackenzie Brown, Ruth Wilcox, Graham Isaac, James Anderson, Tim Board, Sophie Williams. Development of a geometric characterisation methodology for the assessment of dual mobility liners used in total hip replacement. British Orthopaedic Research Society (BORS), Virtual meeting, 2021. Podium presentation.

Mackenzie Brown, Ruth Wilcox, Graham Isaac, James Anderson, Tim Board, Douglas van Citters, Sophie Williams. Semi-quantitative Assessment of Retrieved Dual Mobility Liners for Total Hip Replacement. Orthopaedic Research Society (ORS), Florida USA, 2022. Poster presentation.

Mackenzie Smeeton, Ruth Wilcox, Graham Isaac, James Anderson, Tim Board, Douglas van Citters, Sophie Williams. Retrieval analysis of dual mobility polyethylene liners for total hip replacement. International Combined Orthopaedic Research Societies (ICORS), Edinburgh UK, 2022. Oral poster presentation.

Mackenzie Smeeton, Ruth Wilcox, Graham Isaac, James Anderson, Tim Board, Douglas van Citters, Sophie Williams. Retrieval analysis of dual mobility polyethylene liners for total hip replacement. British Hip Society (BHS), Edinburgh UK, 2023. Podium presentation.